Quantitative structure activity relationships for the biotransformation and toxicity of halogenated benzene-derivatives

Implications for enzyme catalysis and reaction mechanisms

Promotor:	Dr. C. Veeger *Hoogleraar in de Biochemie*
Co-promotor:	Dr. Ir. I.M.C.M. Rietjens Universitair hoofddocent Vakgroep Biochemie

Quantitative structure activity relationships for the biotransformation and toxicity of halogenated benzene-derivatives

Implications for enzyme catalysis and reaction mechanisms

Proefschift

Ter verkrijging van de graad van
doctor in de landbouw- en milieuwetenschappen,
op gezag van de Rector Magnificus,
Dr. C.M. Karssen, in het openbaar te verdedigen
op vrijdag 7 juni 1996 des ochtends om elf uur in de Aula
van de Landbouwuniversiteit te Wageningen.

door

Nicole Hubertine Pauline Cnubben
geboren 13 februari 1967, te Meerssen.

CIP-DATA KONINKLIJKE BIBLIOTHEEK, DEN HAAG

Cnubben, Nicole Hubertine Pauline Cnubben

Quantitative structure activity relationships for the biotransformation and toxicity of halogenated benzene-derivatives: implications for enzyme catalysis and reaction mechanisms / Nicole Hubertine Pauline Cnubben. - [S.I. : s.n.]
Thesis University Wageningen. - With summary in Dutch.
ISBN 90-5485-520-7
Subject headings: QSAR / biotransformation / toxicity / benzene-derivatives.

The studies described in this thesis were carried out at the Department of Biochemistry, Agricultural University Wageningen, Dreijenlaan 3, 6703 HA Wageningen, The Netherlands.

This work was supported by the Netherlands Organization for Scientific Research (NWO), section Medical Sciences.

Ter nagedachtenis aan mijn vader
Voor mijn familie
Voor Peter

Contents

Abbreviations and symbols

AO	atomic orbital
ARNT	aromatic hydrocarbon receptor nuclear translocator
ATP	adenosine 5'-triphosphate
BD	benzodioxole
BSA	bovine serum albumine
BUN	blood urea nitrogen
CO	carbonmonoxide
DMA	dimethylamine
DMG	dimethylglycine
DMSO	dimethylsulphoxide
E_a	activation energy
EDTA	ethylenediaminetetraacetate
E(HOMO)	energy of the highest occupied molecular orbital
E(LUMO)	energy of the lowest unoccupied molecular orbital
E(SOMO)	energy of the single occupied molecular orbital
FAD	flavin adenine dinucleotide
FMN	flavin mononucleotide (riboflavin-5'-phosphate)
FMO	flavin-containing monooxygenase
GC-MS	gas chromatography - mass spectrometry
GSH	reduced glutathione
GST	glutathione S-transferase
GS-X	glutathione conjugate of compound X.
γGT	γ-glutamyl transpeptidase
HOMO	highest occupied molecular orbital
HPLC	high performance liquid chromatography
HXO	hypohalous acid
IR	infra red
IS	internal standard
K_m^s	apparent Michaelis constant K_m
K_d^s	apparent K_d of the cytochrome P450-substrate complex
ln	natural logarithm
log P	logarithm of experimental octanol/water partition coefficient
LUMO	lowest unoccupied molecular orbital
Me_2SO	dimethylsulphoxide

MO	molecular orbital
MP-8	microperoxidase 8
NAD(P)H	reduced nicotinamide-adenine dinucleotide
NAT	N-acetyltransferase
NMR	nuclear magnetic resonance
PAPS	3'-phosphoadenosine 5'-phosphosulphate
PCB	polychloorbiphenyl
PCN	pregnenolone-16α-carbonitrile
PPAR	peroxisome proliferator-activated receptor
QSAR	quantitative structure activity relationship
SEM	standard error of the mean
SOMO	single occupied molecular orbital
S	substrate
SO	oxygenated substrate
ST	sulphotransferase
tBuOOH	tertiair butyl hydroperoxide
TCA	trichloroacetic acid
TLC	thin layer chromatography
TMAO	trimethylamine N-oxide
TSP	sodium 3-trimethylsilyl-(2,2,3,3-$^{2}H_4$)-propionate
UDPG	uridine 5'-diphospho-glucuronyltransferase
UV	ultra violet light
ε_x	extinction coefficient at x nm
λ_{max}	position of absorption maximum

CHAPTER 1

Introduction.

General aspects of biotransformation.

Living organisms are exposed to a great variety of natural and man-made substances, such as pharmacological agents, industrial chemicals, environmental pollutants, food additives etcetera. These chemical compounds may enter the body accidently or on purpose through the skin, the gastrointestinal tract or the respiratory tract. The fate of these compounds in the body is generally dependent on their physico-chemical characteristics. For instance, highly lipophilic compounds will accumulate in fat tissues due to their affinity for a hydrophobic environment, whereas reactive compounds may react with cellular macromolecules, thereby altering their structure and/or function.

Fortunately, organisms are equipped with a special defense system able to deal with most of the low molecular weight compounds. This system consists of a complex enzymatic machinery aiming to modify these body-foreign compounds (xenobiotica) into more hydrophilic products (metabolites), thereby enhancing efficient excretion into the bile or urine. This sophisticated process of metabolic transformation of molecules, catalyzed by several enzyme systems, is called biotransformation. For most xenobiotics, metabolic processes are not just one-step events, but occur via multiple competing and sequential pathways. Classically, biotransformation reactions are categorized essentially into three groups; phase I, II and III. Phase I reactions involve the introduction of a polar functional group into the molecule by oxidation, reduction or hydrolysis. In phase II reactions, a reactive centre of a polar xenobiotic or of a metabolite from the phase I reaction is conjugated generally with a more hydrophilic moiety. This can be for example a glutathione, sulphate, glucuronide or acetate moiety. Finally, phase III consists of elimination systems like the ATP-dependent P-glycoprotein and the glutathione S-conjugate export pumps [Ishikawa, 1992].

Initially, biotransformation was only regarded as a detoxification mechanism for exogenous as well as endogenous substances. However, biotransformation is often associated with the introduction of a chemically reactive function into the molecule. As a consequence, the ultimate or intermediate metabolites may elicit adverse effects through interaction with critical cellular targets, eventually leading to disturbance of biochemical and physiological processes. This aspect of biotransformation is called bioactivation. The bioactivating properties of the biotransformation system, however, may also serve as a basis for the generation of pharmacologically active compounds within specific areas of the body to produce the actual therapeutic effect of the administered drug. The balance between detoxification and bioactivation eventually determines the expression of toxicity upon xenobiotic exposure.

Insight into the relationships between the structure and metabolism of xenobiotics is urgently needed for the costly design and safety assessment of new compounds in drug and agrochemical industries. Organisms are frequently exposed to an almost unlimited number of natural chemicals and other xenobiotics, and data on the biological effects of all these compounds are far from complete or even lacking. This requires the definition of molecular structural features in order to classify the biological activities of compounds. The recognition that substrate characteristics are often related to biological activity of xenobiotics, has prompted the development of QSARs or Quantitative Structure Activity Relationships. Initially, much studies were devoted to obtain relationships between biological effects and substituent parameters like log P or π, Hammett σ and/or Taft $E\sigma$ values to describe hydrophobic, electronic and steric influences [for review see: Hansch and Zang, 1993; Lewis, 1990]. In those studies relationships were primarily described for transport of compounds through multicompartmental systems, substrate-receptor interactions and the ability to reach the site of action. Later, it became increasingly evident that for many xenobiotics biotransformation plays a critical role in the development of chemically induced toxicities, because of the formation of reactive intermediates and metabolites. The enzymatic generation of reactive species is often the response-determining step. Hence, knowledge on the metabolic fate of xenobiotics and the molecular mechanisms of biotransformation enzymes involved, is of crucial importance to the understanding of the nature, site and mechanism of action of these compounds. Therefore, more and more attention has been devoted to quantitative structure metabolism relationships. In this way, molecular and biochemical toxicology aim to contribute to the setting of priorities in toxicological research and to the development of safer chemicals used as drugs, food additives and agrochemicals.

Scope of this thesis.

The main objective of the studies presented in this thesis was the description of QSARs for the cytochrome P450 and glutathione S-transferase mediated biotransformation and toxicity of small aromatic molecules. The superfamilies of cytochromes P450 and glutathione S-transferases are the most important and numerous phase I and phase II biotransformation enzymes, respectively, involved in the detoxification and bioactivation of a great variety of chemicals. The aim of the present thesis was to describe QSARs on the basis of insight in the molecular mechanisms of the enzymes involved. This insight is used to define the specific substrate characteristic(s) that influence the reaction and can, thus, provide the appropriate QSAR parameter to explain or even predict the outcomes of a biotransformation reaction. Ultimately, the QSARs may provide a basis for the prediction of the rate and regioselectivity of enzymatic conversion and biotransformation-related toxicity. Besides, QSARs based on insight in the molecular mechanisms of biotransformation enzymes may be helpfull in a more rational design of new biocatalysts.

A general characteristic feature of biotransformation enzymes, especially when compared to other enzymes, is their relatively, broad and partially overlapping substrate specificity and regioselectivity. This property enables the biotransformation system to metabolize an almost unlimited number of compounds by a limited number of enzymes. The broad substrate specificity can be primarily attributed to the relatively large active sites of the enzymes. In order to elucidate molecular mechanisms of enzymes and determine the specific substrate characteristics that influence biotransformation reactions, the contribution of the active site of the enzymes in directing the juxtaposition of the substrates by steric factors have to be minimalized. Therefore, the investigations of this thesis were focussed on relatively small aromatic molecules.

General outline of this thesis.

Halogenated aromatic compounds are widely used in industry, commerce and agriculture and are a major contribution to nowadays environmental pollution. Modern agrochemical and pharmaceutical industries are known to synthesize wide varieties of new halogenated aromatics, to be used as agrochemicals, dyes, drugs or building blocks in the synthesis of new industrially relevant compounds. Organisms

are frequently exposed to these compounds or their degradation products with possible toxicological consequences. Clearly, toxicological testing of all these newly synthesized compounds is a time- and money-consuming problem.

Based on these considerations, the studies of this thesis were undertaken, in order to investigate whether insight into the molecular mechanisms of biotransformation enzymes is helpfull in defining QSARs for the metabolic fate of aromatic compounds. Insight into factors that direct the rates and regioselectivities of biotransformation processes will help to gain insight in factors that direct processes of, and chances on, bioactivation or detoxification of xenobiotics to which the organism is exposed.

In the present study the research was predominantly focussed on nitrogen (amino or nitro) substituted halogenated aromatics, like anilines and nitrobenzenes. These compounds were chosen, because -as outlined above- they are of industrial relevance and used on a large scale, but also because their biotransformation is known to include pathways leading to both detoxification and the generation of reactive intermediates assumed to contribute to the toxicity of amino- and nitrobenzene derivatives (bioactivation). In the present studies in particular, fluorine containing compounds were investigated, due to the unique characteristics of this type of halogen. Introduction of fluorines into a molecule influences the electron distribution in the molecule and its lipophilicity, without introducing any major steric chances since the van der Waals radius of fluorine (1.35Å) is almost similar to that of a hydrogen (1.20Å). Furthermore, fluorine substitution is frequently used for site-specific blocking of metabolic pathways, since the strong C-F bond is thought to prevent reactivity at a fluorinated center. Thus, the introduction of fluorines into a molecule can be used to alter the rate, route and extent of drug metabolism with minimal effect on steric influences [Park and Kitteringham, 1994]. Besides, the metabolism of fluorine containing compounds can be elegantly monitored by ^{19}F-NMR.

In chapter 2 of this thesis, a general description of the enzymes primarily involved in the biotransformation of the amino- and nitrobenzene derivatives is given. For cytochromes P450 and glutathione S-transferases special attention is focussed on the reaction mechanisms involved, because the studies of the present thesis aim to base QSARs on the chemical substrate characteristics and the way in which these characteristics may influence the supposed reaction mechanism.

In chapter 3 and 4 clear examples of QSAR studies are presented directed at understanding either the regioselectivity (chapter 3) or the rate (chapter 4) of the

cytochrome P450 catalyzed aromatic hydroxylation of a series of aniline derivatives. The QSARs obtained are based on the reaction mechanism of the enzyme system involved and computer calculated chemical reactivity parameters of the substrates.

To fully describe the biotransformation pathways of not only fluorinated anilines (identified on the basis of ^{19}F-NMR analysis), but also of other anilines with chlorine, bromine or iodine substituents, methods to quantify the metabolites from aromatic or N-hydroxylation were developed, as far as they were not available from the literature. Chapter 5 describes the development of a new and sensitive chemical assay for the detection of halogenated 2-aminophenols in biological samples. In further studies of the thesis this method could be used for the identification and quantification of 2-aminophenol derivatives in addition to HPLC and NMR analysis.

Using the available methods for the analysis of metabolites of aniline derivatives, studies were carried out to investigate the influence of the nature, number and position of halogen substituents at the aromatic ring of aniline derivatives on metabolic pathways, with special emphasis on the bioactivation to toxic metabolites, and, thus on the toxicity of the respective aromatic compounds. In chapter 6 the effect of halogen substituent patterns on possibilities for bioactivation through the cytochrome P450 catalyzed oxidative dehalogenation, leading to reactive benzoquinoneimine metabolites, was investigated and quantified. In chapter 7 the relationship between the regioselectivity of the hydroxylation of a series of aniline derivatives and their actual toxic endpoint (nephrotoxicity and methemoglobinemia) was studied, providing some general rules for the way in which biotransformation of these compounds is influencing their toxicity.

Finally, attention was focussed on the changes in metabolic profiles observed upon full oxidation of the amino moiety to a nitro substituent. In chapter 8 it is outlined that the molecular orbital based QSARs obtained in chapter 4, but also in recent studies with glutathione S-transferases [Rietjens *et al.*, 1995], can actually explain why the amino derivatives are mainly metabolized through cytochrome P450 dependent metabolic pathways, whereas the nitro analogues are not, and, instead are rather metabolized through glutathione S-transferase catalyzed reactions. Chapter 9 describes a molecular orbital based quantitative structure activity relationship for both the biotransformation and reactivity of a series of fluoronitrobenzenes with nucleophiles. This study provides a clear example of how chemical reactivity parameters of fluoronitrobenzenes direct biotransformation processes and, as a consequence, toxicity in rats.

A final study (chapter 10) actually demonstrates that the QSARs obtained for the regioselectivity and rate of cytochrome P450 catalyzed conversions of the relatively small halogenated benzene derivatives, can be extrapolated from rats to various species, including man.

Altogether, the results of the present thesis fully support that the use of computer calculated molecular orbital parameters are a useful additional tool to study, not only the mechanisms of the enzymes involved in biotransformation of xenobiotics, but also, to explain, or even predict the outcomes of biotransformation pathways in mammalian systems exposed to these chemicals. Finally, the findings described in this thesis are summarized and discussed in chapter 11.

REFERENCES.

Hansch C. and Zhang L., Quantitative structure activity relationships of cytochrome P450, *Drug Metabolism Reviews* **25**, 1-48, 1993.

Ishikawa T., The ATP-dependent glutathione S-conjugate export pump, *Trends Biochem. Sci.* **17**, 463-468, 1992.

Lewis D.F.V., MO-QSARs: a review of molecular orbital-generated quantitative structure activity relationships, Progress in drug metabolism, (Ed. G.G. Gibson), Taylor & Francis, Chapter 5, 205-255, 1990.

Park B.K. and Kitteringham N.R., Effects of fluorine substitution on drug metabolism: pharmacological and toxicological implications, *Drug Metabolism Reviews* **26**, 605-643, 1994.

Rietjens I.M.C.M., Soffers A.E.M.F., Hooiveld G.J.E.J., Veeger C. and Vervoort J., Quantitative structure activity relationships based on computer calculated parameters for the overall rate of glutathione S-transferase catalyzed conjugation of a series of fluoronitrobenzenes, *Chem. Res. Tox.* **8**, 481-488, 1995.

CHAPTER 2

Biotransformation enzymes involved in the detoxification and bioactivation of amino- and nitrobenzene derivatives.

The phase I enzymes play an important role in the enzymatic oxidation of xenobiotic chemicals. A number of these enzymes, contain a heme-cofactor (e.g. cytochromes P450) or a FAD-cofactor (e.g. flavin-containing monooxygenase, monoamine oxidase) as the site of dioxygen activation [Gibson and Skett, 1989; Guengerich, 1990]. The phase II enzymes are involved in the conjugation of compounds, generally yielding water-soluble metabolites, which can be excreted in bile or urine. In this section the phase I enzymes cytochrome P450 and flavin-containing monooxygenase as well as the phase II enzymes glutathione S-transferase, N-acetyltransferases, UDP-glucuronyltransferase and sulphotransferase will be discussed, because they are relevant for the biotransformation reactions of the present thesis (see Figure 1).

2.1. Phase 1 biotransformation enzymes.

2.1.1. Cytochrome P450 enzyme system.

General.

Cytochromes P450 constitute a family of enzymes that play a key role in the oxidative, peroxidative and reductive biotransformation of a surprisingly large number of structurally unrelated compounds. The cytochrome P450-dependent monooxygenases are involved in many steps of the biosynthesis and biodegradation of endogenous compounds such as steroids, fatty acids and prostaglandins, as well as in the conversion of exogenous compounds such as drugs and environmental

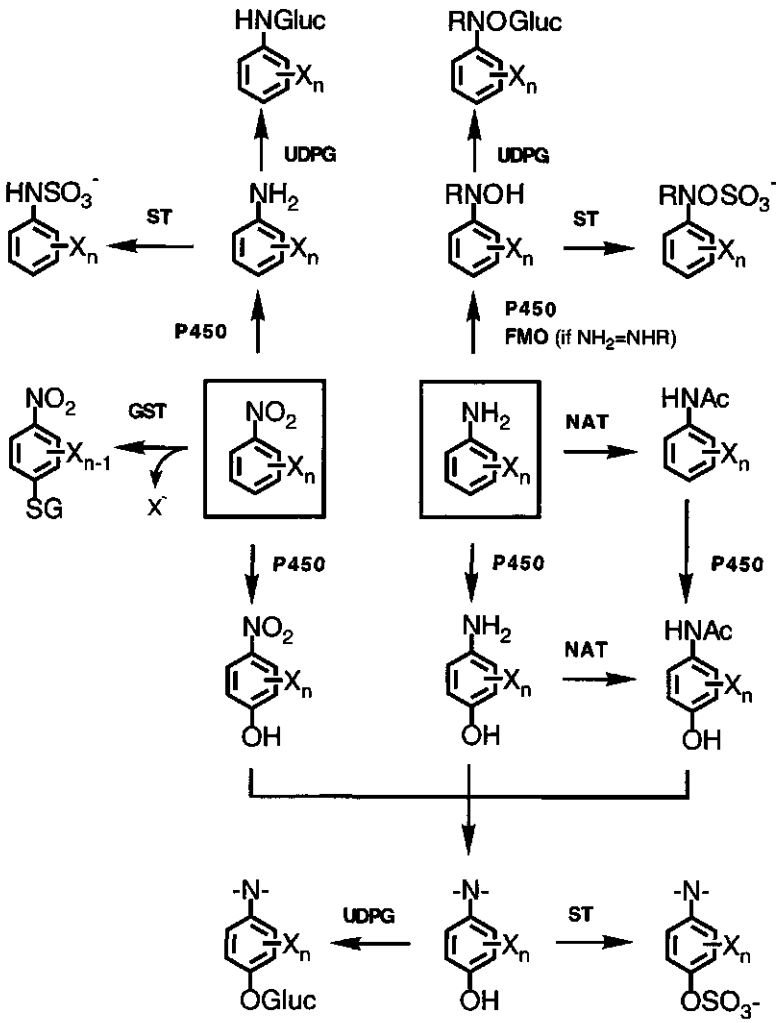

Figure 1: Schematic representation of the biotransformation pathways of amino- and nitrobenzene derivatives.

P450, cytochrome P450; FMO, flavine monooxygenase; GST, glutathione S-transferase; UDPG, UDP-glucuronyltransferase; ST, sulphotransferase; NAT, N-acetyltransferase.

pollutants, allowing their elimination from living organisms [Guengerich, 1993]. Furthermore, due to their ability to convert a vast array of substrates, cytochromes P450 and also other heme-containing enzymes are recognized as powerfull biocatalysts for industrial and environmental applications such as for example the production of fine-chemicals or the introduction of the genes of these enzymes into microorganisms that can be used for the bioremediation of contaminated sites. As a result, there is great and broad interest in the relationship between P450 structure and the mechanisms of substrate recognition and catalysis [Hasemann *et al.*, 1995]. Another reason underlying the considerable interest in P450 proteins, originates from the fact that their actions are not always benificial. Cytochromes P450 are frequently involved in chemical carcinogenesis, since they catalyze the oxidative activation of carcinogens to reactive electrophilic intermediates, that bind covalently to DNA, thus damaging the genetic material and activating oncogenes. In addition the reactive metabolites may induce the activation of the protein kinase C cascade leading to the phosphorylation of key nuclear transcription factors involved in the regulation of DNA replication [Parke, 1994].

Cytochromes P450 are found ubiquitously in animal and plant kingdoms [Nelson *et al.*, 1993]. The P450 enzymes inherite their name from the Soret absorption maximum around 450 nm of the reduced Fe^{2+}-CO complex which is characteristic for the axial thiolate ligation, provided by the cysteinyl residue [Omura and Sato, 1964]. In mammalia, these enzymes are found within almost every cell type of the body. The liver is the organ, which not only expresses most of the different cytochrome P450 genes, but also contains the highest P450 amounts, and, is thereby the major site of the metabolism of xenobiotics, drugs and endogenous compounds.

The unique property of the cytochrome P450 enzyme system to metabolize such a large variety of compounds originates from the existance of several types of cytochrome P450 enzymes (the so-called multiplicity), their inducibility as well as their broad and partially overlapping substrate specificity [Gonzalez, 1989; Guengerich, 1993].

The cytochrome P450 gene family.

More than 250 genes of the so-called superfamily of cytochromes P450 can be found in mammalia, birds, reptiles, fish, yeast, bacteria and plants. This superfamily is composed of families and subfamilies of enzymes that have been sequenced, characterized and classified on the basis of their primary amino acid

sequence homology [Nelson *et al.*, 1993; Nebert, 1989; Nebert, 1991]. In general, one gene family exhibits up to 36% resemblance to a cytochrome P450 of another family, whereas within a single subfamily the genes always share greater than 59% sequence similarity [Gonzales, 1994; Paine, 1995]. Two general functional classes of P450 exist. One class containing P450s for the conversion of fatty acids (CYP4), steroids (CYP17, 19, 21 and 27) and cholesterol (CYP7 and 11), which are well conserved with respect to their catalytic activities and display a rather rigid substrate and product specificity, due to their critical role in steroid and bile acid synthesis [Gonzalez *et al.*, 1994]. The other class of P450s consists of the enzymes encoded for by genes of the CYP1, 2, 3 and 4 families, which are predominantly involved in the metabolism of exogenous compounds [Paine, 1995]. The levels of the individual cytochromes P450 may vary considerably among species and individuals dependent on age, hormonal status, dietary factors (caffeine, charbroiled meat, alcohol), xenobiotic exposure (barbiturates, smoking, drugs) and genetic polymorphisms. Polymorphism in cytochrome P450 gene expression in humans has been described for the drug nifedipine (CYP3A4) [Paine, 1995], S-mephenytoin (CYP2C19) [de Morais *et al.*, 1994] and debrisoquine (CYP2D6) [Gonzalez and Idle, 1994; Gonzalez and Meyer, 1991; Gouch *et al.*, 1990]. Differences in the overall cytochrome P450 patterns among individuals, but also differences in the catalytic activities and regulatory pathways of cytochromes P450 may result in altered metabolism and hence can lead to different pharmacological or toxic responses. This aspect of variability is of present concern in pharmacological industries [Nedelcheva and Gut, 1994]. For instance, the CYP2C subfamilies are the most abundantly expressed P450s in the rat liver, whereas in humans the CYP3A subfamily predominates [Gonzalez, 1992; Paine, 1995], indicating that extrapolation of biotransformation and toxicity data from rodents to humans in some cases is very difficult or even impossible.

The best known forms of the cytochromes P450 involved in the biotransformation and bioactivation of drugs and other xenobiotics belong to the CYP 1A, 2A, 2B, 2D, 2E and 3A gene families. Cytochromes P450 of the 1A1 and 1A2 subfamilies are mainly involved in the metabolism of respectively polycyclic hydrocarbons and arylamines, amino acid and protein pyrolysates [Gonzalez, 1992; Shimada and Nakamura, 1987]. CYP2A6 exhibits activity towards activation of benzo(a)pyrene, aflatoxin B_1 and nitroso compound metabolism [Crespi *et al.*, 1990; Guengerich, 1992]. CYP2B6 is involved in the activation of the prodrug cyclophoshamide [Chang and Waxman, 1993]. The CYP2D6 is well known due to its

polymorphic expression in man and is involved in the biotransformation of debrisoquine and sparteine. CYP2E1 plays an important role in the metabolism of numerous low molecular weight halogenated hydrocarbon species (e.g. CCl_4, $CHCl_3$), benzenes and dialkylnitrosamines [Guengerich *et al.*, 1991; Yang *et al.*, 1990]. The most abundantly expressed hepatic enzyme CYP3A4 has been demonstrated to catalyze the conversion of numerous large compounds like aflatoxin B_1, nifedipine and testosteron [Gallagher *et al.*, 1994].

Regulation and induction.

The cytochrome P450 patterns are extremely variable among individuals (genetic polymorphism) and are partially dependent on xenobiotic exposure (P450 induction or inhibition) [Nedelcheva *et al.*, 1994]. Induction leads to variation in the cytochrome P450 enzyme patterns, and thereby to modulation of biotransformation activities. The regulation of the cytochromes P450 is very complex, involving increase of transcription and translation as well as mRNA- and protein stabilisation [Nedelcheva *et al.*, 1994; Nelson *et al.*, 1993; Okey *et al.*, 1990]. The mechanism of induction of cytochromes P450 is dependent on the type of inducer.

In general, cytochrome P450 inducers are classified into five classes, named after the prototype inducer, which are the polycyclic aromatic hydrocarbon-, the phenobarbital-, the ethanol-, the glucocorticoid- and the peroxisome-proliferator-inducible cytochromes P450. The aromatic hydrocarbon (Ah) receptor is involved in the regulation of the CYP1A1 and 1A2 genes. This receptor is composed of two heterodimeric subunits consisting of a ligand binding subunit and a subunit called the Ah receptor nuclear translocator (ARNT). Inducers like TCDD (2,3,7,8-tetrachlorodibenzo-p-dioxin) or other polycyclic aromatic hydrocarbons, bind to the Ah receptor and this couple binds to the ARNT protein. The complex is translocated to the cell nucleus, where it binds to a specific region of the CYP1A1 gene, the so-called xenobiotic regulatory element. The transcription of the CYP1A1 gene is stimulated by this interaction by a yet not fully understood mechanism [Guengerich, 1993]. CYP1A2 is to a minor extent coinduced with CYP1A1, although an additional mechanism for CYP1A2 induction has been demonstrated to exist. This alternative mechanism is mediated by benzodioxole (BD) compounds such as safrole, isosafrole and myristicin,which are involved in the regulation of the CYP1A2 gene, and act by mechanisms which are independent of the Ah receptor [Adams *et al.*, 1993; Ryu *et al.*, 1995]. It has been suggested that formation of a BD metabolite-cytochrome P450

complex is asssociated with decreased turnover and accumulation of distinct P450 enzymes [Cook and Hodgson, 1985; Steward *et al.*, 1985]. The barbiturates constitute the second type of P450 inducers, and primarily induce the CYP2B subfamilies and to a minor extent the CYP2A, 3A and 2C subfamilies [Waxman and Azaroff, 1992]. The exact mechanism by which the cell recognizes this group of inducers is not yet established. One has speculated that a phenobarbital-type receptor exists that eventually leads to increased transcription of the CYP2B gene and as a result increased levels of mRNA. In the presence of barbiturates a positive regulator protein is produced that displaces the repressor allowing the enhanced production of P450 mRNA [Shaw and Fulco, 1992]. Molecular shape has been suggested to be a factor in the ability of compounds to induce P450s, with globular compounds of specified molecular dimensions being better inducers of CYP2B1, and compounds with planar configurations inducing P4501A [Lewis *et al.*, 1986; Lewis *et al.*, 1987]. The ethanol inducible CYP2E subfamily is regulated by substrates such as ethanol, aceton or isoniazide, primarily through protein and mRNA stabilization. Binding of the substrate or its metabolite to CYP2E1 protects the protein from rapid degradation. Pregnenolone-16α-carbonitrile (PCN) or dexamethasone act as inducers of the glucocorticoid inducible CYP3A subfamily, predominantly due to activation of gene transcription and consequently mRNA increase [Simmons *et al.*, 1987]. Finally, the genes of the enzymes belonging to the P4504A subfamily are transcriptionally activated by a structurally diverse groups of chemicals known as the peroxisome proliferators (e.g. clofibric acid, linoleic acid). Induction has been reported to be mediated by a receptor named PPAR, peroxisome proliferator-activated receptor [Issemann and Green, 1990]. The PPARs are activated by peroxisome proliferators in a process in which the ligand-receptor complex is thought to bind to the regulatory regions of responsive genes, thereby enhancing transcription [Muerhoff *et al.*, 1992].

Crystal structures of cytochromes P450.

The mammalian cytochrome P450 enzymes are membrane-bound and as such have been resistant to crystallization and detailed structural characterization. Due to the hydrophobic character, the protein has a tendency to aggregate rather than form distinct crystals. The relationship between the amino acid sequences of P450s and their three-dimensional structures is crucial for a better understanding of their function, such as substrate selectivity, stereospecificity of hydroxylation reactions and interactions with electron-transfer partners. Until the crystal structure of a

mammalian cytochrome P450 is available, three-dimensional models of eukaryotic P450s constructed from amino acid sequence alignments with $P450_{BM3}$, $P450_{cam}$, $P450_{ery}$ and $P450_{terp}$ are helpful in identifying potential residues in cytochromes P450 that might be important in the function of these enzymes and these residues are candidates for site-directed mutagenesis [Hasemann *et al.*, 1995; Lewis, 1995; Nelson and Strobel, 1989; Ouzounis and Melvin, 1991; Zvelebil *et al.*, 1991].

The cytochromes P450 are divided into two classes based on their sequence homology and the identity of their redox-partner protein. The class I P450s comprise the soluble bacterial and membrane-bound mitochondrial P450 systems which consist of three components, namely FAD reductase, a non-heme iron-sulfur protein, putidaredoxin (bacterial) or adrenodoxin (mitochondrial), and the cytochrome P450 protein. The microsomal cytochromes P450 belong to the class II enzymes and receive their NADPH-derived electrons directly from a FAD/FMN containing reductase [Guengerich, 1993; Hasemann *et al.*, 1995; Li and Poulos, 1994].

The soluble class I cytochrome $P450_{cam}$ (product of the CYP101 gene), which catalyzes the conversion of camphor to 5-*exo*-hydroxycamphor, has served for some time as the only prototypical cytochrome P450 in providing detailed chemical, physical, and structural information in order to understand detailed structure-function relationships for the superfamily. Recently, the structure of additional class I enzymes cytochrome $P450_{terp}$ (product of the CYP108 gene) and cytochrome $P450_{eryF}$ (product of the eryF gene) as well as the first structure of a class II enzyme, the hemoprotein domain of cytochrome $P450_{BM3}$ (product of the CYP102 gene) became available [Boddupalli *et al.*, 1992; Cupp-Vickery and Poulos, 1995; Ravichandran *et al.*, 1993]. $P450_{terp}$ is a bacterial enzyme which catalyzes the oxidation of α-terpineol. $P450_{eryF}$ catalyzes the 6S-hydroxylation of the large substrate 6-deoxyerythronolide B, the initial reaction in a multistep pathway to convert 6-deoxyerythronolide B into the antibiotic, erythromycin. $P450_{BM3}$ is a flavocytochrome monooxygenase isolated from *Bacillus Megaterium* and catalyzes the hydroxylation and epoxidation of several fatty acid substrates. Although BM3 is also a soluble bacterial enzyme, it is considered to be a better prototype for microsomal P450s than the soluble $P450_{cam}$, $P450_{terp}$ and $P450_{eryF}$ as it is grouped within the class II P450s based on both sequence homology and its requirements for a FAD/FMN containing reductase domain as a source of electrons. Therefore, BM3 more closely resembles the sequence and functional properties of eukaryotic microsomal P450s. BM3 is unique among P450s in that the holoenzyme is catalytically self-sufficient, since it consists of both a FAD/FMN containing

reductase domain and a heme-containing P450 domain fused into a single 119000 dalton polypeptide.

Although the sequence identity between the (crystallized) P450s is generally low, these proteins have a similar overall topology [Cupp-Vickey and Poulos, 1995; Hasemann *et al.*, 1995]. The most highly conserved region of the P450 structure is the α-helical domain located in the protein core, namely the I and L helices and the heme binding region. The long I helix which extends across the entire molecule is a structural feature characteristic of all P450s. Much attention has been focussed on the role of the conserved threonine, a residue of the I helix, in oxygen scission during catalysis. This threonine has been proposed to act as the proton donor to bound dioxygen during the reaction cycle [Gerber and Sligar, 1992; Raag *et al.*, 1990]. However, in cytochrome $P450_{eryF}$, where an alanine is located at a position homologous to that of threonine in the other P450s, a possible participation of the substrate in a network of hydrogen bonds, providing a proton shuttle pathway to the iron linked dioxygen, has been suggested [Cupp-Vickery and Poulos, 1995]. The underlying reason for the threonine to alanine substitution in $P450_{eryF}$ might be, that its large substrate would be sterically hindered by the side-chain methyl group of a threonine residue.

The heme prosthetic group is embedded between the I and L helices of the α domain. The cysteine pocket is the most significant feature in all cytochromes P450 as it provides the axial heme ligand, a conserved cysteine residue. The residue tryptophan 96 of cyt $P450_{BM3}$ is virtually invariant in most microsomal P450s, and is thought to be involved in electron transfer from the FMN moiety of reductase to the heme [Lewis, 1995]. In $P450_{BM3}$ the active site heme is accessible through a long hydrophobic channel formed primarily by the β-domain and the B' and F helices of the α domain, lined with mostly non-aromatic hydrophobic residues. At the entrance of the substrate binding pocket an exposed hydrophobic patch is formed, that may be important for the initial docking of a lipophilic substrate, since these residues are solvent exposed, mobile and located adjacent to the binding pocket [Ravichandran *et al.*, 1993].

Substantial differences in structure are observed for the B', F and G helices, which together form the majority of the substrate-access channel, and for the regions of importance in redox partner binding. The structural differences around the substrate binding pocket could confer different substrate specificities. For instance, the extended structure of the B' helix of $P450_{terp}$ and the F-G loop of both $P450_{terp}$ and $P450_{BM3}$ provide a much more open or accessible binding pocket as that seen in

$P450_{cam}$ [Hasemann *et al.*, 1995]. Due to the large structural variation of the substrate-binding pocket of the different P450s, the possibility to predict the potential residues that determine substrate specificity of other P450s whose three-dimensional structures have not been determined, is limited. Indeed, situations are known where very small residue changes (even one residue) are known to change catalytic specificity in a remarkable way [Lindberg and Negishi, 1989].

Catalytic cycle

The cytochromes P450 possess a so-called monooxygenase activity, indicating that one oxygen atom combines with two electrons and two protons to form H_2O, whereas the other oxygen is inserted into the substrate, following the stoichiometry, where S represents the substrate;

$$NAD(P)H + H^+ + O_2 + S \text{ -----> } NAD(P)^+ + H_2O + SO.$$

The catalytic mechanism of monooxygenation can be divided in two events; oxygen activation and substrate oxidation. The most important steps of the catalytic cytochrome P450 cycle are presented in Figure 2.

The cytochrome P450 system is associated with the membrane of the smooth endoplasmatic reticulum and consists of several components which are involved in the electron transport from NADPH or NADH to the cytochrome P450 enzyme, the protein which ultimately catalyzes the final electron transfer to molecular oxygen and the insertion of an oxygen atom into the substrate. The components that take part in the electron transfer to cytochrome P450 are the flavoproteins NADPH- or NADH-cytochrome reductase (the first and second electron) and the hemoprotein cytochrome b5 (the second electron). For an optimal catalytic activity, the cytochrome P450 multi-enzyme system also requires the presence of phospholipids, important components of membranes [Lu *et al.*, 1976]. The phospholipids have been suggested to assist in complex formation between P450 and its redox partners [Strobel *et al.*, 1970]. The presence of such a hydrophobic environment has been assumed to target hydrophobic endogenous compounds or xenobiotica to these proteins, resulting in a higher effective concentration in the neighbourhood of the active site [Ebel *et al.*, 1978; Parry *et al.*, 1976].

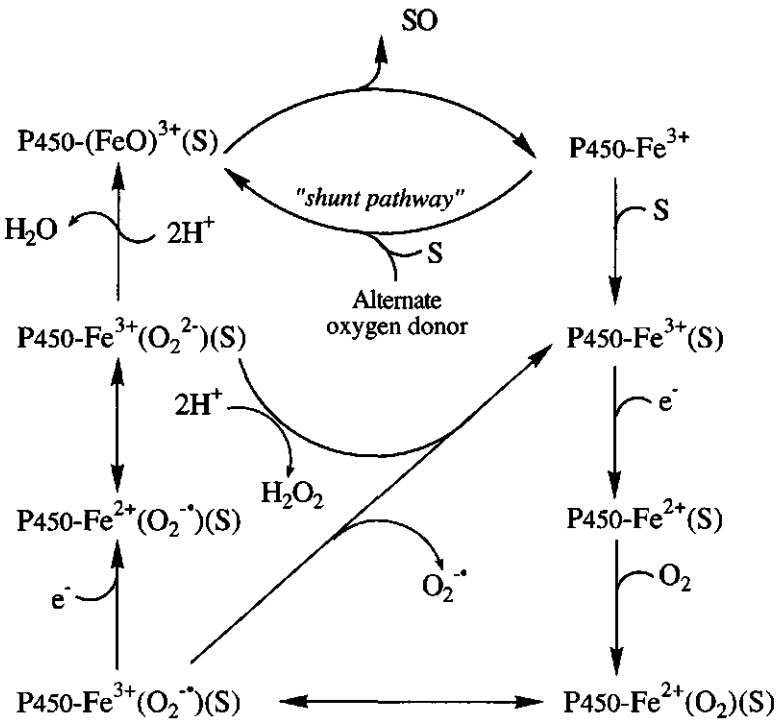

Figure 2: The reaction cycle of cytochrome P450. The heme-cofactor of cytochrome P450 at the resting state is schematically indicated as P450-Fe^{3+} and the substrate as S. Some general features on the catalytic intermediates of this enzyme are discussed in the text.

The individual steps in the P450 catalytic cycle are summarized briefly below.

P450-Fe^{3+}

The active sites of the cytochromes P450 contain an iron protoporphyrin IX acting as the cofactor in the catalysis of oxygenation of large sets of substrates. Four ligands of the heme iron are contributed by the nitrogen atoms of the porphyrin ring. The fifth, axial ligand, that is coordinated to the iron atom, is a thiolate anion provided by a cysteinyl residue of the apoprotein. The sixth ligand position of the iron is occupied by an exchangeable water molecule or an OH-containing group, provided by a tyrosine. A remarkable difference between the cytochromes P450 and other heme-containing enzymes, like peroxidases and catalase, is supposed to be the

presence of a cysteine instead of a histidine or tyrosine residue respectively as the axial ligand. This cysteine in cytochromes P450 is responsible for the characteristic absorption at 450 nm of the reduced Fe^{2+}-CO complex. Upon occupation of the sixth ligand, the iron atom is in the plane of the porphyrin ring in the hexacoordinated low spin (S=1/2) Fe^{3+} form, where the five 3d electrons of the iron are maximally paired. When the sixth ligand position is unoccupied, the iron atom is out of the plane of the porphyrin ring and in the pentacoordinated, high spin (S=5/2) Fe^{3+} form, where the five 3d electrons of the iron are maximally unpaired.

P450-Fe^{3+}·S

Substrates may interact in three ways with the active site centre of cytochromes P450. The type 1 substrates show high affinity for the high spin state and have been proposed to interact with a hydrophobic site near the heme group. Reversed type 1 substrates have a higher affinity for the low spin state. Finally, type 2 substrates such as the nitrogen containing compounds, have been assumed to occupy the sixth axial ligand position, which is reflected by a high to low spin shift.

For some P450s (e.g. $P450_{cam}$) the substrate binding, shifts the high spin-low spin equilibrium in favor of the high spin configuration and results in an increase in the redox-potential, thereby facilitating the first one-electron reduction of the enzyme-substrate complex. However, the iron spin-state of most of the mammalian P450s is not correlated with the redox-potential or a faster reduction rate [Kominami and Takemori, 1982]. Despite the lack of a correlation between the degree of shift of the spin equilibrium, the change in redox-potential and the rate of cytochrome P450 reduction [Guengerich, 1983], it is generally assumed that substrate-binding facilitates the uptake of the first electron. Besides a possible increase in the redox-potential, substrate binding to cytochrome P450 may also enhance both the rate of association and the affinity of the reductase-P450 complex and consequently the efficiency of electron flow from reductase to P450 [Backes and Eyer, 1989].

P450-Fe^{2+}·S

For the mammalian microsomal P450s, the first electron comes from NADPH, transferred by the flavoprotein NADPH-cytochrome P450 reductase via their FAD and FMN cofactors to the heme complex of cytochromes P450 converting its ferric to the ferrous state. The reductase functions as a brigde between the NADPH, a two electron donor, and cytochrome P450, an one electron acceptor, via a multistep reaction cycle proposed by Iyanagi *et al.* [1981]. Cytochromes P450 are

also known to possess reducing activity, and this may occur at this stage of the catalytic cycle. Under anaerobic conditions, certain xenobiotics such as halogenated alkanes, azo dyes, nitro compounds and quinones, may accept electrons directly from the reduced P450-Fe^{2+} complex [Goeptar *et al.*, 1995].

P450-$Fe^{2+}(O_2)$·S <-> P450-$Fe^{3+}(O_2^{-\bullet})$·S

After the one-electron reduction, dioxygen can be coordinated to the sixth position, thus forming the hexacoordinated P450-$Fe^{2+}(O_2)$·S.
Mossbauer spectroscopy on this one-electron reduced cytochrome $P450_{cam}$ substrate dioxygen complex indicated that the electron resides on the oxygen molecule instead of on the iron; P450-$Fe^{3+}(O_2^{-\bullet})$·S [Sharrock *et al.*, 1976]. At this point, a reactive superoxide anion can dissociate returning the enzyme to its Fe^{3+}·S state.

P450-$Fe^{2+}(O_2^{-\bullet})$·S <-> P450-$Fe^{3+}(O_2^{2-})$·S.

The second electron can be provided by either NADPH via NADPH-cytochrome P450 reductase as well as by NADH via NADH-cytochrome reductase and cytochrome b5. For mitochondrial and bacterial cytochrome P450 the first and second electron are both donated by the NADH-flavoprotein ferredoxin system. The transfer of a second electron and of a proton leads to a transient intermediate structure, which is assumed to be formally equivalent to a peroxide like complex, cytochrome P450-$Fe^{3+}(OOH^-)$·S, although this is yet not unambigously proven. At this stage the reactive hydrogen peroxide may be released, leading to uncoupling of the P450 catalytic cycle. The P450-$Fe^{3+}(OOH^-)$ species has been implicated in the oxidation of substrates that contain a carbonyl-group. When the carbonyl group is correctly positioned in the active site, the P450-$Fe^{3+}(OOH^-)$ is intercepted to produce a carbonyl-adduct, rather than decompose to the usual cytochrome P450 high-valent iron-oxo species (see below) [Akthar and Wright, 1991].

Cleavage of the dioxygen bond

Cytochromes P450 are capable of cleaving the dioxygen bond in two ways, namely the heterolytic or homolytic bond scission. Organic hydroperoxides and peroxyacids are frequently used to model the putative P450-$Fe^{3+}(OOH^-)$ complex formed immediately prior to dioxygen bond cleavage during the reaction cycle of this enzyme, the so-called "peroxide shunt" pathway [Mansuy *et al.*, 1989]. As shown in Figure 3, heterolytic cleavage of the dioxygen bond generates the high-valent iron-oxo porphyrin cation radical species (homologous to compound I of peroxidases),

together with a ROH molecule, while homolytic cleavage results in the formation of an iron-oxo species (homologous with compound II of peroxidases) and reactive alkoxy radicals (RO•) capable of hydrogen abstraction from the substrate.

A main function of the cysteinyl ligand is presumed to be the assistance in the heterolytic cleavage of the dioxygen bond, through electron donation. This is based for instance on the observation that the ratio of heterolysis to homolysis increases substantially, when the proximal histidinyl ligand in myoglobin is replaced by a cysteine [Adachi *et al.*, 1993]. The observed preference for heterolysis is probably due to a greater electron push provided by the cysteine thiolate relative to that of the histidine imidazole [Adachi *et al.*, 1993; Allentoff *et al.* 1992; Higuchi *et al.*, 1990]. Additionally, the cleavage-mode of the dioxygen bond has been demonstrated to depend on the polar nature of the peroxy bond [Lee and Bruice, 1985], the architecture of the P450 active site and the structural dimensions of the hydroperoxides. The latter two factors are related to the degree of water present in the active site, which assists in the highly regulated delivery of protons into the active site by way of a hydrogen-bonding network [Correia *et al.*, 1995].

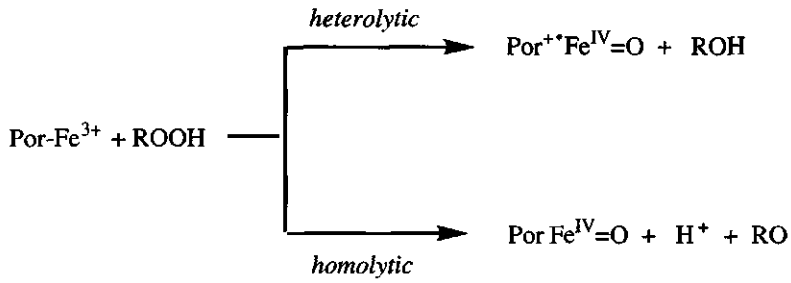

Figure 3: Hetero- versus homolytic dioxygen bond scission in cytochrome P450. The porphyrin of P450 is schematically represented as "Por".

P450 (FeO)$^{3+}$ S.

Upon heterolytic cleavage of the dioxygen bond, the so-called cytochrome P450 high-valent iron-oxo porphyrin cation radical complex is formed [Larroque *et al.* 1990]. The porphyrin radical cation thus produced is stabilized by resonance over the extensive network of conjugated double bonds of the porphyrin. Knowledge on the exact nature of the active species is based on indirect evidence obtained from studies on other hemo-proteins (peroxidases) and iron-porphyrin model systems [Mansuy, 1987; Mansuy *et al.*, 1989]. The active species, for convenience

represented as $(FeO)^{3+}$, is generally assumed to be the enzyme form catalyzing the oxidation and oxygenation reactions. Since most cytochrome P450 mediated reactions are proposed to be one electron-step processes, the ultimate oxidant is also often represented as $Fe^{IV}(O\cdot)$ to present its radical character (see Figure 4) [Akhtar and Wright, 1991]. Artificial oxygen donors, such as organic peroxides, iodosobenzene or $NaIO_4$, are frequently used in mechanistic and biotransformation studies and may substitute molecular oxygen and reducing equivalents to produce the formal $(FeO)^{3+}$ intermediate in what is termed "the shunt pathway" [Hrycay *et al.*, 1976; Ortiz de Montellano, 1985; White and Coon, 1980]. Subsequent insertion of one atom of oxygen into the substrate and subsequent product release restores cytochrome P450-Fe^{3+}, the resting state of the enzyme. Some generally accepted mechanisms and hypotheses for the cytochrome P450 $(FeO)^{3+}$ catalyzed substrate conversion are presented hereafter.

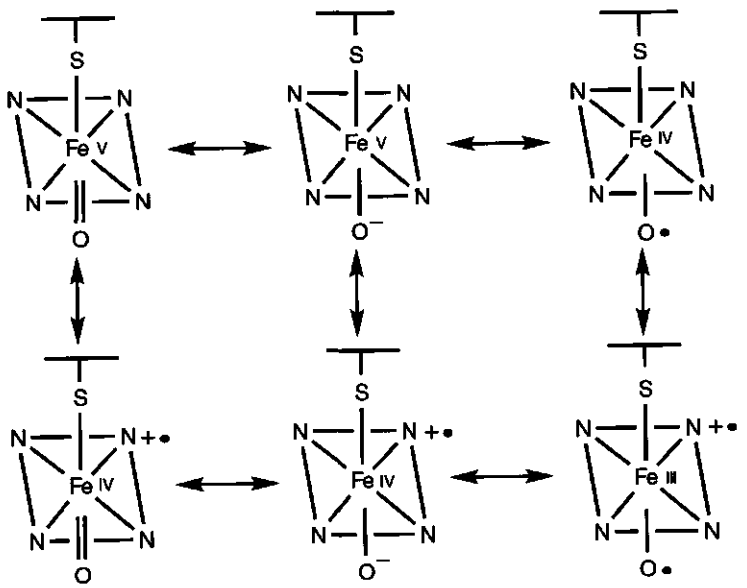

Figure 4: Different proposed resonance structures of the reactive high valent iron-oxo intermediate of cytochrome P450 catalyzing the substrate conversion [Akhtar and Wright, 1991; Ortiz de Montellano, 1986].

Rate of catalysis

The overall rate is a complex product of subsequent steps. The rate-determining step in the overall cytochrome P450 catalytic sequence, varies depending on the particular P450 protein under consideration, the substrate and the reaction mechanism. Within the P450 cycle, the electron reduction steps, the actual interaction of the $(FeO)^{3+}$ with the oxidizable substrate, or product release can be rate-limiting. Electron transfer is essential for the turnover of the P450 enzymes and is often the rate-limiting step. Oxidation rates are often found to be much higher when the rate-limiting electron donation steps are circumvented by the use of artificial oxygen donors [Macdonald *et al.*, 1989]. In electron abstracting catalysis, the rate of electron abstraction is considered to be dependent on the oxidation-reduction potential $E_{1/2}$ of the $(FeO)^{3+}$ intermediate of the cytochrome P-450 enzyme, but also on the inter-radial distance between the reaction centres, the dielectric constant in that region and the oxidation potential of the substrate [Guengerich, 1990; MacDonald *et al.*, 1989].

Chemical mechanisms of oxidative and reductive cytochrome P450 mediated conversion of substituted aromatics.

The reactions catalyzed by cytochrome P450 include carbon hydroxylation of aliphatic and π-bonded systems, epoxidations, heteroatom oxygenations, heteroatom release, oxidative dehalogenation, deamination, azo-reduction, nitro reduction, reductive dehalogenation, oxidative desulfation and cleavage of C-C, C-N, C=S bonds. The unique characteristic of P450 enzymes to catalyze the conversion of a large set of compounds by different types of reactions orginates from the fact that the mechanisms of P450 mediated catalysis may be understood in terms of a few basic principles [Guengerich 1990, Guengerich and MacDonald, 1990]. There is a generally accepted view that the fundamental chemical steps used with the different P450 enzymes and reactions are rather constant [Guengerich, 1995]. Concerning the oxidation reactions, the basis of this view lies in the ability of the high-valent iron-oxo intermediate of P450 to perform one-electron oxidation through the abstraction of hydrogen atoms or electrons (non-bonded or π electrons) or to perform radical addition to π-bonds. These initial steps are followed by an oxygen rebound or by radical recombination reactions to complete the oxidation process and to yield the product [Guengerich *et al.*, 1995; Guengerich and MacDonald, 1990; Mansuy *et al.*, 1989].

Only the basic molecular mechanisms of the types of metabolic transformations that are within the scope of this thesis (aliphatic and aromatic hydroxylation, epoxidation, heteroatom oxidation, oxidative dehalogenation and nitroreduction) will be considered here in more detail.

Aliphatic hydroxylation.

It is now widely accepted that during the cytochrome P450-catalyzed hydroxylation of alkanes, the high-valent iron-oxo species abstracts a hydrogen atom from the substrate to generate an intermediate carbon-centered substrate radical. This intermediate radical then collapses with an iron-bound hydroxyl radical to form an alcohol in a process termed oxygen rebound (see Figure 5) [Atkinson *et al.*, 1993 & 1994, Guengerich and MacDonald, 1984 & 1990; Mansuy *et al.* 1989]. Computational models are developed for the cytochrome P450 hydrogen abstraction reactions [Korzekwa *et al.*, 1990; Yin *et al.*, 1995]. Results with for example cyclopropanes that undergo radical rearrangements (radical clocks) implicate radical intermediates with rates of oxygen rebound in the order of $> 10^{11}$ s^{-1}. Since the oxygen rebound step is very fast, the intermediate free radical has no chance to escape fom the active site [Atkinson *et al.*, 1994, Atkinson and Ingold, 1993].

$$(FeO)^{3+} + H\text{-}CR_3 \xrightarrow[H\bullet\ \text{abstraction}]{} (FeOH)^{3+} + \bullet CR_3 \xrightarrow[\bullet OH\ \text{rebound}]{} Fe^{3+} + HO\text{-}CR_3$$

Figure 5: Generally accepted mechanism for the cytochrome P450 mediated aliphatic hydroxylation.

Hydroxylation of an α-carbon atom substituted on a nitrogen (α-carbon hydroxylation) by a similar oxygen rebound mechanism has been implicated as precursor steps in N-dealkylation reactions [Guengerich *et al.*, 1995]. Hydrogen atom abstraction or more likely electron abstraction followed by the participitation of the cytochrome P450 $(FeO)^{2+}$ entitity in base-catalyzed deprotononation of the α-proton followed by an oxygen rebound step, has been proposed as the mechanism for formation of the instable carbinol amine, which finally decomposes into a dealkylated product and aldehyde (see Figure 6) [Macdonald *et al.*, 1989].

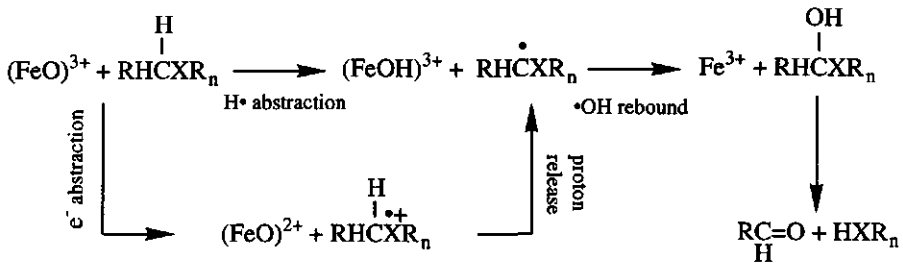

Figure 6: Proposed mechanism for heteroatom dealkylation (X represents O, N or S).

Aromatic hydroxylation and epoxidation.

The mechanism of oxidation of double bonds of alkenes or of aromatic rings by the high valent iron-oxo species of cytochrome P450 has been studied extensively and involves intermediate free radicals or cations formed by interaction of the $(FeO)^{3+}$ species with the π-type electrons (abstraction or addition). The intermediate substrate radicals or adducts undergo intramolecular reactions resulting in formation of epoxides, keto-products or phenols.

Alkenes undergo monooxygenation primarily to yield epoxides, although a series of products derived from 1,2-migration or porphyrin N-alkylation, the latter leading to inactivation of the heme-based catalyst, are also observed [Guengerich and MacDonald, 1990; Mansuy *et al.*, 1989; Ortiz de Montellano *et al.*, 1982].

The most likely pathways proposed for epoxidation and aromatic hydroxylation are schematically outlined in Figure 7 and 8. These mechanisms represent either a direct addition of the $(FeO)^{3+}$ intermediate to the π-system of the aromatic ring or alkene, leading to formation of a so-called "radical σ-adduct" or, an initial one electron abstraction from the substrate by the $(FeO)^{3+}$ intermediate followed by addition of the $(FeO)^{2+}$ entity to the substrate cation radical, resulting in a so-called "cation σ-adduct". The radical or cation σ-adduct subsequently may rearrange to their hydroxylated metabolite directly or via formation of a keto or an epoxide product [Burka *et al.*, 1983; Guengerich and Macdonald, 1990; Korzekwa *et al.*, 1989]. Experimental as well as theoretical studies on aromatic hydroxylation (i.e.

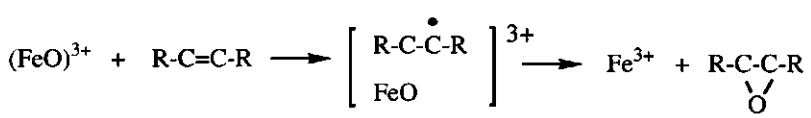

Figure 7: Generally accepted mechanism for the alkene epoxidation by cytochome P450.

σ-addition pathway:

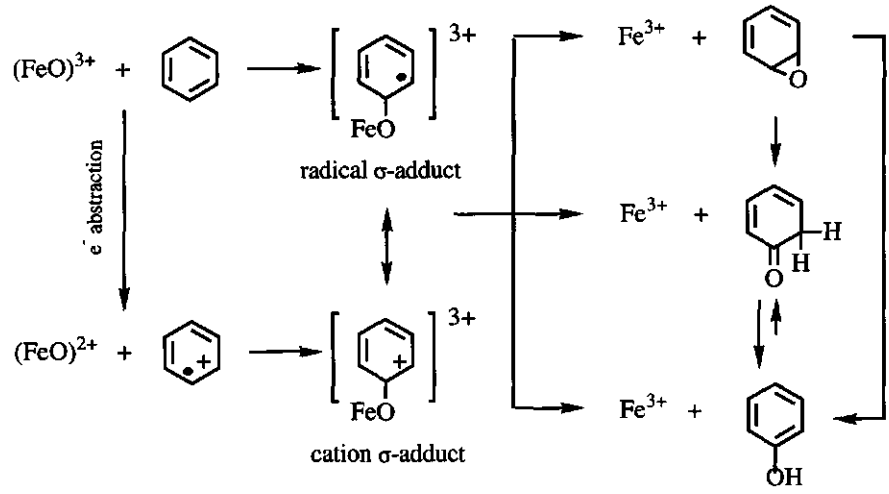

proton abstraction pathway (X = O, N, S):

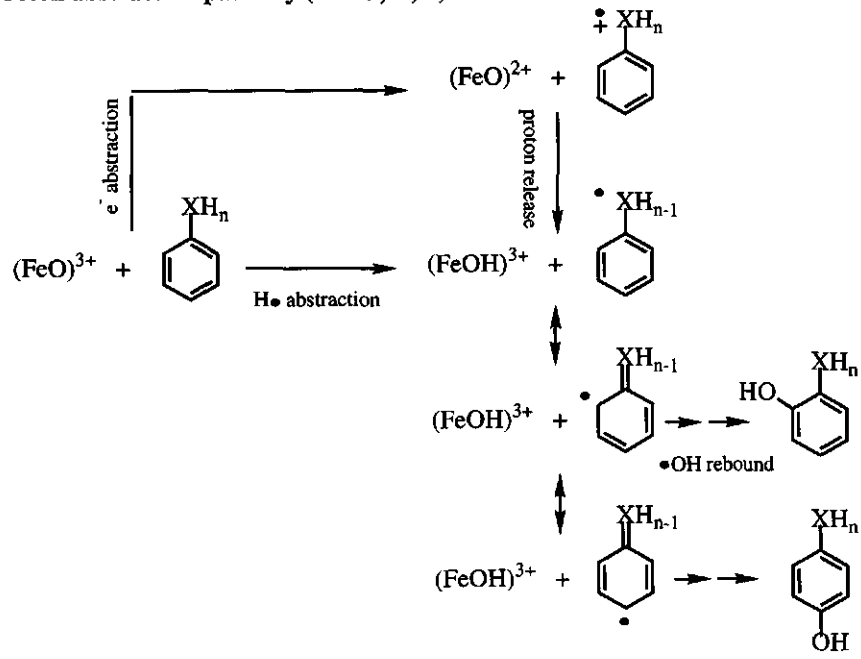

Figure 8: Hypotheses for the cytochrome P450 catalyzed aromatic hydroxylation [e.g. Armstrong, 1987; Guengerich and MacDonald, 1990].

phenol formation) indicate that an initial electrophilic attack of the $(FeO)^{3+}$ species on the substrate -without formation of epoxides as the precursor- is the preferred mechanism [Guengerich and Macdonald, 1990; Korzekwa *et al.*, 1989; Rietjens *et al.*, 1995; Riley and Hanzlik, 1994]. The results of Korzekwa suggest that the extent of charge transfer and spin density on the substrate resulting in either a radical or cation σ-adduct intermediate species may be substituent dependent, with electron donating groups favoring the cation species. It has been proposed that the "radical σ-adduct" favors epoxide formation, whereas the "cation σ-adduct" favors direct phenol or ketone formation. [Korzekwa *et al.*, 1985]. The aromatic epoxides instead of giving rise to phenolic metabolites may rather result in formation of rather catechol metabolites, upon epoxide hydrolase catalyzed conjugation with water, followed by aromatization, or of glutathione conjugation derived metabolites [Rietjens *et al.*, 1993].

Aromatic hydroxylation of substrates containing heteroatoms with a relatively low oxidation potential (N, S, P, O) have been proposed to proceed by either hydrogen atom abstraction, or electron abstraction and proton release from the heteroatoms, followed by rearrangement of the radicals and oxygen rebound to form the product [Armstrong, 1987]. For *p*-substituted anisoles the cytochrome P450 oxidative metabolism -also aromatic hydroxylation- could be predicted qualitatively on the basis of spin distributions, energy differences between substrates, metabolic intermediates and products taken only hydrogen abstraction mechanisms into account [Groot *et al.*, 1995, Koymans *et al.*, 1993]. However, a direct addition of a cytochrome P450 $(FeO)^{3+}$ intermediate to a π-bond or to a lone pair [*e.g.* Riley and Hanzlik, 1994] as hypothetical mechanism for aromatic hydroxylation was not taken into account in those studies. Recently, a mechanistic study on the oxidative metabolism of [3,5-$^2H_2$]-4-iodoanisole, explained aromatic hydroxylation via direct aromatic hydroxylation. The formation of 2-hydroxy-4-iodoanisole was proposed to occur almost entirely by direct aromatic hydroxylation with no epoxide or cyclohexadienone as the intermediates, whereas the 3-hydroxylation could proceed via direct aromatic hydroxylation or formation of cyclohexadienone intermediates, without epoxide intermediates [Rizk and Hanzlik, 1995]. The hypothesis that 3-hydroxylation occurs without epoxide formation, is in accordance with the observation that the 2,3- or 3,4-chlorobenzene epoxides rearrange to respectively 2- and 4-chlorophenol, without formation of 3-chlorophenol [Selander *et al.*, 1975]. To suggest a completely different mechanism for OH incorporation at different sites in one molecule seems unlikely.

N-oxygenation.

N-oxygenation is a process that is mechanistically related to, α-carbon hydroxylation and subsequent N-dealkylation (see above) (Figure 9). Understanding the processes of the partitioning between N-dealkylation and N-oxygenation is important, because in some cases the two pathways can lead to quite different products. In N-oxygenation oxidation occurs at the nitrogen, whereas in N-dealkylation the oxygen is transferred to the carbon adjacent to the heteroatom. It has been proposed that N-oxygenation/N-dealkylation proceeds via an initial one-electron oxidation at the nitrogen by the high-valent iron-oxo intermediate of cytochrome P450. Support for an one-electron oxidation pathway for N-oxygenation and N-dealkylation was provided by several lines of evidence: cycloalkylamines undergo rearrangements characteristic of one-electron transfer processes [Bondon *et al.*, 1989; Hanzlik and Tullman, 1982; Macdonald *et al.*, 1982], the rate of the cytochrome P450 mediated dimethylaniline oxidation was found to correlate with the substrate oxidation-reduction potential [Macdonald *et al.*, 1989], low isotope effects were observed for N-dealkylation reactions [Guengerich *et al.*, 1995] and the formation of alkyl radicals was reported upon oxidation of 1,4-dihydro-4-alkylpyridines [Augusto *et al.*, 1982; Lee *et al.*, 1988]. The partitioning of the resulting putative aminium radicals between radical recombination and α-deprotonation (i.e. between N-oxygenation and N-dealkylation) is influenced by the ease of deprotonation and aminium radical stability. N-oxygenation of amines does not occur unless 1) no α-

heteroatom oxygenation

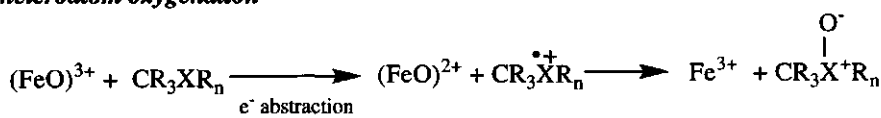

N-hydroxylation

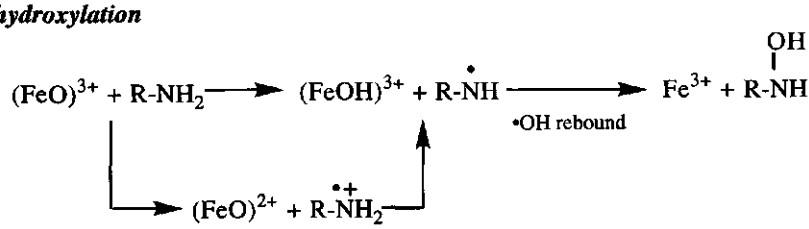

Figure 9: Proposed general mechanisms for the cytochrome P450-catalyzed N-dealkylation and N-hydroxylation.

protons are available as is the case for the primary arylamines (see Figure 9), 2) α-protons are inaccesible due to Bredt's rule as is the case for quinidine (Bredt's rule prevents abstraction of α proton at the individual bridgehead nitrogen for steric reasons) [Guengerich *et al.*, 1986] or 3) radical stability is provided by neighbouring electron donating groups [Guengerich, 1990].
Finally, for heteroatoms with a relatively high ionization potential, a hydrogen abstraction pathway, instead of a single electron transfer pathway with subsequent proton release, may be preferred [Armstrong, 1987; Guengerich and Macdonald, 1984].

Oxidative dehalogenation.

Cytochromes P450 catalyze reductive as well as oxidative dehalogenation of halogenated and aliphatic compounds, and the respective reactions are modulated by oxygen tension but also the chemical nature of the substrate [Lefever and Wackett, 1994]. Here, attention is focussed on the mechanisms with respect to the oxidative dehalogenation of aromatic compounds.

Cytochrome P450-mediated oxidative dehalogenation of aromatic compounds to phenolic derivatives has been observed for fluorinated [Daly *et al.*, 1968; Den Besten *et al.*, 1993; Li *et al.* 1985, Rietjens *et al.*, 1992], chlorinated [Daly *et al.*, 1968], brominated [Zheng and Hanzlik, 1992] and recently iodinated [Rizk and Hanzlik, 1995] compounds. Several pathways are thought to be involved in the oxidative dehalogenation of aromatics. For 4-fluorinated phenols and anilines as well as pentafluorochlorobenzene, elimination of the fluoride as an anion results in formation of respectively benzoquinone(imine) and a benzohaloquinone cation as the primary reaction products, which can be reduced subsequently to give the phenolic derivative [Den Besten *et al.*, 1993; Rietjens and Vervoort; 1991; Rietjens *et al.*, 1992]. The P450-catalyzed deiodination of 4-iodoanisole to 4-methoxyphenol is suggested to involve C-O bond formation via direct attack of the $(FeO)^{3+}$ intermediate on the aromatic ring followed by reductive cleavage of the C-iodine bond, with electrons coming from P450 reductase. The observation that no ^{18}O from $H_2{}^{18}O$ is incorporated into 4-methoxyphenol indicates that the phenolic oxygen originates from molecular oxygen via the cytochrome $(FeO)^{3+}$ species [Rizk and Hanzlik, 1995].

Noteworthy, it has been proposed that halogenated aromatics may also be metabolized by direct oxidation of the halogen on the aromatic ring to an intermediate that produces the phenolic derivative and eliminates the halogen as

(HXO) [Macdonald, 1983; Rietjens *et al.*, 1992; Van Ommen and Van Bladeren P.J., 1989]. This hypothetical mechanism was based on the observation that cytochrome P450 oxidizes iodobenzene to iodosobenzene [Burka *et al.*, 1980]. Later, Guengerich demonstrated that except iodine, also bromine substituents can be oxidized by using the 4-*tert*-butyl-2,5-bis[1-hydroxy-1-(trifluoromethyl)-2,2,2-trifluoroethyl] halobenzenes of which the oxidized reaction products are relatively stable [Guengerich, 1989]. In terms of understanding mechanisms of P450 catalysis this type of reaction is interesting, however the physiological importance remains to be established yet.

Finally, during the cytochrome P450-mediated monooxygenation a halogen can be lost from its position via an intramolecular migration to the carbon position adjacent to the hydroxylated position. This phenomenon, the so-called "NIH shift" (named after the National Institute of Health), has been reported especially for chloro- and bromo-substituents [Daly *et al.*, 1972].

Nitroreduction

Cytochromes P450 are also able to catalyze the reductions of some particular substrates (e.g. nitrocompounds, CCl_4), especially under low dioxygen pressure or under anaerobic conditions. The reduction of nitro moieties is a well known metabolic reaction that frequently leads to bioactivation. Besides cytochromes P450, several other enzymes such as NADPH-cytochrome c reductase, DT-diaphorase, aldehyde oxidase, bacterial nitroreductases in the intestinal tract of mammalians and xanthine oxidase have been shown to possess significant nitro reductase activity for various type of nitro compounds [Harada and Omura, 1980; Levin and Dent, 1982; Suzuki *et al.*, 1989; Tatsumi *et al.*, 1978].

The cytochrome P-450 catalyzed reduction of the nitro moiety to the amino analogue in a six electron pathway is proposed to proceed by the transfer of electrons

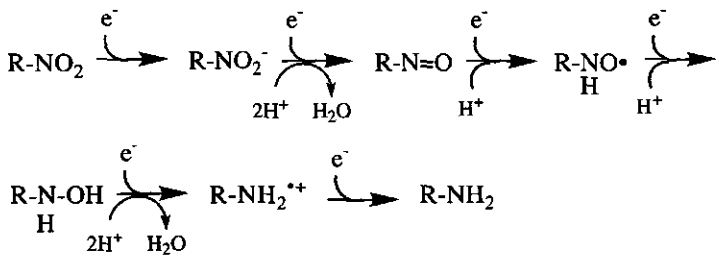

Figure 10: Proposed mechanism for nitro reduction [Goeptar *et al.*, 1995].

from the ferrous cytochrome P450 to the substrate (see Figure 10) [Harada and Omura, 1980]. Electron spin resonance studies demonstrated that the nitro group is reduced in a one electron reaction to yield a nitro anion radical [Mason and Holtzman, 1975; Sealy *et al.*, 1978]. Under aerobic conditions these radicals react with oxygen to form superoxide radical anions and H_2O_2 which cause an oxidative stress type of cytotoxicity [O'Brien *et al.*, 1990]. Upon the addition of a second electron and two protons the nitroso intermediate is formed as the intermediate [Levin and Dent, 1982]. Subsequent reduction of the nitroso compound results in the formation of a hydronitroxide free radical, which in turn is reduced to the hydroxylamine [Goeptar *et al.*, 1995]. Finally, the phenylhydroxylamine is reduced to the aniline analogue [Suzuki et al., 1989].

Regioselective metabolism in cytochrome P450 catalyzed reactions.

The regioselective metabolism of xenobiotics by the cytochromes P450 is a consequence of the topographical features of the apoproteins around the active sites in combination with chemical characteristics of the substrates itself [Korzekwa and Jones, 1993; White *et al.*, 1984]. Small substrates have the potential for high active site mobility [Koerts *et al.*, 1995; Raag and Poulos, 1992]. Substrates that can rotate more freely in the active site may be expected to have greater variations in binding orientations and therefore greater differences in stereoselectivities [Jones *et al.*, 1995]. If cytochrome P450 has no steric or binding requirements for its substrate, a model based only on the electronic characteristics of oxidant and substrate would be sufficient [Korzekwa and Jones, 1993; Oguri *et al.*, 1994; Rietjens *et al.*, 1993]. However, for substrates of large size and structural rigidity, like benzo[*a*]pyrene, or substrates which interact with specific amino acid residues in the active site, like debrisoquine in P450 2D6 or camphor in P450cam, severe constraints against mobility exist once they are bound to the active site. Because of a lack of detailed structures of the mammalian P450 enzymes, alternatives are developed to probe the active site topology of P450 enzymes, in order to obtain insight into factors that determine substrate selectivity and regioselective metabolism.

Lewis studied the active sites of P450 by detailed knowlegde on the substrate characteristics like molecular dimensions, the presence of certain structural features and electronic properties [Lewis *et al.*, 1987]. Inspection of the molecular structures of cytochrome P450 1A-specific compounds revealed that they are all rigid, planar molecules due to the presence of a number of fused aromatic rings, characterized by a small depth and a large area-to-depth ratio. The majority of cytochromes P450 2B

substrates have structures containing at least one non-fused aromatic ring and a overall non-planar geometry, often adopting a V-shaped conformation and are characterized by a small area-to-depth ratio. A common structural feature of the cytochrome P450 2E substrates is that they are relatively small-sized molecules, whereas the cytochrome P450 3A substrates are large-sized molecules [Lewis *et al.*, 1987; Lewis *et al.*, 1994]. Recently, it was demonstrated by ^{1}H-NMR that more than one aromatic base substrate molecule can enter the active site of cytochrome P450cam and bind both in the hydrophobic cavity and at the heme metal [Banci *et al.*, 1994]. To understand the factors that determine the substrate specificity of cytochromes P450, De Voss and Ortiz de Montellano succesfully used a docking program to predict, whether compounds entirely unrelated to camphor are substrates for cytochrome P450cam, a protein that normally uses camphor as the substrate and for which a crystal structure is available [De Voss and Ortiz de Montellano, 1995]. Another experimental approach for probing the active site of P450s is based on prosthetic heme alkylation reactions. This proceeds by a reaction of cytochromes P450 with aryl moieties to give an iron-phenyl complex that oxidatively rearranges to N-phenylprotoporphyrin IX regioisomers with the phenyl group on the pyrrole rings A, B, C and/or D. The four pyrroles are not equivalent in their capacity to accept the phenyl radical, because of differences in steric hindrance of each pyrrole ring by amino acids of the P450 peptide in the vicinity of the oxygen binding site. Using aryl moieties of diverse structures provides information on the openess above the pyrrole rings. The regiochemistry of the iron nitrogen adducts demonstrated that the active sites of 1A1, 2B1, 2B2 and 2E1 have similar structural motifs, with pyrrole rings B and C at least partially masked by protein residues and a more open region above rings A and D [Ortiz de Montellano, 1987; Swanson *et al.* 1991; Tuck and Ortiz de Montellano, 1992; Mackman *et al.*, 1996].

Besides models that provide information on the three-dimensional structure of the active site, also models that explain regioselective metabolism were proposed. Based upon the regiospecificity of the cytochrome P4501A1 catalyzed biotransformation of benzo[*a*]pyrene and its di-hydrodiol derivatives Jerina proposed that the catalytic site of this P450 has a space for substrate binding of a size equivalent to nine benzene rings. Upon superposition of a polycyclic aromatic compound on the nine benzene ring model, the regioselectivity and stereoselectivity of the P450 1A1 mediated metabolisme could be predicted [Jerina *et al.*, 1982]. Recently, it has been demonstrated that seven human, five rodent and two bacterial P450s were all able to convert benzo[*a*]pyrene to the 7(R),8(R)-diol and the

9(R),10(R)-diol with an extremely high degree of stereoselectivity, which is likely due to the large size of the substrate molecule and its constraints in the active site [Jones *et al.*, 1995]. For smaller molecules, however, it was proposed that more orientations in the active site are possible. NMR relaxation studies were used to investigate the preferred orientation in the binding of acetaminophen to P450 1A1 and 2B1 isoforms. Using ^{15}N and ^{13}C NMR T_1 relaxation rate measurements, it was suggested that P450 1A1 produces the N-acetyl-p-benzoquinoneimine preferentially, because of closer proximity of the heme iron to the amide nitrogen, whereas P450 2B1 produces 3-hydroxyacetaminophen preferentially because of closer proximity of the heme iron to the phenolic oxygen [Myers *et al.*, 1994]. Remarkably however, using ^{1}H NMR T_1 relaxation rate measurements, the nitrogen of the acetamido group was reported to be closer to the heme iron in P450 2B1, than in P4501A1 [Van de Straat *et al.*, 1987].

X-ray crystal structures and site-directed mutagenesis of P450cam gave valuable information on the substrate-P450 interactions. The camphor is bound through its carbonyl group via a hydrogen bridge to Tyr 96 so that oxygen insertion can occur at C5. However, the absolute regiospecificity of camphor hydroxylation is lost when camphor is metabolized by the Tyr96Phe mutant enzyme which is unable to form a hydrogen bond with the substrate. The five different products observed, when camphor is hydroxylated by the Tyr96Phe mutant enzyme suggests that camphor itself can bind in multiple orientations when it is not anchored through a hydrogen bond [Raag and Poulos, 1992]. X-ray crystal structures have been determined for complexes of cytochrome P450cam with the substrates camphane, adamantane and thiocamphor. Unlike the natural substrate camphor, which hydrogen bonds to Tyr 96 and is metabolized to a single product, camphane, admantane and thiocamphor do not form a hydrogen bond with the enzyme and all are hydroxylated at multiple positions. Again it was concluded that the lack of a substrate-enzyme hydrogen bond allows substrates greater mobility in the active site explaining this lower regiospecificity of metabolism [Raag and Poulos, 1991].

Current advances in computational chemistry allow the modelling of the more relevant cytochrome P450 $(FeO)^{3+}$ intermediate. Molecular dynamic studies on the orientation of thiocamphor in the active site of P450cam indicated, that the orientation in the active site is different in the presence of the reactive high-valent iron-oxo species, than in the absence of that oxygen and in addition is more consistent with the formation of the 5-alcohol as being the major product [Paulsen and Ornstein, 1993]. Moreover, on the basis of molecular dynamic simulations with

inclusion of all atoms within a 16Å "belly" region surrounding the reactive iron-oxo species of P450cam, the predicted regioselectivities of the hydroxylation of d-camphor, d-camphane, d-thiocamphor [Harris and Loew, 1995] and the stereochemistry of the styrene and β-methylstryrene epoxides formed by P450cam [Fruetel *et al.*, 1992] were in excellent agreement with experimental results.

In conclusion, more knowledge on the active site structure of the different P450 enzymes in the reactive $(FeO)^{3+}$ state, specific interactions of substrates with amino-acid residues or the heme in the active site, insight into molecular reaction mechanisms and chemical substrate characteristics that determine the reaction chemistry, may eventually lead to a good prediction of substrate specificity and stereoselective metabolism of xenobiotics.

2.1.2. Flavin-containing monooxygenase.

The flavin-containing monooxygenases (FMO) are a family of enzymes that metabolize a variety of structurally diverse pesticides, therapeutic agents and other xenobiotics. The mammalian FMO enzymes are catalogued into five different groups FMO1, FMO2, FMO3, FMO4 and FMO5 on the basis of their amino acid sequence identities [Lawton, 1994]. The expression of the FMOs is regulated by hormonal and dietary factors, but the effects on induction appear to be species- and tissue dependent [Cashman, 1995].

These endoplasmatic reticulum-bound flavoproteins utilize NADPH and molecular oxygen to catalyze the monooxygenation of nucleophilic heteroatoms like nitrogen, sulphur, phosphorous [Ziegler, 1980; Ziegler 1988; Cashman, 1995], but also the selenium atom [Ziegler, 1992]. FMOs are able to N-oxidize virtually all lipophilic secondary and tertiary amines. Remarkably, FMOs also tend to hydroxylate aromatic carbon atoms which are located *ortho* or *para* to an hydroxyl or amine moiety, such as the 2-hydroxylation of 1-naphtylamine, the 1-hydroxylation of 2-naphtylamine and the 4-hydroxylation of 4-fluoro-N-methylaniline, probably via rearrangement of N-hydroxy-metabolites [Boersma *et al.*, 1993; Hammonds *et al.*, 1985].

The physiological function of the FMOs remains undefined, although some potential endogenous substrates have been identified. In human, substantial evidence has been obtained indicating that FMO serves an important role in the detoxication of the vast majority of naturally occurring alkaloids and medicinal tertairy amines to

polar, readily excretable and pharmacologically less toxic derivatives. Thus, a deficiency in the FMO-mediated oxygenation may limit detoxification processes. For example deficiency in N-oxygenation of trimethylamine (derived from choline), a reaction catalyzed by FMO, leads to the "fish odor" syndrom and psychosocial reactions including low self-esteem, clinical depression, paranoia and addiction to drugs [Ayesh, 1993].

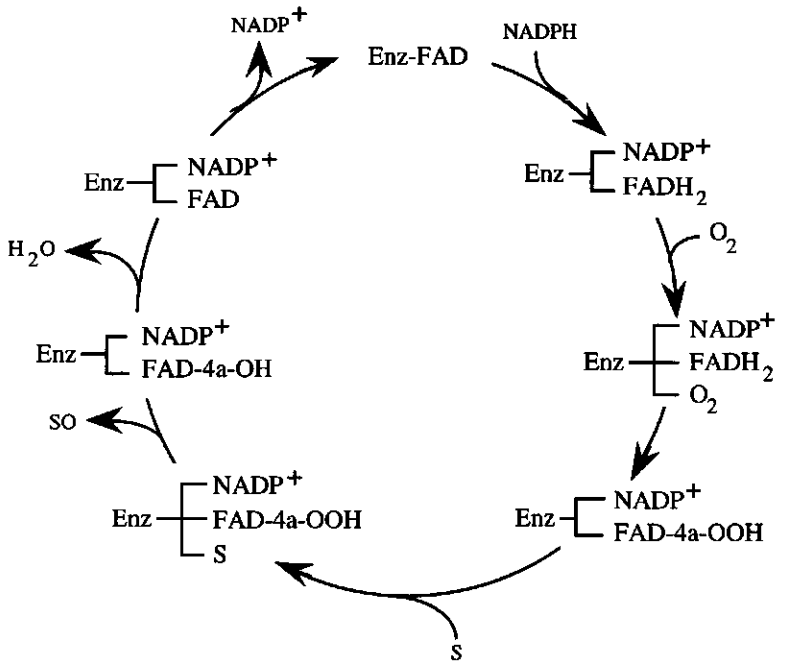

Figure 11: Schematic presentation of the catalytic cycle of FMO. S and S-O are the substrate and oxygenated substrate, respectively [Poulsen and Ziegler, 1995].

Occasionally, FMO promotes the formation of toxic metabolites as seems to be the case with for example the tertairy amine verapamil. Verapamil N-oxide, which is efficiently formed by FMO, is unstable and undergoes decomposition to a hydroxylamine and 3,4-dimethoxystyrene. These unanticipated metabolites may contribute to the cardiotoxicity observed with verapamil [Cashman, 1995].

The catalytic mechanism is fairly well accepted for FMO1 from hog liver. It

is assumed that the major steps of the catalytic cycle are essentially the same for the other FMO subfamilies. The major steps in the FMO1 catalytic cycle are summarized in Figure 11. The fully oxidized flavoprotein is reduced by NADPH to the dihydroflavin which generates the so-called C(4a)-hydroperoxyflavin intermediate in a reaction with molecular oxygen. FMO is known to catalyze the oxygenation of the substrate by means of this remarkably long-lived intermediate. Upon addition of the xenobiotic substrate, the hydroperoxyflavin reacts with the substrate to form product and C(4a)-hydroxyflavin. Thus, the preloaded FMO active site oxidant waits in a ready position to oxygenate substrate, which contrasts the cytochromes P450 that only forms the high-valent iron-oxo species after the substrate binds to the enzyme. The reaction cycle is completed by dehydration of the resulting C(4a)-hydroxyflavin and release of $NADP^+$ from the enzyme [Poulsen and Ziegler, 1995; Cashman, 1995; Guengerich, 1990].

2.2. Phase 2 biotransformation enzymes.

2.2.1. Glutathione S-transferases.

Structure, function and catalysis.

The glutathione S-transferases are a ubiquitous group of enzymes that catalyze the addition of the tripeptide glutathione (γ-L-Glu-L-CysGly) to a variety of endogenous and xenobiotic compounds containing electrophilic functional groups. This reaction is the first step in mercapturic acid pathway. Glutathione is the most prominent low molecular weight thiol present in cells, and competes with nucleophilic entities in cellular macromolecules for reaction with electrophiles. Although microsomal forms of glutathione S-transferase have been detected [Morgenstein *et al.*, 1988], glutathione S-transferase activity is mainly located in the cytosol. Physiological substrates of glutathione S-transferases are phospholipid hydroperoxides, α,β-unsaturated carbonyl-compounds, fatty acid epoxides and DNA-hydroperoxides. Most glutathione S-transferases exhibit very broad substrate specificity and catalyze a variety of reaction types, including epoxide ring openings, nucleophilic aromatic substitution reactions and Michael additions [Armstrong, 1987; Ji *et al.*, 1993; Robertson and Jernstrom, 1986]. Recently, it became evident that glutathione S-transferases also catalyze the retro-Michael reaction of GSH conjugates of α,β-unsaturated carbonyl compounds [Chen and Armstrong, 1995]. Their ability to

initiate the metabolism of a broad range of alkylating agents suggests that this family of proteins plays a central role in the detoxication of many carcinogens as well as anticancer chemotherapeutic agents.

The cytosolic glutathione S-transferases found in mammalian species appear to be a supergene family of isoenzymes and are organized into four principle gene classes designated alpha, mu, pi and the newly discovered theta [Pemble *et al.*, 1994]. Two allelic glutathione S-transferase polymorphisms in humans are known, *GSTM1* and *GSTT1*. Both are characterized by gene deletions in >1/3 of the population [Nelson *et al.* 1995; Pemble *et al.*, 1994; Smith *et al.*, 1994]. Some epidemiological studies suggest a link to smoking induced lung cancer with the absence of M1 [Nazar-Stewart *et al.*, 1993; Zhong *et al.*, 1991], the relevance of T1 is not clearly understood yet. Glutathione S-transferases exist as dimeric proteins comprised of two subunits. Both homo- and heterodimeric proteins are found within a gene class, and each monomer has a kinetically independent active site. Inter-gene class heterodimers are not known.

The active site of the glutathione S-transferases is organized into two structural domains with distinct functional roles, a glutathione binding domain (domain I or classically G-site) at the N-terminus and a hydrophobic xenobiotic substrate binding domain (domain II or classically H-site) at the C-terminus. Comparison of the crystal structures of the alpha, mu and pi glutathione S-transferases revealed an overall similarity in the glutathione-binding domain I, while most of the sequence variation presumably associated with the different catalytic properties of the isoenzymes is located in domain II, the xenobiotic binding site [Ji *et al.*, 1992]. Crystal structure analysis revealed that the active site of the pi and mu enzymes is larger and more open to the solvent as compared to the alpha class glutathione S-transferases, since the extended C-terminus -which forms an extra α-helix- blocks one entrance to the active site and makes up part of the substrate binding site [Sinning *et al.*, 1993]. Specific amino acid residues as well as structural elements have been demonstrated to be directly involved in defining the catalytic characteristics of the glutathione S-transferases. Fifteen hydrogen bond or salt bridge contacts are involved in the interaction between glutathione and the enzyme, among which the hydrogen bond between the sulfur of GSH and the side-chain hydroxyl group of the strictly conserved tyrosine 6 near the N-terminus plays a critical role in catalysis as demonstrated by site-directed mutagenesis [Liu *et al.*, 1992]. This interaction appears to activate the thiol anion by lowering the pKa of the sulhydryl group and appears to help orient the thiolate anion in the active site such that half of

its surface is shielded by hydrophobic residues and the other half is exposed for reaction with the electrophilic substrate [Ji *et al.*, 1992]. However, the equivalent residue of Tyr 6 in the theta-class structure is not present in the active site, but its role appears to have been replaced by either a nearby serine or another tyrosine residue located in the C-terminal domain of the enzyme [Wilce *et al.*, 1995]. Domain II provides a great deal of the hydrophobic surface that interacts with the xenobiotics and the products of the reactions. Using molecular modeling techniques a predictive substrate model for class mu rat glutathione S-transferase 4-4 was constructed, containing three interaction sites responsible for Lewis acid-Lewis base interaction as well as a region responsible for aromatic interactions with the substrates [Groot *et al.*, 1995].

The rate of the glutathione S-transferase catalyzed reaction can be limited by a number of different chemical or physical steps in the mechanism, such as formation of the Meisenheimer complex in a glutathione S-transferase catalyzed nucleophilic aromatic substitution reaction, assistance of specific amino-acid residues in substrate activation, stabilisation of the transition state or dissociation of the product. The mu class isoenzyme 3-3, which is particularly efficient in catalyzing aromatic nucleophilic substitution reactions, appears to stabilize the transition state of the Meisenheimer complex by hydrogen bonding interactions between the *pro-R o*-nitrogroup of 1-chloro-1-(S-glutathionyl)-2,4-dinitrocyclohexadienate anion and the hydroxyl groups of Tyr6 and Tyr115 and between the *p*-nitro group and an enzyme-bound water [Graminski *et al.*, 1989; Ji *et al.*, 1993]. Further structural and mechanistic analysis on the functional properties of Tyr 115 in mu class isoenzyme 3-3 revealed that the hydroxyl group of this residue provides electrophilic assistance in addition of glutathione to arene oxide substrates [Johnson *et al.*, 1993]. Interaction of the flexible C-terminal tail with the N-terminal domain helps to limit the rate of product release from the active site of mu class isoenzymes in nucleophilic aromatic substitution reactions [Zhang *et al.*, 1992; Johnson *et al.*, 1993]. Recently, it was demonstrated that the chemical reactivity for nucleophilic attack of fluoronitrobenzenes in the glutathione S-transferase catalyzed reaction might also be rate-limiting [Rietjens *et al.*, 1995].

Bioactivation and detoxification via glutathione conjugation.

In general, the conjugation of an electrophilic compound with glutathione is a detoxification reaction, but there are several examples where glutathione conjugation plays an important role in the bioactivation of chemicals by different types of

mechanisms. For example, glutathione conjugation of quinone- and quinoneimine-derivatives targets the metabolites to the kidneys, where subsequent processing by the proximal tubular brush border enzyme γ-glutamyltranspeptidase are thought to be involved in the selective toxicity of these compounds by a yet unknown mechanism [Fowler *et al.*, 1991; Fowler *et al.*, 1994, Lock *et al.*, 1993]. Conjugation to glutathione has been demonstrated to be the initial step in the bioactivation of haloalkenes. After subsequent degradation to the corresponding cysteine conjugates, β-lyase mediated formation of reactive thiol compounds are proposed to be responsible for the nephrotoxicity caused by haloalkenes [Commandeur *et al.*, 1995]. Glutathione is also involved in the conjugative activation of vicinal dihaloalkanes to the reactive episulfonium ion intermediate, which forms adducts with DNA [Guengerich, 1992].

Glutathione S-transferases are of particular interest because they have been implicated in the development of resistance of cells and organisms towards pesticides, herbicides and chemotherapeutic alkylating agents [Tew, 1994]. Increased conjugation with glutathione as well as an increased efflux of the GS-conjugates from the cell by ATP-dependent GS-X pumps, is a mechanism frequently associated with this type of drug resistance [Ishikawa, 1992].

2.2.2. N-acetyltransferases

N-acetylation is a major biotransformation pathway for compounds with an amino group. N-acetyltransferases catalyze the transfer of the acetyl group from endogenous acetyl coenzyme A to molecules that contain a primary amine function. Besides drugs and other chemicals like arylamine and hydrazine derivatives, also certain biogenic amines such as histamine and serotonin are substrates for the N-acetyltransferases [Weber *et al.*, 1990]. Structure activity studies of a series aniline-derivatives with substituents that differ in hydrophobicity, position, number, size and charge demonstrated that some *ortho*-substituted derivatives are not acetylated, probably due to steric hindrance [Andres *et al.*, 1987].

At least two groups of N-acetyltransferases are identified, one being monomorphic (NAT1) and the other being polymorphic (NAT2) [Blum *et al.*, 1990]. The polymorphism in N-acetyltransferase activity leads to the existance of the so-called 'fast' and 'slow' acetylator phenotypes. N-acetylation has been recognized to play a modulatory role in the metabolic activation of mutagenic and carcinogenic aromatic amines and various food pyrosylates that are classified as carcinogenic [Weber *et al.*, 1990]. From patterns of epidemiology slow acetylators appear to be

more susceptible to develop bladder cancer, probably as a result of their decreased capacity to prevent N-hydroxylation of arylamines [Guengerich, 1992]. Fast acetylators are predisposed to colorectal cancer by enhancing the genotoxicity of amine food pyrolysis products in the gastrointestinal tract via acetylation of N-hydroxy arylamines [Turesky *et al.*, 1991; Hein *et al.*, 1994].

2.2.3. UDP-glucuronyltransferase.

The membrane-bound glycoproteins UDP-glucuronyltransferases are a group of proteins responsible for the transfer of the glucuronyl group from uridine 5'-diphosphoglucuronate to a large number of lipophilic compounds with a nucleophilic functional group (Figure 12), resulting in formation of water-soluble O-, S-, N- and even C-glucuronides excreted into urine or bile [Armstrong, 1987; Mulder *et al.* 1990].

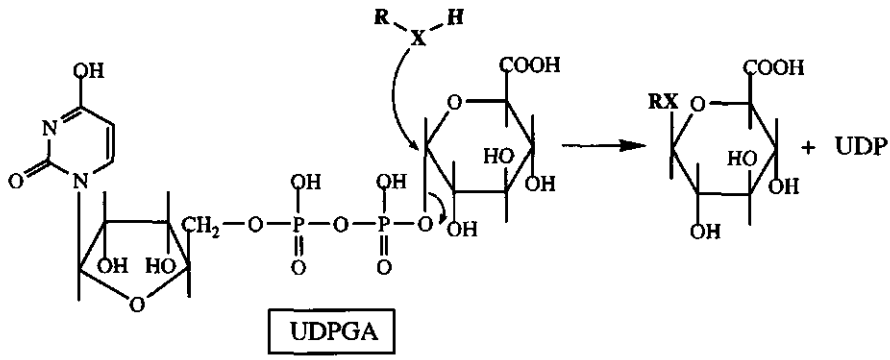

Figure 12: The mechanism of glucuronidation is a S_N2 reaction, the nucleophilic functional group of the substrate attacks the C1 of the pyranose ring to which UDP is attached in an α-glycosidic bond [Mulder *et al.*, 1990].

Located on the lumal side of the membranes of the endoplasmatic reticulum, these enzymes are closely associated with the cytochrome P450 monooxygenase dependent system and are involved in vectorial transport and metabolism of drugs through the phospholipid bilayer [Batt *et al.*, 1994].

At least two groupes of UDP-glucuronyltransferases exist with different substrate binding preferences; one being concerned with small planar molecules of relatively low lipid solubility and the other binding larger non-planar lipophilic substrates [Ghauri *et al.*, 1992]. The UDP-glucuronyltransferases exist as a multigene

family and the level of expression of each isoenzyme is the result of interplay between genetics, tissue specific and environmental regulators. At least ten human forms have been identified. The UDP-glucuronyltransferases are involved in the metabolism of endogenous compounds like biliburin, retinoic acid and in maintaining the steady state of steroid and thyroid hormones [Batt *et al.*, 1994].

Whereas glucuronidation in general constitutes a reaction of detoxification and elimination via urine or bile, this biotransformation pathway is also implicated in the bioactivation of N-hydroxylarylamines of e.g. 4-aminobiphenyl and 2-naphthylamine. Reactive nitrenium ions that can covalently bind to epithelial macromolecules and are believed to be responsible for arylamine-induced bladder and colon carcinogenesis, may be generated in the bladder via hydrolysis of N-hydroxy-N-glucuronides in slightly acidic urine or in the colon upon the action of bacterial β-glucuronidase [Guengerich, 1992].

2.2.4. Sulphotransferase.

The cytosolic sulphotransferases catalyze the transfer of the sulphuryl group from 3'-phosphoadenosine 5'-phosphosulphate (PAPS) to nucleophiles such as alcohols, phenols and amines (Figure 13). The availability of the PAPS precursor, inorganic sulphate, can be a limiting factor in sulphation activity [Mulder *et al.*, 1990].

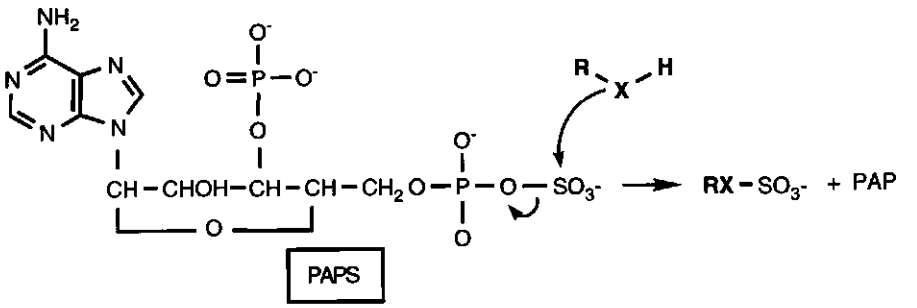

Figure 13: *Reaction catalyzed by sulphotransferases involving a nucleophilic attack of the substrate on the sulphuryl group of PAPS.*

The sulphotransferase constitute a large gene family and the activities of sulphotransferase enzymes are regulated by both genetic polymorphisms and hormonal factors. Numerous cDNAs encoding these enzymes have been isolated from different species including the rat, mouse, human, guinea pig, plant and cow

[Kong *et al.*, 1994]. In the past, these enzymes were most often classified on the basis of their substrate specificities toward simple phenols, phenolic monoamines and hydroxysteroids. Recently, however, the sulphotransferase genes have been grouped into distinct gene families, since the substrate-based classification of these enzymes appears to be inappropriate due to the broad and overlapping substrate specificity of the individual sulphotransferases [Yamazoe *et al.*, 1994].

In general, the sulphotransferase enzymes exhibit a high affinity and a low capacity, whereas glucuronidation has a low affinity and a high capacity for the same substrates [Temellini *et al.*, 1991].

Sulphation of endogenous (e.g. bile salts, steroids, catecholamines) or foreign chemicals has been recognized as an important pathway of metabolic inactivation, through enhancing the polarity and solubility of compounds and thereby hasten their excretion from the body. However, for a number of chemicals, such as N-hydroxylamines, arylhydroxamic acids and benzylic alcohols, sulphation has been implicated into the bioactivation to reactive intermediates [Miller, 1994].

3. Frontier orbital theory.

Frontier orbital theory has been already frequently used in the field of organic chemistry to explain the regioselectivity in nucleophilic and electrophilic aromatic substitutions [Fleming, 1989; Fukui *et al.*, 1954]. This section gives a short introduction which is mainly based on the monograph by Fleming, in order to provide a basis to understand how the frontier orbital theory can be used to study and predict outcomes of enzyme catalysis and, thus, outcomes of biotransformation processes.

Atomic and molecular orbitals

Atoms consist of a nucleus containing protons and neutrons surrounded by electrons which are localized in so-called atomic orbitals. Each orbital can contain two electrons with opposite electron spin. The chemical characteristics of an atom depend on especially the electrons in the outer-shell orbitals, the so-called valence shell orbitals. When molecules are formed from atoms, atomic orbitals (AO's) from one atom are combined with those of another atom to give the molecular orbitals (MO) of the newly formed molecule. These MO's are not, as the AO's localised around one atomic nucleus, but can be delocalised over all atomic nuclei of the molecule.

The hydrogen atom

The simplest example to describe and explain the mixing of two AO's to give MO's is the formation of a molecule of hydrogen (H_2) from two hydrogen atoms (H). The two 1s AO's of the two H-atoms can combine to make two MO's, named the σ-bonding orbital and the σ* anti-bonding orbital, as depicted in Figure 14.

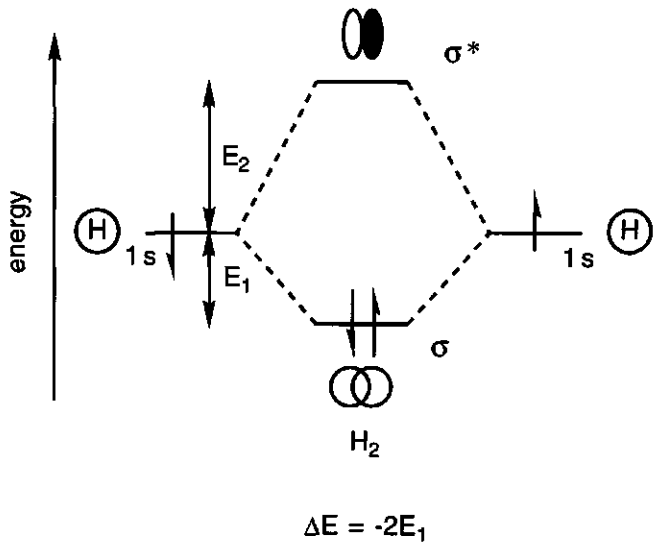

Figure 14: Combination of two hydrogen atom AO's to give the two MO's of the hydrogen molecule. In σ, the two AO combine with a similar phase, leading to a binding interaction, since the electrons are in an orbital with significant density between the two positively charged nuclei. The absolute value of E_1 is less than E_2, because the positioning of the two negative charges in one orbital costs some energy. The energy gain of this interaction is $2E_1$.

Two atoms of helium do not combine to form a He_2 molecule, because two electrons would go into the σ-binding orbital and two into the σ*-antibonding orbital. The energy needed to force the molecules together in an antibonding combination is greater than that gained from the bonding combination. Since $2E\sigma^*$ is greater than $2E\sigma$, extra energy is thus required to keep the two helium atoms together.

Thus, the interaction between an occupied and an unoccupied orbital will result in an energy gain -as for the H_2 molecule-, while the interaction between two filled orbitals leads to an energy loss.

Intermolecular MO-interactions: contributions to the energy of activation for a reaction

When two reacting species start to interact, the orbitals of one reactant will start to interact with the orbitals of the other reactant. Combinations between empty orbitals will not have effect on the energy of the system, as there are no electrons involved. However, the interaction between the filled orbitals of the one reactant (HOMO) with the filled orbitals of the other reacant (HOMO) will all require energy (Figure 15A). The energy required is a reason for the existance of an activation energy for a reaction. The interaction between a filled MO of the nucleophile (HOMO) and an unoccupied MO of the electrophile (LUMO) will give rise to an energy gain as schematically presented in Figure 15. The interaction of an orbital below the HOMO, for example HOMO-1, with an orbital above the LUMO, for example LUMO+1, will also contribute to the energy of the interaction and hence to lowering the energy of the transition state, but the effect is usually less than that of the HOMO/LUMO interaction. The HOMO/LUMO interaction thus contributes most to the energy gained, that can be used to overcome the activation barrier of the reaction.

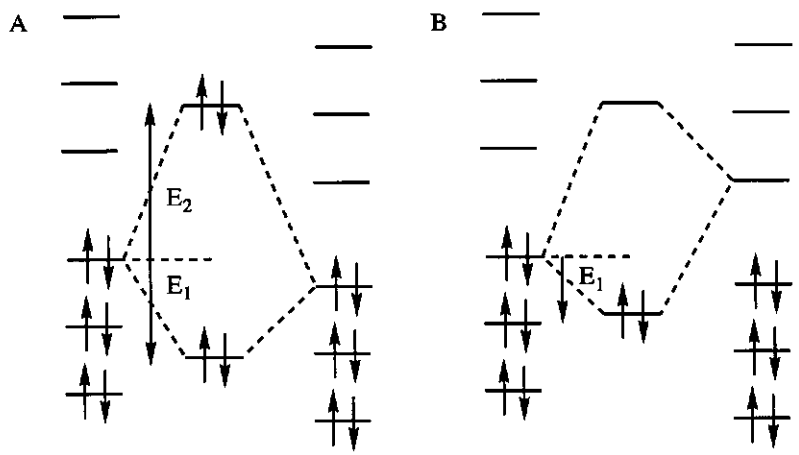

Figure 15: The interaction of the HOMO of one molecule with the HOMO of another (A); The interaction of the HOMO of one molecule with the LUMO of another (B)

Klopman and Salem have defined a formula for the energy change (ΔE), when two molecular orbitals of two reactants overlap. Based on considerations described in detail elsewhere (Fleming) this equation can be simplified to the following form for a reaction between a nucleophile and an electrophile:

$$\Delta E = - \frac{Q_{nucl.} \bullet Q_{elec.}}{\varepsilon \bullet R} + \frac{2(c_{nucl.} \bullet c_{elec.} \bullet \beta)^2}{E_{HOMO(nucl.)} - E_{LUMO(elec.)}}$$

The Coulombic term *The frontier orbital term*

E(HOMO), E(LUMO) = energy levels of the HOMO and LUMO; β = resonance integral; c_{nucl}, c_{elec} = coefficients of the HOMO of the reaction centre in the nucleophile and of the LUMO of the reaction cente in the electrophile; c^2_{nucl}, c^2_{elec} = orbital density of the HOMO or the LUMO on the reaction centre of the nucleophile or electrophile, respectively; $Q_{nucl.}$, $Q_{elec.}$ = total charges on the reaction centre in the nucleofile or the electrophile, respectively ; ε = local dielectric constant; R = distance between the reaction centres.

The formula describes that, the relative energy changes involved in the interaction between two reactants can be described by a Coulomb term (the first term) and a so-called frontier orbital term (the second term) in which the HOMO and LUMO interaction are described. For hard electrophiles and hard nucleophiles, which are known to have relatively high-energy LUMOs and low-energy HOMOs respectively, the term E_{HOMO}-E_{LUMO} becomes very large, which makes the frontier orbital term less important than the Coulomb term. However, as most reactants in biochemical reactions are not fully charged and have relatively delocalized electron distributions, they can be considered as soft nucleophiles or soft electrophiles. Radicals are considered to be soft, since most of them are uncharged and in most reactions react with uncharged molecules. The frontier orbital of a radical is called the SOMO (singly occupied molecular orbital). Because the Coulombic forces are small and the frontier orbital interactions are large, radical reactions are frontier orbital controlled. This implies that this type of reaction will be determined by the parameters that determine the frontier orbital term, e.g. the energy as well as the density of the reactive orbitals. The high-valent iron-oxo species of the P450 enzyme has been proposed to possess radical character (see also section 2.1.1., p. 29-30), and therefore

this intermediate can be considered to possess a SOMO. As this intermediate acts as a a electrophilic species, the SOMO might interact with the HOMO of the substrate.

Together these considerations form the basis for the application of frontier orbital theory in making QSAR's for the relative rate of conversion between different molecules, and/or the regioselectivity (i.e. the relative rate at various reaction centres in one molecule) of a biotransformation reaction.

REFERENCES.

Adachi S., Nagano S., Ishimori K., Watanabe Y., Morishima I., Egawa T., Kitagawa T. and Makino R., Roles of proximal ligand in heme proteins: Replacement of proximal histidine of human myoglobin with cysteine and tyrosine by site-directed mutagenesis as models for P450, chloroperoxidase, and catalase, *Biochemistry* **32**, 241-252, 1993.

Adams N.H., Levi P.E. and Hodgson E., Regulation of cytochrome P-450 isoenzymes by methylenedioxyphenyl compounds, *Chem.-Biol. Interactions* **86**, 255-274, 1993.

Akhtar M. and Wright J.N., A unified mechanistic view of oxidative reactions catalysed by P450 and related Fe-containing enzymes, *Nat. Prod. Rep.* **8**, 527-551, 1991.

Allentoff A.J., Bolton J.L., Wilks A., Thompson J.A. and Ortiz de Montellano P.R., Heterolytic versus homolytic peroxide bond cleavage by sperm whale myoglobin and myoglobin mutants, *J. Am. Chem. Soc.* **114**, 9744-9749, 1992.

Andres H.H., Vogel R.S., Tarr G.E., Johnson L. and Weber W.E., Purification, physicochemical, and kinetic properties of liver acetyl-CoA: arylamine N-acetyltransferase from rapid acetylator rabbits *Molecular Pharmacology* **31**, 446-456, 1987.

Armstrong R.N., Enzyme catalyzed detoxication reactions: mechanisms and stereochemistry, *CRC Critical Reviewes in Biochemistry* **22**, 39-88, 1987.

Atkinson J.K., Hollenberg P.F., Ingold K.U., Johnson C.C., Le Tadic M.-H., Newcomb M., Putt D.A., Cytochrome P450-catalyzed hydroxylations of hydrocarbons: Kinetic deuterium isotope effects for the hydroxylation of an ultrafast radical clok, *Biochemistry* **33**, 10630-10637, 1994.

Atkinson J.K. and Ingold K.U., Cytochrome P450 hydroxylation of hydrocarbons: Variation in the rate of oxygen rebound using cyclopropyl radical clocks including two new ultrafast probes, *Biochemistry* **32**, 9209-9214, 1993.

Augusto O., Beilan H.S., Ortiz de Montellano P.R., The catalytic mechanism of cytochrome P450: spin-trapping evidence for one-electron substrate oxidation. *J. Biol. Chem.* **257**, 11288-11295, 1982.

Ayesh R., Mitchell S.C., Zhang A., and Smith R.L., The fish odor syndrome: biochemical, familial and clinical aspects, *Br. Med. J.* **307**, 655-657, 1993.

BackesW.L. and Eyer C.S., Cytochrome P450 LM2 reduction, *J. Biol. Chem.* **264**, 6252-6259, 1989.

Banci L., Bertini I., Marconi S., Pierattelli R. and Sligar S.G., Cytochrome P450 and aromatic bases, A ^{1}H NMR study, *J. Am. Chem. Soc.* **116**, 4866-4873, 1994.

Batt A.M., Magdalou J., Vincent-Viry M., Ouzzine M., Fournel-Gigleux S., Galteau M.M., Siest G., Drug metabolizing enzymes related to laboratory medicine: cytochromes P450 and UDP-glucuronosyltransferases, *Clinica Chimica Acta* **226**, 171-190, 1994.

Blum M., Grant D.M., McBride W., Heim M., and Meyer U.A., Human arylamine N-acetyl-transferase genes: isolation, chromosomal localization, and functional expression, *DNA Cell Biol.* **9**, 193-203, 1990.

Bock K.W., Metabolic polymorphism affecting activation of toxic and mutagenic arylamines, *Trends Pharmacol. Science* **13**, 223-226, 1992.

Boddupalli S.S., Hasemann C.A., Ravichandran K.G., Lu J.-Y., Goldsmith E.J., Deisenhofer J., Peterson J.A., Crystallization and preliminary x-ray diffraction analysis of $P450_{terp}$ and the hemoprotein domain of $P450_{BM-3}$, enzymes belonging to two distinct classes of the cytochrome P450 superfamily, *Proc. Natl. Acad. Sci.* **89**, 5567-5571, 1992.

Boersma M.G., Cnubben N.H.P., van Berkel W.J.H., Blom M., Vervoort J. and Rietjens I.M.C.M., Role of cytochrome P450 and flavin containing monooxyenase in the biotransformation of 4-fluoro-N-methylaniline, *Drug Metabolism and Disposition* **21**, 218-230, 1993.

Bogaards J.J.P., Van Ommen B., Wolf C.R. and Van Bladeren P.J., Human cytochrome P450 enzyme selectivities in the oxidation of chlorinated benzenes, *Toxicology and Applied Pharmacology* **132**, 44-52, 1995.

Bondon A., Macdonald T.L., Harris .M. and Guengerich F.P. Oxidation of cycloalkylamines by cytochrome P450. Mechanism based inactivation, adduct formation, ring expansion and nitrone formation, *J. Biol. Chem.* **264**, 1988-1997, 1989.

Burka L.T., Plucinski T.M. and Macdonald T.L., Mechanisms of hydroxylation by cytochrome P450; metabolism of monohalobenzenes by phenobarbital-induced microsomes, *Proc. Natl. Acad. Sci.* **80**, 6680-6684, 1983.

Burka L.T., Thorsen A. and Guengerich F.P., Enzymatic monooxygenation of halogen atoms: Cytochrome P-450 catalyzed oxidation of iodobenzene by iodosobenzene, *J. Am. Chem. Soc.* **102**, 7615-7616, 1980.

Cashman J.R., Structural and catalytic properties of the mammalian flavin-containing monooyxgenase, *Chem. Res. Toxicol.* **8**, 165-181, 1995.

Chang T K.H., Weber G.F., Crespi C.L. and Waxman D.J., Differential activation of cyclophosphamide and ifosphamide by cytochromes P450 2B and 3A in human liver microsomes. *Cancer Research* **53**, 5629-5637, 1993.

Chen J. and Armstrong R.N., Stereoselective catalysis of a Retro-Michael reaction by class Mu glutathione transferases. Consequences for the internal distribution of products in the active site, *Chem. Res. Toxicol.* **8**, 580-585, 1995.

Commandeur, J.N.M., Stijntjes G.J., and Vermeulen N.P.E., Enzymes and transport systems involved in the formation and disposition of glutathione S-conjugates, Role in bioactivation and detoxication mechanisms of xenobiotics, *Pharmac. Rev.* **47**, 271-330, 1995.

Cook J. and Hodgson E., The induction of cytochrome P450 by isosafrole and related

methylenedioxyphenyl compounds, *Chem.-Biol. Interactions* **54**, 299-315, 1985.

Coon M.J., Ding X., Pernecky S.J. and Vaz A.D.N. Cytochrome P450: progress and predictions, *The FASEB Journal* **6**, 669-673, 1992.

Correia M.A., Yao K., Allentoff A.J., Wrighton S.A., Thompson J.A., Interactions of peroxyquinols with cytochromes P450 2B1, 3A1 and 3A5, Influence of the apoprotein on heterolytic versus homolytic O-O bond cleavage, *Arch. Biochem. Biophys.* **317**, 471-478, 1995.

Crespi C.L., Penman B.W., Leaky J.A., Arlotto M.P., Stark A., Parkinson A., Turner T. and Steimel D., Human cytochrome P4501A3: cDNA sequence, role of the enzyme in the metabolic activation of promutagens, comparison to the nitrosoamine activation by human cyctochrome P4502E1, *Carcinogenesis* **3**, 1293-1301, 1990.

Cupp-Vickery J.R. and Poulos T.L., Structure of cytochrome P450 eryF involved in erthromycin biosynthesis, *Stuctural Biology* **2**, 144-153, 1995.

Daly J.W., Guroff G., Udenfriend S. and Witkop B., Hydroxylation of alkyl and halogen substituted anilines and acetanilides by microsomal hydroxylases, *Biochem. Pharmacol.* **17**, 31-36, 1968.

Daly J.W., Jerina D.M. and Witkop B., Arene oxides and the NIH shift: The metabolism, toxicity and carcinogenity of aromatic compounds, *Experientia* **28**, 1129-1264, 1972.

Den Besten C., Van Bladeren P.J., Duizer E., Vervoort J. and Rietjens I.M.C.M., Cytochrome P450-mediated oxidation of pentafluorophenol to tetrafluorobenzoquinone as the primary reaction product, *Chem. Res. Toxicol.* **6**, 674-680, 1993.

De Voss J.J. and Ortiz de Montellano P.R., Computer-assisted, structure-based prediction of substrates for cytochrome P450cam, *J. Am. Chem. Soc.* **117**, 4185-4186, 1995.

Ebel R.E., O'Keeffe, Peterson J.A.,. Substrate binding to hepatic microsomal cytochrome P450, *J. Biol. Chem.* **253**, 3888-3897, 1978.

Fleming I. (ed.), Radical reactions, in: Frontier Orbitals and Organic Chemical Reactions, John Wiley & Sons, New York, 182-186, 1989.

Fruetel J.A., Collins J.R., Camper D.L., Loew G.H. and Ortiz de Montellano P.R.O., Calculated and experimental absolute stereochemistry of the styrene and β-methylstyrene epoxides formed by cytochrome P450cam, *J. Am. Chem. Soc.* **114**, 6987-6993, 1992.

Fukui K., Yonezawa T., Nagata C., and Shingu H., Molecular orbital theory of orientation in aromatic, heteroaromatic and other conjugated molecules, *J. Chem. Phys.* **22**, 1433-1442, 1954.

Gallagher E.P. Wienkers L.C., Stapleton P.L., Kunze K.L., Eaton D.L., Role of CYP1A2 and CYP3A4 in the bioactivation of alfatoxin B1 (AFB1) by human liver microsomes. *Cancer Research* **54**, 1-8, 1994.

Gerber N.C. and Sligar S.G., Catalytic mechanism of cytochrome P-450: evidence for a distal charge relay, *J. Am. Chem. Soc.* **114**, 8742-8743, 1992.

Ghauri F.Y., Blackledge C.A., Glen R.C., Sweatman B.C., Lindon J.C., Beddell C.R., Wilson I.D. and

Nicholson J.K., Quantitative structure-metabolism relationships for substituted benzoic acids in the rat, *Biochem. Pharmacol.* **44**, 1935-1946, 1992.

Gibson G.G. and Skett P. (Eds.), in: Introduction to drug metabolism, Chapman and Hall, New York, 1989.

Goeptar A.R., Scheerens H. and Vermeulen N.P.E., Oxygen and xeniobiotic reductase activities of cytochrome P450, *Critical Reviews in Toxicology* **25**, 25-65, 1995.

Gonzalez F.J., Human cytochromes P450: problems and prospects, *TIPS Reviews* **131**, 346-352, 1992.

Gonzalez F.J., The molecular biology of cytochrome P450s, *Pharmacological Reviews* **40**, 243-288, 1989.

Gonzalez F.J. and Idle J.R., Pharmacogenetic phenotyping and genotyping, present status and future potential, *Clin. Pharmacokinet.* **26**, 59-70, 1994.

Gonzalez F.J. and Meyer U.A., Molecular genetics of the debrisoquine-spartein polymorphism, *Clin. Pharm. Ther.* **50**, 233-238, 1991.

Gough A.C., Miles J.S., Spurr N.W., Moss J.E., Gaedigk A., Eichelbaum M. and Wolf C.R., Identification of the primary gene defect at the cytochrome P450 CYP2D locus, *Nature* **347**, 773-776, 1990.

Graminski G.F., Zhang P., Sesay M.A., Ammon H.L. and Armstrong R.N., Formation of the 1-(S-glutathionyl)-2,4,6-trinitrocyclohexadienate anion at the active site of glutathione S-transferase: Evidence for enzymic stabilization of σ-complex intermediates in nucleophilic aromatic substitution reactions, *Biochemistry* **28**, 6252-6258, 1989.

Groot M.J. de, Donné-Op den Kelder G., Commandeur J.N.M., Lenthe J.H. van, Vermeulen N.P.E., Metabolite predictions for para-substituted anisoles based on ab initio complete active space self-consistent field calculations, *Chem. Res. Toxicol* **8**, 437-443, 1995.

Groot M.J. de, van der Aar E.M., Nieuwenhuizen P.J., van der Plas R.M., Donné-Op den Kelder G., Commandeur J.N.M. and Vermeulen N.P.E., A predictive substrate model for rat glutathione S-transferase 4-4, *Chem. Res. Toxicol.* **8**, 649-658, 1995.

Guengerich F.P., Oxidation-reduction properties of rat liver cytochrome P-450 and NADPH-cytochrome P-450 reductase related to catalysis in reconstituted systems, *Biochemistry* **22**, 2811-2820, 1983.

Guengerich F.P., Oxidation of halogenated compounds by cytochrome P-450, peroxidases and model metalloporphyrins, *J. Biol. Chem.* **264**, 17198-17205, 1989.

Guengerich F.P., Enzymatic oxidation of xenobiotic chemicals, *Biochemisty and Molecular Biology* **25**, 97-153, 1990.

Guengerich F.P., Metabolic activation of carcinogens, *Pharmac. Ther.* **54**, 17-61, 1992.

Guengerich F.P., Cytochrome P450 enzymes, *American Scientist* **81**, 440-447, 1993.

Guengerich F.P., Bell L.C. and Okazaki O., Interpretations of cytochrome P450 mechanisms from

kinetic studies, *Biochimie* **77**, 573-580, 1995.

Guengerich F.P. and Macdonald T.L., Chemical mechanisms of catalysis by cytochromes P450 : A unified view, *Acc. Chem. Res.* **17**, 9-16, 1984.

Guengerich F.P. and Macdonald T.L., Mechanisms of cytochrome P-450 catalysis, *The FASEB Journal* **4**, 2453-2459, 1990.

Guengerich F.P., Muller-Enoch D., Blair I.A., Oxidation of quinidine by human liver cytochrome P450., *Mol. Pharmacol.* **30**, 287-.295, 1986.

Guengerich F.P., Kim P. and Iwasaki M., Role of human cytochrome P450IIE1 in the oxidation of many low molecular weight cancer suspects, *Chem. Res. Toxicol.* **4**, 168-179, 1991.

Gulick A.M. and Fahl W.E., Mammalian glutathione S-transferases: regulation of an enzyme system to achieve chemotherapeutic efficacy, *Pharmac. Ther.* **66**, 237-257, 1995.

Hammons G.J., Guengerich F.P., Weis C.C., Beland F.A., and Kadbular F.F., Metabolic oxidation of carcinogenic arylamines by rat, dog and human hepatic microsomes and by flavin-containing and cytochrome P-450 monooxygenase, *Cancer Research* **45**, 3578-3585, 1985.

Hansch C. and Zhang L., Quantitative structure activity relationships of cytochrome P450, *Drug Metabolism Reviews* **25**, 1-48, 1993.

Hanzlik R.P. and Tullman R.H., Suicidal inactivation of cytochrome P450 by cyclopropylamines. Evidence for cation radical intermediates, *J. Am. Chem. Soc.* **104**, 2048-2050, 1982.

Harada N. and Omura T., Participation of cytochrome P450 in the reduction of nitro compounds by rat liver microsomes, *J. Biochem.* **87**, 1539-1554, 1980.

Harris D. and Loew G., Prediction of regiospecific hydroxylation of camphor analogs by cytochrome P450cam, *J. Am. Chem. Soc.* **117**, 2738-2746, 1995.

Hasemann C.A., Kurumbail R.G., Boddupalli S.S., Peterson J.A., Deisenhof J., Structure and function of cytochromes P450: a comparative analysis of three crystal structures, *Structure* **15**, 41-62, 1995.

Hein D.W., Rustan T.D., Ferguson R.J., Doll M.A., Gray K., Metabolic activation of aromatic and heterocyclic N-hydroxyarylamines by wild-type and mutant recombinant human NAT1 and NAT2 acetyltransferases, *Arch. Toxicol.* **68**, 129-133, 1994.

Higuchi T., Uzu S. and Hirobe M. Synthesis of a highly stable iron porphyrin coordinaetd by alkylthiolate anion as a model for cytochrome P450 and its catalytic activity in O-O bond cleavage, *J. Am. Chem. Soc.* **112**, 7051-7053, 1990.

Hlavica P., Regulatory mechanisms in the activation of nitrogenous compounds by mammalian cytochrome P450 isoenzymes, *Drug Metabolism Reviews* **26** (1&2), 325-348, 1994.

Hrycay E.G., Gustafsson J.-A., Ingelman-Sundberg M. and Ernster L., The involvement of cytochrome P450 in hepatic microsomal steroid hydroxylation reactions supported by sodium periodate, sodium chlorite, and organic hydroperoxides, *Eur. J. Biochem.* **61**, 43-52, 1976.

Ishikawa T., The ATP-dependent glutathione S-conjugate export pump, *Trends Biochem. Sci.* **17**, 463-468, 1992.

Isseman I. and Green S., Activation of a member of the steroid hormone receptor superfamily by peroxisome proliferators, *Nature* **347**, 645-650, 1990.

Iyanagi T., Makino R. and Koichi Anan F., Studies on the microsomal mixed-function oxidase system: Mechanism of action of hepatic NADPH-cytochrome P450 reductase, *Biochemistry* **20**, 1722-1730, 1981.

Jerina D.M., Michaud D.P., Feldmann R.J., Armstrong R.N., Vyas K.P., Thakker D.R., Yagi H., Thomas P.E., Ryan D.E. and Levin W., Stereochemical modeling of the catalytic site of cytochrome P450c. In: Sato R., Kato R. (eds.) Microsomes, drug oxidations, and drug toxicity. Tokyo: Japan Scientific Societies Press, 195-201, 1982.

Ji X., Armstrong R.N., and Gilliland G.L., Snapshots along the reaction coordinate of an S_NAr reaction catalyzed by glutathione transferase, *Biochemistry* **32**, 12949-12954, 1993.

Ji X., Zhang P., Armstrong R.N., Gilliland G.L., The three-dimensional structure of a glutathione S-transferase from the Mu gene class. Stuctural analysis of the binary complex of isoenzyme 3-3 and glutathione at 2.2-Å resolution, *Biochemistry* **31**, 10169-10184, 1992.

Johnson W., Liu S., Ji X., Gilliland G.L. and Armstrong R.N., Tyrosine 115 participates both in chemical and physical steps of the catalytic mechanism of a glutathione S-transferase, *J. Biol. Chem.* **268**, 11508-11511, 1993.

Jones J.P., Shou M., and Korzekwa, Stereospecific activation of the procarcinogen benzo[a]pyrene: A probe for the active sites of the cytochrome P450 superfamily, *Biochemistry* **34**, 6956-6961, 1995.

Koerts J., Rietjens I.M.C.M., Boersma M.G. and Vervoort J., ^1H NMR T_1 relaxation rate study on substrate orientation of fluoromethylanilines in the actives sites of microsomal and purified cytochrome P450 1A1 and 2B1, *FEBS Letters* **368**, 279-284, 1995.

Kominami S. and Takemori S., Effect of spin state on reductions of cytochrome P450 from bovine adrenocortical microsomes, *Biochem. Biophys. Acta* **709**, 147-153, 1982.

Kong, Ah-Ng Tony and Fei P., Molecular cloning of three sulfotransferase cDNAs from mouse liver, *Chemico-Biological interactions* **92**, 161-168, 1994.

Korzekwa K.R. and Jones J.P., Predicting the cytochrome P450 mediated metabolism of xenobiotics, *Pharmacogenetics* **3**, 1-18, 1993.

Korzekwa K.R., Jones J.P., and Gillette J.R., Theoretical studies on cytochrome P450 mediated hydroxylation: A predictive model for hydrogen atom abstractions, *J. Am. Chem. Soc.* **112**, 7042-7046, 1990.

Korzekwa K., Swinney D.C., and Trager W.F, Isotopically labelled chlorobenzenes as probes for the mechanisms of cytochrome P450 catalyzed aromatic hydroxylation, *Biochemistry* **28**, 9019-

9027, 1989.

Korzekwa K., Trager W., Gouterman M., Spangler D. and Loew G.H., Cytochrome P450 mediated aromatic oxidation: A theoretical study, *J. Am. Chem. Soc.* **107**, 4273-4279, 1985.

Koymans L., Donné-Op de Kelder G.M., te Koppele J.M., and Vermeulen N.P.E., Generalized cytochrome P450-mediated oxidation and oxygenation reactions in substituted aromatic substrates with activated N-H, O-H, C-H or S-H substituents, *Xenobiotica* **23**, 633-648, 1993.

Larroque C., Lange R., Maurin L., Bienvenue A. and van Lier J.E., On the nature of the cytochrome P450scc "ultimate oxidant": characterization of a productive radical intermediate, *Arch. Biochem. Biophys.* **282**, 198-201, 1990.

Lawton M.P., Cashman J.R., Cresteil T., Dolphin C., Elfarra A., Hines R.N., Hodgson E., Kimura T., Ozols J., Phillips I., Philpot R.M., Poulsen L.L., Rettie A.E., Williams D.E., and Ziegler D.M., A nomenclature for the mammalian flavin-containing monooxygenase gene family based on amino acid sequence identities. *Arch. Biochem. Biophys.* **308**, 254-257, 1994.

Lee J.S., Jacobsen N.E., Ortiz de Montellano P.R., 4-Alkyl radical extrusion in the cytochrome P450 catalyzed oxidation of 4-alkyl-1,4-dihydropyridines, *Biochemistry* **27**, 7703-7710, 1988.

Lee W.A. and Bruice T.C., Homolytic and heterolytic oxygen-oxygen bond scissions accompanying oxygen transfer to iron(III)porphyrins by percarboxylic acids and hydroperoxides. A mechanistic criterion for peroxidase and cytochrome P450, *J. Am. Chem. Soc.* **107**, 513-514, 1985.

Lefever M.R. and Wackett L.P., Oxidation of low molecular weight chloroalkanes by cytochrome P450CAM, *Biochem. Biophys. Res. Commun.* **201**, 373-378, 1994.

Levin A.A., and Dent J.G., Comparison of the metabolism of nitrobenzene by hepatic microsomes and cecal microflora from Fischer-344 rats in vitro and the relative importance of each in vivo. *Drug Metab. Dispos.* **10**, 450-454, 1982.

Lewis D.F.V., MO-QSARs: a review of molecular orbital-generated quantitative structure activity relationships, Progress in drug metabolism, (Ed. G.G. Gibson), Taylor & Francis, Chapter 5, 205-255, 1990.

Lewis D.F.V., Three-dimensional models of human and other mammalian microsomal P450s constructed from an alignment with P450102 ($P450_{bm3}$), *Xenobiotica* **25**, 333-366, 1995.

Lewis D.F.V., C. Ioannides and D.V. Parke, Molecular dimensions of the substrate binding site of cytochrome P-448, *Biochem. Pharmacol.* **35**, 2179-2185, 1986.

Lewis D.F.V., Ioannides C. and Parke D.V., Structural requirements for substrates of cytochromes P-450 and P-448, *Chem.-Biol. Interact.* **64**, 39-60, 1987.

Lewis D.F.V., Moereels H., Lake B.G., Ioannides C. and Parke D.V., Molecular modeling of enzymes and receptors involved in carcinogenesis: QSARs and compact-3D, *Drug Metabolism Reviews* **26**, 261-285, 1994.

Li H. and Poulos T.L., Structural variation in heme enzymes: a comparative analysis of peroxidase and P450 crystal structures, *Structure* **2**, 461-464, 1992.

Li J.J., Purdy R.H., Appelman E., Klicka J.K. and Li S.A., Catechol formation of fluoro- and bromo-substituted estradiols by hamster liver microsomes, *Molec. Pharmacol.* **27**, 559-565, 1985.

Lindberg R.L.P. and Negishi M., Alteration of mouse cytochrome $P450_{coh}$ substrate specificity by mutation of a single amino-acid residue, *Nature* **339**, 632-634, 1989.

Liu S., Zhang P., Ji X., Johnson W.W., Gilliland G.L. and Armstrong R.N., Contribution of tyrosine 6 to the catalytic mechanism of isoenzyme 3-3 of glutathione S-transferase, *J. Biol. Chem.* **267**, 4296-4299, 1992.

Lo H.H., Brown P.I., Rankin G.O., Acute nephrotoxicity induced by isomeric dichloroanilines in Fischer 344 rats, *Toxicology* **63**, 215-231, 1990.

Lo H.H., Brown P.I. and Rankin G.O., Trichloroaniline effects on renal function in vivo and in vitro, *Toxicology Letters* **57**, 319-328, 1991.

Loida P.J., Sligar S.G., Paulsen M.D., Arnold G.E. and Ornstein R.L., Stereoselective hydroxylation of norcamphor by cytochrome P450cam, *J. Biol. Chem.* **270**, 5326-5330, 1995.

Lu A.Y.H., Levin W., Vore M., Conney A.H., Thakker D.R., Holder D.R., and Jerina D.M., Metabolism of benzo(a)pyrene by purified liver microsomal cytochrome P448 and epoxide hydrase, In: *Carcinogenesis* 1, Polynuclear Aromatic hydrocarbons: Chemistry, metabolism and carcinogenesis pp. 115-126. Freudenthal R.I. and Jones P.W. (eds.) Raven Press, New York., 1976.

Macdonald T.L., Chemical mechanisms of halocarbon metabolism, *CRC Critical Reviews in Toxicology* **11**, 85-120, 1983.

Macdonald T.L., Gutheim W.G., Martin R.B., and Guengerich F.P., Oxidation of substituted N,N-dimethylanilines by cytochromes P450: estimation of the effective oxidation-reduction potential of cytochrome P450, *Biochemistry* **28**, 2071-2077, 1989.

Macdonald T.L., Zirvi K., Burka L.T., Peyman P., Guengerich F.P., Mechanism of cytochrome P450 inhibition by cyclopropylamines, *J. Am. Chem Soc.* **104**, 2050-2052, 1982.

Mackman R., Guo Z., Guengerich F.P. and Ortiz de Montellano P.R., Active site topology of human cytochrome P450 2E1, *Chem. Res. Toxicol.* **9**, 223-226, 1996.

Mansuy D., Cytochrome P450 and synthetic models, *Pure & Applied Chemistry* **59**, 759-770, 1987.

Mansuy D., Battioni P. and Battioni J.-P., Chemical model systems for drug-metabolizing cytochrome P450 dependent monooxygenases [review], *Eur. J. Biochem.* **184**, 2647-285, 1989.

Mason R.P. and Holzman J.L., The mechanism of microsomal and mitochondrial nitroreductase. Electron spin resonance evidence for nitroaromatic free radical intermediates, *Biochemistry* **14**, 1626-1632, 1975.

Miller J.A., Sulfonation in chemical carcinogenesis-history and present status, *Chemico-Biological*

Interactions **92**, 329-341, 1994.

Monks T.J., and Lau S.S., Commentary: renal transport processes and glutathione conjugate-mediated nephrotoxicity, *Drug Metab. Dispos.* **15**, 437-441, 1987.

Morais de S.M.F., Wilkinson G.R., Blaisdell J., Nakamura K., Meyer U.A. and Goldstein J.A., The major genetic defect responsible for the polymorphism of (S)-mephenytoin metabolism in humans, *J. Biol. Chem.* **269**, 15419-15422, 1994.

Morgenstein R. and DePierre J.W., Membrane-bound glutathione transferases. In: Glutathione conjugation. Eds.: Sies H. and Ketterer B., Academic Press, London, 157-175, 1988.

Muerhoff A.S., Griffin K.J. and Johnson E.F., The peroxisome proliferator-activated receptor mediates the induction of CYP4A6, a cytochrome P450 fatty acid ω-hydroxylase, by clofibric acid, *J. Biol. Chem.* **267**, 19051-19053, 1992.

Mulder G.J., Coughtrie M.W.H. and Burchell B., (ed), Conjugation reactions in drug metabolism, Taylor & Francis, Chapter 4, Glucuronidation, 1990.

Myers T.G., Thummel K.E., Kalhorn T.F., and Nelson S.D., Preferred orienations in the binding of 4'-hydroxyacetanilide (acetaminophen) to cytochrome P450 1A1and 2B1 isoforms as determined by ^{13}C- and ^{15}N-NMR relaxation studies, *J. Med. Chem.* **37**, 860-867, 1994.

Nazar-Stewart V., Motulsky A.G., Eaton D.L., White E., Hornung S.K., Leng Z.-T., Stapleton P. and Weiss N.S., The glutathione S-transferase m polymorphism as a marker for susceptibility to lung carcinoma, *Cancer Research* **53**, 2313-2318, 1993.

Nedelcheva V. and Gut I., P450 in the rat and man: methods of investigation, substrate specificities and relevance to cancer, *Xenobiotica* **24**, 1151-1175, 1994.

Nelson D.R., Kamataki T., Waxman D.J., Guengerich F.P., Estabrook R.W., Feyereisen R., Gonzalez F.J., Coon M.J., Gunsalus I.C., Gotoh O., Okuda K. and Nebert D.W., The P450 superfamily-update on new sequences, gene mapping, accession numbers, early trivial names of enzymes, and nomenclature, *DNA Cell Biol.* **12**, 1-51, 1993.

Nelson H.H., Wiencke J.K., Christiani D.C., Cheng T.J., Zuo Z.-F., Schwartz B.S., Lee B.-K., Spitz M.R., Wang M., Xu X., Kelsey K.T., Ethnic differences in the prevalence of the homozygous deleted genotype of glutathione S-transferase theta, *Carcinogenesis* **16**, 1243-1245, 1995.

O'Brien P.J., Wong W.C., Silva J. and Skan S., Toxicity of nitrobenzene compounds towards isolated hepatocytes: dependence on reduction potential, *Xenobiotica* **20**, 945-955, 1990.

Oguri K., Yamada H. and Yoshimura H., Regiochemistry of cytochrome P450 isozymes, *Annu. Rev. Pharmacol. Toxicol.* **34**, 251-279, 1994.

Okazaki O. and Guengerich F.P., Evidence for specific base catalysis in N-dealkylation reactions catalyzed by cytochrome P450 and chloroperoxidase, *J. Biol. Chem.* **268**, 1546-1552, 1993.

Omura T. and Sato R., The carbon monoxide binding pigment of liver microomes, *J. Biol. Chem.* **239**, 2370-2378, 1964.

Ortiz de Montellano P.R., Cytochrome P450; structure, mechanism and biochemistry, Plenum Press, New York and London, 1986.

Ortiz de Montellano P.R., Control of the catalytic activity of prosthetic heme by the structure of hemoproteins, *Acc. Chem Res.* **20**, 289-294, 1987.

Ortiz de Montellano P.R., Kunze K.L., Beilan H.S. and Wheeler C., Destruction of cytochrome P450 by vinyl fluoride, fluroxene and acetylene. Evidence for a radical intermediate in olefin oxidation, *Biochemistry* **21**, 1331-1339, 1982.

Ouzounis C.A. and Melvin W.T., Primary and secondary structural patterns in eukaryotic cytochrome P450 families correspond to structures of helix-rich domain of *Pseudomonas putida* cytochrome P450cam, *Eur. J. Biochem.* **198**, 307-315, 1991.

Paine A.J., Heterogeneity of cytochrome P450 and its toxicological significance, *Human and Experimental Toxicology* **14**, 1-7, 1995.

Parry G., Palmer D.N. and Williams D.J., Ligand partitioning into membranes, its significance in determining Km and Ks values for cytochrome P450 and other membrane bound receptors and enzymes, *FEBS Letters* **67**, 123-129.

Parke D.V., The cytochromes P450 and mechanims of chemical carcinogenesis, *Environmental health perspectives* **102**, 852-853, 1994.

Paulsen M.D. and Ornstein R.L., Substrate mobility in thiocamphor-bound cytochrome P450cam: an explanation of the conflict between the observed product profile and the X-ray structure, *Protein Engineering* **6**, 359-365, 1993.

Pemble S., Schroeder K.R., Spencer S.R., Meyer D.J., Hallier E., Bolt H.M., Ketterere B. and Taylor J.B., Human glutathione S-transferase theta (GSTT1): cDNA cloning and the characterization of a genetic polymorphism, *Biochem. J.* **300**, 271-276, 1994.

Porter T.D. and Coon M.J., Cytochrome P450, multiplicity of isoforms, substrates, and catalytic and regulatory mechanisms, *J. Biol. Chem.* **266**, 13469-13472, 1991

Poulsen L.L. and Ziegler D.M., Multisubstrate flavin-containing monooxygenase: applications of mechanism to specificity. *Chem.-.Biol. Interact.* **96**, 57-73, 1995.

Raag R., Martinins S.A., Sligar S.G. and Poulos T.L., Crystal structure of the cytochrome $P450_{cam}$ active site mutant Thr252Ala, *Biochemistry* **30**, 11420-11429, 1991.

Raag R. and Poulos T.L., Crystal structures of cytochrome P-450cam complexed with camphane, thiocamphor and adamantane: factors controlling P450 substrate hydroxylations, *Biochemistry* **30**, 2674-2684, 1991.

Raag R. and Poulos T.L., X-Ray crystallographic structural studies of cytochrome P450cam: Factors controlling substrate metabolism, pp. 1-44 in: Relationships between structure and function of cytochrome P450; experiments, calculations, models, Frontiers in Biotransformation, Vol. 7. (eds. K. Ruckpaul and H. Rein), Akademie Verlag, Berlin, 1992.

Rankin G.O., Yang D.J., Cressey-Veneziano K., Casto S., Wang R.T. and Brown P.I., In vivo and in vitro nephrotoxicity of aniline and its monochlorophenylderivatives in the Fischer 344 rat, *Toxicology* **38**, 269-283, 1986a.

Rankin G.O., Yang D.J., Teets V.J., Lo H.H. and Brown P.I., 3,5-Dichloroaniline-induced nephrotoxicity in the Sprague-Dawley rat, *Toxicology Letters* **30**, 173-179, 1986b.

Ravichandran K.G., Boddupalli S.S., Hasemann C.A., Peterson J.A., Deisenhofer J., Crystal structure of hemoprotein domain of P450BM-3, a prototype for microsomal P450's, *Science* **261**, 731-736, 1993.

Reinemer P., Dirr H.W., Ladenstein R., Huber R., Lo Bello M., Federici G. and Parker M.W., Three-dimensional structure of class π glutathione S-transferases from human placenta in complex with S-hexylglutathione at 2.8 Å resolution, *J. Molec. Biol.* **227**, 214-226, 1992.

Reinemer P., Dirr H.W., Ladenstein R., Schäffer J., Gallay O., and Huber R., The three dimensional structure of class π glutathione S-transferase in complex with glutathione sulfonate at 2.3 Å resolution, *EMBO J.* **10**, 1997-2005, 1991.

Rietjens I.M.C.M., Soffers A.E.M.F., Hooiveld G.J.E.J., Veeger C. and Vervoort J., Quantitative structure activity relationships based on computer calculated parameters for the overall rate of glutathione S-transferase catalyzed conjugation of a series of fluoronitrobenzenes, *Chem. Res. Tox.* **8**, 481-488, 1995.

Rietjens I.M.C.M., Soffers A.E.M.F., Veeger C. and Vervoort J. Regioselectivity of cytochrome P450 catalyzed hydroxylation of fluorobenzenes predicted by calculated frontier orbital substrate characteristics, *Biochemistry* **32**, 4801-4812, 1993.

Rietjens I.M.C.M., and Vervoort J., Bioactivation of 4-fluorinated anilines to benzoquinoneimines as primary reaction products, *Chem.-Biol. Interact.* **22**, 263-281, 1991.

Rietjens I.M.C.M., and Vervoort J., A new hypothesis for the mechanism for the cytochome P450 dependent aerobic conversion of hexahalogenated benzenes to pentahalogenated phenols, *Chem. Res. Toxicol.* **5**, 10-19, 1992.

Riley P. and Hanzlik R.P., Electron transfer in P450 mechanisms. Microsomal metabolism of cyclopropylbenzene and *p*-cyclopropylanisole, *Xenobiotica* **24**, 1-16, 1994.

Rizk P.N. and Hanzlik R.P., Oxidative and non-oxidative metabolism of 4-iodoanisole by rat liver microsomes, *Xenobiotica* **25**, 143-150, 1995.

Robertson I.G.C. and Jernstrom B., The enzymatic conjugation of glutathione with bay-region diol-epoxides of benzo[*a*]pyrene, benz[*a*]anthracene and chrysene, *Carcinogenesis* **7**, 1633-1636, 1986.

Ryu D.-Y., Levi P.E. and Hodgson E., Regulation of cytochrome P-450 isoenzymes CYP1A1, CYP1A2 an CYP2B10 by three benzodioxole compounds, *Chem.-Biol. Interact.* **96**, 235-247, 1995.

Sealy R.C., Swartz H.M. and Olive P.L., Electron spin resonance-spin trapping. detection of superoxide formation during aerobic microsomal reduction of nitro-compounds, *Biochem. Biophys. Res. Commun.* **82**, 680-684, 1978.

Sharrock M., Debrunner P.G., Schulz C., Lipscomb J.D., Marshall V. and Gunsalus I.C., Cytochrome P450cam and its complexes. Mossbauer parameters of the heme iron, *Biochim. Biophys. Acta* **420**, 8-26, 1976.

Shaw G.-C. and Fulco A.J., Barbiturate-mediated regulation of expression of the cytochrome P450BM-3 gene of *Bacillus megaterium* by Bm3R1 protein, *J. Biol. Chem.* **267**, 5515-5526, 1992.

Shimada T. and Nakamura S.I., Cytochrome P450 mediated activation of procarcinogens and promutagens to DNA damaging products by measuring expression of umu-gene in Salmonella typhimurium TA1535, Biochem. Pharmacol. **36**, 1979-1987, 1987.

Simmons D.L., McQuiddy P. and Kasper C.B., Induction of the hepatic mixed function oxidase system by synthetic glucocorticoids: transcriptional and post-transcriptional regulation, *J. Biol. Chem.* **262**, 36-332. 1987.

Sinning I., Kleywegt G.J., Cowan S.W., Reinemer P., Dirr H.W., Huber R., Gilliland G.L., Armstrong R.N., Ji X., Board P.G., Olin B., Mannervik B. and Jones T.A., Structure determination and refinement of human alpha class glutathione transferase A1-1, and a comparison with the Mu and Pi class enzymes., *J. Mol. Biol.* **232**, 192-212, 1993.

Steward A.R., Wrighton S.A., Pasco D.S., Fagan J.B., Li D. and Guzelian P.S., Synthesis and degradation of 3-methylcholanthrene-inducible cytochromes P-450 and their mRNAs in primary monolayer cultures of adult rat hepatocytes, *Arch. Biochem. Biophys.* **241**, 494-508, 1985.

Strobel H.W., Lu A.Y.H., Heidema J., and Coon M.J., Phosphatidylcholine requirement in the enzymatic reduction of hemoprotein P450 and in fatty acid, hydrocarbon, and drug hydroxylation, *J. Biol. Chem.* **245**, 4851-4854, 1970.

Suzuki J. Meguro S., Moriat O., Hirayama S. and Suzuki S., Comparison of in vivo binding of aromatic nitro and amino compounds to rat hemoglobin, *Biochem. Pharmac.* **38**, 3511-3519, 1989.

Swanson B.A., Dutton D.R. Lunetta J.M., Yang C.S. and Ortiz de Montellano P.R., The active sites of cytochromes P450 IA1, IIB1, IIB2, and IIE1, *J. Biol. Chem.* **266**, 19258-19264, 1991.

Tatsumi K., Kitamura S., Yoshimura H. and Kawazoe Y. Susceptibility of aromatic nitro compounds to xanthine oxidase-catalyzed reduction. *Chem. Pharm. Bull.* **26**, 1713-1717, 1978.

Temellini E., Franchi M., Giuliani L. and Pacifici G.M., Human liver sulphotransferase and UDP-glucuronosyltransferase: structure-activity relationship for phenolic subsrates, *Xenobiotica* **21**, 171-177, 1991.

Tew K.D., Gluathione-associated enzymes in anticancer drug resistance, *Cancer Research* **54**, 4313-4320, 1994.

Tuck S.F. and Ortiz de Montellano P.R., Topological mapping of the active sites of cytochrome P4502B1 and P4502B2 by in situ rearrangement of aryl-iron complexes, *Biochemistry* **31**, 6911-6916, 1992.

Turesky R.J., Lang N.P., Butler M.A., Teitel C.H., and Kadbular F.F., Metabolic activation of carcinogenic heterocyclic amines by human liver and colon, *Carcinogenesis* **12**, 1839-1845, 1991.

Valentovic M.A., Ball J.G., Anestis D.K., Beers K.W., Madan E., Hubbard J.L. and Rankin G., Aute renal and hepatic toxicity of 2-haloanilines in Fischer 344 rats, *Toxicology* **75**, 121-131, 1992.

Van de Straat R., de Vries J., de Boer H.J.R., Vromans R.M. and Vermeulen N.P.E., Relationship between paracetamol binding to and its oxidation by two cytochrome P-450 isoenzymes - a proton nuclear magnetic resonance and spectrophotometric study, *Xenobiotica* **17**, 1-9, 1987.

Van Ommen B., and Van Bladeren P.J., Possible reactive intermediates in the oxidative biotransformation of hexachlorobenzene. *Drug Metab. Drug Interact.* **7**, 213-243, 1989.

Waxman D.J. and Azaroff L., Phenobarbital induction of cytochrome P450 gene expression, *Biochem. J.* **281**, 577-592, 1992.

Weber W.W., Levy G.N. and Hein D.W., Acetylation. In *Conjugation reactions in drug metabolism*, Ed: Mulder G.J., pp 163-191, 1990.

White R.E. and Coon M.J., Oxygen activation by cytochrome P450, *Ann. Rev. Biochem.* **49**, 315-356, 1980.

White R.E., McCarthy M.-B., Egeberg K.D. and Sligar S.G., Regioselectivity in the cytochromes P450: control by protein constraints and by chemical reactivities, *Arch. Biochem. Biophys.* **228**, 493-502, 1984.

Wilce M.C.J., Board P.G., Feil S.C. and Parker M.W., Crystal structure of a theta-class glutathione transferase, *The EMBO Journal* **14**, 2133-2143, 1995.

Yamazoe Y., Nagata K., Ozawa S., Kato R., Structural similarity and diversity of sulfotransferases, *Chem.-Biol. Interact.* **92**, 107-117, 1994.

Yang C.S., Yoo J.-S.H., Ishizaki H. and Hong Y., Cytochrome P450IIE: Roles in nitrosamine metabolism an mechanisms of regulation, *Drug Metabolism Reviews* **22**, 147-159, 1990.

Yin H., Anders M.W., Korzekwa K.R., Higgins L., Thummel K.E., Kharasch E.D. and Jones J.P., Designing safer chemicals: Predicting the rates of metabolism of halogenated alkanes, *Proc. Natl. Acad. Sci.* **92**, 11076-11080, 1995.

Zhang P., Liu S., Shan S., Ji X., Gilliland G.L. and Armstrong R.N., Modular mutagenesis of exons 1, 2, and 8 of a glutathione S-transferase from the mu class. Mechanistic and structural consequences for chimeras of isoenzyme 3-3, *Biochemistry* **31**, 10185-10193, 1992.

Zhong S., Howie A.F., Ketterer B., Taylor J., Hayes J.D., and Beckett G.J., Wathen C.G., Wolf C.R., and Spurr N.K., Glutathione S-transferase μ polymorphism as a marker for susceptibility to lung carcinoma, *Cancer Res.* **12**, 1533-1537, 1991.

Ziegler D.M., Flavin-containing monooxygenases: catalytic mechanisms and substrate specificities, *Drug Metab. Rev.* **19**, 1-32, 1988.

Ziegler D.M., in *Enzymatic basis of detoxication* Vol.1, Chapt.9, Microsomal flavin-containing monooxygenase: oxygenation of nucleophilic nitrogen and sulphur compounds, pp. 201-227 (W.B. Jakoby, ed.) Academic Press, New York, 1980.

Ziegler D.M., Graf P., Poulsen L., Sies H., and Stal W., NADPH-dependent oxidation of reduced ebselen, 2-selenylbenzanilide, and of 2-(methylseleno)benzanilide catalyzed by pig liver flavin-containing monooxygenase, *Chem. Res. Toxicol.* **5**, 163-166, 1992.

Zvelebil M.J.J.M., Wolf C.R. and Sternberg M.J.E., A predicted three-dimensional structure of human cytochrome P450: implications for substrate specificity, *Protein Engineering* **4**, 271-282, 1991.

CHAPTER 3

Study on the regioselectivity and mechanism of the aromatic hydroxylation of monofluoroanilines.

N.H.P. Cnubben, J. Vervoort, C. Veeger and I.M.C.M. Rietjens.

Chemico-Biological Interactions **85**, 151-172, 1992.

SUMMARY.

The *in vitro* and *in vivo* metabolism of monofluoroanilines was investigated. Special attention was focussed on the regioselectivity of the aromatic hydroxylation by cytochromes P450 and the mechanism by which this reaction might proceed. The results clearly demonstrate that the *in vitro* and *in vivo* regioselectivity of the aromatic hydroxylation by cytochromes P450 is dependent on the fluoro-substituent pattern of the aromatic aniline-ring. Results from experiments with liver microsomes from differently pretreated rats demonstrate that the observed regioselectivity for the aromatic hydroxylation is not predominantly determined by the active site of the cytochromes P450. To investigate the underlying reason for the observed regioselectivity, semi-empirical molecular orbital calculations were performed. Outcomes of these calculations show that neither the frontier orbital densities of the LUMO/LUMO+1 (lowest unoccupied molecular orbital) of the monofluoroanilines nor the spin-densities in their NH• radicals can explain the observed regioselectivities. The frontier orbital densities of the HOMO/HOMO-1 (highest occupied molecular orbital) of the monofluoroanilines however, qualitatively correlate with the regioselectivity of the aromatic hydroxylation. Based on these results, it is concluded that the cytochrome P450 dependent aromatic hydroxylation of monofluoroanilines does not proceed by hydrogen or electron abstraction from the aniline substrate to give an aniline-NH• radical. The results rather suggest that cytochrome P450 catalyzed aromatic hydroxylation of monofluoroanilines proceeds by an electrophilic attack of the $(FeO)^{3+}$ species of cytochrome P450 on a specific carbon atom of the aromatic aniline-ring.

INTRODUCTION.

Halogenated arylamines are widely used in industry for the synthesis of dyes, pesticides and herbicides [1]. Mammalian exposure to these compounds might arise from industrial pollution and from the production of these chemicals as a result of biological or combustional degradation of agrochemicals.

Cytochrome P450 enzymes catalyze the oxidative biotransformation of these aromatic compounds. This conversion results in more polar aminophenol metabolites, which can be conjugated in subsequent reactions followed by excretion from the body [2-4]. The mechanism by which cytochrome P450 hydroxylates aromatic compounds is still a matter of debate [5-7].

Based on literature [5,6] several mechanisms for the cytochrome P450 dependent aromatic hydroxylation of arylamines can be proposed, which are presented in Figure 1A and B, taking 3-fluoroaniline as a model compound.

The first two mechanisms proceed by formation of a fluoroaniline-NH• radical. This radical results from a reaction in which the cytochrome P450 $(FeO)^{3+}$ species abstracts a hydrogen atom from the aminogroup of the aniline substrate (mechanism 1). However, for molecules with heteroatoms of low ionization potential, like nitrogen, the aniline-NH• radical might as well result from a single electron transfer to cytochrome P450, followed by the loss of a proton from the fluoroaniline cation (mechanism 2)[5]. Once the NH• radical is formed, the reaction pathway proceeds by recombination of the substrate NH• radical with a hydroxide radical, donated by the $(FeOH)^{3+}$ moiety of the cytochrome P450 (oxygen rebound mechanism). This results in the formation of adducts, which rearrange to the energetically more favorable aminophenols, via keto-enol tautomerization. The third mechanism, depicted in Figure 1B, involves a radical attack of the cytochrome P450 $(FeO)^{3+}$ intermediate on the aniline-ring to give a so-called σ-adduct [6]. The reaction proceeds by a collapse of this σ-complex to give the aminophenols, either directly or through the formation of epoxides or ketones as an intermediate step [6,7].

The objective of the present study was to investigate which of these reaction pathways is more likely for the aromatic hydroxylation of arylamines. Monofluoroanilines were taken as model compounds, because (i) the fluoro-substituent will not cause significant steric hindrance as its Van der Waals radius (1.35 Å) almost equals that of a hydrogen substituent (1.20 Å); (ii) the metabolism of fluoroanilines can be studied by ^{19}F-NMR, which implies that all products from hydroxylation can be detected and quantified in a single run by the same method.

The *in vitro* and *in vivo* regioselectivity for the aromatic hydroxylation of the monofluoroanilines was studied and compared to the outcomes of molecular orbital calculations. It was expected that, if the aromatic hydroxylation proceeds by

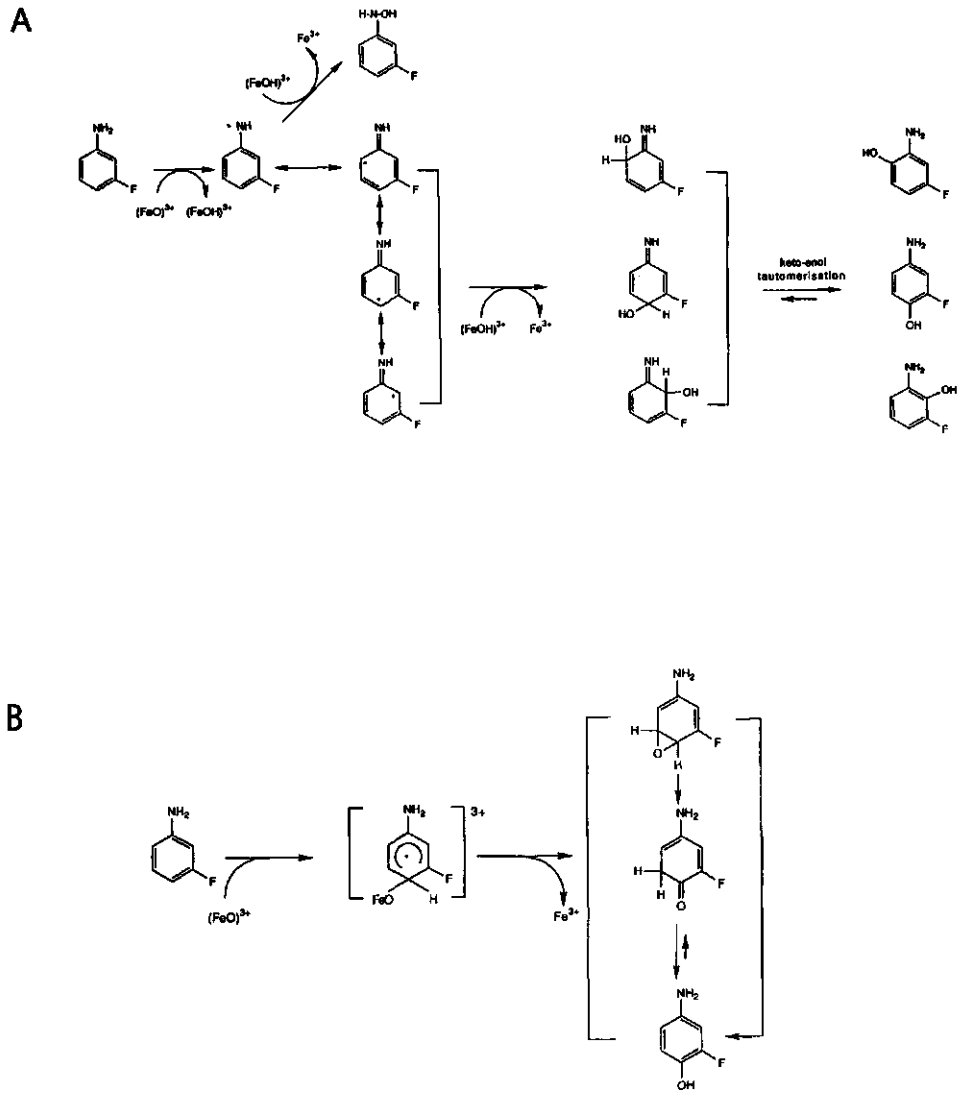

Figure 1 Reaction pathway for the hydroxylation of the monofluoroanilines, proceeding by (A) the so-called "oxygen rebound" mechanism. Formation of the aniline-NH• radical might result from either abstraction of a hydrogen atom from the aminogroup of the fluoroaniline (mechanism 1) or from electron abstraction followed by proton release in two separate steps (mechanism 2) [see Ref. 5], or (B) the attack of the cytochrome P450 $(FeO)^{3+}$ intermediate at the aniline-ring to give a σ-adduct [see Refs. 5-7]

formation of a NH• radical, the regioselectivity of the reaction depends on the spin distribution of the radical in the aromatic ring, *i.e.* the SOMO (single occupied molecular orbital) density of the NH• radical. However, when the reaction proceeds by formation of the σ-adduct, the site at which the cytochrome P450 $(FeO)^{3+}$ radical interacts with the aniline-substrate, will determine the regioselectivity. Because radical reactions are generally frontier-orbital controlled [8], the site of attack of the $(FeO)^{3+}$ SOMO-electron can be expected to be directed by either the HOMO (highest occupied molecular orbital) or the LUMO (lowest unoccupied molecular orbital) density of the aniline molecule.

Generally, these assumptions are based on the fact that not only the active site of the cytochrome P450 and the steric characteristics of the substrates, but also the electronic characteristics of the substrates will contribute to the regioselectivity of their aromatic hydroxylation by cytochromes P450 [9]. This paper also describes experiments carried out to ascertain that regioselectivity for the aromatic hydroxylation of the monofluoroanilines is indeed not predominantly determined by steric effects in the active site of the cytochromes P450.

MATERIALS AND METHODS.

Reference compounds.

2-Fluoroaniline, 3-fluoroaniline, 4-fluoroaniline were obtained from Janssen Chimica (Beerse, Belgium). Potassium fluoride was from Merck (Darmstadt, FRG). 2-Fluoro-4-nitrophenol was synthesized according to the method described by Vogel [10] for the synthesis of 2- and 4-nitrophenol. Using 2-fluorophenol (Janssen Chimica) and potassium nitrate (Merck) as starting materials, this procedure resulted in a reaction mixture containing 2-fluoro-4-nitrophenol and 2-fluoro-6-nitrophenol. These two products were separated by crystallisation of 2-fluoro-4-nitrophenol in pentane. The same procedure was followed for the synthesis of 3-fluoro-2-nitrophenol using 3-fluorophenol (Janssen Chimica) and potassium nitrate as starting materials.

3-Fluoro-4-aminophenol, 5-fluoro-2-aminophenol, 4-fluoro-2-aminophenol, 3-fluoro-2-aminophenol and 2-fluoro-4-aminophenol were synthesized by chemical reduction of respectively 3-fluoro-4-nitrophenol (Fluorochem, Derbyshire, UK), 5-fluoro-2-nitrophenol (Janssen Chimica), 4-fluoro-2-nitrophenol (Fluorochem), 3-fluoro-2-nitrophenol and 2-fluoro-4-nitrophenol under 3 atm. H_2 (24 h) in the presence of Pd/C (0.1 % w/v) (Janssen Chimica) using ethylacetate as the solvent. Because the synthesized 3-fluoro-2-nitrophenol and 2-fluoro-4-nitrophenol were not completely pure, their reduced compounds (3-fluoro-2-aminophenol and 2-fluoro-4-

nitrophenol) were further purified on silicagel 60 (70-230 Mesh) (Merck) using a mixture of ethylacetate-ethanol-acetic acid (15:3:2 by vol.) as eluent.

2-Fluoro-6-aminophenol was synthesized by the demethylation of 3-fluoro-*o*-anisidine (Aldrich, Steinheim, FRG) in hydrobromic acid and acetic acid at 130°C, essentially as described by Bhatt *et al.* [11].

2-Fluoracetanilide, 3-fluoro-4-acetamidophenol, 3-fluoracetanilide, 2-fluoro-4-acetamidophenol, 4-fluoracetanilide and 5-fluoro-2-acetamidophenol were synthesized by acylation of the corresponding amino-compound following the procedure described by Vogel [12].

4-Fluoro-N-hydroxyaniline was synthesized by the reduction of 4-fluoronitrobenzene as described by Coleman *et al.* [13]. In short, a mixture of 2 g 4-fluoronitrobenzene (Aldrich) and 1 g ammoniumchloride in 30 ml H_2O was stirred vigorously. Over a period of 15 minutes pulverized zinc was added in small portions, whereupon the mixture was refluxed at 60°C. After 1 h, the hot suspension was filtered to remove the zinc oxide residues. The filtrate was saturated with NaCl and cooled on ice. The yellow precipitate presented 4-fluoro-N-hydroxyaniline and was isolated.

In vivo exposure to 2-, 3- or 4-fluoroaniline.

Male Wistar rats (300-350 g) were housed individually in metabolism cages. The animals were given food and water *ad libitum*. Control urine was collected for 24 h before dosing. After these 24 h, the rats were orally dosed with 50 mg 2-, 3- or 4- fluoroaniline per kg body weight in olive oil. Urine was collected for 24 h after oral dosing and stored at -20°C.

Preparation of microsomes.

Microsomes were prepared from the perfused livers of male Wistar rats (≈ 300 g), which were untreated or treated with inducers of the cytochrome P450 enzymes, namely phenobarbital (Brocacef, Maarssen, The Netherlands)(0.1% in drinking water for 7 days), acetone (Merck, Darmstadt, FRG)(1.5 ml, 30% in water, administered by oral gavage, 24 h before sacrificing), dexamethasone (Sigma, St Louis, MO, USA)(300 mg/kg bodyweight, using a stock solution of 90 mg/ml in water containing 2% Tween-80, administered by oral gavage, daily for 4 days), 3-methylcholanthrene (Sigma, St Louis, MO, USA)(30 mg/kg body weight, using a stock solution of 6 mg/ml in olive oil, i.p., daily for 3 days), and isosafrole (Janssen, Beerse, Belgium)(150 mg/kg bodyweight, using a stock solution of 50 mg/ml in olive oil, i.p. daily for 3 days).

Following homogenisation of the livers in Tris-sucrose buffer (50 mM Tris, 0.25 M sucrose, pH 7.4) and centrifugation at 10,000 x *g* (20 min), the supernatants

were centrifuged for 75 min. at 105,000 x *g*. The microsomal pellet was washed once with Tris-sucrose buffer and finally suspended in potassium phosphate pH 7.25 containing 20% glycerol and 1 mM EDTA. The final preparation was immediately frozen in liquid nitrogen and stored at -80°C until use.

Cytochrome P450 contents were determined as described by Omura and Sato [14]. Protein was assayed by the method of Lowry [15] using bovine serum albumin (Sigma, St Louis, MO, USA) as the standard.

Microsomal incubations.

Microsomal incubations were carried out at 37°C in 0.1 M potassium phosphate, pH 7.6, containing 1 μM microsomal cytochrome P450 and 10 mM 2-, 3- or 4-fluoroaniline added as 1% (v/v) of a stock solution in DMSO. The reaction was started by addition of NADPH (1 mM final concentration) and terminated after 10 min by freezing the reaction mixture in liquid nitrogen for ^{19}F-NMR measurements or by adding 1.0 ml of the reaction mixture to 0.3 ml 20% trichloroacetic acid (TCA) for the chemical detection of 4-aminophenol.

Chemical detection of 4-aminophenol.

4-Aminophenol was determined by the method of Brodie and Axelrod [16] as follows: to 1 ml precipitated supernatant, 100 μl 5% phenol reagent (5% w/v phenol in 2.5 M NaOH) and 200 μl 2.5 M Na_2CO_3 were added. After 45 min. at room temperature, the absorbance at 630 nm was measured. The extinction coefficient for aminophenol in this assay was determined to be 30.5 mM^{-1} cm^{-1}.

Enzyme hydrolysis of conjugates in urine samples.

To hydrolyse glucuronide conjugates, 8 units (40 μl) of β-glucuronidase (from *E. coli* K_{12}, Boehringer, Mannheim, Germany) in 1200 μl 0.2 M KH_2PO_4/Na_2HPO_4 pH 6.2 were added to an equal volume of urine sample. The mixture was made anaerobic by four cycles of evacuating and filling with argon and incubated for 1 h at 37°C.

To hydrolyse the sulphate and glucuronide conjugates 40 μl of the arylsulphatase/β-glucuronidase enzyme mixture from *Helix pomatia* (Boehringer, Mannheim, Germany) in 1200 μl 0.1 M potassium acetate pH 5.2 were added to an equal volume of urine sample. The mixture was made anaerobic and incubated for 16 h at 37°C. 4-Fluoro-2-aminophenylsulphate could only be hydrolyzed by arylsulphatase treatment after its isolation from the urine by Bio-Gel P2 column chromatography, carried out as described before [17].

^{19}F-NMR measurements.

^{19}F-NMR measurements were performed on a Bruker CXP 300 and a Bruker AMX 300 spectrometer operating at 282.3 MHz as described before [18]. Proton decoupling (inverse gated decoupling) was achieved with the Waltz-16 pulse sequence [19] at -16 dB from 20 W (CXP 300) and -22 dB from 50 W (AMX 300).

Norell (Landisville, NJ) 10 mm NMR-tubes were used. The sample volume was 1.71 ml, containing 100 µl ^2H_2O for locking the magnetic field. The samples were made oxygen free by four cycles of evacuating and filling with argon. Between 60000 and 80000 scans were recorded for spectra from microsomal incubations. For urine spectra between 2000 and 3000 scans were recorded.
Chemical shifts are reported relative to $CFCl_3$ [20].

Concentrations of the various metabolites observed in the ^{19}F-NMR spectra were determined by comparison of the integrals of their ^{19}F-NMR resonances to the integral from the ^{19}F-NMR resonance of parafluorobenzoic acid, added to each sample as an internal standard.

Molecular orbital computer calculations.

Computer calculations were performed on a Silicon Graphics Iris 4D/85 using Quanta/Charmm (Polygen inc., U.K.). The semi-empirical molecular orbital method was used, applying the AM1 Hamiltonian from the AMPAC program (Quantum Chemistry Program Exchange no 506) (Indiana University, Bloomington, IN, USA) [21]. All calculations were carried out with PRECISE criteria. For all calculations the self-consistent field was achieved. Geometries were optimized for all bond lengths, bond angles and torsion angles using the Fletcher-Powell criteria.

The frontier electron densities of the monofluoroanilines were calculated as indicated by Fukui [22] to assess the contribution of the occupied orbital just below the HOMO, *i.e.* HOMO-1, and the unoccupied orbital above the LUMO, *i.e.* LUMO+1.

In this study, the outcomes of the *in vacuo* AM1 calculations are related to the electronic behaviour of these substrates in the relative hydrophobic environment of the active site pocket of the cytochromes P450. Due to solvation effects and a different dielectric constant, the intrinsic properties of the compounds might be influenced. However, it is assumed that this phenomenon not influences the relative difference of parameters between a series of closely related compounds, like the monofluoroanilines. The outcomes of these *in vacuo* computer calculations can thus be used as an approach to study relative differences within this series of related compounds.

RESULTS.

Identification of urine metabolites of monofluoroanilines.

The *in vivo* biotransformation of the monofluoroanilines was studied by ^{19}F-NMR analysis of the 24-h urine of rats exposed to these compounds. Figure 2 presents the ^{19}F-NMR spectra obtained. The ^{19}F-NMR chemical shifts were identified under our standard experimental conditions (0.1 M potassium phosphate, pH 7.6, 1% DMSO, 7°C) using commercially available and synthesized reference compounds. Table 1 summarizes the ^{19}F-NMR chemical shifts of the urine metabolites of the monofluoroanilines. Identification of the ^{19}F-NMR resonances of the glucuronidated and sulphated metabolites was based on the hydrolysis of the compounds with arylsulphatase and/or β-glucuronidase. Table 2 presents the results of the enzyme hydrolysis of conjugated metabolites in the urine of monofluoroaniline exposed rats.

The urinary metabolites of 2-fluoroaniline were previously identified by Vervoort *et al.* [18]. Only two minor metabolites remained unidentified at that time. The identity of one of these minor metabolites follows from results of this study. The unidentified resonance at -138.2 ppm can now be ascribed to 3-fluoro-2-aminophenylsulphate. This follows from the observation that arylsulphatase/β-glucuronidase treatment, but not β-glucuronidase, resulted in loss of this signal at -138.2 ppm and in a proportional increase of a resonance at -136.9 ppm, identified as the ^{19}F-NMR signal of 3-fluoro-2-aminophenol using the synthesized reference compound.

The data presented in Table 2 also demonstrate that β-glucuronidase treatment of urine samples from 3-fluoroaniline exposed rats resulted in loss of the resonances at -136.0 ppm and -136.3 ppm with a concomitant proportional increase of the resonances at, respectively -139.7 ppm (2-fluoro-4-acetamidophenol) and -140.1 ppm (2-fluoro-4-aminophenol). This identifies the resonances of both glucuronidated species. Treatment of the urine from 3-fluoroaniline exposed rats with arylsulphatase/β-glucuronidase resulted not only in loss of the signals of the glucuronidated compounds, but also in the disappearance of the resonances at -132.5 and -133.8 ppm giving rise to proportional increase of the resonances at -139.7 ppm (2-fluoro-4-acetamidophenol) and -140.1 ppm (2-fluoro-4-aminophenol). This identifies the resonances of both sulphated species. The resonance at -119.7 ppm was not affected to a significant extent by either of these enzymatic treatments (Table 2). Only treatment with arylsulphatase/β-glucuronidase resulted in a slight decrease of the resonance at -119.7 ppm and a concomitant proportional increase of the resonance at -127.5 ppm (4-fluoro-2-aminophenol). To identify this resonance at -119.7 ppm, the metabolite was purified using BioGel-P2 column chromatography.

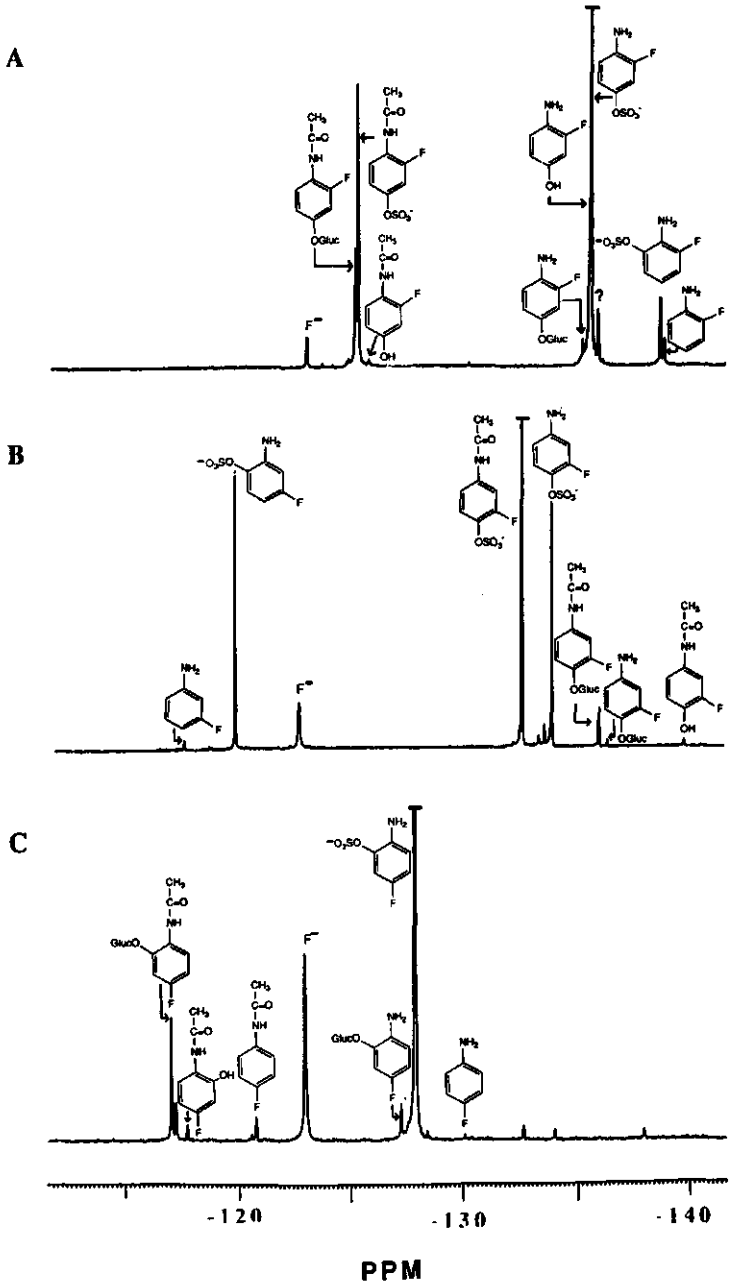

Figure 2 ^{19}F-NMR spectra of 24-hr urine of monofluoroanilines exposed male Wistar rats. (A) 2-fluoroaniline, (B) 3-fluoroaniline, and (C) 4-fluoroaniline. Each animal received 50 mg/kg fluoroaniline dissolved in olive oil.

Table 1: Chemical shift of ^{19}F-NMR resonances of monofluoroaniline metabolites in 0.1 M potassium phosphate, pH 7.6, 7°C. The chemical shifts are relative to $CFCl_3$.

Compound	**Chemical shift (ppm)**
Fluoride anion	-123.0
2-Fluoroaniline	-138.4
2-Fluoroacetanilide	-128.5
3-Fluoro-4-aminophenol	-134.9
3-Fluoro-4-aminophenylglucuronide	-134.7
3-Fluoro-4-aminophenylsulphate	-135.1
3-Fluoro-4-acetamidophenol	-125.7
3-Fluoro-4-acetamidophenylglucuronide	-125.0
3-Fluoro-4-acetamidophenylsulphate	-125.1
3-Fluoro-2-aminophenol	-136.9
3-Fluoro-2-aminophenylsulphate	-138.2
3-Fluoroaniline	-117.6
3-Fluoroacetanilide	-116.5
2-Fluoro-4-aminophenol	-140.1
2-Fluoro-4-aminophenylglucuronide	-136.3
2-Fluoro-4-aminophenylsulphate	-133.8
2-Fluoro-4-acetamidophenol	-139.7
2-Fluoro-4-acetamidophenylglucuronide	-136.0
2-Fluoro-4-acetamidophenylsulphate	-132.5
2-Fluoro-6-aminophenol	-141.3
4-Fluoro-2-aminophenol	-127.5
4-Fluoro-2-aminophenylsulphate	-119.7
4-Fluoroaniline	-130.0
4-Fluoroacetanilide	-121.0
4-Fluoro-N-hydroxyaniline	-125.7
5-Fluoro-2-aminophenol	-127.5
5-Fluoro-2-aminophenylglucuronide	-126.9
5-Fluoro-2-aminophenylsulphate	-127.8
5-Fluoro-2-acetamidophenol	-117.6
5-Fluoro-2-acetamidophenylglucuronide	-117.0

Once the metabolite had been separated from other urine compounds, arylsulphatase/β-glucuronidase treatment, but not β-glucuronidase treatment, resulted in its conversion to 4-fluoro-2-aminophenol. This identifies the resonance at -119.7 ppm as 4-fluoro-2-aminophenylsulphate.

β-Glucuronidase treatment of urine samples from 4-fluoroaniline exposed rats resulted in a loss of the resonances at -117.0 ppm and -126.9 ppm, accompanied by a concomitant proportional increase of the resonances at -117.6 ppm (5-fluoro-2-acetamidophenol) and -127.5 ppm (5-fluoro-2-aminophenol) (Table 2). This

Table 2: Identification of the ^{19}F-NMR resonances of the glucuronidated and sulphated metabolites in the urine of Wistar rats dosed with 2-fluoroaniline, 3-fluoroaniline or 4-fluoroaniline. The urine samples were either untreated (**I**), β-glucuronidase treated (**II**) or arylsulphatase/β-glucuronidase treated (**III**) (N=2). See section Materials and Methods for exact procedure.

^{19}F-NMR resonance (ppm)	**Metabolites in urine (% of total ^{19}F-intensity)**			**Identified as**
	I	**II**	**III**	
2-Fluoroaniline				
-123.0	0	0	0	Fluoride anion
-125.0	10.5	0	0	3-F-4-acetamidophenylglucuronide
-125.1	15.7	17.2	0	3-F-4-acetamidophenylsulphate
-125.7	0.9	10.6	29.5	3-F-4-acetamidophenol
-134.7	4.1	0	0	3-F-4-aminophenylglucuronide
-134.9	0	3.5	55.1	3-F-4-aminophenol
-135.1	49.7	50.0	0	3-F-4-aminophenylsulphate
-135.4	4.48	2.5	2.2	Unknown
-136.9	0	0	6.1	3-F-2-aminophenol
-138.2	6.6	6.2	0.4	3-F-2-aminophenylsulphate
-138.4	6.4	6.6	9.6	2-Fluoroaniline
3-Fluoroaniline				
-117.6	1.2	1.4	1.6	3-Fluoroaniline
-119.7	22.3	21.9	14.9	4-F-2-aminophenylsulphate
-123.0	15.2	14.9	15.8	Fluoride anion
-127.5	0	0.4	8.5	4-F-2-aminophenol
-132.5	37.3	36.5	0	2-F-4-acetamidophenylsulphate
-133.3	1.8	2.1	0	Unknown
-133.6	2.7	2.9	0	Unknown
-133.8	20.0	20.0	0	2-F-4-aminophenylsulphate
-136.0	5.5	0	0	2-F-4-acetamidophenylglucuronide
-136.3	1.1	0	0	2-F-4-aminophenylglucuronide
-139.7	0.6	5.8	40.1	2-F-4-acetamidophenol
-140.1	0	1.2	24.1	2-F-4-aminophenol
4-Fluoroaniline				
-117.0	7.7	0	0	5-F-2-acetamidophenylglucuronide
-117.6	0	8.2	8.4	5-F-2-acetamidophenol
-123.0	11.2	10.9	11.2	Fluoride anion
-126.9	3.1	0	0	5-F-2-aminophenylglucuronide
-127.5	0	3.0	69.1	5-F-2-aminophenol
-127.8	69.6	69.2	1.6	5-F-2-aminophenylsulphate
-130.0	1.5	1.7	1.7	4-Fluoroaniline
-132.5	0.9	0.9	0	Unknown
-133.9	0.5	0.4	0	Unknown
-134.6	0	0	0.9	Unknown
-135.2	1.1	0.9	0	Unknown
-138.0	1.0	0.9	0	Unknown
-139.7	0	0	0.3	Unknown
-144.6	0	0	1.1	Unknown

identifies both glucuronidated species. Arylsulphatase/β-glucuronidase treatment of this urine resulted in a loss of the resonance at -127.8 ppm giving rise to a concomitant proportional increase of the resonance at -127.5 ppm (5-fluoro-2-aminophenol), indicating that the resonance at -127.8 ppm presents 5-fluoro-2-aminophenylsulphate.

In vivo regioselectivity for aromatic hydroxylation of the monofluoroanilines.

Table 3 shows the quantitative urine metabolite patterns of the monofluoroanilines in rats as determined by ^{19}F-NMR urine analysis. The H_2O-extracted and ethanol-extracted faeces of the exposed rats were also analysed by ^{19}F-NMR, but no fluoro-containing metabolites were detected. On the basis of Figure 2 and Table 3 it can be concluded that, during *in vivo* biotransformation, 2-fluoroaniline is predominantly hydroxylated at the *para* C4 position (87.0% of the administered dose) and to a much lesser extent (2.7%) at the *ortho* C6 position. No increased fluoride anion elimination was detected in the urine as a result of the 2-fluoroaniline exposure. This result, in combination with the fact that the urinary recovery is high (98.6 ± 1.2%), indicates that hydroxylation at the fluorinated carbonatom does not occur *in vivo*.

The *in vivo* conversion of 3-fluoroaniline leads to 17.2% *ortho* C6 hydroxylated and 50.2% *para* C4 hydroxylated metabolites. Hydroxylation at the *ortho* C2 position, leading to 2-fluoro-6-aminophenol, was not observed. In the urine of 3-fluoroaniline exposed rats, a considerable amount of fluoride anions was present (7.2% of the dose of 3-fluoroaniline administered).

The 4-fluoroaniline exposed rats excreted predominantly *ortho* C2/6-hydroxylated metabolites in the urine, namely 76.4% of the administered dose. To find out whether the fluoride anions, observed in the urine, represent *para* C4-hydroxylated defluorinated metabolites, the urine was acid hydrolysed to remove the acetyl-, glucuronide- and sulphate-groups from the conjugated metabolites, and the amount of C4-aminophenol was determined by a chemical assay. From the results obtained (data not shown) it appeared that 86.4% of the fluoride anions in the urine could be accounted for by urinary C4-hydroxylated metabolites.

Altogether, regioselectivity for the *in vivo* aromatic C2 : C4 : C6 hydroxylation of the monofluoroanilines was 0.00 : 0.97 : 0.03 for 2-fluoroaniline, 0.00 : 0.74 : 0.26 for 3-fluoroaniline and 0.90 (C2/6) : 0.10 (C4) for 4-fluoroaniline. Thus, the data from the *in vivo* experiments shown in Table 3 clearly demonstrate an influence of the position of the fluoro-substituent on the regioselectivity of the aromatic aniline hydroxylation.

Table 3: Excretion of metabolites (0-24 h) in the urine of male Wistar rats dosed orally with 50 mg 2-, 3- or 4-fluoroaniline/kg bodyweight. Identification and quantification was performed using ^{19}F-NMR. The fluoride anion values were corrected for the amount of fluoride anion present in control urine. Values are presented as mean ± SEM. Values between brackets present ppm values for the unknown metabolites. n=4 for each value.

Derivative	**% of excreted metabolites in 24h urine**		
	2-fluoroaniline	**3-fluoroaniline**	**4-fluoroaniline**
parent compound	5.1 ± 0.4	3.8 ± 0.2	1.3 ± 0.4
fluoride anion	N.D.	8.5 ± 0.2	10.4 ± 0.7
N-acetyl	N.D.	2.6 ± 0.0	1.3 ± 0.1
4-acetamidophenylglucuronide	10.2 ± 0.6	7.6 ± 1.1	*
4-acetamidophenylsulphate	18.7 ± 0.3	29.5 ± 1.6	*
4-aminophenylglucuronide	3.4 ± 0.1	1.4 ± 0.2	*
4-aminophenylsulphate	55.4 ± 0.7	19.0 ± 1.7	*
4-acetamidophenol	0.5 ± 0.0	0.7 ± 0.1	*
4-aminophenol	N.D.	0.9 ± 0.1	*
2-acetamidophenylglucuronide	N.D.	N.D.	11.7 ± 0.9
2-acetamidophenylsulphate	N.D.	N.D.	N.D.
2-aminophenylglucuronide	N.D.	N.D.	2.5 ± 0.1
2-aminophenylsulphate	2.7 ± 0.3	20.2 ± 0.6	66.9 ± 0.9
2-acetamidophenol	N.D.	N.D.	0.9 ± 0.2
2-aminophenol	N.D.	N.D.	N.D.
unknown	3.9 ± 0.1 (-135.4)	2.8 ± 0.1 (-133.3)	1.9 ± 0.3 (-117.1)
		2.5 ± 0.1 (-133.6)	0.4 ± 0.1 (-120.5)
			0.7 ± 0.2 (-128.3)
			0.4 ± 0.0 (-129.4)
			0.8 ± 0.1 (-132.5)
			0.4 ± 0.1 (-133.9)
			0.6 ± 0.0 (-138.0)
24h recovery as % of the administered dose	98.6 ± 1.2	85.0 ± 3.1	93.2 ± 0.9

* ^{19}F-NMR invisible.

N.D. not detected.

The in vitro regioselectivity for the aromatic hydroxylation of monofluoroanilines.

The effect of a fluoro-substituent in the aniline ring on regioselectivity of its aromatic hydroxylation was also studied *in vitro* using microsomal incubations. Figure 3 presents the ^{19}F-NMR spectra of the microsomal conversions of 2-fluoroaniline, 3-fluoroaniline and 4-fluoroaniline. From these results it appears that microsomal conversion of 2-fluoroaniline leads to formation of 3-fluoro-4-

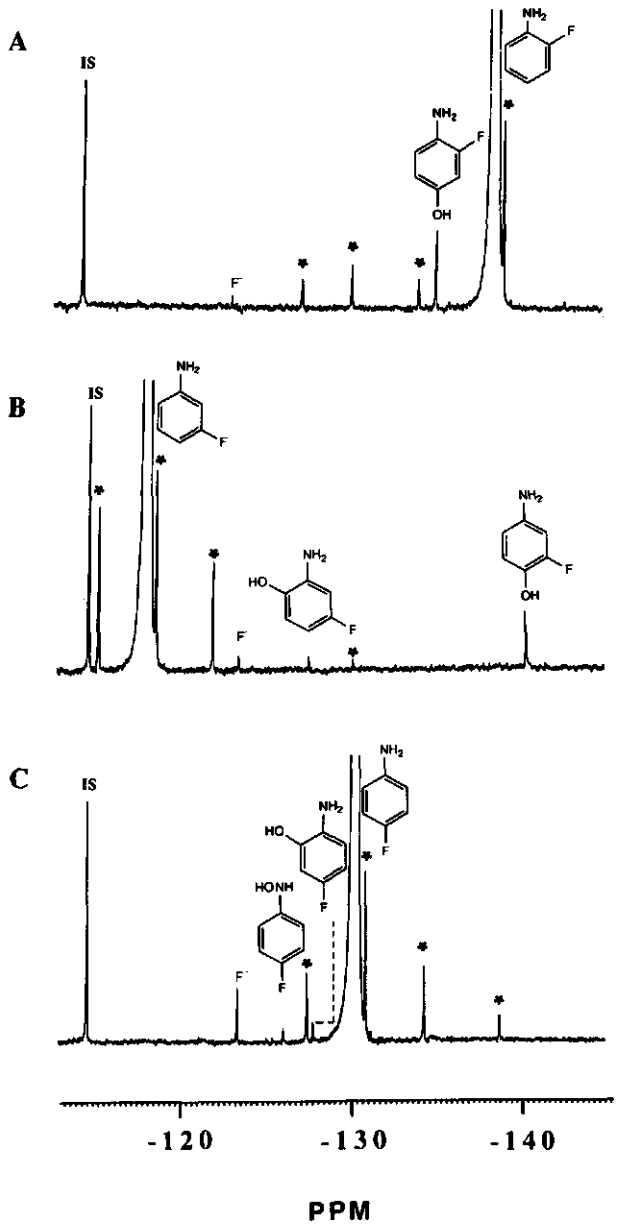

Figure 3 ^{19}F-NMR spectra of liver microsomal incubations with monofluoroanilines. (A) 2-fluoroaniline, (B) 3-fluoroaniline, and (C) 4-fluoroaniline. Liver microsomes were from untreated rats. The resonances marked with an asterisk are due to impurities of the monofluoroanilines, because these resonances are also present in control incubations without NADPH or microsomes. The resonance marked IS is from the internal standard 4-fluorobenzoic acid.

aminophenol as the main metabolite (Figure 3a). No formation of 3-fluoro-2-aminophenol (-136.9 ppm), resulting from *ortho* C6 hydroxylation was observed. Microsomal conversion of 3-fluoroaniline resulted in the metabolites 2-fluoro-4-aminophenol and 4-fluoro-2-aminophenol (Figure 3b). 2-Fluoro-4-aminophenol is the main metabolite, indicating that also *in vitro para* C4-hydroxylation is the favoured route for the biotransformation of 3-fluoroaniline. Formation of 2-fluoro-6-aminophenol (-141.3 ppm), resulting from hydroxylation at C2, was not observed at the detection limit of the measurement (± 1 μM).

The *in vitro* biotransformation of 4-fluoroaniline resulted in the formation of 5-fluoro-2-aminophenol and fluoride anions. By a chemical assay it was determined that these fluoride anions represent C4-aminophenol (data not shown).

Thus, analogous to the *in vivo* conversion, the conversion of monofluoroanilines in an *in vitro* microsomal system results in preferential hydroxylation in the order C4>C6 for 2-fluoroaniline, C4>C6>C2 for 3-fluoroaniline and C2/6>C4 for 4-fluoroaniline.

Involvement of microsomal cytochromes P450 in the regioselectivity for aromatic hydroxylation of 3-fluoroaniline.

Further experiments described in this paper were performed to study the origin of the observed regioselectivities in more detail.

First, the possible involvement of stereoselective influences of the active site of the cytochromes P450 on the regioselectivity of the aromatic hydroxylation was investigated. This was done using 3-fluoroaniline as the substrate.

In Table 4 the C2:C4:C6 hydroxylation ratios are presented for the conversion of 3-fluoroaniline by liver microsomal preparations from rats pretreated with different cytochrome P450 inducers. Although these ratios slightly change dependent on the type of microsomes used, the results in Table 4 clearly demonstrate that C4-hydroxylation of 3-fluoroaniline remains the major route of conversion for all types of microsomal preparations and *ortho* C6 hydroxylation is always significantly favoured over *ortho* C2 hydroxylation. Only aromatic hydroxylation by liver microsomes of isosafrole and 3-methylcholanthrene pretreated rats leads to some *ortho* C2 hydroxylation of 3-fluoroaniline, however to a lesser extent than *ortho* C6 hydroxylation.

In a previous study, the microsomal *para* C4-hydroxylation of aniline and the monofluoroanilines was investigated and it was shown that induction of different cytochromes P450 affects *para* C4-hydroxylation of all three monofluoroanilines and aniline in a similar way [23]. For aniline, it was reported that different purified hepatic cytochrome P450 enzymes are able to hydroxylate this compound, especially

TABLE VI

CALCULATED FRONTIER ORBITAL CHARACTERISTICS OF THE HOMO/HOMO-1 AND LUMO/LUMO+1 OF THE MONOFLUOROANILINES

Compound	HOMO/HOMO-1 frontier orbital density on atom								E_{HOMO} eV	E_{HOMO-1} eV
	C1	C2	C3	C4	C5	C6	N[a]	Rest of the molecule		
2-Fluoroaniline	0.31	0.35	0.03	0.38	0.12	0.18	0.55	0.08	-8.65	-9.68
3-Fluoroaniline	0.26	0.20	0.11	0.47	0.05	0.36	0.51	0.04	-8.75	-9.64
4-Fluoroaniline	0.32	0.23	0.09	0.44	0.09	0.23	0.46	0.14	-8.55	-10.02
	LUMO/LUMO+1 frontier orbital density on atom								E_{LUMO} eV	E_{LUMO+1} eV
	C1	C2	C3	C4	C5	C6	N[a]	Rest of the molecule		
2-Fluoroaniline	0.33	0.36	0.33	0.26	0.35	0.30	0.02	0.05	0.27	0.34
3-Fluoroaniline	0.32	0.30	0.40	0.26	0.32	0.31	0.02	0.07	0.28	0.37
4-Fluoroaniline	0.43	0.26	0.28	0.40	0.29	0.25	0.05	0.04	0.29	0.31

[a]The nitrogen atom is attached to the C1 atom.

al. [25] and Vervoort *et al.* [18], who dosed rats with 2-fluoroaniline and analysed the urinary metabolites using respectively HPLC and ^{19}F-NMR. The present study reports a small amount of *ortho* hydroxylated product, 2-aminophenylsulphate, present as 2.7% of all fluorinated metabolites in the urine of a 2-fluoroaniline exposed rat. Probably one of the unidentified metabolites of Eadsforth *et al.* [25] should be ascribed to this 2-aminophenylsulphate.

4-Fluoroaniline appeared to become predominantly C2/6 hydroxylated (82% of the fluorine intensity present in the urine) and to a minor extent (9%) C4-hydroxylated. Upon C4-hydroxylation, the fluorine atom is preferentially lost from the molecule giving rise to fluoride anion formation by a reaction pathway previously described [26, 27].

3-Fluoroaniline appeared to become hydroxylated at its *para* C4 and *ortho* C6 position, but hardly or not at all at its *ortho* C2 position. For 3-fluoroaniline both *in vitro* and *in vivo* the percentage of metabolites that resulted from *ortho* C6 hydroxylation (11-20%) was higher than the corresponding percentage for 2-fluoroaniline (0-2.7%). This implies that a fluoro-substituent at C3 in the aniline molecule activates the *ortho* C6 position for aromatic hydroxylation compared to the situation with a fluoro-substituent at C2. The difference in C2 and C6 hydroxylation observed for 3-fluoroaniline metabolism is also remarkable. This difference cannot be ascribed to steric hindrance by the fluorine atom attached to C3, preventing hydroxylation at C2. This can be concluded from the fact that the Van der Waals radius of a fluorine substituent (1.35 Å), is very close to that of a hydrogen substituent (1.20 Å).

Additional experiments demonstrated that in *in vitro* incubations with liver microsomes from rats pretreated with different cytochrome P450 inducers and, thus, containing different cytochrome P450 enzyme patterns, the regioselectivity of the aromatic hydroxylation of 3-fluoroaniline was not significantly influenced, whereas total conversion was influenced by a factor of only 4.7 at most. This eliminates the possibility that the regioselectivity is predominantly dictated by the way of substrate binding to the active site of the cytochrome P450, because it is highly unlikely that all the different cytochromes P450 dictate the juxtaposition of this relative small substrate in their hydrophobic active site in a similar way. It also eliminates the possibility that the various hydroxylated monofluoroaniline products are mainly formed by different cytochrome P450 enzymes, because in such a case induction of different P450 patterns would be expected to change the relative contribution of the various hydroxylated products to the metabolite pattern more significantly than was observed. This conclusion is further supported by data from Furuya *et al.* [28] who reported that C2, C4 and C6 hydroxylated metabolites from acetanilide could all be formed by one cytochrome P450 (P450 IA2) expressed in yeast.

Further experiments described in the present study were undertaken to investigate whether the origin of the observed differences in regioselectivity for the monofluoroanilines could be ascribed to intrinsic electronic characteristics of the substrates. As outlined in Figure 1 the kind of electronic characteristics that will determine the regioselectivity varies with the mechanism for the cytochrome P450 dependent hydroxylation. When the reaction proceeds by hydrogen or electron abstaction from the amino moiety, regioselectivity will be influenced by the radical distribution of the NH• radical formed. Whereas a reaction proceeding by addition of the $(FeO)^{3+}$ intermediate in the active site of the P450 will be directed by the density distribution of one of the frontier orbitals. Results from molecular orbital calculations clearly demonstrate that nor the spin distribution in the 3-fluoroaniline-NH• radical nor the LUMO/LUMO+1 frontier orbital density in 3-fluoroaniline can explain the observed difference in C6 and C2 hydroxylation of the compound. Furthermore, the data on the spin distribution in the 2-fluoroaniline and 3-fluoroaniline NH• radical and the LUMO/LUMO+1 frontier orbital density in 2-fluoroaniline and 3-fluoraniline also do not clearly explain the activation of the C6 position for hydroxylation when the fluoro-substituent is at C3 instead of C2. Even when an interaction of the $(FeO)^{3+}$ SOMO of cytochrome P450 with the aniline LUMO/LUMO+1, followed by formation of an epoxide as an intermediate is considered, the LUMO/LUMO+1 densities cannot explain the preferential hydroxylation of C6 over C2 in 3-fluoroaniline.

Additional results demonstrated that both these phenomena are much better explained by the calculated HOMO/HOMO-1 frontier orbital density distribution of the monofluoroaniline molecules. In 3-fluoroaniline, the HOMO/HOMO-1 frontier orbital density at C6 is 2.0 times higher than the corresponding value in 2-fluoroaniline, while the energies of the HOMO and HOMO-1 are almost the same for 2-fluoroaniline and 3-fluoroaniline. From this it follows that, based on these HOMO/HOMO-1 densities, in 3-fluoroaniline compared to 2-fluoroaniline the C6 position is activated for hydroxylation by a σ-addition mechanism. The observed difference in 3-fluoroaniline C2 and C6 hydroxylation can also be elegantly explained by the difference in HOMO/HOMO-1 density at these positions, being 0.20 and 0.36 respectively.

In vivo formation of N-acetylated aminophenols might proceed through a cytochrome P450 dependent hydroxylation of the fluoroanilines, followed by N-acetylation of the hydroxylated product. However, formation of these metabolites can also result from N-acetylation followed by cytochrome P450 dependent hydroxylation of the N-acetylfluoroanilines. This implies that the regioselectivity of the aromatic hydroxylation would also be dictated by molecular orbital characteristics of the N-acetylfluoroanilines. For this reason, molecular orbital

calculations as the ones presented in Table 5 and 6 for the monofluoroanilines, were performed for their N-acetylated derivatives. The results obtained (data not shown), show similar SOMO characteristics of the corresponding N-acetyl radical resulting from hydrogen abstraction and also similar results for the frontier orbital density distributions of the N-acetylated monofluoroaniline derivatives as for their non-acetylated analogues. From this result it is concluded that, even if part of the *in vivo* conversion proceeds through N-acetylation as the first step, HOMO/HOMO-1 characteristics of the substrates for the cytochrome P-450 dependent conversion still provide the best explanation for the regioselectivity observed for the aromatic hydroxylation.

Because the HOMO/HOMO-1 frontier orbital densities in the monofluoroaniline molecules explain the observed differences in regioselectivity for the hydroxylation in a better way than the LUMO/LUMO+1 frontier orbital densities of the fluoroanilines and the spin densities in their corresponding NH• radicals, it is concluded that the aromatic hydroxylation of the monofluoroanilines proceeds predominantly by the σ-addition mechanism and not by an initial hydrogen or electron abstraction from the amino moiety as suggested before for arylamines [27,29]. In addition, because the interaction between the $(FeO)^{3+}$ intermediate in the active site of the cytochrome P450 and the aniline can be described on the basis of an interaction of the $(FeO)^{3+}$ SOMO with the aniline HOMO/HOMO-1, the $(FeO)^{3+}$ attack can even be classified as electrophilic.

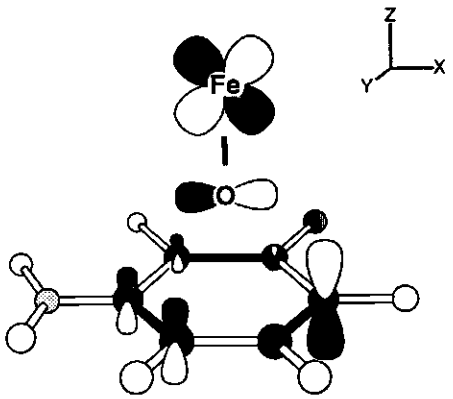

Figure 4 Schematic presentation of the interaction of the HOMO of 3-fluoroaniline with the d_{xz}-p_x SOMO of the $(FeO)^{3+}$ intermediate of cytochrome P450. A similar orbital interaction might occur in the yz plane [see Ref. 7].

nitrogen; carbon; hydrogen; and fluor.

Finally, the question can be addressed whether hydroxylation of the monofluoroanilines at the *ortho* and *para* positions requires fast rotation of the substrate molecule in the active site of the cytochrome P450. Such a rotation would be in contradiction to results from ^{1}H-NMR studies on the longitudinal relaxation behaviour of protons of paracetamol [30] or acetanilide [31] in the active site of cytochrome P450.

However, from the molecular orbital calculations of the present study it follows that the monofluoroaniline HOMO orbitals are π-type orbitals, as schematically presented for 3-fluoroaniline in Figure 4.

If the aniline were positioned in the active site with the $(FeO)^{3+}$ axis perpendicular to its aromatic ring, the interaction of the aniline HOMO with the $(FeO)^{3+}$ d_{xz}-p_x as the SOMO orbital [32] might occur as depicted in Figure 4. An interaction of the aniline HOMO with the $(FeO)^{3+}$ d_{yz}-p_y as the SOMO orbital is also possible, because the unpaired electron can be present in either of these $(FeO)^{3+}$ SOMO orbitals. In this case, the interaction of the $(FeO)^{3+}$ at the *ortho* and *para* positions of the aniline substrate becomes feasible without the requirement for fast rotation of the substrate in the active site.

In conclusion, the results of the present study indicate that the best working hypothesis for further research is, that the cytochrome P450 dependent aromatic hydroxylation of monofluoroanilines proceeds predominantly by the σ-addition mechanism initiated by an electrophilic attack of the $(FeO)^{3+}$ on the aniline molecule.

Acknowledgements.

The authors gratefully acknowledge Mr J. Haas for assistance with animal handling. This study was supported by the Netherlands Organisation for the Advancement of Scientific Research (N.W.O.).

REFERENCES.

1 J.W. Gorrod and D. Manson, The metabolism of aromatic amines, *Xenobiotica* **16**, 933-955, 1986.

2 J.N. Smith and R.T. Williams, Studies in detoxication: the fate of aniline in the rabbit, *Biochem. J.* **44**, 242-250, 1949.

3 D.V. Parke, Studies in detoxication: the metabolism of [^{14}C]-aniline in the rabbit and other animals, *Biochem. J.* **77**, 493-503, 1960.

4 D.J. McCarthy, W.R. Waud, R.F. Struck and D.L. Hill, Disposition and metabolism of

aniline in Fischer 344 rats and C57BL/6 x C3H F_1 mice, *Cancer Res.* **45**, 174-180, 1985.

5 R.N. Armstrong, Enzyme-catalyzed detoxification reactions: mechanism and stereochemistry, *CRC Crit. Rev. Biochem.* **22**, 39-88, 1987.

6 F.P. Guengerich and T.L. MacDonald, Mechanisms of cytochrome P-450 catalysis, *FASEB J.* **4**, 2453-2459, 1990.

7 P.R. Ortiz de Montellano (ed.), Oxygen activation and transfer, in: Cytochrome P-450: Structure, Mechanism and Biochemistry, Plenum Press, New York, 217-271, 1986.

8 I. Fleming (ed.), Radical reactions, in: Frontier Orbitals and Organic Chemical Reactions, John Wiley & Sons, New York, 182-186, 1989.

9 R.E.White, M-B McCarthy, K.D. Egeberg and S.G. Sligar, Regioselectivity in the cytochromes P-450: Control by protein constraints and by chemical reactivities, *Arch. Biochem. and Biophys.* **228**, 493-502, 1984.

10 A.J. Vogel, in: B.S. Furniss, A.J. Hannaford, P.W.G. Smith and A.R. Tatchell (eds.), Vogel's Textbook of Practical Organic Chemistry, Longman Scientific & Technical, London, 978, 1989.

11 M.V. Bhatt and S.U. Kulkarni, Cleavage of ethers, Synthesis, 249-282, 1983.

12 A.J. Vogel,in: B.S. Furniss, A.J. Hannaford, P.W.G. Smith and A.R. Tatchell (eds.), Vogel's Textbook of Practical Organic Chemistry, Longman Scientific & Technical, London, 684, 1978.

13 G.H. Coleman, C.M. McClosky and F.A. Stuart, Nitrosobenzene, *Org. Synthesis* **25**, 80-83, 1946.

14 T. Omura and R. Sato, The carbon monoxide pigment of liver microsomes, I. Evidence for its haemoprotein nature, *J. Biol. Chem.* **239**, 2370-2378, 1964.

15 O.H. Lowry, N.J. Rosebrough , A.L. Farr and A.J. Randall, Protein measurements with Folin phenol reagent, *J. Biol. Chem.* **193**, 265-275, 1951.

16 B.B. Brodie and J. Axelrod, The estimaton of acetanilide and its metabolic products, aniline, N-acetyl p-aminophenol and p-aminophenol (free and conjugated) in biological fluids and tissues, *J. Pharmacol. Exp. Ther.* **94**, 22-28, 1948.

17 I.M.C.M. Rietjens, J. Koerts, S. Boeren and J. Vervoort, Biosynthesis and chemical determination of polyfluoro-4-hydroxyanilines, *Recl. Trav. Chim. Pays-Bas* **110**, 216-221, 1991.

18 J. Vervoort, P.A. De Jager,J. Steenbergen and I.M.C.M. Rietjens, Development of a ^{19}F-n.m.r. method for studies on the in vivo and in vitro metabolism of 2-fluoroaniline, *Xenobiotica* **20**, 657-670, 1990.

19 A.J. Shaka, J. Keeler and R. Freeman, Evaluation of a new broad band decoupling sequence: Waltz 16, *J. Magn. Res.* **53**, 313-340, 1983.

20 V. Wray, in: G.A. Webb (ed.), Annual Reports on NMR Spectroscopy, Vol. 14, Academic Press, London, 252, 1983.

21 M.J.S. Dewar, E.G. Zoebisch, E.F. Healy and J.J. Stewart, AM1: A new general purpose

electrons of the substrate, this attack is no longer the rate-limiting step of the reaction. Additional results of the present study demonstrate that the apparent Michaelis constant K_m^s of the NADPH/oxygen-supported 4-hydroxylation of the anilines decreases with increasing hydrophobicity of the aniline derivatives. Because the spectral dissociation constant K_d^s of the aniline-cytochrome P450 complex appeared to be severalfold lower than the K_m^s, it was concluded that other parameters than binding, influence the K_m^s of the cytochrome P450-catalyzed aniline 4-hydroxylation. In conclusion, the present paper presents a MO-QSAR for the cytochrome P450 catalyzed conversion of a series of aniline derivatives. The implications of these findings for the catalytic cycle of cytochrome P450 are being discussed.

INTRODUCTION.

Cytochromes P450 play an important role in the monooxygenation of aromatic xenobiotics. The present study focuses on the cytochrome P450-catalyzed conversion of halogenated anilines. Aniline derivatives are used in industry for the synthesis of agrochemicals and pigments [1]. Their cytochrome P450-catalyzed conversion is known to result in both detoxification as well as in bioactivation. Bioactivation can result, for example, from the cytochrome P450-catalyzed arylamine N-hydroxylation [2, 3] or from the cytochrome P450-catalyzed oxidative dehalogenation of 4-halogenated anilines, resulting in formation of electrophilic reactive quinoneimines as the primary metabolites [4]. Cytochrome P450-dependent monooxygenation of anilines with a non-halogenated position *para* with respect to the amino moiety results in formation of 4-aminophenols as the primary metabolites. 4-Aminophenol can either be conjugated and be excreted into urine [5, 6] or bile [7] and/or act as an acute nephrotoxin producing severe necrosis of the proximal tubuli [5, 6, 8, 9].

Regarding the exposure of mammals to halogenated anilines as a consequence of environmental pollution, it is reasonable to assume that these xenobiotics are present at a rather low concentration in the mammalian body. The capacity of the cytochrome

[1]**Abbreviations**: MO-QSAR, molecular orbital-based quantitative structure-activity relationship; HXO, hypohalous acid (for example, HClO = hypochlorous acid); SOMO, singly occupied molecular orbital; HOMO, highest occupied molecular orbital; HOMO-1, first occupied molecular orbital at the highest energy level below the HOMO; E(HOMO), energy of the HOMO; E_a, activation energy; TCA, trichloroacetic acid. Definitions: K_m^s, apparent Michaelis constant K_m for aniline derivatives in mM; K_d^s, apparent K_d of the cytochrome P450-substrate complex in mM; k_{cat}^s, apparent maximum velocity in nmol converted per nmol cytochrome P450 per minute; ε, molar extinction coefficient in $mM^{-1} \cdot cm^{-1}$.

P450 enzyme system for 4-hydroxylation of a homologous series of halogenated anilines present at subsaturating substrate concentrations can be characterized by and will be dependent on both k_{cat} and K_m [10]. Thus, insight into possibilities for prediction of kinetic parameters will provide insight in possibilities for prediction of conversion characteristics of these aniline derivatives.

Therefore, the objective of the present study was to investigate whether physico-chemical and/or electronic characteristics of a homologous series of aniline derivatives provide a basis to obtain molecular orbital based quantitative structure-activity relationships (MO-QSAR's)[1] for the kinetic characteristics of their 4-hydroxylation by the cytochromes P450.

Anilines with a non-halogenated 4-position were used as the model compounds. Aniline derivatives with a halogenated 4-position were not included, because the cytochrome P450-catalyzed 4-hydroxylation of an aniline with a halogenated 4-position was demonstrated previously to proceed by a reaction pathway different from that of an aniline with a non-halogenated 4-position [4].

MATERIALS AND METHODS.

Chemicals.

4-Aminophenol was obtained from Aldrich (Steinheim, FRG). Phenol and 2-iodophenol were purchased from Merck (Darmstadt, FRG). 2-Fluoro-, 3-fluoro-, 2-chloro, 3-chloro-, 2-bromo-, 3-bromo- and 3-iodophenol were from Janssen Chimica (Beerse, Belgium). Aniline, 2-fluoroaniline, 3-fluoroaniline, 2-chloroaniline, 3-chloroaniline, 2-bromoaniline, 3-bromoaniline, 2-iodoaniline, 3-iodoaniline, 2,6-difluoroaniline, 2,5-difluoroaniline, 2,3-difluoroaniline, 3,5-difluoroaniline, 2,3,6-trifluoroaniline and 2,3,5,6,-tetrafluoroaniline were also purchased from Janssen Chimica. The purity of all compounds was >98%. Iodosobenzene was synthesized by the base-catalyzed hydrolysis of diacetoxyiodobenzene (Fluka, Switzerland), essentially as described by Saltzman and Sharefkin [11], and added to the incubations from a 20 mM sonicated suspension in 10% Me_2SO in demineralized water.

The biosynthesis of polyfluoroaminophenols.

3,5-Difluoro-, 2,6-difluoro-, 2,3-difluoro-, 2,5-difluoro-, 2,3,5-trifluoro- and 2,3,5,6-tetrafluoro-4-aminophenol were prepared by biosynthesis as follows. Male Wistar rats (300-350 g) were housed individually in metabolism cages. The animals were given food and water *ad libitum*. The rats were orally dosed with 100 mg of the appropriate polyfluoroaniline (respectively 2,6-difluoro-, 3,5-difluoro-, 2,3-difluoro-, 2,5-difluoro-, 2,3,6-trifluoro- and 2,3,5,6-tetrafluoroaniline) per kg body weight in

olive oil. The urine was collected for 48 h after oral dosing. The N-acetyl, glucuronide, and sulphate moieties were removed from the urinary aminophenol conjugates by acid hydrolysis, performed by the addition of 1 volume of 12 N HCl to 10 volumes of the urine sample, followed by heating at 100°C for 30 minutes. After hydrolysis the solution was neutralized with 12N NaOH and the polyfluoro-4-aminophenols were isolated from the mixture by extraction into ethyl acetate. The solvent was removed by evaporation, and the residue was further purified on silicagel 60 (70-230 mesh) (Merck) using a mixture of ethyl acetate-ethanol-acetic acid (15:3:2 by v/v) as eluent. The fractions were analyzed using ^{19}F-NMR, the polyfluoro-4-aminophenol-containing fractions were pooled, and the concentration of the fluorinated 4-aminophenols was determined using ^{19}F-NMR. The stock solutions of the 4-aminophenols thus obtained were immediately used for the determination of molar extinction coefficients in the chemical assay for 4-aminophenol (see hereafter). The purity of the polyfluoro-4-aminophenols was > 95% as determined by ^{19}F-NMR and > 85 % on the basis of HPLC analysis with UV detection at 240 nm. The identity of the biosynthetized 4-aminophenols was derived from ^{19}F-NMR and ^{1}H-NMR spectral characteristics. 2,3-Difluoro-4-aminophenol: ^{19}F-NMR (0.1 M potassium phosphate pH 7.6, relative to $CFCl_3$)(ppm): -160.5 (F3)(dd, $^{3}J_{F3\text{-}F2}$ = 20.0 Hz, $^{4}J_{F3\text{-}H5}$ = 9.0 Hz), -165.3 (F2)(dd, $^{3}J_{F2\text{-}F3}$ = 20.0 Hz, $^{4}J_{F2\text{-}H6}$ = 9.6 Hz) and ^{1}H-NMR (acetone-*d6*, relative to acetone)(ppm): 6.55 (H5)(m, $^{3}J_{H5\text{-}H6}$ = 9.0 Hz, $^{4}J_{H5\text{-}F3}$ = 9.0 Hz, $^{5}J_{H5\text{-}F2}$ = 2.5 Hz), 6.46 (H6)(m, $^{3}J_{H6\text{-}H5}$ = 9.0 Hz, $^{4}J_{H6\text{-}F2}$ = 9.6 Hz, $^{5}J_{H6\text{-}F3}$ = 2.5 Hz); 2,5-difluoro-4-aminophenol: ^{19}F-NMR (0.1 M potassium phosphate pH 7.6, relative to $CFCl_3$)(ppm): -141.4 (F5)(m, $^{3}J_{F5\text{-}H6}$ = 11.5 Hz, $^{4}J_{F5\text{-}H3}$ = 8.0 Hz, $^{5}J_{F5\text{-}F2}$ = 15.0 Hz,), -146.0 (F2)(m, $^{3}J_{F2\text{-}H3}$ = 12.0 Hz, $^{4}J_{F2\text{-}H6}$ = 8.0 Hz, $^{5}J_{F2\text{-}F5}$ = 15.0 Hz) and ^{1}H-NMR (acetone-*d6*, relative to acetone)(ppm): 6.64 (H3)(dd, $^{3}J_{H3\text{-}F2}$ = 12.0 Hz, $^{4}J_{H3\text{-}F5}$ = 8.0 Hz), 6.61 (H6)(dd, $^{3}J_{H6\text{-}F5}$ = 11.5 Hz, $^{4}J_{H6\text{-}F2}$ = 8.0 Hz); 3,5-difluoro-4-aminophenol: ^{19}F-NMR (0.1 M potassium phosphate pH 7.6, relative to $CFCl_3$)(ppm): -133.7 (F3/F5)(d, $^{3}J_{F3/F5\text{-}H2/H6}$ = 9.5 Hz) and ^{1}H-NMR (acetone-*d6*, relative to acetone)(ppm): 6.38 (H2/H6)(d, $^{3}J_{H2/H6\text{-}F3/F5}$ = 9.5 Hz); 2,6-difluoro-4-aminophenol: ^{19}F-NMR (0.1 M potassium phosphate pH 7.6, relative to $CFCl_3$)(ppm): -137.8 (F2/F6)(d, $^{3}J_{F2/F6\text{-}H3/H5}$ = 10.0 Hz) and ^{1}H-NMR (acetone-*d6*, relative to acetone)(ppm): 6.24 (H3/H5)(d, $^{3}J_{H3/H5\text{-}F2/F6}$ = 10.0 Hz); 2,3,5-trifluoro-4-aminophenol: ^{19}F-NMR (0.1 M potassium phosphate pH 7.6, relative to $CFCl_3$)(ppm): -140.7 (F5)(m, $^{3}J_{F5\text{-}H6}$ = 10.5 Hz, $^{4}J_{F5\text{-}F3}$ = 10.0 Hz, $^{5}J_{F5\text{-}F2}$ = 11.0 Hz), -158.5 (F3)(m, $^{3}J_{F3\text{-}F2}$ = 20.5 Hz, $^{4}J_{F3\text{-}F5}$ = 10.0 Hz, $^{5}J_{F3\text{-}H6}$ = 2.5 Hz), -171.0 (F2)(m, $^{3}J_{F2\text{-}F3}$ = 20.5 Hz, $^{4}J_{F2\text{-}H6}$ = 8.0 Hz, $^{5}J_{F2\text{-}F5}$ = 11.0 Hz) and ^{1}H-NMR (acetone-*d6*, relative to acetone)(ppm): 6.54 (H6)(m, $^{3}J_{H6\text{-}F5}$ = 10.5 Hz, $^{4}J_{H6\text{-}F2}$ = 8.0 Hz, $^{5}J_{H6\text{-}F3}$ = 2.5 Hz); 2,3,5,6-tetrafluoro-4-aminophenol: ^{19}F-NMR (0.1 M potassium phosphate pH 7.6, relative to $CFCl_3$)(ppm): -167.6 (F3/F5)(d, $^{3}J_{F3/F5\text{-}}$

$_{F2/F6}$ = 20.0 Hz), -171.4 (F2/F6)(d, $^3J_{F2/F6\text{-}F3/F5}$ = 20.0 Hz) and ^{1}H-NMR (acetone-d_6, relative to acetone)(ppm): ^{1}H-NMR resonances were not observed in the aromatic region.

Preparation of microsomes.

Microsomes were prepared from the perfused livers of male Wistar rats (ca. 300 g), which were untreated or treated with inducers of the cytochrome P450 enzymes, namely phenobarbital (Brocacef, Maarssen, The Netherlands), β-naphthoflavone (Sigma, St Louis, USA), isosafrole (Janssen, Beerse, Belgium), and acetone (Merck, Darmstadt, FRG), essentially as described before [12]. Cytochrome P450 contents were determined as described by Omura and Sato [13]. Protein was assayed by the method of Lowry [14] using bovine serum albumin (Sigma) as the standard.

Microsomal incubations.

Microsomal incubations were carried out at 37°C in 0.1 M potassium phosphate (pH 7.6) containing 1 μM microsomal cytochrome P450 and 0-20 mM (as indicated) (halogenated) aniline added as 1% (v/v) of a stock solution in Me_2SO. The reaction was started by the addition of NADPH or iodosobenzene (both at 1 mM final concentration) and terminated after 10 min (NADPH) or 1 min (iodosobenzene), respectively, by adding 1.0 mL of the reaction mixture to 0.3 mL 20% (w/v) trichloroacetic acid (TCA). The cytochrome P450-mediated microsomal conversion of the aniline derivatives to their 4-aminophenols was observed to be linear in time for at least 10 minutes in a NADPH/O_2-supported reaction and 75 seconds in an iodosobenzene-supported reaction. For the NADPH series control incubations were carried out in the absence of NADPH. For the iodosobenzene series control incubations were carried out for each substrate concentration in the absence of microsomal cytochrome P450. This was done in order to correct for the chemical reaction between iodosobenzene and the aniline substrates also resulting in 4-hydroxylation of the substituted anilines. This correction was 5-40% dependent on the substrate concentration and aniline derivative used.

Chemical detection of 4-aminophenol.

Halogenated 4-aminophenols were determined essentially by the method of Brodie and Axelrod [15]. In short, to 1 mL of TCA-precipitated supernatant were added 100 μL phenol reagent (5% w/v phenol in 2.5 M NaOH) and 200 μL 2.5 M Na_2CO_3. After 60 minutes at room temperature the absorbance at 630 nm was measured. Introduction of a halogen substituent in the indophenol influences its molar extinction coefficient at 630 nm [16]. For this reason the ε_{630nm} of all halogenated 4-

aminophenol-derived indophenols had to be determined to allow quantification of the 4-aminophenol formation for the various halogenated anilines. For the chlorinated, brominated and iodinated 4-aminophenols the respective halogenated indophenols were prepared from the reaction of a suitable halogenated phenol with non-halogenated 4-aminophenol, instead of by the reaction of the non-substituted phenol with the halogenated 4-aminophenol as prescribed by the method of Brodie and Axelrod [15]. Figure 1 schematically presents this approach. For the monohalogenated 4-aminophenols this "reversed" method proved to result in a reliable molar extinction coefficient of the halogenated indophenols (see Results). In short, the molar extinction coefficients of the halogenated indophenols derived from the 2- and 3-halogenated 4-aminophenols were determined by adding respectively 300 µL of 20% TCA, 130 µL of 3- or 2-halogenated phenol reagent (5% w/v halogenated phenol in 2.5 N NaOH) and 260 µL of 2.5 M Na_2CO_3 to 1 mL sample, containing 0-50 µM 4-aminophenol in 1% Me_2SO (v/v) in water. The molar extinction coefficients for the polyfluoroindophenols were determined by the regular method of Brodie and Axelrod [15] using the polyfluorinated 4-aminophenols obtained from biosynthesis.

NMR measurements.

^{19}F-NMR measurements were performed on a Bruker AMX 300 NMR spectrometer essentially as described before by Vervoort *et al.* [17]. Quantification of the fluorinated compounds in the samples was achieved by comparison of the integrals of their ^{19}F-NMR resonances to the integral of the resonance of 4-fluorobenzoic acid, which was added as an internal standard. The splitting patterns of the ^{1}H-NMR and ^{19}F-NMR resonances of the biosynthesized 4-aminophenols dissolved in acetone-d_6 were measured on a Bruker AMX 500 MHz. ^{19}F-NMR measurements were performed using a ^{1}H probehead tuned to the ^{19}F frequency (470.5 MHz).

Determination of K_d^s.

The apparent spectral dissociation constants (K_d^s) of the microsomal cytochromes P450 for a halogenated aniline were determined by spectral analysis of microsomal protein titrated with the substrate according to the method described by Schenkman *et al.* [18]. Liver microsomes from isosafrole-pretreated rats were used, *i.e.*, the same type of microsomes used for the kinetic experiments, because these microsomes showed the highest activity with the aniline-substrates (see Results). A solution of 1 µM microsomal cytochrome P450 in 0.1 M potassium phosphate buffer (pH 7.6) containing 20% glycerol was titrated with aliquots (1-5 µL) of halogenated aniline in 10% Me_2SO in demineralized water at 25°C. In a similar way, the reference sample was titrated with aliquots of a 10% Me_2SO solution without the halogenated aniline. A few minutes after each addition, a difference absorption spectrum was

recorded from 350 nm to 500 nm with a computer-controlled Aminco DW-2000 spectrophotometer. The scan rate was 2 nm s^{-1}. The apparent spectral dissociation constants of the substrates (K_d^s) were determined by fitting the data to the equation $\Delta A = \Delta A_{max} [S] / (K_d^s + [S])$ ($\Delta A = A_{433nm} - A_{405\text{-}410nm}$).

Kinetic analysis.

The apparent Michaelis constant K_m^s (mM) for the aniline substrates and the apparent maximum reaction rate k_{cat}^s (nmol halogenated 4-aminophenol per nmol cytochrome P450 per min) at infinite aniline concentration for the 4-hydroxylation of the aniline-derivatives by cytochrome P450 were determined from fitting the data to the standard Michaelis-Menten equation $v = V_{max} * [S]/(K_m + [S])$ using the program of KaleidaGraph, version 2.0.2. (Abelbeck Software). In spite of its multistep reaction cycle, it appeared possible to analyze the kinetics of the cytochrome P450-catalyzed 4-hydroxylation of the various anilines by Michaelis-Menten kinetics, the correlation coefficient "*r*" of the fits being greater than 0.97 in all cases.

Molecular orbital computer calculations.

Computer calculations were performed on a Silicon Graphics Iris 4D/85 with Quanta/Charmm (Molecular Simulations, UK). The semi-empirical molecular orbital method was used, applying the AM1 Hamiltonian from the AMPAC program (Quantum Chemistry Program Exchange, No. 506, Indiana University, Bloomington, IN). All calculations were carried out with PRECISE criteria. For all calculations the self-consistent field was achieved. Geometries were optimized for all bond lengths, bond angles, and torsion angles with the Fletcher-Powell criteria.

The frontier electron densities for electrophilic attack, calculated from the characteristics of the highest occupied molecular orbital (HOMO) and of the first occupied molecular orbital at the highest energy level below the HOMO (HOMO-1) as indicated by Fukui *et al.* [19], were not significantly different from HOMO densities, because of a relatively large difference between the energy of the HOMO [E(HOMO)] and the E(HOMO-1) for all aniline derivatives used in this study. Therefore, the values of the HOMO were used in this study.

These AM1 molecular orbital calculations generate data for compounds *in vacuo*, while the outcomes of these molecular orbital calculations are related to the electronic behaviour of the substrates in the relative hydrophobic environment of the active site pocket of the cytochromes P450. Solvation effects and a different dielectric constant in the active site of the enzyme might influence the frontier orbital characteristics of the substrates compared to the *in vacuo* situation. However, it is assumed that this phenomenon will not significantly influence the relative differences between parameters of a series of closely related compounds, like the halogenated

anilines. The outcomes of these *in vacuo* computer calculations can thus be used to obtain insight into the relative differences within this series of related substrates of cytochromes P450.

RESULTS.

Determination of the molar extinction coefficients of the halogenated indophenols.

According to the method of Brodie and Axelrod, 4-aminophenols can be quantified by their reaction with excess phenol to give a colored indophenol derivative, with an absorption maximum around 630 nm in a base environment [15]. A precise quantification of halogenated 4-aminophenols requires exact values for the molar extinction coefficients of their corresponding halogenated indophenols in the chemical

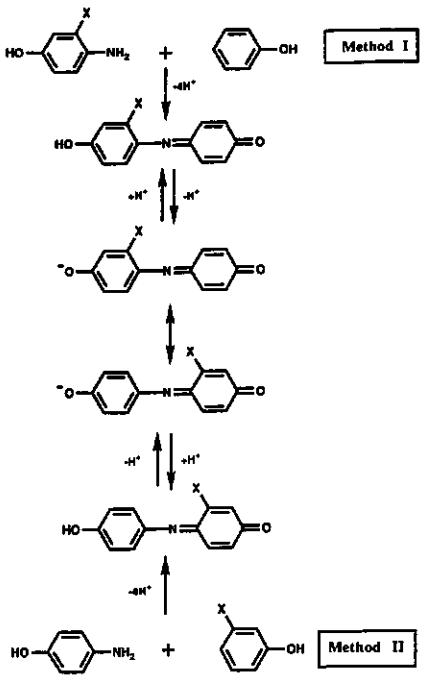

Figure 1: Reaction scheme for the formation of the substituted indophenols by two different methods yielding the same reaction product. Method I represents the method according to Brodie and Axelrod [15]; Method II represents the modified method described in this article. X represents the halogen substituent(s).

assay. For the chlorinated, brominated and iodinated 4-aminophenols, a different approach to determine the molar extinction coefficients of the halogen-substituted indophenols was used. This approach is illustrated in Figure 1. Due to resonance stabilization of the indophenol the reaction product resulting from a reaction of a halogenated 4-aminophenol with excess phenol (Method I) will be similar to the indophenol formed from a reaction of 4-aminophenol with excess of a properly halogenated phenol (Method II). Using this approach, the molar extinction coefficients of the various monohalogenated indophenols were determined using 4-aminophenol calibration samples reacting with an excess of different commercially available halogenated phenols. The values for the molar extinction coefficients thus obtained are presented in Table 1 (Method II). To validate this method, the molar extinction coefficient of the non-halogenated indophenol was determined by both the regular

Table 1: The molar extinction coefficients of the indophenol-derivatives at 630 nm, (I) determined by the regular method of Brodie and Axelrod (Method I, Figure 1), (II) determined by the modified method described in this article (Method II, Figure 1), and (III) obtained from the literature [16, 20].

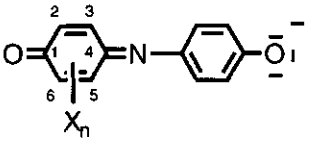

Indophenol	Molar extinction coefficient in $mM^{-1} \cdot cm^{-1}$		
	I	II	III
Parent	30.5	30.5	31.6 [a]
2-Fluoro-	n.d	26.3	26.0 [b]
3-Fluoro-	n.d	26.7	26.0 [b]
2-Chloro-	n.d.	25.9	28.2 [a]
3-Chloro-	n.d.	20.8	22.4 [a]
2-Bromo-	n.d.	25.4	
3-Bromo-	n.d.	18.7	
2-Iodo-	n.d.	27.2	
3-Iodo-	n.d.	18.0	
3,5-Difluoro-	14.5	n.d.	
2,5-Difluoro-	20.0	n.d.	
2,3-Difluoro-	16.8	n.d.	
2,6-Difluoro-	20.0	n.d.	
2,3,5-Trifluoro-	12.5	n.d.	
2,3,5,6-Tetrafluoro-	7.7	n.d.	

[a] The molar extinction coefficients are determined by Corbett [16]. The value for the non-halogenated indophenol was determined at 637 nm instead at 630 nm. [b] These molar extinction coefficients were determined after 45 min. instead of 60 min. [20]. [c] n.d., not determined.

procedure of Brodie and Axelrod (Method I, Table1) and the modified method (Method II, Table 1). Furthermore, the values for the molar extinction coefficients of some of the indophenol-derivatives available in the literature [16] were compared to the values obtained by the modified method (Table 1). From these data it can be concluded that the newly developed "reversed" Method II provides reliable molar extinction coefficients for the monohalogenated 4-aminophenol derived indophenols. For the polyfluorinated 4-aminophenols the molar extinction coefficients were determined by Method I with the biosynthesized fluorinated aminophenols.

Influence of the microsomal cytochrome P450 pattern on the 4-hydroxylation of the halogenated anilines.

Before starting measurements to determine K_m^s and k_{cat}^s characteristics for the cytochrome P450-catalyzed 4-hydroxylation of the aniline derivatives, it was investigated which type of microsomes is best able to catalyze the 4-hydroxylation of these compounds. Figure 2 presents the results of the conversion of the halogenated anilines used in this study at 3 mM substrate concentration by liver microsomes with a different cytochrome P450 enzyme pattern. The 4-hydroxylation reaction is cytochrome P450 mediated as no conversion was observed without NADPH, without microsomes, or in the presence of CO [20]. The results obtained clearly demonstrate

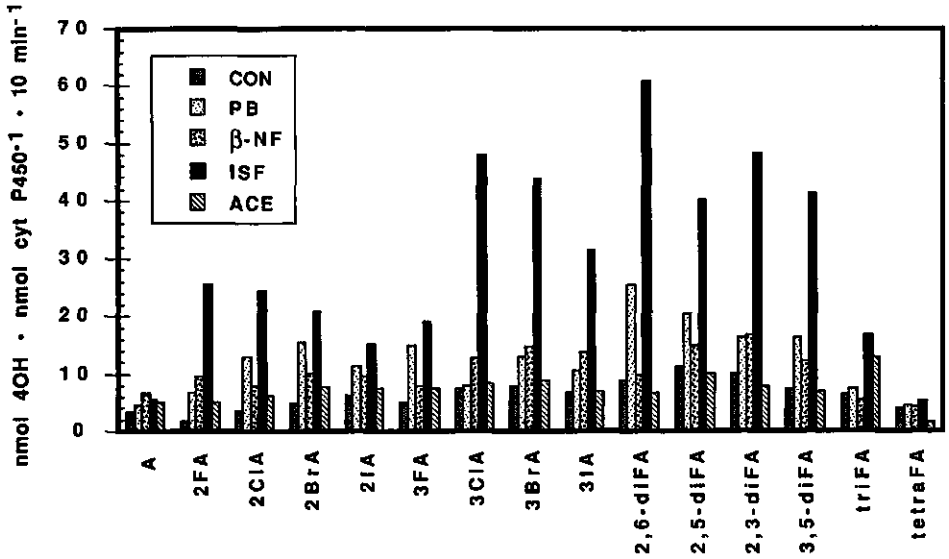

Figure 2: The 4-hydroxylation rate of the aniline-derivatives at a substrate concentration of 3 mM by liver microsomes from untreated rats (CON) [■] and rats which were pretreated with phenobarbital (PB) [▩], β-naphthoflavone (βNF) [▩], isosafrole (ISF) [■] or acetone (ACE) [▨] as cytochrome P450 inducers.

that the 4-hydroxylation for all aniline-derivatives, at a substrate concentration of 3 mM, is highest when liver microsomes of isosafrole (inducer of P450 1A1/1A2)-pretreated animals were used. Liver microsomes of phenobarbital, β-naphthoflavone, or acetone (inducers of respectively P450 2B1/2B2, 1A1 or 2E1)-pretreated animals also showed increased activities compared to liver microsomes from control animals, although to a lesser extent than the liver microsomes from the isosafrole-pretreated animals.

In order to ascertain that the differences in the 4-hydroxylation rate at 3 mM are not due to differences in K_m^s of the different cytochrome P450 preparations for the aniline substrates, further experiments were performed in which, for some of the aniline derivatives, the k_{cat}^s and K_m^s values for their conversion by the various types of microsomes were determined. Table 2 presents the results obtained. The k_{cat}^s values obtained clearly demonstrate that also at saturating substrate concentrations the cytochrome P450-mediated 4-hydroxylation of the aniline substrates is highest for liver microsomes from isosafrole-pretreated rats. On the basis of the highest rates for conversion obtained with liver microsomes of isosafrole-pretreated rats, this microsomal preparation was used for further experiments.

Table 2: The k_{cat}^s and K_m^s for the 4-hydroxylation of 3-substituted anilines by liver microsomes of differently pretreated rats [a].

Substrate	CON	PB	βNF	ISF	ACE
			k_{cat}^s for 4-hydroxylation [b]		
3-fluoroaniline	1.1 ± 0.0 (100)	1.6 ± 0.2 (145)	1.3 ± 0.1(118)	4.9 ± 0.2 (445)	1.2 ± 0.0 (109)
3-chloroaniline	0.9 ± 0.0 (100)	1.4 ± 0.1 (156)	1.5 ± 0.1 (167)	4.6 ± 0.2 (511)	0.9 ± 0.1 (100)
3-bromoaniline	0.9 ± 0.0 (100)	1.1 ± 0.1 (122)	1.6 ± 0.1 (178)	5.1 ± 0.0 (567)	0.9 ± 0.0 (100)
3-iodoaniline	0.7 ± 0.0 (100)	1.1 ± 0.0 (157)	1.6 ± 0.2 (229)	3.8 ± 0.5 (543)	0.7 ± 0.0 (100)
			K_m^s (mM)		
3-fluoroaniline	2.1 ± 0.2	0.4 ± 0.1	1.4 ± 0.2	3.5 ± 0.5	1.4 ± 0.3
3-chloroaniline	0.8 ± 0.1	0.2 ± 0.0	0.3 ± 0.0	0.3 ± 0.0	0.5 ± 0.1
3-bromoaniline	0.8 ± 0.0	0.2 ± 0.0	0.4 ± 0.1	0.3 ± 0.0	0.7 ± 0.1
3-iodoaniline	0.5 ± 0.1	0.4 ± 0.1	0.2 ± 0.0	0.2 ± 0.0	0.3 ± 0.1

[a] Values presented are the mean ± standard error of the mean. The values between parentheses represent % of the values of liver microsomes from untreated rats. Microsomes were from the livers of untreated (CON) and phenobarbital (PB)-, β-naphthoflavone (βNF)-, isosafrole (ISF)- or acetone (ACE)-pretreated rats. [b] In units of nmol halogenated 4-aminophenol per nmol cytochrome P450 per min.

Kinetic parameters of the 4-hydroxylation of halogenated anilines in a NADPH-supported microsomal cytochrome P450 system.

In order to examine to which extent the catalytic parameters K_m^s and k_{cat}^s for the cytochrome P450-mediated 4-hydroxylation of anilines are influenced by their substituent pattern, microsomal incubations with a series of aniline derivatives were performed. The k_{cat}^s and K_m^s obtained for the 4-hydroxylation of the aniline derivatives in a NADPH- and oxygen-supported microsomal cytochrome P450 system are presented in Table 3. The k_{cat}^s values for the cytochrome P450-catalyzed 4-hydroxylation do not differ considerably for the various anilines, except for 2,3,5,6-tetrafluoroaniline, which appeared to become 4-hydroxylated at a relatively low conversion rate compared to that of the other anilines.

In contrast, the K_m^s for the 4-hydroxylation of the various aniline derivatives in a NADPH- and oxygen-supported reaction varies considerably with changes in the substituent pattern (Table 3). These results imply that differences in the catalytic efficiency constant k_{cat}^s/K_m^s - a constant of importance for the in vivo conversion of xenobiotics [10] - for the NADPH- and oxygen-supported microsomal cytochrome P450-mediated 4-hydroxylation of halogenated anilines are mainly caused by differences in the K_m^s value.

Table 3: The K_m^s and k_{cat}^s for the NADPH/O_2- and iodosobenzene-driven microsomal cytochrome P450-mediated 4-hydroxylation of aniline derivatives [a].

	microsomal system supported by			
	NADPH/O_2		iodosobenzene	
Substrate	K_m^s (mM)	k_{cat}^s (min^{-1})	K_m^s (mM)	k_{cat}^s (min^{-1})
aniline	17.0 ± 2.0	5.6 ± 0.2	15.3 ± 3.4	215.0 ± 15.1
2-fluoroaniline	7.4 ± 0.3	6.2 ± 0.2	9.1 ± 0.8	93.8 ± 9.6
2-chloroaniline	0.6 ± 0.3	3.5 ± 0.2	14.3 ± 1.1	129.9 ± 17.8
2-bromoaniline	0.4 ± 0.0	2.8 ± 0.2	9.0 ± 1.2	92.7 ± 2.0
2-iodoaniline	0.2 ± 0.1	2.7 ± 2.3	8.2 ± 0.2	98.1 ± 0.7
3-fluoroaniline	3.5 ± 0.5	4.9 ± 0.2	17.9 ± 2.7	43.7 ± 3.5
3-chloroaniline	0.3 ± 0.0	4.6 ± 0.2	12.6 ± 1.7	44.9 ± 1.7
3-bromoaniline	0.3 ± 0.0	5.1 ± 0.0	8.5 ± 3.6	32.1 ± 1.7
3-iodoaniline	0.2 ± 0.0	3.8 ± 0.5	8.3 ± 2.2	57.2 ± 6.0
2,6-difluoroaniline	2.0 ± 0.3	8.9 ± 0.1	18.8 ± 2.0	27.7 ± 5.8
2,5-difluoroaniline	1.6 ± 0.0	4.4 ± 0.2	15.4 ± 0.5	8.9 ± 0.8
2,3-difluoroaniline	1.6 ± 0.1	9.5 ± 0.4	9.9 ± 2.5	11.4 ± 2.7
3,5-difluoroaniline	1.5 ± 0.3	6.8 ± 0.4	n.q.[b]	n.q.
2,3,6-trifluoroaniline	0.9 ± 0.0	3.2 ± 0.1	11.24 ± 2.3	6.4 ± 2.6
2,3,5,6-tetrafluoroaniline	0.3 ± 0.0	0.4 ± 0.0	n.q.	n.q.

[a] Values presented are the mean ± standard error of the mean (n=2-4).[b] n.q. = not quantified because the amount 4-aminophenol formed in the 1 min. iodosobenzene supported reaction was too low to be accurately quantified (< 1 nmol 4-aminophenol per min).

Binding characteristics of some aniline derivatives to cytochromes P450.

To provide some insight into factors influencing the K_m^s for 4-hydroxylation, the binding interaction of the aniline derivatives with the cytochromes P450 was studied by determining spectral dissociation constants (K_d^s) of the complex between substituted anilines and the cytochromes P450 of isosafrole-induced liver microsomes. In these series of experiments aniline derivatives with a hydrogen, fluorine, chlorine, bromine or iodine at the 3-position were used as the model compounds. Upon binding of these anilines to the cytochromes P450, a characteristic decrease of the high-spin Soret absorbance at 405-410 nm and a concomitant increase of the low-spin absorbance at 433 nm were observed . This so-called type II spectral interaction is generally assumed to result from a direct interaction of the substrate with the heme [18] and was observed for all anilines tested (spectra not shown). The apparent spectral dissociation constants were determined and are summarized in Table 4. Comparison of the apparent K_d^s (Table 4) and K_m^s (Table 3) values demonstrates that the K_m^s values are 6-40 fold higher than the corresponding K_d^s values. This means that not only the binding of these substrates to the cytochromes P450 (K_d^s), but also other steps in the catalytic cytochrome P450 cycle, for example, the electron reduction steps, substrate conversion and/or product release, influence the K_m^s values for the cytochrome P450 mediated 4-hydroxylation.

Table 4: Apparent spectral dissociation constants (K_d^s) of isosafrole-induced liver microsomal cytochromes P450 for 3-substituted anilines.

Substituent at the 3-position of the aniline ring.	**Apparent spectral dissociation constant K_d^s (mM)**
H	0.447 ± 0.022
F	0.088 ± 0.006
Cl	0.012 ± 0.000
Br	0.015 ± 0.003
I	0.032 ± 0.007

[a] Data are presented as the mean ± standard error of the mean (n=2-3).

Relations between substrate characteristics and catalytic characteristics for the NADPH- and oxygen-driven cytochrome P450-mediated 4-hydroxylation of halogenated anilines.

In order to gain insight into factors influencing the conversion characteristics K_m^s and k_{cat} for the cytochrome P450-catalyzed 4-hydroxylation of the aniline-

derivatives relations between catalytic characteristics and substrate characteristics were investigated.

The decrease of K_m^s for the cytochrome P450-mediated 4-hydroxylation of substituted anilines in a NADPH- and oxygen-supported reaction (Table 3) appears to be linked with an increase of the substrate's lipophilicity. From this observation it follows that the lipophilicity of the halogenated anilines is an important factor determining the relative differences in K_m^s between this series of substrates.

The k_{cat}^s values were related to other substrate characteristics, *i.e.*, their so-called frontier orbital characteristics. This can be explained as follows. On the basis of the frontier orbital theory the relative reactivities of different molecules, and, as a result, their chances for conversion, *i.e.*, their k_{cat}^s values, will be dependent on their frontier orbital characteristics [19, 21]. The frontier orbital characteristics known to influence relative differences in reactivity are (i) the frontier orbital density for electrophilic or nucleophilic attack at the reaction centre, and (ii) the energy of the frontier orbital of interest. When the aromatic hydroxylation of the substrates proceeds by an electrophilic attack of the cytochrome P450 $(FeO)^{3+}$ singly occupied molecular orbital (SOMO) on the aromatic substrate, the HOMO characteristics of the substrate are of importance. A high HOMO density on the reaction center and a relatively higher (*i.e.*, less negative) energy of the HOMO can both result in higher reactivity. A stronger interaction between the substrate HOMO and the cytochrome P450 $(FeO)^{3+}$ SOMO will result in a stronger reduction of the activation energy (E_a), which is related to the natural logarithm (ln) of k_{cat}. If an electrophilic attack of the cytochrome P450 $(FeO)^{3+}$ intermediate on the frontier π electrons of the substrate is the rate-limiting factor in their cytochrome P450-catalyzed conversion, a correlation between HOMO parameters of the substrates and k_{cat} for 4-hydroxylation can be expected.

Table 5 presents these HOMO characteristics of the various aniline substrates. The data demonstrate that the E(HOMO) of the anilines varies with the substituent pattern at the aromatic ring. In Figure 3 the ln of the k_{cat}^s for the cytochrome P450-catalyzed 4-hydroxylation of the aniline derivatives is plotted against the corresponding E(HOMO) values. Linear regression analysis reveals the absence of a correlation between these parameters (r=0.49). Only for 2,3,5,6-tetrafluoroaniline the relatively low conversion rate qualitatively corresponds with a relatively low E(HOMO). These results suggest that the electrophilic attack of the cytochrome P450 $(FeO)^{3+}$ intermediate on the substrate's frontier π electrons is not the rate-limiting step for conversion of the anilines in the NADPH/oxygen-supported conversion by cytochromes P450.

Table 5: AM1 calculated frontier orbital characteristics of the aniline-derivatives.

Substrate	E(HOMO) (eV)	HOMO density on the reaction centre C4.
aniline	-8.52	0.24
2-fluoroaniline	-8.65	0.20
2-chloroaniline	-8.62	0.21
2-bromoaniline	-8.67	0.22
2-iodoaniline	-8.65	0.22
3-fluoroaniline	-8.75	0.25
3-chloroaniline	-8.73	0.24
3-bromoaniline	-8.76	0.24
3-iodoaniline	-8.76	0.23
2,6-difluoroaniline	-8.81	0.18
2,5-difluoroaniline	-8.83	0.21
2,3-difluoroaniline	-8.90	0.21
3,5-difluoroaniline	-9.01	0.27
2,3,6-trifluoroaniline	-9.01	0.19
2,3,5,6-tetrafluoroaniline	-9.24	0.21

Cytochromes P450-catalyzed 4-hydroxylation of aniline derivatives using iodosobenzene as an artificial single oxygen source.

In addition to a step involved in substrate conversion other steps of the catalytic P450 cycle may be rate-limiting. The exact nature of the rate-limiting step might even be dependent on the type of substrate converted and the microsomal system applied [22, 23]. In addition to the oxygen transfer from the cytochrome P450 $(FeO)^{3+}$ intermediate to the substrate, the NADPH-cytochrome-reductase mediated electron transfer from NADPH to the cytochrome P450/substrate complex (first electron) or to the one-electron-reduced cytochrome P450/substrate/oxygen complex (second electron), have been reported to represent possible rate-limiting steps [22-25]. It is known that several factors, for instance, a conformational change of the enzyme induced by substrate binding, an increase in redox potential, or a shift in spin equilibrium upon substrate binding may influence the electron flow from the NADPH-dependent cytochrome P450 reductase to the cytochrome P450-substrate complex [22, 26-27]. If the reduction step is the rate-limiting step in the $NADPH/O_2$ driven cytochrome P450-mediated 4-hydroxylation of the aniline derivatives, this would explain why the actual overall rate varies (slightly) from one substrate to another. To circumvent these possible rate-limiting electron-donating steps, artificial oxygen donors can be used to create the cytochrome P450 $(FeO)^{3+}$ species and support the substrate oxygenation by the cytochrome P450 enzyme. In this study iodosobenzene was used as the artificial oxygen donor because it is well accepted that the iodosobenzene-

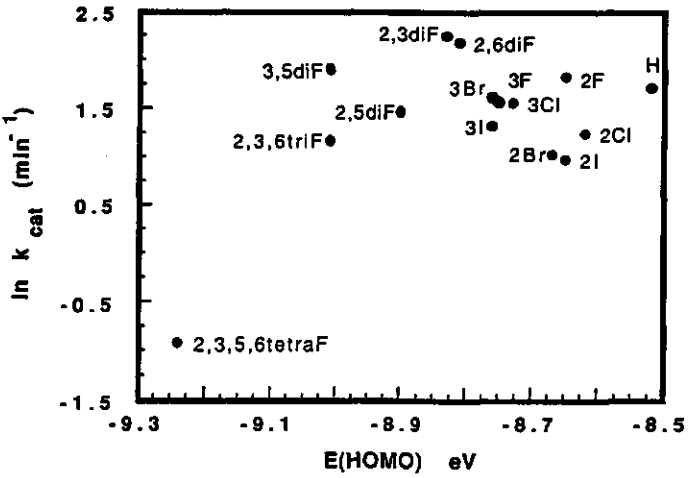

Figure 3: ln k_{cat}^{S} for the NADPH/O_2-supported microsomal 4-hydroxylation of a series of halogenated anilines plotted against their E(HOMO) values (r=0.49). Liver microsomes from isosafrole-pretreated rats were used. Theoretically k_{cat} should be divided by h/k•T to make the parameter dimensionless before calculating the natural logarithm. However, because this would result in a change of the y-axis values by a constant factor, this theoretically appropriate correction was omitted and the natural logarithm of k_{cat} was plotted.

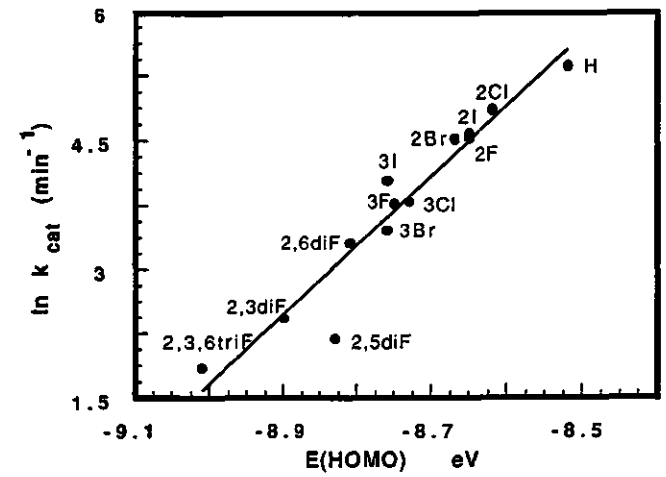

Figure 4: Correlation of the ln k_{cat}^{S} for the 4-hydroxylation of halogenated anilines in an iodosobenzene supported microsomal cytochrome P450 reaction with the E(HOMO) values of these substrates (r=0.96).

supported reaction proceeds by the same active cytochrome P450 $(FeO)^{3+}$ species as the NADPH/oxygen-driven conversion [28]. In addition to the k_{cat}^S and K_m^S values of the NADPH/oxygen driven aniline 4-hydroxylation Table 3 also presents the k_{cat}^S and K_m^S values obtained when the 4-hydroxylation of the halogenated anilines by liver microsomes from isosafrole-pretreated rats was studied in an iodosobenzene-driven reaction. The data demonstrate that the K_m^S values for the iodosobenzene-driven 4-hydroxylation are higher as compared to the NADPH/oxygen-supported conversion. Furthermore, the results presented in Table 3 demonstrate that the turnover rates for the iodosobenzene-driven reactions are several times higher than the ones observed for the NADPH/oxygen-driven cytochrome P450 conversions. These considerably increased k_{cat}^S values indicate that the rate-determining step during NADPH/oxygen-driven microsomal cytochrome P450-mediated 4-hydroxylation of the aniline derivatives is indeed circumvented in the iodosobenzene-driven system. The results in Table 3, also demonstrate that upon the use of iodosobenzene as the artificial oxygen donor considerable differences in the k_{cat}^S for 4-hydroxylation emerge for the various aniline derivatives. The variation observed is much larger than that obtained for the NADPH/oxygen-supported cytochrome P450 reaction (Table 3).

In Figure 4, the iodosobenzene-supported ln k_{cat}^S values for the 4-hydroxylation of the halogenated anilines are plotted against their E(HOMO) values (Table 5). The figure obtained demonstrates a correlation ($r=0.96$) between the ln k_{cat}^S for the iodosobenzene-supported 4-hydroxylation of the halogenated anilines and the E(HOMO) of these substrates. This observation indicates that the E(HOMO) values of the aniline derivatives determine the maximum cytochrome P450-mediated 4-hydroxylation rate, when iodosobenzene is used as the artificial oxygen source. Thus, in this iodosobenzene-supported cytochrome P450 system the interaction of the electrophilic SOMO of the cytochrome P450 $(FeO)^{3+}$ intermediate with the frontier HOMO electrons of the aniline derivatives, becomes the rate-limiting step in catalysis.

In addition to the E(HOMO), the HOMO density on the reaction center C4 could be a factor influencing the substrate's reactivity for electrophilic attack [29]. Table 5 presents these HOMO densities at the C4 atoms of the halogenated anilines. From the values presented, it can be derived that the relative differences in HOMO density at the C4 atoms of the halogenated anilines are relatively small and cannot account for the differences of at least a factor 31 observed between the maximum 4-hydroxylation rates of the various anilines. Therefore, the relative difference in the E(HOMO) values between these related halogenated anilines appears to be the predominant factor in regulating their relative reactivities for electrophilic attack and, thus, the relative differences in their iodosobenzene-supported cytochrome P450-mediated 4-hydroxylation rate.

DISCUSSION.

In the present study the 4-hydroxylation of the halogenated anilines, catalyzed by the microsomal cytochrome P450, was investigated. Liver microsomes from isosafrole-pretreated rats appeared to be most capable of catalyzing the cytochrome P450-dependent 4-hydroxylation of the aniline derivatives. This suggests a predominant role for cytochrome P450 1A2 in the 4-hydroxylation of all the anilines studied. This result is in accordance with the observation of Ryan *et al.* [30], who demonstrated that purified reconstituted rat hepatic cytochrome P450 1A2 is one of the cytochrome P450 enzymes best capable of aniline 4-hydroxylation. Using microsomes from isosafrole-pretreated rats, further studies were especially focused on the importance of the physico chemical and electronic characteristics of the aniline substrates in relation to their cytochrome P450-mediated conversion to the 4-aminophenol metabolites.

Results of the present study demonstrate a relation between the K_m^s values for 4-hydroxylation of a series of aniline derivatives and the hydrophobicity of these substrates. It can be concluded that the hydrophobicity of the substrate is an important factor in determining the K_m^s values, of the aniline derivatives. This observation is in accordance with results obtained by Burka *et. al.* [31] for the K_m^s for hydroxylation of monohalogenated benzenes by phenobarbital-induced microsomes. The K_m^s was shown to correlate with the Hansch's π parameter of the substrates [31]. For the iodosobenzene-driven 4-hydroxylation it was demonstrated that the K_m^s values are higher as compared to the K_m^s values of the NADPH/O_2-driven supported conversion. This observation is best ascribed to the fact that iodosobenzene competes with the substrate for the binding site of the cytochrome P450 enzymes as has been demonstrated by Lichtenberg [32].

Additional results of the present study demonstrate that the spectral dissociation constant K_d^s, reflecting the binding interaction between the aniline substrate and the cytochrome P450 enzyme, is 6-40 times less than the K_m^s value for 4-hydroxylation. This leads to the conclusion, that not only the binding of the substrate to the cytochromes P450 (K_d^s), but also other steps in the catalytic cytochrome P450 cycle, such as for example electron donation, substrate conversion and/or product release, are involved in determining the K_m^s values for the cytochrome P450-mediated 4-hydroxylation. An alternative explanation could be that the K_d^s determined from the type II binding spectra does not represent the K_d, *i.e.*, the binding, of importance for substrate conversion. Taking into account that type II spectral characteristics are generally accepted to result from an interaction of the amino moiety with the Fe^{3+} of the cofactor, it is possible that this type of binding is not the one representative for substrate binding that eventually leads to product formation. Additional support for the

fact that binding characteristics determined for the resting Fe^{3+} form of the cytochrome P450 may not be relevant for the binding interaction characteristics for the activated $(FeO)^{3+}$ form comes from a study reported by Paulsen and Ornstein [33]. They demonstrate that binding of camphor to the Fe^{3+} form and that to the activated $(FeO)^{3+}$ form are different indeed. This implies that the K_d of the binding step influencing the K_m might be a different one than the one that can be obtained from type II difference spectra.

Additional results of the present study clearly demonstrate that reaction steps preceding the substrate conversion by the cytochrome P450 $(FeO)^{3+}$ intermediate play a main role in rate limitation of the NADPH/oxygen-supported aniline 4-hydroxylation. This follows from the observation that k_{cat}^s significantly increases when these reaction steps are surpassed by the use of iodosobenzene instead of NADPH and molecular oxygen to support the cytochrome P450 reaction. This result indicates that the interaction of the cytochrome P450 $(FeO)^{3+}$ intermediate with the aniline substrate is not the rate-limiting step in the NADPH/oxygen-driven catalysis. The most important observation of the iodosobenzene experiments, however, was a clear correlation ($r=0.96$) observed between the ln k_{cat}^s for the iodosobenzene-supported cytochrome P450-catalyzed 4-hydroxylation of the various aniline derivatives and their E(HOMO). This observation implies that the 4-hydroxylation proceeds by the interaction of the HOMO electrons of the substrate with the cytochrome P450 $(FeO)^{3+}$ SOMO. For the iodosobenzene-driven reaction this interaction becomes the rate-limiting step in catalysis. However, because iodosobenzene is generally accepted to generate the same reactive cytochrome P450 $(FeO)^{3+}$ intermediate as formed in the NADPH/O_2 supported pathway [28], it can be concluded that the normal NADPH- and oxygen-driven aniline 4-hydroxylation also proceeds by an electrophilic attack of the SOMO of the cytochrome P450 $(FeO)^{3+}$ intermediate on the HOMO π electrons of the aromatic aniline ring. Such a mechanism would be in accordance to the one proposed before on the basis of studies on the regioselectivity of the aromatic hydroxylation of monofluoroanilines and fluorobenzenes [12, 34]. Only when the reactivity of the substrate is too low, such as for example for 2,3,5,6-tetrafluoroaniline, the interaction of the cytochrome P450 $(FeO)^{3+}$ SOMO with the HOMO electrons of the substrate might become the rate-limiting step in the NADPH/O_2-supported reaction cycle.

Acknowledgements.

The authors gratefully acknowledge Mr. J. Haas and Mr. G. van Tintelen for assistance with animal handling. This study was supported by the Netherlands Organisation for the Advancement of Scientific Research (N.W.O.).

REFERENCES.

1 Gorrod J.W. and Manson D., (1986) The metabolism of aromatic amines, *Xenobiotica* **16**, 933-955.

2 Eyer P., (1988) Detoxication of N-oxygenated arylamines in erythrocytes. An overview, *Xenobiotica* **18**, 1327-1333.

3 Uehleke H., (1973) The role of cytochrome P-450 in the N-oxidation of individual amines, *Drug Metabolism and Disposition* **1**, 299-313.

4 Rietjens I.M.C.M. and Vervoort J., (1991) Bioactivation of 4-fluorinated anilines to benzoquinoneimines as primary reaction products, *Chem. -Biol. Interactions* **77**, 263-281.

5 Gartland K.P.R., Bonner F.W., Timbrell J.A. and Nicholson J.K., (1989) Biochemical characterisation of *para*-aminophenol-induced nephrotoxic lesions in the F344 rat, *Arch. Toxicol.* **63**, 97-106.

6 Gartland K.P.R., Eason C.T., Bonner F.W. and Nicholson J.K., (1990) Effects of biliary cannulation and buthionine sulphoximine pretreatment on the nephrotoxicity of para-aminophenol in the Fisher 344 rat, *Arch. Toxicol.* **64**, 14-25.

7 Klos C., Koob M., Kramer C. and Dekant W., (1992) *p*-Aminophenol nephrotoxicity: Biosynthesis of toxic glutathione conjugates, *Toxicol. Appl. Pharmacol.* **115**, 98-106.

8 Newton J.F., Kuo C.-H., Gemborys M.W., Mudge G.H. and Hook J.B., (1982) Nephrotoxicity of *p*-aminophenol, a metabolite of acetaminophen, in the Fischer 344 rat, *Toxicol. Appl. Pharmacol.* **65**, 336-344.

9 Calder I.C., Yong A.C., Woods R.A., Crowe C.A., Ham K.N. and Tange J.D., (1979) The nephrotoxicity of *p*-aminophenol, II. The effect of metabolic inhibitors and inducers, *Chem.-Biol. Interactions* **27**, 245-254.

10 Armstrong R.N., (1987) Enzyme-catalyzed detoxification reactions: mechanism and stereochemistry, *CRC Crit. Rev. Biochem.* **22**, 39-88.

11 Saltzman H. and Sharefkin J.G., (1973) Iodosobenzene, Organic Synthesis, Collective Volume V, John Wiley & Sons, 658-659.

12 Cnubben N.H.P., Vervoort J., Veeger C. and Rietjens I.M.C.M., (1992) Study on the regioselectivity and mechanism of the aromatic hydroxylation of monofluoroanilines, *Chem.-Biol. Interactions* **85**, 151-172.

13 Omura T. and Sato R., (1964) The carbon monoxide pigment of liver microsomes, I. Evidence for its haemoprotein nature, *J. Biol. Chem.* **239**, 2370-2378.

14 Lowry O.H., Rosebrough N.J., Farr A.L. and Randall A.J., (1951) Protein measurements with Folin phenol reagent, *J. Biol. Chem.* **193**, 265-275.

15 Brodie B.B. and Axelrod J., (1948) The estimation of acetanilide and its metabolic products, aniline, N-acetyl p-aminophenol and p-aminophenol (free and total conjugated) in biological fluids and tissues, *J. Pharmac. Exp. Ther.* **94**, 22-28.

16 Corbett J.F., (1970) Benzoquinone imines Part VIII. Mechanism and kinetics of the reaction

of p-benzoquinone monoimines with monohydric phenols, *J. Chem. Soc.*, 1503-1508.

17 Vervoort J., De Jager P.A., Steenbergen J. and Rietjens I.M.C.M., (1990) Development of a ^{19}F-n.m.r. method for studies on the in vivo and in vitro metabolism of 2-fluoroaniline, *Xenobiotica* **20**, 657-670.

18 Schenkman J.B., (1970) Studies on the nature of the type I and type II spectral changes in liver microsomes, *Biochemistry* **9**, 2081-2091.

19 Fukui K., Yonezawa T., Nagata C. and Shingu H., (1954) Molecular orbital theory of orientation in aromatic, heteroaromatic and other conjugated molecules, *J. Chem. Phys.* **22**, 1433-1442.

20 Rietjens I.M.C.M. and Vervoort J., (1989) Microsomal metabolism of fluoroanilines, *Xenobiotica* **19**, 1297-1305.

21 Fleming I. (1989), Molecular orbitals and frontier orbitals, in: Frontier Orbitals and Organic Chemical Reactions (Fleming I., Ed.), pp. 182-186, John Wiley & Sons, New York.

22 Guengerich F.P., (1990) Enzymatic oxidation of xenobiotic chemicals, *Biochemistry and Molecular Biology* **25**, 97-153.

23 White R.E. and Coon M.J., (1980) Oxygen activation by cytochrome P-450, *Ann. Rev. Biochem.* **49**, 315-356.

24 Miwa G.T., West S.B., Lu A.Y.H., (1978) Studies on the rate-limiting enzyme component in the microsomal monooxygenase system, *J. Biol. Chem.* **253**, 1921-1929.

25 Peterson J.A. and Prough R.A. (1986), Cytochrome P-450 reductase and cytochrome b5 in cytochrome P-450 catalysis, in: Cytochrome P-450: Structure, mechanism and biochemistry (Ortiz de Montellano P.R., Ed.), pp. 89-117, Plenum Press, New York.

26 Ruckpaul K., Rein H. and Blanck J. (1989), Regulation mechanisms of the activity of the hepatic endoplasmic cytochrome P-450, in: Frontiers in biotransformation: Basis and mechanisms of regulation of cytochrome P-450 (Ruckpaul K. and Rein H., Eds.), pp. 1-65, Taylor & Francis, London.

27 Murray M. and Reidy G.F., (1990) Selectivity in the inhibition of mammalian cytochromes P-450 by chemical agents, *Pharmacol. Rev.* **42**, 85-101.

28) Ortiz de Montellano P.R. (1986), Oxygen activation and transfer, in: Cytochrome P-450: Structure, mechanism and biochemistry (Ortiz de Montellano P.R., Ed.), pp. 217-271, Plenum Press, New York.

29 Vervoort J., Rietjens I.M.C.M., Berkel W.J.H. and Veeger C., (1992) Frontier orbital study on the 4-hydroxybenzoate-3-hydroxylase-dependent activity with benzoate derivatives, *Eur. J. Biochem.* **206**, 479-484.

30 Ryan D.E. and Levin W., (1990) Purification and characterization of hepatic microsomal cytochrome P-450, *Pharmac. Ther. Vol.* **45**, 153-239.

31 Burka L.T., Plucinski T.M. and Macdonald T.L., (1983) Mechanisms of hydroxylation by cytochrome P-450: Metabolism of monohalobenzenes by phenobarbital-induced microsomes, *Proc. Natl. Acad. Sci. USA* **80**, 6680-6684.

32 Lichtenberg F., Nastainczyk W. and Ullrich V., (1976) Cytochrome P450 as an oxene transferase, *Biochem. Biophys. Res. Commun.* **70**, 939-946.

33 Paulsen M.D. and Ornstein R.L., (1993) Substrate mobility in thiocamphor-bound cytochrome $P450_{cam}$: an explanation of the conflict between the observed product profile and the X-ray structure, *Protein Engng.* **6**, 359-365.

34 Rietjens I.M.C.M., Soffers A.E.M.F., Veeger C. and Vervoort J., (1993) Regioselectivity of cytochrome P-450 catalyzed (poly)fluorobenzene hydroxylation predicted by calculated frontier orbital substrate characteristics, *Biochemistry* **32**, 4801-4812.

CHAPTER 5

A spectrophotometric assay for the detection of 2-aminophenols in biological samples.

N.H.P. Cnubben, B. Blaauboer, S. Juyn, J. Vervoort and I.M.C.M. Rietjens

Analytical Biochemistry **220**, 165-171, 1994.

SUMMARY.

A sensitive and efficient spectrophotometric assay is described for the determination of 2-aminophenols in biological samples. Using ferric ions as a metal catalyst, 2-aminophenol dimerizes in an acidic aqueous environment to 2-hydroxy-isophenoxazin-3-one, an intensively coloured dye. The newly developed assay is suitable for the detection of 2-aminophenols in the μM range. The paper demonstrates that this chemical assay is also applicable for the determination of 2-aminophenols substituted with a halogen at the *ortho*, *meta* or *para* position of the aromatic ring with respect to the amino moiety, λ_{max}, and the molar extinction coefficient varying with the substituent pattern. Results obtained for fluorinated 2-aminophenol detection in biological samples by either this new method or ^{19}F-NMR are similar. This observation corroborates that the newly developed assay is suitable for detection of 2-aminophenols in biological samples.

INTRODUCTION.

Halogenated aniline derivatives are compounds used for the manufacture of numerous dyes, drugs, pesticides and herbicides [1]. Upon the cytochrome P450-dependent aromatic hydroxylation of these aniline derivatives, the compounds are converted into preferentially 2- and 4-aminophenols [2-5]. For the detection of 4-aminophenols, a sensitive, accurate and efficient chemical assay has been described

achieved by the addition of 100 µl 12N HCl to 1 ml of urine sample, followed by heating at 100°C for 30 minutes. The hydrolyzed samples were adjusted with 12 N NaOH to pH 7 and extracted three times with 3 ml diethylether to separate the 2-aminophenols from the mixture. After evaporation of the diethylether, 300 µl 20% TCA were added to the residue. This was followed by the addition of 1 ml demineralized water and 100 µl 40 mM ferric ammonium sulfate dodecahydrate. The 2-aminophenol content of these samples was determined as described above. A urine sample of a rat before exposure to an aniline derivative, treated in a similar way, was used as the reference.

Determination of 2-aminophenols in microsomal incubations.

Prior to analysis by the chemical assay, samples from microsomal incubations were frozen in liquid nitrogen and -upon thawing- centrifuged at 13,000 rpm for 10 minutes at 4°C. Diethyl ether extraction of the 2-aminophenols from the supernatant was carried out as described above for the urine samples, and appeared to be essential, because the presence of KP_i buffer prevents the formation of the yellow colour initiated by the addition of ferric ammonium sulfate dodecahydrate. The diethyl ether extraction also liberates 2-aminophenols (partially) bound to the microsomal protein by hydrophobic interactions, leading to an underestimation of the amount of 2-aminophenol actually present in the sample.

NMR measurements.

^{19}F-NMR measurements were performed on a Bruker AMX 300 spectrometer operating at 282.3 MHz essentailly as described before [2]. D_2O (Isotec, USA) was used for locking the magnetic field. The samples were made oxygen-free by four cycles of evacuating and filling with argon. Concentrations of the various compounds observed in the ^{19}F-NMR spectra were determined by comparison of the integrals of their ^{19}F-NMR resonances to the integral from the ^{19}F-NMR resonance of *para*-fluorobenzoic acid, added to each sample as an internal standard.

^{1}H-NMR measurements were performed on a Bruker AMX 500 spectrometer using 40° pulses and a repetition time of 3s. For ^{1}H-NMR measurements acetone-d_6 was used as the solvent.

Analysis by infra red.

Fourier Transform infrared spectra of the yellow dye and the synthesized 2-amino-isophenoxazin-3-one in KBr were recorded on a Biorad FTS-7 Fourier transform spectrometer.

Analysis by mass spectrometry

Electron Impact MS was performed using a Finnigan-MAT-95 mass spectrometer. GC-MS was not applied because of the high melting points of the compounds.

RESULTS

Calibration curve.

Figure 1 shows the calibration curve for formation of the coloured dye with increasing concentration of 2-aminophenol using the optimal conditions with respect to λ_{max} and reaction time (400 nm, 90 min). Figures 2 and 3 demonstrate that the λ_{max} of the 2-aminophenol-derived yellow dye in chloroform is 400 nm (Figure 2) and that the reaction is completed within 90 minutes (Figure 3). Figure 3 also demonstrates that the reaction product responsible for the absorbance at 400 nm is stable for at least another 30 minutes beyond the 90 minutes of the assay.

The calibration curve obtained (Figure 1) shows a linear relationship between the 2-aminophenol concentration and the absorbance at 400 nm (yellow colour) between 20 and -at least- 100 µM. From 0-20 µM a deviation from the linear relationship between 20-100 µM is observed, pointing at a concentration of about 10 µM that remains undetected. Obviously, the calibration curve for the 20-100 µM region must be corrected for this apparent "lag". Therefore, the calibration curve, valid between 20-100 µM, is best described by means of the following equation: A_{400nm} = -0.034 + 8.66•[2-aminophenol] with the concentration of 2-aminophenol in mM and at a value ≥ 0.020 mM.

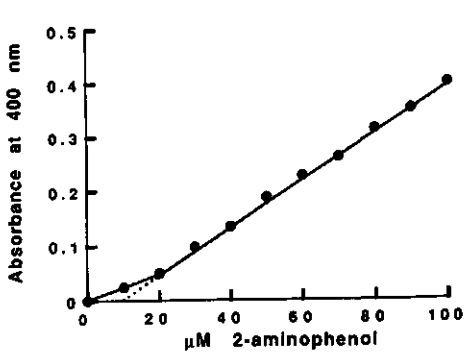

Figure 1: Calibration curve for the determination of 2-aminophenol.

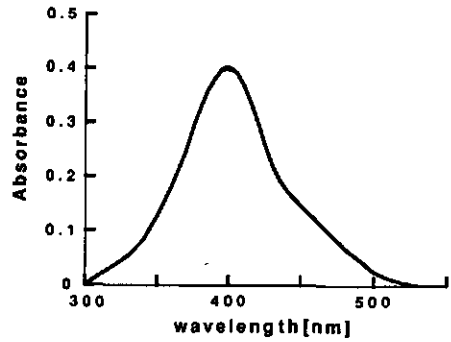

Figure 2: The visible absorption spectrum of the yellow dye in chloroform formed upon the reaction of 100 µM 2-aminophenol with ferric ammonium sulfate dodecahydrate.

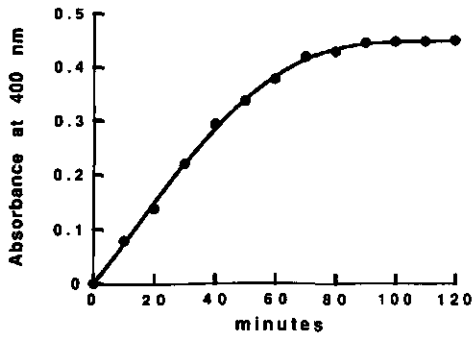

Figure 3: Influence of reaction time on the absorbance at 400 nm of the yellow dye in chloroform. To a 1-ml sample containing 100 nmol 2-amino-phenol, 0.3 ml 20% trichloroacetic acid and 0.1 ml 40 mM ferric ammonium sulfate dodecahydrate were added. The reaction mixtures were extracted with 2 ml chloroform at different time-intervals.

Identity of the yellow dye.

The identity of the yellow dye, formed upon a reaction of ferric ions with 2-aminophenol in an acidic aqueous environment, was investigated by means of mass spectrometry, ^{1}H-NMR measurements and Fourier Transform infrared spectrometry. Initially it was assumed that the yellow dye might be 2-amino-isophenoxazin-3-one [9-11]. The synthesized 2-amino-isophenoxazin-3-one (m.p 254-256°C) and the yellow dye (m.p. 262-264°C) appeared to have a mass of respectively *m/z* 212 (100%), 185 (53%), 184 (27%) and *m/z* 213 (100%), 185 (80%). The ^{1}H-NMR resonances of the

synthesized 2-amino-isophenoxazin-3-one and the yellow dye formed in the chemical assay show the same characteristics namely two doublets, two triplets and two singlets, although the resonances of the latter are all shifted to higher field. The IR spectrum of the synthesized 2-amino-isophenoxazin-3-one confirmed its structure as it was identical to the IR spectrum of this compound published in the literature [17]. Surprisingly, the IR spectrum of the yellow dye demonstrated to be identical to the IR spectrum of 2-hydroxy-isophenoxazin-3-one published in the same paper [17]. Finally, comparison of the results from mass analysis, ^{1}H-NMR and melting points to data published in the literature for phenoxazin-3-ones [17-18] further confirms the identity of the yellow compound as 2-hydroxy-isophenoxazin-3-one.

The influence of halogen substituents at the 2-aminophenol on the formation of the yellow colour in the chemical assay.

To investigate the effect of halogen substituents at the aromatic ring of the 2-aminophenol on the formation of the yellow dye as well as the reliability of the newly developed assay, monofluorinated 2-aminophenols were used. The presence of a fluorine substituent provides the possibility to analyze 2-aminophenol containing samples in a quantitative way using ^{19}F-NMR spectroscopy and to compare this to the results of the newly developed chemical assay.

Table 1 demonstrates that for fluorine-substituted 2-aminophenols the λ_{max} of the respective coloured reaction products in chloroform and the corresponding molar extinction coefficients vary significantly with the substituent pattern. However, from the results in Table 1 it appears that the presence of a fluorine substituent at the *ortho*,

Table 1: Spectral characteristics of the 2-aminophenol derived dyes in chloroform.

Compound	λ_{max} (nm)	ε-value ($mM^{-1} \cdot cm^{-1}$) for C ≥ 0.020 mM[a]	b[a]
2-Aminophenol	400	8.66	-0.034
2-Amino-3-fluorophenol	402	3.44	-0.022
2-Amino-4-fluorophenol	433	5.38	-0.026
2-Amino-5-fluorophenol	402	10.14	-0.033

[a] The calibration curve is described by the equation $A = b + \varepsilon \cdot C \cdot l$. A represents the absorbance of the corresponding yellow dye in $CHCl_3$ at λ_{max}, ε is the molar extinction coefficient in $mM^{-1} \cdot cm^{-1}$, C is the concentration of the halogen-subsituted 2-aminophenol in mM, l is the light pathway in cm and b is the correction factor.

meta or *para* position of the aromatic ring with respect to the amino moiety does not prevent the formation of the yellow dye. The structures of the dimerization products of the fluorinated 2-aminophenols were identified essentially as described above. The ^{1}H-NMR characteristics, *m/z* values and corresponding structures of the dimerization products of the fluorinated 2-aminophenols are presented in Table 2.

Table 2: Spectral characteristics of the dimerization products of the 2-aminophenol derivatives in the chemical assay.

2-Amino-phenol derivative	Dimerization product	Mass and ^{1}H-NMR spectral characteristics
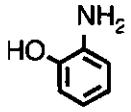	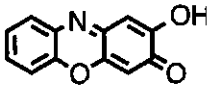	^{1}H-NMR (acetone-d_6): 9.01 (OH)(broad s), 7.83 (H9)(d, $^3J_{H-H}$= 7.6 Hz), 7.63 (H7)(tr, $^3J_{H-H}$= 7.6 Hz, $^3J_{H-H}$= 7.5 Hz), 7.52 (H6)(d, $^3J_{H-H}$= 7.6 Hz), 7.49 (H8)(tr, $^3J_{H-H}$= 7.6, $^3J_{H-H}$= 7.5 Hz), 6.76 (H1)(s), 6.42 (H4)(s). *m/z*: 213 (100%), 185 (80%).
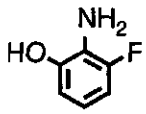	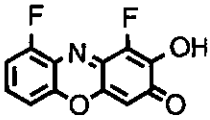	^{1}H-NMR (acetone-d_6): 9.52 (OH)(broad s), 7.71 (H6)(d, $^3J_{H-H}$= 7.9 Hz), 7.55-7.38 (H7+H8)(m), 6.43 (H4)(s) *m/z*: 249, compound was not purified from the "minor product".
	Main product (70%) 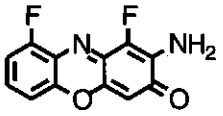	^{1}H-NMR (acetone-d_6): 7.68 (H6)(d, $^3J_{H-H}$= 7.8 Hz), 7.55-7.38 (H7+H8)(m), 6.51 (NH_2)(broad s), 6.48 (H4)(s) *m/z*: 248, compound was not purified from the "main product".
	Minor product (30%)	
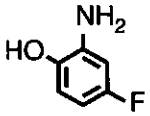	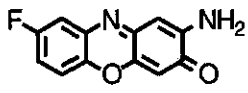	^{1}H-NMR (acetone-d_6): 7.50 (H6)(dd, $^3J_{H-H}$= 8.8 Hz, $^4J_{H-F}$= 4.9 Hz), 7.43 (H9)(dd, $^3J_{H-F}$= 9.1 Hz, $^4J_{H-H}$= 2.8 Hz), 7.28 (H7)(m, $^3J_{H-H}$= 8.8 Hz, $^3J_{H-F}$= 8.6 Hz, $^4J_{H-H}$= 2.8 Hz), 6.47 (H1)(s), 6.42 (NH_2)(broad s), 6.30 (H4)(s). *m/z*: 230 (100%), 203 (39%), 202 (28%).
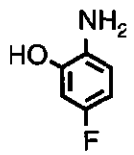	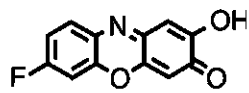	^{1}H-NMR (acetone-d_6): 9.05 (OH)(broad s), 7.89 (H9)(dd, $^3J_{H-H}$= 8.8 Hz, $^4J_{H-F}$= 6.1 Hz), 7.38 (H6)(dd, $^3J_{H-F}$= 9.0 Hz, $^4J_{H-H}$= 2.6 Hz,), 7.30 (H8)(m, $^3J_{H-H}$= 8.8 Hz, $^3J_{H-F}$= 8.8 Hz, $^4J_{H-H}$= 2.6 Hz), 6.75 (H1)(s), 6.43 (H4)(s). *m/z*: 231 (100%), 203 (73%).

Verification of the assay.

Additional experiments were performed to investigate the applicability of the newly developed 2-aminophenol assay for the detection of 2-aminophenols in biological samples such as urine samples and microsomal incubations. For this reason, urine samples from rats exposed to fluoroanilines and samples from microsomal incubations with fluorinated anilines were analyzed by both the chemical assay and by ^{19}F-NMR.

Urine samples were analyzed after acid hydrolysis, carried out to eliminate conjugated N-acetyl, sulphate and glucuronic acid residues from the 2-aminophenols. Table 3 summarizes the values obtained for these urine samples using both the chemical assay and ^{19}F-NMR. The ^{19}F-NMR spectra of these urine samples have been published before [12]. It is clear that both methods provide similar results. Thus, urine components and other monofluoroaniline metabolites which may also be extracted into the diethylether do not interfere with this chemical assay. Quantification of 2-aminophenols in the urine of 3-fluoroaniline exposed rats using the chemical assay may in theory be hampered by the fact that hydroxylation of 3-fluoroaniline can lead to the formation of two isomeric 2-aminophenols. However, ^{19}F-NMR analysis of the urine of 3-fluoroaniline-exposed rats revealed that only 2-amino-5-fluorophenol derived metabolites are present in the urine, thus eliminating this theoretical problem [12].

Table 3: Comparison of the chemical assay with ^{19}F-NMR analysis for the estimation of 2-aminophenol in urine samples of monofluoroaniline exposed rats.

	μmol 2-aminophenol in urine after acid hydrolysis.	
Dosed compound	**^{19}F-NMR**	**Chemical assay**
2-Fluoroaniline	4.8 ± 0.1	4.5 ± 0.5
3-Fluoroaniline	19.6 ± 0.7	19.0 ± 0.1
4-Fluoroaniline	97.8 ± 1.1	99.8 ± 3.7

Note. Data are presented as means ± standard error of the mean.

Table 4 presents the results of the analysis of samples from microsomal incubations of monofluoroanilines using ^{19}F-NMR and the chemical assay. In these microsomal samples the 2-aminophenol metabolites are formed in the μM range upon the cytochrome P450-mediated conversion of the aniline derivatives.

derivative, providing a basis for quantification of the respective 2-aminophenols upon characterization of their respective calibration curves.

Using the fluorinated analogues, it could be demonstrated that analysis by the newly developed chemical assay provides similar results for the 2-aminophenol concentration in urinary and microsomal samples as obtained by ^{19}F-NMR. Thus, the newly developed chemical assay presented here provides an efficient, reliable and more sensitive method for the detection of (halogen substituted) 2-aminophenols in biological samples than the existing colorimetric methods.

Acknowledgements.

The authors gratefully acknowledge Mr. A van Veldhuizen and Mr. C. Teunis from the Department of Organic Chemistry, for help with ^{1}H-NMR measurements, fourier transform infrared spectrometry and mass spectrometry. The preliminary results of J. v. Leeuwen on the spectrophotometry of this chemical assay is also acknowledged. The authors wish to thank Mr. S. Boeren for helpful discussion. This study was supported by the Netherlands Organisation for the Advancement of Scientific Research (N.W.O.).

REFERENCES.

1 Gorrod, J.W., and Manson, D., The metabolism of aromatic amines, *Xenobiotica* **16**, 933-955, 1986.

2 Vervoort, J., Jager, P.A., Steenbergen, J., and Rietjens, I.M.C.M., Development of a ^{19}F-n.m.r. method for studies on the in vivo and in vitro metabolism of 2-fluoroaniline, *Xenobiotica* **20**, 657-670, 1990.

3 Baldwin, M.K., and Hutson, D.H., The metabolism of 3-chloro-4-fluoro-aniline in dog and rat, *Xenobiotica* **10**, 135-144, 1980.

4 Eadsforth, C.V., Logan, C.J., Morrison, B.J., and Warburton, P.A., 2,4-Difluoroaniline and 4-fluoroaniline exposure: monitoring by methaemoglobin and urine analyses, *Int. Arch. Occup. Environ. Health* **54**, 223-232, 1984.

5 Ehlhardt, W.J., and Howbert, J.J., Metabolism and disposition of *p*-chloroaniline in rat, mouse and monkey, *Drug metabolism and disposition* **19**, 366-369, 1991.

6 Brodie, B.B., and Axelrod, J., The estimaton of acetanilide and its metabolic products, aniline, N-acetyl p-aminophenol and p-aminophenol (free and conjugated) in biological fluids and tissues, *J. Pharmacol. Exp. Ther.* **94**, 22-28, 1948.

7 Feigl, F., (Ed.), *o*-Aminophenol; test with glyoxal and calcium oxide, in: Spot tests in organic analysis, Elsevier, 2nd edn., 1960, p. 413.

8 Snell, F.D., and Snell, C.T., (Eds.), *o*-Aminophenol, in: Colorimetric methods of analysis, Vol. 4, D. v. Nostrand Co. Inc., Princeton, 3th edn, 1954, p. 201.

9 King, C.M., and Kriek, E., The differential reactivity of the oxidation products of *o*-aminophenols toward protein and nucleic acid, *Biochimica et Biophysica Acta* **111**, 147-153, 1965.

10 Nagasawa, H.T., and Gutmann, H.R., The oxidation of *o*-aminophenols by cytochrome *c* and cytochrome oxidase, I: Enzymatic oxidations and binding of oxidation products to bovine serum albumine, *J. Biol. Chem.* **234**, 1593-1599, 1959.

11 Nagasawa, H.T., Gutmann, H.R., and Morgan, M.A., The oxidation of *o*-aminophenols by cytochrome *c* and cytochrome oxidase, II: Synthesis and identification of oxidation products, *J. Biol. Chem.* **234**, 1600-1604, 1959.

12 Cnubben, N.H.P., Vervoort, J., Veeger, C., and Rietjens, I.M.C.M., Study on the regioselectivity and mechanism of the aromatic hydroxylation of monofluoroanilines, *Chem.-Biol. Interactions*, **85**, 151-172, 1992.

13 Fischer, O., and Jonas, O., Beitrag zur oxydation der aromatischen orthodiamine und orthoamidophenole, *Berichte der Deutschen Chemischen Gesellschaft*, **27**, 2782-2785, 1894.

14 Cavill, G.W.K., Clezy, P.S., and Tetaz, J.R., The chemistry of mould metabolites. Part II. A partial structure for polystictin, *J. Chem. Soc.*, 2646-2651, 1957.

15 Rietjens, I.M.C.M., and Vervoort, J., Microsomal metabolism of fluoroanilines, *Xenobiotica* **19**, 1297-1305, 1989.

16 Omura, T., and Sato, P., The carbon monoxide pigment of liver microsomes, I: Evidence for its haemoprotein nature, *J. Biol. Chem.* **239**, 2370-2378, 1964.

17 Musso, H., und Matthies, H.-G., Über orceinfarbstoffe, V) IR- und UV-spektren, hydroxy- und amino-substituierter phenoxazone, *Chem. Ber.* **90**, 1814-1827, 1957.

18 Bolognese, A., and Scherillo G., *J. Heterocyclic Chem.*, **23**, 1003-1006, 1986.

19 Miller, D.M., Buettner, G.R., and Aust, S.D., Transition metals as catalysts of "autoxidation" reactions, *Free Radical Biology & Medicine* **8**, 95-108, 1990.

20 Charles, R.G., and Freiser, H., Structure and behaviour of organic analytical reagents. II. Stability of chelates of *o*-aminophenol and of *o*-aminobenzenethiol, *J. Am. Chem. Soc.* **74**, 1385-1387, 1952.

21 Sims, P., The stability constants of some metal chelates of ortho aminophenols, *J. Chem. Soc.*, 3648-3649, 1959.

22 King, C.M., Gutmann, H.R., and Chang, S.F., The oxidation of *o*-aminophenols by cytochrome *c* and cytochrome oxidase, IV Interaction of 2-imino-1,2-fluorenoquinone and of 2-imino-2,3-fluorenoquinone with bovine serum albumin, *J. Biol. Chem.*, **238**, 2199-2205, 1963.

23 Butenandt, A., Schiedt, U., und Biekert, E., Über ommochrome, III. Mitteilung: Synthese des xanthommatins, *Ann. Chem. Liebigs* **588**, 106-116, 1954.

24 Lenk, W., and Sterzl, H., Peroxidase activity of oxyhaemoglobin in vitro, *Xenobiotica* **14**, 581-588, 1984.

25 Diepolder, E., Ueber Oxydationsproducte des *o*-Aminophenols, *Berichte der Deutschen Chemischen Gesellschaft* **35**, 2816-2822, 1902.

CHAPTER 6

The effect of varying halogen substituent patterns on the cytochrome P450-catalyzed dehalogenation of 4-halogenated anilines to 4-aminophenol metabolites.

N.H.P. Cnubben, J. Vervoort, M. G. Boersma and I.M.C.M. Rietjens.

Biochemical Pharmacology **49**, 1235- 1248, 1995.

SUMMARY.

The cytochrome P450-catalyzed biotransformation of 4-halogenated anilines was studied *in vitro* with special emphasis on the dehalogenation to 4-aminophenol metabolites. The results demonstrated that a fluorine substituent at the C4 position was more easily eliminated from the aromatic ring than a chloro-, bromo- or iodo-substituent. HPLC analysis of *in vitro* biotransformation patterns revealed that the dehalogenation of the C4-position was accompanied by formation of non-halogenated 4-aminophenol, without formation of NIH-shifted metabolites. Changes in the apparent V_{max} for microsomal oxidative dehalogenation appeared to correlate with the electronegativity of the halogen substituent at C4, the fluorine substituent being the one most easily eliminated. A similar decrease in the rate of dehalogenation from a fluoro- to a chloro- to a bromo- to an iodo-substituent was observed in a system with purified reconstituted cytochrome P450 IIB1, in a tertiair butyl hydroperoxide supported microsomal cytochrome P450 system as well as in a system with microperoxidase 8. This microperoxidase 8 is a heme-based mini-enzyme without a substrate binding site, capable of catalyzing cytochrome P450-like reaction chemistry. Together, these results excluded the possibility that the difference in the rate of dehalogenation with a varying C4-halogen substituent arose from a change in the contribution of cytochrome P450 enzymes involved in oxidative dehalogenation with a change in the halogen

substituent. Rather, they strongly suggested that the difference was indeed due to an intrinsic electronic parameter of the various C4 halogenated anilines dependent on the type of halogen substituent. Additional *in vitro* experiments with polyfluorinated anilines demonstrated that elimination of the C4-fluorine substituent became more difficult upon the introduction of additional electron withdrawing fluorine substituents in the aniline-ring. ^{19}F-NMR analysis of the metabolite patterns showed that the observed decrease in 4-aminophenol formation was accompanied by a metabolic switch to 2-aminophenols and N-hydroxyanilines, while products resulting from NIH-type mechanisms were not observed. For a C4-chloro-, bromo-, or iodo-substituted 2-fluoroaniline the V_{max} for the oxidative dehalogenation was reduced by the additional electron withdrawing fluorine substituent at the C2 position in a similar way. In conclusion, the results of the present study strongly indicate that the possibilities for cytochrome P450 mediated dehalogenation of 4-halogenated anilines to 4-aminophenol metabolites are dependent on: (i) the characteristics of the halogen that has to be eliminated, the most electronegative and smallest halogen being the one most easily eliminated, and (ii) the electron-withdrawing capacities of other substituents in the aromatic ring, electron-withdrawing substituents decreasing the relative rate of the reaction. Together these data lead to the conclusion that the halogen is eliminated as a halogen anion.

INTRODUCTION.

The accumulation of halogen-containing aliphatic and aromatic compounds is a major factor adding to environmental pollution. The phenomenon originates in the widespread use of halogenated compounds in industry, commerce and medicine and in the relatively high persistence of these xenobiotics. Removal of halogen substituents is considered to be a crucial step in the bioconversion and biodegradation of halogenated compounds [1-5]. In mammals and microorganisms cytochromes P450 are important enzymes involved in biodehalogenation processes [6, 7].

In our previous studies on the dehalogenation of 4-fluorinated anilines and phenols a reaction mechanism was proposed for the cytochrome P450-mediated oxidative defluorination of 4-fluoroanilines to 4-aminophenol metabolites and of pentafluorophenols to tetrafluorohydroquinone metabolites [8, 9]. Figure 1 schematically presents this pathway. The reaction proceeds by formation of chemically

Abbreviations: MP-8, microperoxidase 8; HXO, hypohalous acid (for example, HClO = hypochlorous acid); tBuOOH, tert butyl hydroperoxide; NMR, nuclear magnetic resonance; HPLC, high performance liquid chomatography.

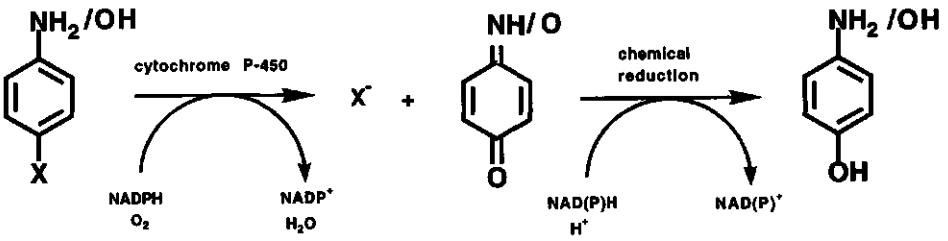

Figure 1: Proposed reaction pathway for the cytochrome P450-catalyzed dehalogenation of 4-halogenated anilines and phenols. X represents a fluoro atom [8, 9].

reactive benzoquinone(imine) as the primary reaction product. Because of this possible formation of reactive primary reaction products the cytochrome P450-mediated oxidative dehalogenation of aromatic compounds is of considerable interest [8-10]. Subsequent chemical reduction of benzoquinone(imine) leads to the formation of the final 4-aminophenol (or hydroquinone) metabolite (Figure 1). Based on the electron balance of the cytochrome P450 reaction and formation of benzoquinone(imine) as the primary reaction product, the fluorine substituent is supposed to be eliminated as an anion.

Studies on the cytochrome P450-catalyzed dehalogenation of aliphatic-halogenated hydrocarbons demonstrated the ease with which halogen elimination decreased in the order iodine > bromine > chlorine > fluorine [3, 5, 11-13]. The strength of the carbon-halogen bond is known to increase in the same order [1, 7]. As a result, a C-F bond is generally considered inert and difficult to break, suggesting that dehalogenation of chlorinated, brominated and iodinated compounds is easier than dehalogenation of the fluorinated analogues. Incorporation of a fluorine substituent into drugs or agrochemicals has even been suggested as a means of blocking biodegradation or bioactivation of the compounds [14-20].

Daly *et al.* [21], however, studying the conversion of various aniline derivatives, reported 4-chloroaniline to be less readily converted to 4-aminophenol than 4-fluoroaniline, although the phenomenon was not studied in more detail. In addition, in a previous study on the conversion of pentafluorochlorobenzene, the cytochrome P450-catalyzed reaction appeared to preferentially eliminate the C4 fluorine substituent and not the chlorine substituent [10], again suggesting that for an aromatic compound and in contrast to the aliphatic compounds, the elimination of a fluorine might be easier than elimination of a chlorine substituent. Furthermore, the observation reported by Li *et al.* [22] of a much lower net rate of 2-dehalogenation of 2-bromoestradiol compared

with that of 2-fluoroestradiol, also suggests the relatively easier elimination of an aromatic fluorine substituent than of other aromatic halogen substituents. These authors attributed their observation to the inability of the brominated substrate to bind to the cytochrome P450 enzyme due to steric hindrance, but the phenomenon might also be due to electronic differences between the fluoro- and bromo-substituent.

The objective of the present study was to investigate the influence of the nature and number of the halogen substituents on the cytochrome P450-catalyzed biodehalogenation of aromatic compounds in more detail. The results are expected to provide additional information on the importance of halogen characteristics for their possible elimination from an aromatic molecule in a cytochrome P450-catalyzed reaction and, thus, on the mechanism of the reaction. Furthermore, an extension of the studies from fluorinated to other halogenated aromatics is of importance considering the more widespread use of chlorinated and brominated aromatics than of their fluorinated analogues.

4-Halogenated anilines were taken as the model compounds because defluorination of 4-fluoroaniline was already demonstrated to occur extensively in previous studies [23-25].

MATERIALS AND METHODS.

Chemicals

Aniline, 2-fluoro-, 3-fluoro-, 4-fluoro-, 4-chloro-, 4-bromo- and 4-iodoaniline were purchased from Janssen Chimica (Beerse, Belgium). All di- and polyfluoroanilines and nitrobenzenes were obtained from Fluorochem (Derbyshire, UK). 2-Aminophenol and 4-fluoronitrobenzene were from Aldrich and 4-aminophenol was from Merck (Darmstadt, Germany). The purity of all compounds was > 98%.

Nitrosobenzene was purchased from Aldrich. 4-Fluoro-, 4-chloro-, 4-bromo- and 4-iodonitrosobenzene were synthesized according to Kennedy and Stock [26]. For 3 min 25 mL 15% (w/v) potassium peroxomonosulphate (minimal 4.5% active oxygen, Janssen Chimica) were added to a solution of 10 mmol C4-halogenated aniline in 20 mL glacial acetic acid, cooled in an ice bath. After 2 minutes mixing, the reaction mixture was immediately extracted twice with 25 mL hexane. The nitrosobenzene was further purified on a LiChroprep Si60 column using an ISCO HPLC system with hexane as the eluens. The flow-rate was 6.0 mL/min and fractions of 10 mL were collected. Detection was at 295 nm. The characteristic green-colored nitrosobenzene containing fractions were collected and concentrated to a volume of 5 mL by evaporation of the solvent. In order to prevent the decomposition of the unstable nitrosobenzenes this fraction was not evaporated to dryness. The

concentration of the C4-halogenated nitrosobenzene was determined by ^{1}H-NMR on a Bruker AC 200 spectrometer using dichloromethane as the internal standard. The stock solutions of the nitrosobenzene derivatives thus obtained were immediately used for the determination of molar extinction coefficients in the chemical assay for N-oxidation products (see below).

Synthesis of the fluorinated N-hydroxyanilines was performed by the chemical reduction of the nitrobenzene analogue essentially as described by Vogel [27] and Coleman *et al.* [28] or by the chemical reduction of the synthetized nitrosobenzenes in 0.1 M KPi buffer (pH 7.6) containing 20 mM ascorbic acid.

3-Fluoro-4-aminophenol, 2-fluoro-4-aminophenol and 5-fluoro-2-aminophenol were synthesized as described before [24].

2-Amino-3,5-difluorophenol, 2-amino-5-chlorophenol, 2-amino-5-bromophenol and 2-amino-5-iodophenol were synthesized according to Boyland and Sims [29] using, respectively, 2,4-difluoroaniline, 4-chloroaniline, 4-bromoaniline and 4-iodoaniline as the starting material. In short, 15 g potassium persulphate (Janssen Chimica) were added to a solution of 5 g 4-halogenated aniline in 20 mL ethanol, 250 mL water and 50 mL 2N potassium hydroxide for 8 hr under continuous stirring. The mixture was kept overnight and filtered. After washing with ether, the solution was acidified with 2N sulphuric acid and the precipitate separated from the mixture by filtration. The filtrate was neutralized with 2N potassium hydroxide and the water-content was reduced to 25-50 mL by freeze-drying. The solution was extracted three times with 100 mL butanol, the collected butanol phases were evaporated under reduced pressure and the residue obtained was crystallized from 90% ethanol. The sulphate esters obtained, were hydrolysed for 45 minutes at 100°C in 3N HCl. After cooling, the solution was neutralized and the 2-aminophenols were extracted from the mixture with diethylether. After evaporation of the solvent, the brownish precipitate was dissolved in 3 mL dichloromethane and applied to a LiChroprep Si60 column (310 mm x 25 mm, particle size 40-63 μm) (Merck, Darmstadt, Germany) using an ISCO HPLC system with 2% (v/v) ethanol in dichloromethane as the eluens. The flow-rate was 5 mL/min and fractions of 10 mL were collected. Detection was at 295 nm using an ISCO absorbance detector. The fractions were analysed on 2-aminophenol content by monitoring their reaction in a chemical assay for 2-aminophenols as described elsewhere [30]. The 2-aminophenol-containing fractions were collected and after crystallization the purity of these aminophenols was verified using a Kratos 400 HPLC system, with a LiChrosorb C_8 column (100 mm x 3 mm) (Chrompack, Middelburg, The Netherlands). After eluting for 5 min with nanopure, a linear gradient from 0 to 80% (v/v) methanol in 22 min, followed by 80% (v/v) methanol for 6 min was applied. Detection was at 240 nm using a Waters^{TM} 996 photodiode array detector. From the elution patterns obtained, the purity of the synthesized compounds was

judged to be >95%.

The identity of the synthetized 2-aminophenols was derived from their ^{19}F-NMR and/or ^{1}H-NMR spectral characteristics. 5-Fluoro-2-aminophenol: ^{19}F-NMR (0.1 M potassium phosphate pH 7.6, relative to $CFCl_3$)(ppm): -127.5 (F5)(m, $^{3}J_{F5-H4}$ = 12.0 Hz, $^{3}J_{F5-H6}$ = 12.0 Hz, $^{4}J_{F5-H3}$ = 9.0 Hz) and ^{1}H-NMR (acetone)(ppm): 9.29 (H3)(tr, $^{3}J_{H3-H4}$ = 9.0 Hz, $^{4}J_{H3-F5}$ = 9.0 Hz), 9.22 (H4)(dd, $^{3}J_{H4-F5}$ = 12.0 Hz, $^{3}J_{H4-H3}$ = 9.0 Hz), 9.07 (H6)(d, $^{3}J_{H6-F5}$ = 12.0 Hz); 5-chloro-2-aminophenol: ^{1}H-NMR (acetone)(ppm): 9.42 (H6)(s), 9.33 (H4)(d, $^{3}J_{H4-H3}$ = 8.3 Hz), 9.29 (H3)(d, $^{3}J_{H3-H4}$ = 8.3 Hz); 5-bromo-2-aminophenol: ^{1}H-NMR (acetone)(ppm): 9.55 (H6)(s), 9.42 (H4)(d, $^{3}J_{H4-H3}$ = 8.5 Hz), 9.29 (H3)(d, $^{3}J_{H3-H4}$ = 8.5 Hz); 5-iodo-2-aminophenol: ^{1}H-NMR (acetone)(ppm): 9.71 (H6)(s), 9.60 (H4)(d, $^{3}J_{H4-H3}$ = 8.5 Hz), 9.19 (H3)(d, $^{3}J_{H3-H4}$ = 8.5 Hz); 3-fluoro-2-aminophenol: ^{19}F-NMR (0.1 M potassium phosphate pH 7.6, relative to $CFCl_3$)(ppm): -136.9 (F3)(dd, $^{3}J_{F3-H4}$ = 10.0 Hz, $^{4}J_{F3-H5}$ = 8.5 Hz) and ^{1}H-NMR (acetone)(ppm): 9.25 (H5)(m, $^{3}J_{H5-H6}$ = 8.5 Hz, $^{3}J_{H5-H4}$ = 8.5 Hz, $^{4}J_{H5-F3}$ = 8.5 Hz), 9.11 (H6)(d, $^{3}J_{H6-H5}$ = 8.5 Hz), 9.02 (H4)(dd, $^{3}J_{H4-H5}$ = 8.5 Hz, $^{3}J_{H4-F3}$ = 10.0 Hz); 3,5-difluoro-2-aminophenol: ^{19}F-NMR (0.1 M potassium phosphate pH 7.6, relative to $CFCl_3$)(ppm): -134.5 (F3)(d, $^{3}J_{F3-H4}$ = 9.0 Hz), -127.1 (F5)(tr, $^{3}J_{F5-H6}$ = 9.0 Hz, $^{3}J_{F5-H4}$ = 9.0 Hz) and ^{1}H-NMR (acetone)(ppm): 9.17 (H6)(d)($^{3}J_{H6-F5}$ = 9.0 Hz), 9.10 (H4)(tr) ($^{3}J_{H4-F3}$ = 9.0 Hz, $^{3}J_{H4-F5}$ = 9.0 Hz).

All di- and polyfluorinated 4-aminophenols were prepared by biosynthesis, purified and their identity was derived from ^{19}F-NMR and ^{1}H-NMR spectral characteristics essentially as described previously [31].

Preparation of microsomes

Microsomes were prepared from the perfused livers of male Wistar rats (± 400 g), pretreated with isosafrole (Janssen Chimica) as described previously [24]. For the *in vitro* experiments liver microsomes of isosafrole-pretreated rats were used, since this type of microsome was demonstrated to possess the highest capacity to convert 4-fluoroaniline to its 4-aminophenol [25]. This was also the case for other 4-halogenated anilines (unpublished results). Cytochrome P450 content of the microsomes was measured as described by Omura and Sato [32].

Purification of microperoxidase-8 (MP-8).

MP-8 was purified by proteolytic digestion of horse heart cytochrome c (Sigma, St. Louis, MO USA) essentially as described in the literature [33]. The sample was more than 96% pure based on HPLC analysis [33]. The HPLC analysis was performed on a Waters^{TM} 600 Controller HPLC with a Baker bond WPC 4 column (25 cm x 4.6 mm). A linear gradient from 0.1% trifluoroacetic acid in water to 50%

0.1% trifluoroacetic acid in water and 50%, 0.1% trifluoroacetic acid in acetonitril was applied in 50 min., which was continued isocratically for 5 min. Detection at 214 nm was performed on an ISCO V^4 absorbance detector and detection at 395 nm was performed on an Applied Biosystems 757 absorbance detector. The heme content was determined essentially as described previously [34].

Purification of cytochrome P450 IIB1 and NADPH-cytochrome P450 reductase.

Cytochrome P450 IIB1 and NADPH-cytochrome P450 reductase were purified from liver microsomes of phenobarbital (Brocacef bv., Maarssen, The Netherlands)(0.1% in drinking water for 7 days) pretreated male respectively female Wistar rats essentially as previously described by Boersma *et al.* [35].

In vitro incubations

Cytochrome P450-dependent conversion was studied *in vitro* in microsomal incubations containing (final concentrations) 0.1 M potassium phosphate pH 7.6, between 0 and 15 mM of the halogenated aniline (as indicated) added as 1 % (v/v) of a 100 fold concentrated stock solution in dimethylsulphoxide and 1 μM microsomal cytochrome P450. The reaction was started by the addition of NADPH (1 mM final concentration) or tBuOOH (10 mM final concentration) and carried out at 37 °C for 10 min. The incubations with tBuOOH as the artificial oxygen donor additionally contained NADH (1 mM final concentration) in order to reduce benzoquinoneimine to 4-aminophenol. The conversion of halogenated anilines to their 4-aminophenol metabolites is linear for at least 10 minutes. Incubations with purified, reconstituted cytochrome P450 IIB1 were conducted using similar final incubation conditions as described for the microsomal incubations. Instead of microsomes, the incubations contained 0.5 nmol cytochrome P450 IIB1, 1.24 units NADPH-cytochrome reductase and 20 μg dilauroyl phosphatidylcholine (Sigma) per ml incubation mixture and were preincubated for 6 minutes at 37°C.

The microperoxidase-8 (MP-8) catalyzed conversion was studied in incubations containing (final concentrations) 0.1 M potassium phosphate pH 7.6, between 0 and 12.5 mM of the halogenated aniline (as indicated) added as 1% (v/v) of a 100 fold concentrated stock solution in dimethylsulphoxide, 7.5 μM MP-8 and 1 mM NADH in order to reduce to primary metabolite 4-benzoquinoneimine to 4-aminophenol. The reaction was started by the addition of H_2O_2 (2.5 mM final concentration) and carried out at 37°C for 1 min.

For chemical analysis of 4-aminophenol or N-hydroxyaniline the reaction was terminated by the addition of 0.8 mL of the incubation mixture to 0.24 mL of 20% (w/v) trichloroacetic acid. Upon mixing and centrifugation (5 min, 13000 rpm) the supernatant was used for the chemical determination of 4-aminophenol or N-

hydroxyaniline metabolites as described hereafter. For the chemical analysis of 2-aminophenol metabolites (decribed below) the reaction was terminated by freezing the sample into liquid nitrogen.

Incubations for HPLC and ^{19}F-NMR analysis additionally contained 1 mM ascorbic acid to prevent autoxidation of the aminophenols especially during the overnight ^{19}F-NMR measurement. These incubations were terminated by freezing the samples into liquid nitrogen. Samples were stored at -20°C, thawed and centrifuged (5 min at 13000 rpm). HPLC analysis of these incubations was performed essentially as described above for the check on purity of the synthetised aminophenols. The samples for the ^{19}F-NMR measurements were made oxygen free by four cycles of evacuating and filling with argon.

Chemical determination of hydroxylated metabolites.

4-Aminophenols were determined essentially as described by Brodie and Axelrod [36]. In short, 100 µL phenol reagent (5% w/v phenol in 2.5 N NaOH) and 200 µL 2.5 M Na_2CO_3 were added to 1 mL trichloroacetic acid precipitated supernatant. After 60 minutes at room temperature the absorbance at 630 nm was measured. The presence of a halogen in the indophenol formed in this assay influences its molar extinction coefficient at 630 nm [37]. For this reason the molar extinction coefficients of the halogenated aminophenol derived indophenols were determined to allow quantification of the 4-aminophenol metabolites from the various aniline derivatives. Molar extinction coefficients were 30.5, 26.7, 26.3, 14.5, 20.0, 16.8, and 12.5 $mM^{-1}cm^{-1}$ for the indophenols derived from 4-aminophenol, 3-fluoro-4-aminophenol, 2-fluoro-4-aminophenol, 3,5-difluoro-4-aminophenol, 2,6-difluoro-4-aminophenol, 2,3-difluoro-4-aminophenol and 2,3,5-trifluoro-4-aminophenol, respectively .

Products from C2 hydroxylation of the 4-halogenated anilines were determined by a chemical assay developed for the detection of 2-aminophenols. This newly-developed assay is described in detail elsewhere [30]. In short, a 1 mL microsomal incubation, frozen into liquid nitrogen to stop the reaction, was thawed and centrifuged at 13000 rpm for 10 min at 4°C. The supernatant was extracted three times with 3 mL of diethylether. After evaporation of the diethylether, 300 µL of 20% (w/v) trichloroacetic acid, 1 mL demineralised water and 100 µL 40 mM ammonium iron(III)sulphate dodecahydrate (Janssen Chimica) were added to the residue. After 45 min at room temperature, the reaction mixture was extracted with 2 mL chloroform and the absorbance of the chloroform-phase was measured at λ_{max} of the halogenated 2-aminophenol derived yellow derivative. The values for the 2-aminophenol concentrations of the samples were determined from the calibration curves of 2-aminophenol, 2-amino-5-fluorophenol, 2-amino-5-chlorophenol, 2-amino-5-

bromophenol and 2-amino-5-iodophenol.

The chemical determination of N-oxidation products (N-hydroxyaniline plus nitrosobenzene derivatives) was performed essentially as described by Herr and Kiese [38]. To 1 mL trichloroacetic acid precipitated microsomal supernatant, 0.3 mL 10% (w/v) potassium ferricyanide in 1N HCl and 1 mL demineralized water were added in order to oxidize the N-hydroxyaniline to the corresponding nitrosobenzene. These samples were extracted with 2 mL CCl_4 and the CCl_4 phases were washed twice with 5N H_2SO_4. To 1.0 mL of the washed CCl_4 phases, 1.0 mL of glacial acetic acid and 50 µl 20% (w/v) sodium nitrite were added. After 15 minutes, 100 µl 50% (w/v) ammonium sulphamate (Janssen Chimica) were added and the samples were mixed for 10 min. Finally, the color formation was started by the addition of 250 µl 80% (v/v) acetic acid and 50 µl N-(1-naphtyl)ethylenediamine dihydrochloride (Aldrich, Steinheim, Germany). After 2h in the dark the absorbance of the water phase at 555 nm was measured. Using nitrosobenzene and synthesized 4-fluoro-, 4-chloro-, 4-bromo- and 4-iodonitrosobenzene molar extinction coefficients of 40.4, 32.9, 41.3, 40.9 and 42.2 $mM^{-1} \cdot cm^{-1}$, respectively, were determined.

Kinetic analysis

The apparent V_{max} and K_m values for C4-, C2- and N-hydroxylation were determined by fitting the data to the standard Michaelis-Menten equation: $v = V_{max} * [S] / (K_m + [S])$ with the program of KaleidaGraph, version 2.0.2 (Abelbeck Software). The correlation coefficient of the fits was above 0.97 in all cases.

NMR measurements

^{19}F-NMR measurements were performed on a Bruker AMX 300 NMR spectrometer essentially as described previously by Vervoort *et al.* [39]. Chemical shifts are reported relative to $CFCl_3$. Quantification of the fluorinated compounds in the samples was achieved by comparison of the integrals of their ^{19}F-NMR resonances to the integral of the resonance of 4-fluorobenzoic acid added as an internal standard. The splitting patterns of the ^{1}H-NMR and ^{19}F-NMR resonances of the (bio)synthetized 2- and 4-aminophenols dissolved in acetone-d_6 were measured on a Bruker AMX 500 MHz. ^{19}F-NMR measurements were performed using a ^{1}H-probehead tuned to the ^{19}F frequency (470.5 MHz). ^{1}H-NMR chemical shifts are reported relative to acetone, present in acetone-d_6, used for locking the magnetic field.

RESULTS.

Microsomal cytochrome P450 catalyzed conversion of 4-halogenated anilines.

The influence of the type of C4 halogen substituent in an aniline molecule on the cytochrome P450-catalyzed dehalogenation to 4-aminophenol was investigated by HPLC analysis of microsomal incubations.

Figure 2 presents HPLC chromatograms of the microsomal metabolite patterns of the four 4-halogenated anilines and -for comparison- aniline itself. The reaction is cytochrome P450-mediated as no conversion was observed without NADPH, without

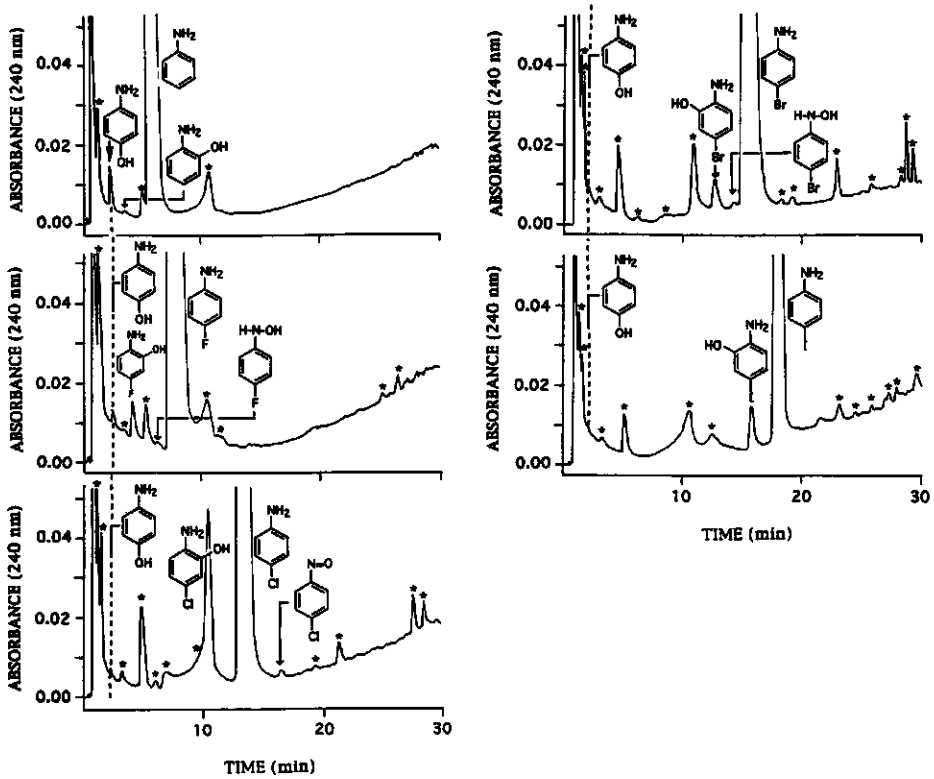

Figure 2: Reversed-phase HPLC chromatograms of the microsomal conversion of A) aniline, B) 4-fluoroaniline, C) 4-chloroaniline, D) 4-bromoaniline and E) 4-iodoaniline with detection at 240 nm. The peaks marked with an asterisk were also present in the chromatograms of control incubations carried out in the absence of NADPH, in the absence of microsomes, or in the absence of the aniline-derivatives.

microsomes or in the presence of CO [25]. Peaks were identified on the basis of their retention times compared to the retention times of the synthetized reference compounds and the similarity of the absorption spectra provided by the diode array detector. From these results it follows that the microsomal cytochrome P450-catalyzed conversion of the anilines results in the formation of 4-aminophenol, (halogenated) 2-aminophenols and/or N-oxidation products (N-hydroxyaniline and nitrosobenzene derivatives). Formation of (halogenated) 3-aminophenols or NIH-shifted metabolites is not observed. In contrast, metabolites resulting from hydroxylation at C4 accompanied by dehalogenation are readily observed, especially for 4-fluoroaniline and 4-chloroaniline. These results support the hypothesis that the cytochrome P450-catalyzed C4-hydroxylation of the 4-halogenated anilines proceeds by dehalogenation of the aromatic ring rather than by hydroxylation at C4 accompanied by an NIH shift of the halogen to the adjacent C3 or C5 position.

In addition to the HPLC experiments, metabolite formation in microsomal incubations was quantified by chemical analysis using specific methods for detection of 2-aminophenol, 4-aminophenol and N-oxidation products (N-hydroxyaniline- plus nitrosobenzene-derivatives). Table 1 presents the kinetic parameters obtained for the microsomal conversion of aniline and the four halogenated anilines. The apparent V_{max} for the formation of 4-aminophenol decreases to 66.8 % of the value of aniline, when the hydrogen at C4 is replaced by a fluorine. Replacement of the hydrogen at C4 by a chlorine, bromine or iodine substituent even further decreases the apparent V_{max} of this reaction. However, the apparent V_{max} values observed for 4-chloro, 4-bromo and 4-iodoaniline vary only slightly (Table 1).

Table 1: Kinetic characteristics of the cytochrome P450-catalyzed aromatic C4-hydroxylation of aniline and its 4-halogenated derivatives determined using liver microsomes from isosafrole pretreated male Wistar rats (n=2-4) [a].

Compound	Apparent V_{max} in nmol product • min^{-1} • nmol cyt $P450^{-1}$	Apparent K_m in mM
Aniline	5.55 ± 0.20 (100%)	17.0 ± 2.0
4-Fluoroaniline	3.71 ± 0.28 (66.8%)	9.3 ± 1.7
4-Chloroaniline	0.54 ± 0.09 (9.7%)	1.2 ± 0.2
4-Bromoaniline	0.39 ± 0.10 (7.0%)	0.7 ± 0.2
4-Iodoaniline	0.38 ± 0.16 (6.8%)	0.3 ± 0.1

[a] Values presented are the means ± standard error of the mean. Values in parentheses represent the % relative to the value for C4-hydroxylation of aniline.

To verify whether the observed change in apparent V_{max} for the dehalogenation to C4 aminophenols was not the result of a general decrease in metabolism from fluorine > chlorine > bromine > iodine, the conversion rates for formation of metabolites resulting from C2 and N-hydroxylation were also determined. Table 2 presents the apparent V_{max} values for the microsomal C2 and N-hydroxylation and also the total maximal conversion rate, calculated as the sum of the V_{max} values obtained for the conversion to 2-aminophenol, 4-aminophenol and N-hydroxyaniline metabolites. The results in Table 2 demonstrate that the total V_{max} for the C2, C4 plus N-hydroxylation is not significantly influenced by the type of C4 halogen substituent. The decrease in the apparent V_{max} for the 4-hydroxylation is accompanied by an increase in hydroxylation of the 4-halogenated anilines at their C2- and N-position. Thus, the results in Table 2 indicate that the observed change in dehalogenation is not a result of a reduced overall capacity of cytochromes P450 to convert the 4-halogenated anilines.

Table 2: Apparent V_{max} values of the cytochrome P450-catalyzed C2-hydroxylation and N-hydroxylation and the total conversion of aniline and its 4-halogenated derivatives determined using liver microsomes from isosafrole pretreated male Wistar rats (n=2-4) [a].

	apparent V_{max} nmol product · min^{-1} · nmol cyt $P450^{-1}$		V_{max} for total conversion [b]
Compound	**2-Aminophenol**	**N-hydroxyaniline**	
Aniline	1.13 ± 0.12	1.42 ± 0.07	8.10 ± 0.39
4-Fluoroaniline	2.27 ± 0.07	3.34 ± 0.09	9.32 ± 0.44
4-Chloroaniline	2.93 ± 0.12	4.35 ± 0.09	7.82 ± 0.30
4-Bromoaniline	2.67 ± 0.04	4.39 ± 0.09	7.45 ± 0.23
4-Iodoaniline	2.93 ± 0.47	2.93 ± 0.17	6.24 ± 0.80

[a] Values presented are the mean ± standard error of the mean. [b] Calculated as the sum of apparent V_{max} for C2-, N- and C4-hydroxylation (see Table 1).

Dehalogenation of 4-halogenated anilines by reconstituted cytochrome P450 IIB1, by a model heme-based catalyst and by a tertiair hydroperoxide supported microsomal cytochrome P450 system.

To demonstrate that the change in the extent of C4 hydroxylation with a change in the type of halogen substituent is not due to a change in tcytochrome P450 enzymes

actually contributing to the oxidative dehalogenation, experiments with purified reconstituted cytochrome P450 IIB1 and microperoxidase 8 (MP-8) were performed. MP-8 is a heme-containing mini-enzyme without a substrate binding site. This mini-enzyme, consisting of a protoporphyrin IX heme covalently bound to an oligopeptide of eight amino acids, has been reported to form a $(FeO)^{3+}$ intermediate similar to the cytochrome P450 enzyme and to catalyze P450 like reactions [40, 41]. Table 3 presents the results for the cytochrome P450 IIB1 and MP-8 mediated conversion of aniline, 4-fluoro-, 4-chloro-, 4-bromo- and 4-iodoaniline to 4-aminophenol. The results clearly demonstrate, for both systems, a decrease in 4-aminophenol formation from aniline > 4-fluoroaniline > 4-chloroaniline > 4-bromoaniline > 4-iodoaniline. Moreover, for cytochrome IIB1 as well as for MP-8, the same dependency in reduction of the rate of 4-aminophenol formation exists as is observed for the conversion by liver microsomes of isosafrole pretreated rats, containing mainly cytochromes P450 IA1/IA2 [42] (Table 1).

Additional experiments were performed to investigate whether the change in the extent of C4 hydroxylation with a change in the type of halogen substituent is not due to a change in rate-limiting steps in the P450 catalysis. The use of the alternative oxygen donor tertiair butyl hydroperoxide is known to provoke a short-cut in the reaction cycle, thereby circumventing several possible rate-limiting reaction steps in a

Table 3: Apparent maximal reaction rates for the microperoxidase 8, purified reconstituted cytochrome P-450 IIB1 and microsomal tBuOOH supported catalyzed C4-hydroxylation of aniline and its 4-halogenated derivatives.

Compound	**Apparent V_{max} nmol product • min^{-1} • nmol cyt P450^{-1}**		
	MP-8	**Cyt P450 IIB1**	**Microsomal tBuOOH supported Cyt P450**
Aniline	3.14 ± 0.06 (100%)	0.97 ± 0.07 (100%)	5.76 ± 0.42 (100%)
4-Fluoroaniline	0.42 ± 0.01 (13.4%)	0.28 ± 0.02 (28.9%)	1.94 ± 0.05 (33.7%)
4-Chloroaniline	0.18 ± 0.01 (5.7%)	0.12 ± 0.01 (12.4%)	0.35 ± 0.05 (6.1%)
4-Bromoaniline	0.15 ± 0.01 (4.8%)	0.07 ± 0.00 (7.2%)	0.21 ± 0.02 (3.6%)
4-Iodoaniline	0.14 ± 0.01 (4.5%)	0.04 ± 0.01 (4.1%)	0.34 ± 0.02 (5.9%)

[a] Values presented are the mean ± standard error of the mean. Values in parentheses represent the % relative to the value for C4-hydroxylation of aniline.

NADPH/oxygen supported reaction [43]. Table 3 presents the results for the tertiair butyl hydroperoxide supported microsomal cytochrome P450-mediated C4 hydroxylation of aniline, 4-fluoro, 4-chloro, 4-bromo and 4-iodoaniline to 4-aminophenol. The results show a similar decrease in 4-aminophenol formation from aniline to 4-iodoaniline as observed for the three other systems used in this study. This observation strongly suggests that for the oxidative dehalogenation of the 4-halogenated anilines occuring in this study, the rate-limiting step might indeed be related to the actual step in which the substrates are converted, and, thus, not -for instance- to electron donating steps.

Effect of additional electronegative substituents on the microsomal C4 hydroxylation of 4-fluorinated aniline derivatives.

To gain insight into the influence of electronic characteristics of the substrate on the dehalogenation of 4-halogenated anilines to 4-aminophenol derivatives, we investigated whether the presence of additional electron withdrawing substituents would affect the elimination of fluorine from the C4 position of the aniline substrate. When electron withdrawing possibilities of the halogen atom that has to be eliminated are a main factor in determining the possibilities for aromatic dehalogenation, it can be expected that additional electron withdrawing fluorine substituents at C2, C3, C5, and/or C6 might hamper C4-defluorination. Furthermore, in addition to the electronegative characteristics of the halogen substituents, the observed decrease in C4 hydroxylation with a change in the type of C4 halogen-substituent (Table 1) might be the result of (i) a change in the reaction mechanisms for dehalogenation with a change in the type of halogen atom, or (ii) increased steric hindrance by the halogen substituent hampering the initial attack of the cytochrome P450 $(FeO)^{3+}$ intermediate at the substituted C4 position of the aniline. However, the van der Waals radius of a fluorine atom almost equals that of a hydrogen atom, resulting in minimal steric influences when the dehalogenation of a series of polyfluorinated anilines is investigated.

Table 4 presents the results obtained. From the data it is clear that the relative ease of fluorine elimination from the C4-fluorinated anilines decreases with an increase in the number of fluorine substituents. Thus, the presence of additional fluorine substituents makes elimination of the fluorine at C4 relatively less easy. The data also demonstrate that an additional fluorine substituent at C3 results in stronger reduction of the relative apparent V_{max} than an additional fluorine at C2. This observation is in accordance with the more pronounced effect of the electron withdrawing fluorine when it is in an *ortho* rather than *meta* position with respect to the fluorine to be removed.

Table 4: Apparent V_{max} values for the C4-hydroxylation of 4-fluorinated anilines compared to the apparent V_{max} values of their non-C4 fluorinated analogues, determined using liver microsomes from isosafrole pretreated male Wistar rats (n=2-4).

Substrate	Apparent V_{max} nmol 4-aminophenol • min^{-1} • nmol cyt $P450^{-1}$	Relative apparent V_{max} as % of the non-C4-fluorinated analogue.
Aniline	5.55 ± 0.20	
4-Fluoroaniline	3.71 ± 0.28	66.8
2-Fluoroaniline	6.23 ± 0.20	
2,4-Difluoroaniline	2.99 ± 0.07	48.0
2,6-Difluoroaniline	8.89 ± 0.05	
2,4,6-Trifluoroaniline	3.21 ± 0.16	36.1
3-Fluoroaniline	4.85 ± 0.12	
3,4-Difluoroaniline	0.90 ± 0.03	18.6
2,3-Difluoroaniline	9.46 ± 0.39	
2,3,4-Trifluoroaniline	1.18 ± 0.04	12.5
3,5-Difluoroaniline	6.82 ± 0.39	
3,4,5-Trifluoroaniline	0.42 ± 0.02	6.2
2,3,6-Trifluoroaniline	3.23 ± 0.12	
2,3,4,6-Tetrafluoroaniline	0.66 ± 0.16	20.3

[a] Values presented are the mean ± standard error of the mean.

Metabolite profiles of the microsomal cytochrome P450 catalyzed conversion of fluorinated aniline-derivatives.

To characterize the overall conversion characteristics of the fluorinated anilines for the apparent V_{max} studies on C4 hydroxylation ^{19}F-NMR spectra of the microsomal incubations were determined.

Figure 3 presents the ^{19}F-NMR spectra of the microsomal conversion of the fluorinated anilines. The ^{19}F-NMR resonances of the metabolites were identified on the basis of (synthetised) reference compounds. For the metabolites 5,6-difluoro-2-aminophenol (Figure 3D), 4,5-difluoro-2-aminophenol (Figure 3D), 4,6-difluoro-2-aminophenol (Figure 3F) and 4,5,6-trifluoro-2-aminophenol (Figure 3F) the ^{19}F-NMR resonances were identified on the basis of a characteristic shift of the ^{19}F-NMR resonance known to exist upon the introduction of a hydroxyl moiety at positions

ortho, meta or para with respect to the fluorine substituent [43, 44].

The ^{19}F-NMR spectra presented in Figure 3 clearly demonstrated that the fluorine substituent at C4 is eliminated from the aromatic aniline-ring upon the cytochrome P450-catalyzed hydroxylation to the fluorinated 4-aminophenols. Metabolites resulting from C4 hydroxylation accompanied by a NIH shift of the fluorine substituent at C4 are not observed. Furthermore, the metabolic patterns show that, as for 4-fluoro, 4-chloro, 4-bromo and 4-iodoaniline, the incorporation of a halogen atom at the C4 position in the (poly)fluoroanilines leads to a metabolic switch from formation of 4-aminophenol to 2-aminophenol and N-hydroxyaniline metabolites.

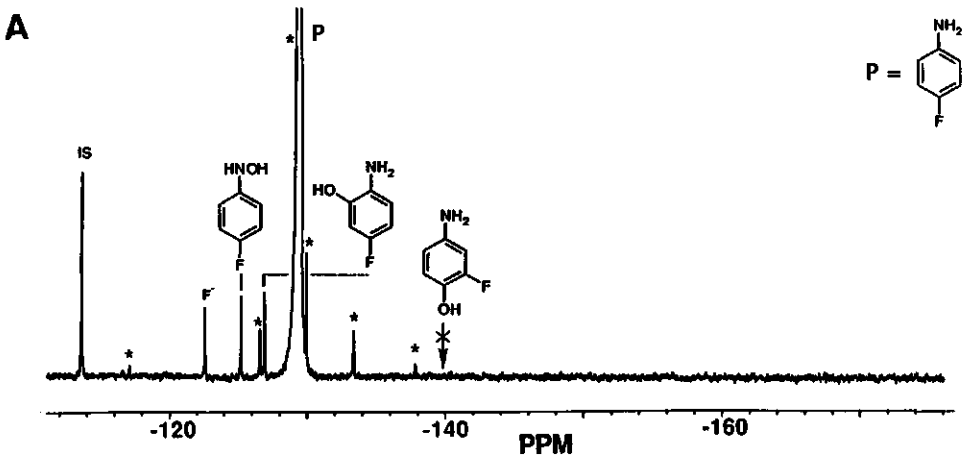

Figure 3: ^{19}F-NMR spectra of the microsomal cytochrome P450-catalyzed conversion of the non-C4 fluorinated anilines (upper part) and their 4-fluorinated analogues (lower part); A) 4-fluoroaniline, B to G, see next pages.

The resonances marked with an asterisk were also present in the ^{19}F-NMR spectra of control incubations carried out in the absence of NADPH. The resonance marked IS is from the internal standard 4-fluorobenzoic acid. The arrows in the spectrum indicate the ppm value where the NIH-shifted metabolites are expected.

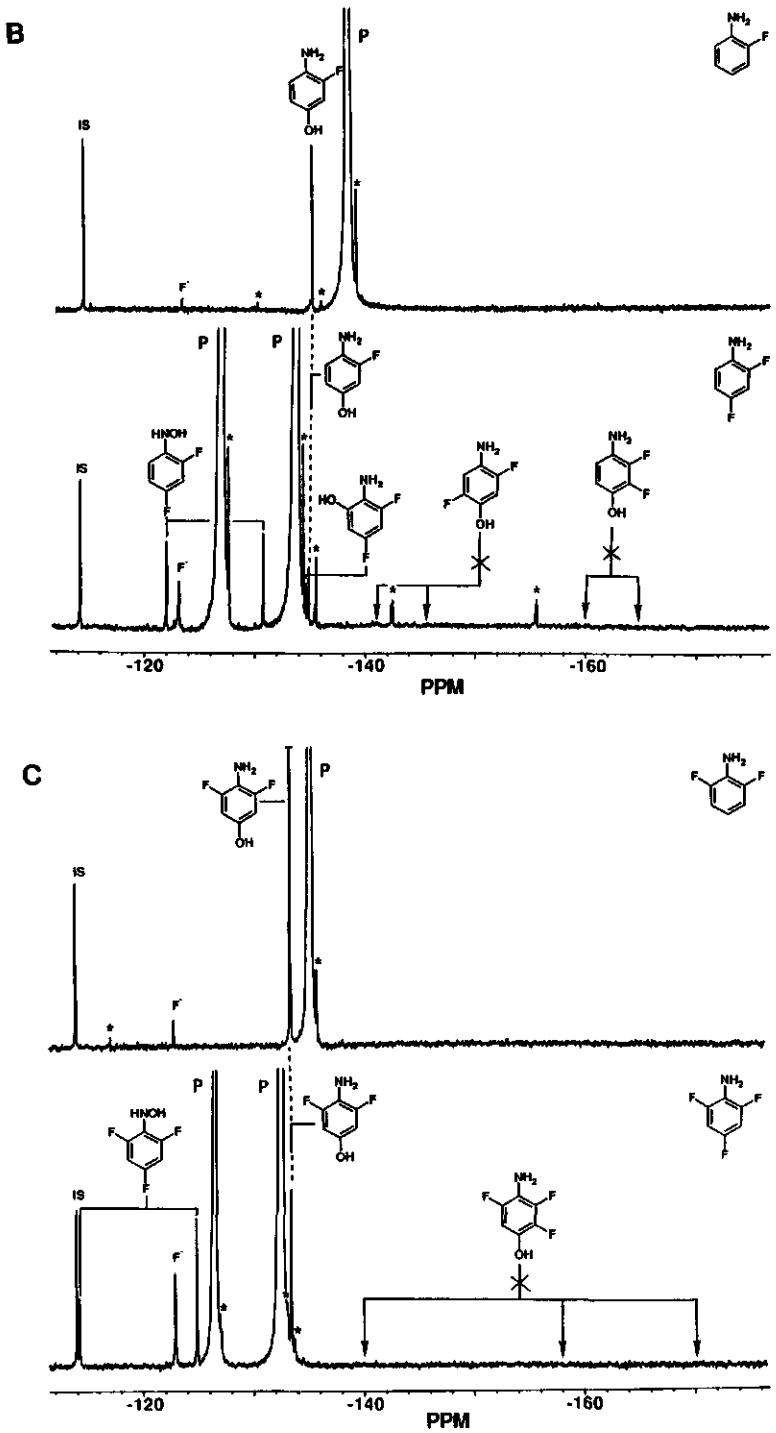

Figure 3 -continued-

B) 2-fluoroaniline and 2,4-difluoroaniline, C) 2,6-difluoroaniline and 2,4,6-trifluoroaniline,

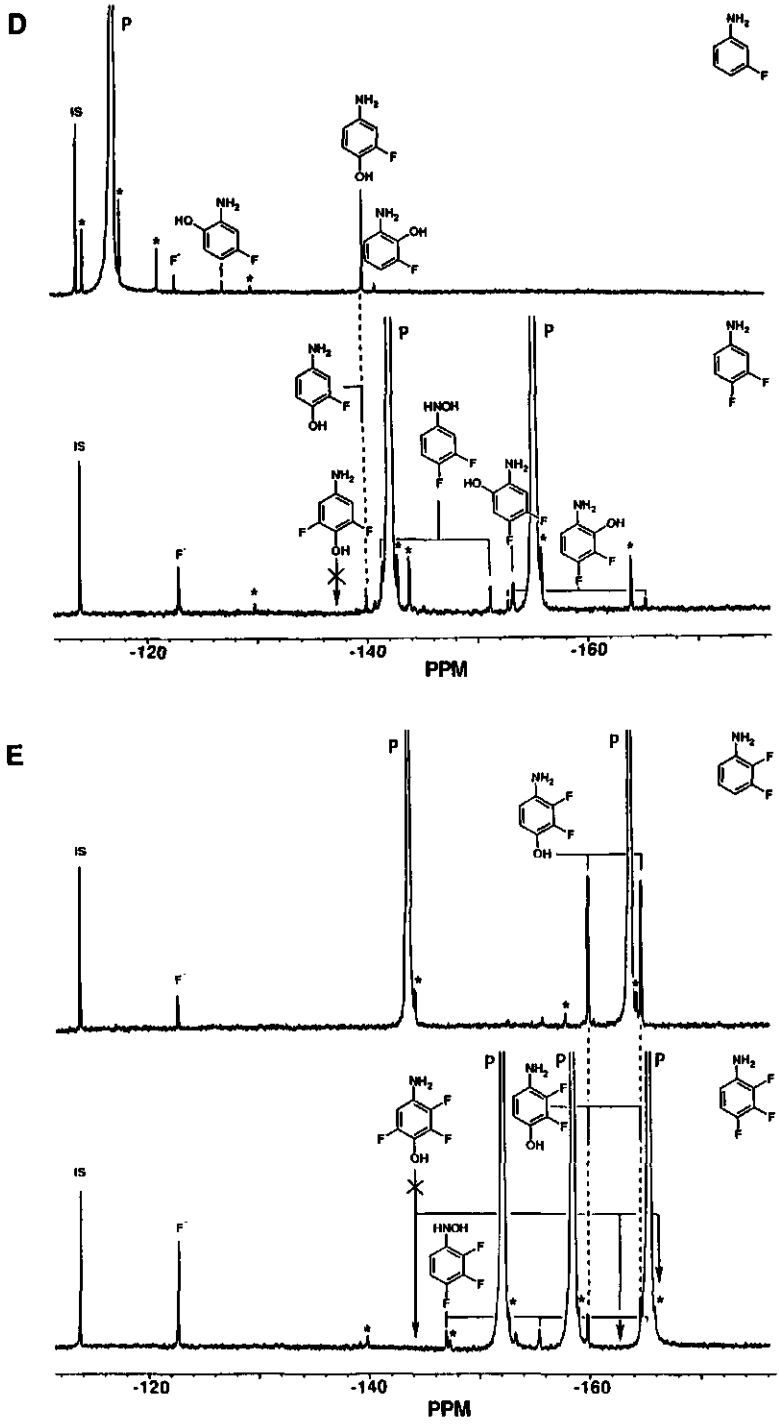

Figure 3 -continued-

D) 3-fluoroaniline and 3,4-difluoroaniline, E) 2,3-difluoroaniline and 2,3,4-trifluoroaniline,

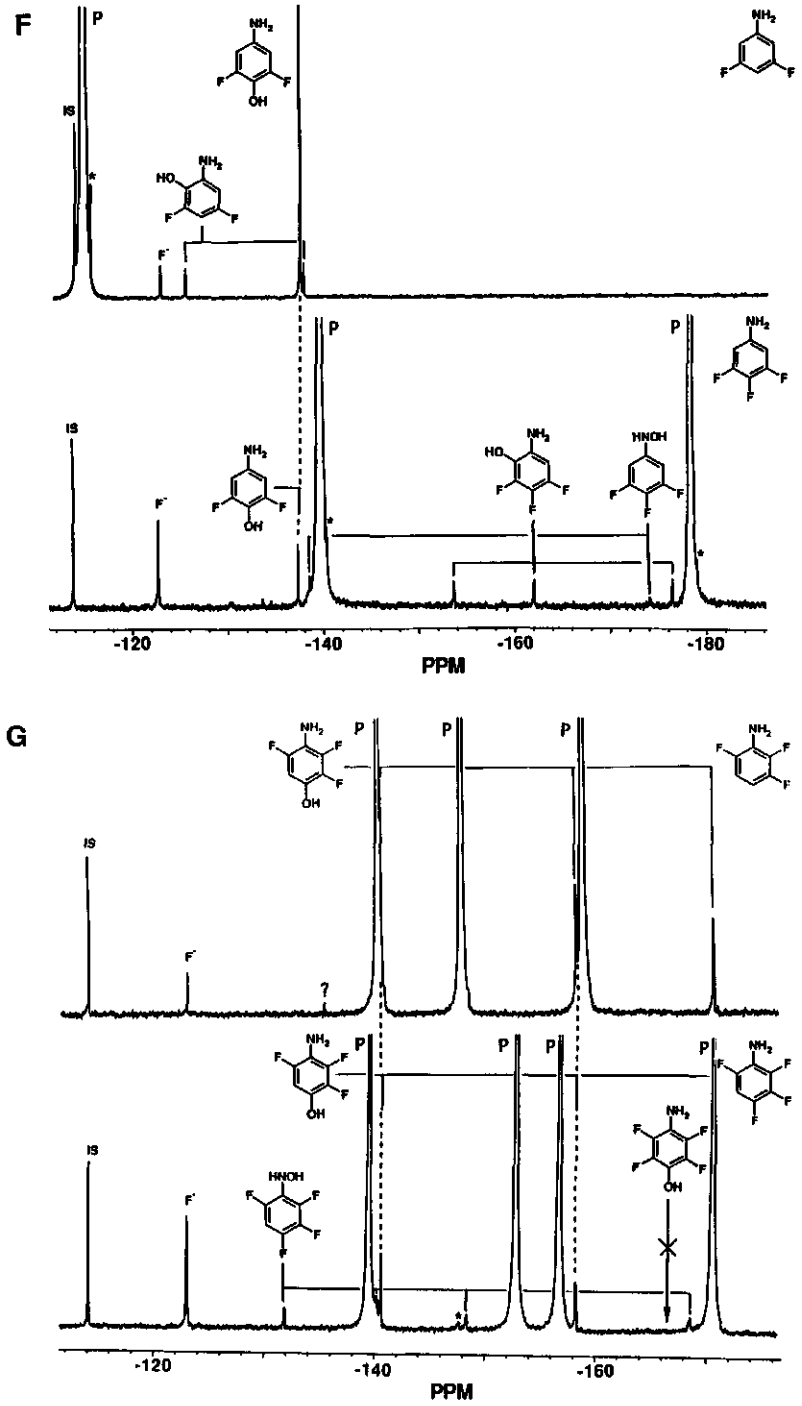

Figure 3 -continued-

F) 3,5-difluoroaniline and 3,4,5-trifluoroaniline, G) 2,3,6-trifluoroaniline and 2,3,4,6-tetrafluoroaniline

Effect of an additional electron-withdrawing substituent on the oxidative dehalogenation of C4 chlorinated, brominated, or iodinated aniline-derivatives.

Analogous to the experiments presented in Table 4, the influence of an additional fluoro-substituent on the oxidative dehalogenation of a C4-chlorinated, brominated and iodinated aniline was studied. This was done to investigate whether an electron withdrawing substituent would also affect the oxidative dehalogenation in the case of a chloro-, bromo-, or a iodo-substituent. Table 5 presents the microsomal cytochrome P450-catalyzed conversion of 2-fluoro-4-halogenated anilines to 3-fluoro-4-aminophenol. The results are in accordance with the observations for the defluorination of the di- and poly-fluorinated anilines. Firstly, the formation of 3-fluoro-4-aminophenol decreases in the order hydrogen >> fluoro >> chloro ≈ bromo ≈ iodo. Secondly, the presence of the additional fluoro substituent hampers oxidative elimination of the halogen at C4 as compared with the non-C2-fluorinated analogues for which the V_{max} of their conversion was already presented in Table 1.

Table 5: The cytochrome P450-catalyzed biotransformation of a series of 2-fluoro-4-halogenated anilines to 3-fluoro-4-aminophenol.

Compound	**Apparent V_{max}** in nmol 4-aminophenol • min^{-1} • nmol cyt $P450^{-1}$	**Relative apparent V_{max}** as % of the non-C4 halogenated analogue
2-Fluoroaniline	6.23 ± 0.20	100.0
2,4-Difluoroaniline	2.99 ± 0.07	48.0
2-Fluoro-4-chloroaniline	0.29 ± 0.00	4.7
2-Fluoro-4-bromoaniline	0.27 ± 0.00	4.3
2-Fluoro-4-iodoaniline	0.29 ± 0.00	4.7

DISCUSSION.

The mechanism of dehalogenation of halogenated aromatic xenobiotics is still a matter of considerable debate. Recently, we proposed a mechanism for the cytochrome P450 catalyzed oxidative defluorination of 4-fluorinated anilines and phenols proceeding by the mechanism depicted in Figure 1. This reaction scheme was based on the formation of a primary reaction product that could be reduced through a two

electron step to the hydroxyaniline or phenol indicating it to be the reactive benzoquinone(imine) [8, 9]. Elimination of the halogen as a halogen anion then follows from the net two electron balance of the cytochrome P450 reaction. Results of the present study demonstrate that the cytochrome P450 catalysed 4-hydroxylation of 4-halogenated anilines proceeds by dehalogenation rather than by hydroxylation accompanied by an NIH-shift. A fluorine substituent is significantly more easily eliminated than a chlorine, bromine or iodine substituent, the dehalogenation rate of 4-chloro-, 4-bromo- and 4-iodoaniline being much more similar. These findings are in accordance with the observations of Ullrich *et al.* who studied the conversion of a comparable group of compounds, the 4-halogenated acetanilides [46].

Using purified reconstituted cytochrome P450 IIB1, tertiair butyl hydroperoxide supported microsomal cytochrome P450 catalysis and microperoxidase 8, a heme-based model system able to catalyze cytochrome P450 like chemistry [41], similar changes in the rate of oxidative dehalogenation with a change in the C4 halogen substituent were observed. Based on these observations it may be concluded that the observed decrease in dehalogenation with a change in the halogen is not dependent on (i) different P450 enzymes contributing to the reaction nor on (ii) changes in orientation of the substrates by the protein core in the large active sites of P450. The observation of similar effects on the V_{max} of the oxidative dehalogenation in the tertiair butyl hydroperoxide driven reaction with a change in the halogen substituent supports the hypothesis that the actual rate-limiting step follows formation of the activated cofactor, and might thus indeed be related to the effect of the halogen substituent on the actual dehalogenation step. Taken together, these results with the purified reconstituted cytochrome P450 IIB1 system, the tertiair butyl hydroperoxide supported microsomal cytochrome P450 and the MP8 model compound, point to the importance of the electronic characteristics of the halogen substituents for the reactivity of the C4-halogenated anilines to participate in cytochrome P450 mediated oxidative dehalogenation reactions.

For all systems tested, *i.e.* microsomes, purified reconstituted cytochrome P450 IIB1, tertiair butyl hydroperoxide supported microsomal cytochrome P450 and microperoxidase 8, the observed relative apparent V_{max} values for dehalogenation of the anilines correlate ($r = 0.95$, 0.98, 0.93 and 0.97 respectively) with the electronegativity of fluorine (4.10), chlorine (2.83), bromine (2.74) and iodine (2.21). The changes in the apparent V_{max} for C4 hydroxylation with a change in the C4 substituent do not correspond to the strength of the carbon halogen bond known to increase in the opposite order, namely, iodine < bromine < chlorine < fluorine [1, 7]. Together, these results point to the importance of electronegativity of the halogen to be eliminated in the cytochrome P450-catalyzed oxidative dehalogenation. This observation supports the conclusion that the halogen is eliminated as a halogen anion.

However, steric hindrance of the initial cytochrome P450 $(FeO)^{3+}$ attack on C4 by the larger chloro-, but especially bromo- and iodo-substituents with Van der Waals radius of respectively 1.80 Å, 1.95 Å and 2.15 Å, might provide an additional explanation for the observed effects of the type of halogen on the apparent V_{max} for the dehalogenation. Such steric hindrance, in combination with the susceptibility of an iodo-substituent in particular to become oxidized by cytochromes P450, as demonstrated by Guengerich using 4-*tert*-butyl-2,5-bis[1-hydroxy-1-(trifluoromethyl)-2,2,2-trifluoro-ethyl]-iodobenzene [47], may even result in a different mechanism. For iodinated aromatic molecules a mechanism for the cytochrome P450-catalyzed deiodination has been suggested that proceeds by an interaction of the reactive cytochrome P450 $(FeO)^{3+}$ intermediate with non-bonding halogen electrons of the iodine [47, 48]. This interaction results in the formation of a haloso compound, and, finally, the formation of the hydroxylated substrate and elimination of the halogen as HXO [49]. Such a possible change in the actual mechanism of dehalogenation may add to a change in the rate of the dehalogenation reaction, especially for 4-iodoaniline. Therefore, additional dehalogenation experiments were performed to provide further evidence for the mechanism proceeding by elimination of the halogen as an anion. The effect of additional electron withdrawing fluorine substituents on the cytochrome P450-catalyzed oxidative dehalogenation of 4-halogenated aniline-derivates to 4-aminophenol metabolites was studied. The results obtained demonstrate that the presence of additional electron withdrawing substituents at the aromatic ring is another factor influencing dehalogenation. The introduction of additional fluorine substituents in a 4-halogenated aniline molecule lessens the possibility of its oxidative dehalogenation and, consequently, leads to a metabolic switch to fluorinated 2-aminophenol and N-hydroxyaniline metabolites. Formation of NIH-shifted metabolites was not observed. The decreasing effect of a fluorine substituent *ortho* with respect to the halogen to be eliminated is larger than that of an aditional *meta* fluorine substituent. This observation further lends weight to a mechanism in which the fluorine elimination is dependent on (*i.e.* hampered by) additional electron withdrawing substituents in the aromatic ring and, thus, a mechanism proceeding by elimination of the halogen as anion.

Altogether, the results of the present paper demonstrate that the possibilities for the cytochrome P450-mediated oxidative dehalogenation of halogenated anilines do not depend exclusively on factors previously reported: *i.e.* the capacity of the amino moiety to lose a proton and donate electrons to create the quinoneimine primary metabolite as indicated by the mechanism depicted in Figure 1 [9]. Additional factors influencing the cytochrome P450-catalyzed oxidative dehalogenation are; (i) the electronegativity of the halogen to be removed, the more electronegative fluorine being more easily eliminated than a chlorine, bromine or iodine, and; (ii) the position,

number and electron-withdrawing capacities of other substituents in the aromatic ring, electron withdrawing substituents decreasing the relative rate of the reaction, with an *ortho* positioned electron withdrawing substituent being more efficient than one positioned *meta* with respect to the reaction centre.

Thus, the results of the present study demonstrate that for the dehalogenation of aromatic halogenated compounds the electronegativity of the halogen to be eliminated is more important than the bond energy of the carbon halogen bond, known to follow the order fluoro > chloro > bromo > iodo. Surprisingly, this implies that the ease of oxidative dehalogenation of the aromatic 4-halogenated anilines follows the opposite order than that reported for dehalogenation of aliphatic halogenated hydrocarbons [3, 5, 11-13]. Previous studies on 2-fluoro- and 2-bromoestradiol [22] and pentafluorochlorobenzene [10], suggest that for other aromatic halogenated compounds the order of elimination of the halogen substituents also decreases in the order fluorine > chlorine > bromine > iodine, and, thus, opposite to the order for aliphatic halogenated hydrocarbons. This difference between aromatic and aliphatic dehalogenation might be due to a different reaction mechanism. The dehalogenation of aliphatic compounds by cytochromes P450 might proceed by one or two electron reductive pathways [3, 5, 50] or -as proposed for the conversion of dihalomethanes- by oxidative α-hydroxylation followed by the loss of a halogen as a result of a nonenzymatic collapse of an unstable intermediate. In contrast, aromatic dehalogenation most likely proceeds by the mechanism for oxidative dehalogenation as presented in Figure 1 [8, 9, 51].

Acknowledgments

The authors gratefully acknowledge the assistance of Ms. M. Peters and Mr. G. van Tintelen with animal handling. We also wish to thank Mr. S. Boeren and Mr. J. de Kok for their help with synthesizing of some halogenated nitrosobenzenes and HPLC experiments. This study was supported by the Netherlands Organisation for the Advancement of Scientific Research (N.W.O.). Part of this study was supported by the E. C. Human Capital and Mobility grant MASIMO no. ERBCHRXCT 920072.

REFERENCES.

1 Anders M.W., Aliphatic halogenated hydrocarbons. In: *Metabolic basis of detoxication*, (Ed. Jakoby), pp. 29-49. Acadamic Press, New York, 1982.

2 Wiersma D.A., Schnellmann R.G. and Sipes I.G., Pathways of halogenated hydrocarbon metabolism. In: *Foreign compound metabolism* (Eds. Caldwell J. and Paulson G.D.), pp. 53-64, Taylor & Francis, New York, 1984.

3 Ahr H.J., King L.J., Nastainczyk W. and Ullrich V., The mechanism of reductive dehalogenation of halothane by liver cytochrome P450. *Biochem. Pharmacol.* **31**, 383-390, 1982.

4 Schenk T., Müller R., Mörsberger F., Otto M.K. and Lingens F., Enzymatic dehalogenation of pentachlorophenol by extracts from *Arthrobacter* sp. strain ATCC 33790, *J. Bacteriol.* **171**, 5487-5491, 1989.

5 Castro C.E., Yokoyama W.H. and Belser N.O., Biodehalogenation; reductive reactivities of microbial and mammalian cytochromes P450 compared with heme and whole-cell models. *J. Agric. Food Chem.* **36**, 915-919, 1988.

6 Uotila J.S., Kitunen V.H., Saastamoinen T., Coote T., Haggblom M.M. and Salkinoja-Salonen M.S., Characterization of aromatic dehalogenases of mycobacterium fortuitum CG-2, *J. of Bacteriol.* **174**, 5669-5675, 1992.

7 MacDonald T.L., Chemical mechanisms of halocarbon metabolism. *CRC Crit. Rev. Toxicol.* **11**, 85-120, 1983.

8 Rietjens I.M.C.M. and Vervoort J., Bioactivation of 4-fluorinated anilines to benzoquinoneimines as primary reaction products. *Chem.-Biol. Interact.* **22**, 263-281, 1991.

9 Den Besten C., Van Bladeren P.J., Duizer E., Vervoort J. and Rietjens I.M.C.M., Cytochrome P450-mediated oxidation of pentafluorophenol to tetrafluorobenzoquinone as the primary reaction product. Chem. Res. Toxicol. 6, 674-680, 1993.

10 Rietjens I.M.C.M. and Vervoort J., A new hypothesis for the mechanism for cytochrome P450 dependent aerobic conversion of hexahalogenated benzenes to pentahalogenated phenols. *Chem. Res. Toxicol.* **5**, 10-19, 1992.

11 Kubic V.L. and Anders M.W., Metabolism of dihalomethanes to carbon monoxide. II. In vitro studies. *Drug Metab. Disp.* **3**, 104-112, 1975.

12 Ahmed A.E. and Anders M.W., Metabolism of dihalomethanes to formaldehyde and inorganic halide. I. *In vitro* studies. *Drug Metab. Disp.* **4**, 357-361, 1976.

13 Stevens J.L., Ratnayake J.H. and Anders M.W., Metabolism of dihalomethanes to carbon monoxide. IV. Studies in isolated hepatocytes. *Tox. Appl. Pharmacol.* **55**, 484-489, 1980.

14 Hecht S.S., LaVoie E.J., Bedenko V., Pingaro L., Katayama S., Hoffmann D., Sardella D.J., Boger E. and Lehr R.E., Reduction of tumorigenicity and of dihydrodiol formation by fluorine substitution in the angular rings of dibenzo(*a,i*)pyrene. *Cancer Research*, **41**, 4341-4345, 1981.

15 Hey M.M., Haaf H., McLachlan J.A. and Metzler M., Indirect evidence for the metabolic dehalogenation of tetrafluorodiethylstilbestrol by rat and hamster liver and kidney microsomes. *Biochem. Pharmacol.* **35**, 2135-2139, 1986.

16 Liehr J.G., Modulation of estrogen-induced carcinogenesis by chemical modifications. *Arch. Toxicol.*, **55**, 119-122, 1984.

17 Liehr J.G., 2-Fluoroestradiol: separation of estrogenicity from carcinogenicity. *Mol. Pharmacol.* **23**, 278-281, 1983.

18 Morgan P., Maggs J.L., Page P.C.B. and Park B.K., Oxidative dehalogenation of 2-fluoro-17a-ethynyloestradiol in vivo. *Biochem. Pharmacol.* **44**, 1717-1724, 1992.

19 Oravec C.T., Daniel F.B. and Wong L.K., Comparative metabolism of 7,12-dimethylbenz[*a*]anthracene and its non-carcinogenic 2-fluoro analogue by syrian hamster embryo cells, *Cancer Letters* **21**, 43-55, 1983.

20 Scribner J.D., Scribner N.K. and Koponen G., Metabolism and nucleic acid binding of 7-fluoro-2-acetamidofluorene in rats: oxidative defluorination and apparent dissociation fom hepatocarcinogenesis of 8-(*N*-arylamide)guanine adducts on DNA, *Chem.-Biol. Interactions* **40**, 27-43, 1982.

21 Daly J.W., Guroff G., Udenfriend S. and Witkop B., Hydroxylation of alkyl and halogen substituted anilines and acetanilides by microsomal hydroxylases. *Biochem. Pharmacol.* **17**, 31-36, 1968.

22 Li J.J., Purdy R.H., Appelman E.H., Klicka J.K. and Li S.A., Catechol formation of fluoro- and bromo-substituted estradiols by hamster liver microsomes. *Molec. Pharmacol.* **27**, 559-565, 1985.

23 Renson J. and Bourdon V., Hydroxylation et défluorination des dérivés fluores de l'aniline. *Arch. Int. Pharmacodyn.* **171**, 240-242, 1968.

24 Cnubben N.H.P., Vervoort J., Veeger C. and Rietjens I.M.C.M., Study on the regioselectivity and mechanism of the aromatic hydroxylation of monofluoroanilines. *Chem.-Biol. Interact.* **85**, 151-172, 1992.

25 Rietjens I.M.C.M. and Vervoort J., Microsomal metabolism of fluoroanilines. *Xenobiotica* **19**, 1297-1305, 1989.

26 Kennedy R.J. and Stock A.M., The oxidation of organic substances by potassium peroxymonosulfate. *J. Org. Chem.* **25**, 1901-1906, 1960.

27 Vogel A.I. In "Vogel's Textbook of Practical Organic Chemistry"' 5th ed. (B.S. Furniss, A.J. Hannaford, P.W.G. Smith, and A.R. Fatchell, eds.), John Wiley & Sons, New York, 1989.

28 Coleman G.H., McCloskey C.M. and Stuart F.A., Nitrosobenzene, *Organic synthesis* **25**, 80-83 (1946).

29 Boyland E. and Sims P., The oxidation of some aromatic amines with persulphate. *J. Chem. Soc.*, 980-985, 1954.

30 Cnubben N.H.P., Blaauboer B., Juyn S., Vervoort J. and Rietjens I.M.C.M., A spectrophotometric assay for the detection of 2-aminophenols in biological samples. *Analytical Biochemistry* **220**, 165-171, 1994.

31 Cnubben N.H.P., Peelen S., Borst J.W., Vervoort J., Veeger C. and Rietjens I.M.C.M., Molecular orbital based quantitative structure activity relationship for the cytochrome P450 catalyzed 4-hydroxylation of halogenated anilines, *Chem. Res. Toxicol.*, **7**, 590-598, 1994 .

32 Omura T. and Sato R. The carbon monoxide-binding pigment of liver microsomes. I. Evidence for its hemoprotein nature. *J. Biol. Chem.* **239**, 2370-2378, 1964.

33 Aron J., Baldwin D.A., Marques H.M., Pratt J.M. and Adams P.A., Hemes and

hemoproteins, 1: Preparation and analysis of the heme-containing octapeptide (microperoxidase 8) and identification of the monomeric form in aqueous solution, *J. Inorg. Biochem.*, **27**, 227-243, 1986.

34 Falk J.E. in Porphyrins and Metalloporhyrins, pp. 181, 240, Elsevier, Amsterdam, 1964.

35 Boersma M.G., Cnubben N.H.P., Van Berkel W.J.H., Blom M., Vervoort J. and Rietjens I.M.C.M., Role of cytochromes P-450 and flavin-containing monooxygenase in the biotransformation of 4-fluoro-N-methylaniline, *Drug Metab. Dispos.*, **21**, 218-230, 1993.

36 Brodie B.B. and Axelrod J., The estimation of acetanilide and its metabolic products, aniline, N-acetyl p-aminophenol and p-aminophenol (free and total conjugated) in biological fluids and tissues. *J. Pharmac. Exp. Ther.* **94**, 22-28, 1948.

37 Corbett J.F., Benzoquinone imimnes Part VII. Mechanisms and kinetics of the reaction of p-benzoquinone monimines with monohydric phenols. *J. Chem. Soc.*, 1503-1508, 1970.

38 Herr F. and Kiese M., Bestimmung von nitrosobenzol im blute. *Naunyn-Schmiedebergs Arch. Exp. Pathol. Pharmakol.* **235**, 3510-353, 1959.

39 Vervoort J., De Jager P.A., Steenbergen J. and Rietjens I.M.C.M., Developement of a ^{19}F-n.m.r. method for studies on the *in vivo* and *in vitro* metabolism of 2-fluoroaniline, *Xenobiotica* **20**, 657-670, 1990.

40 Rusvai E., Vègh M., Kramer M. an Horváth I., Hydroxylation of aniline mediated by heme-bound oxy-radicals in a heme peptide model system, *Biochem. Pharmacol.*, **37**, 4577-4581, 1988.

41 Nakamura S., Mashino T., and Hirobe M., ^{18}O Incorporation from $H_2{}^{18}O_2$ in the oxidation of N-methylcarbazole and sulphides catalyzed by microperoxidase-11, *Tetrahedron Letters*, **33**, 5409-5412, 1992.

42 Ryan D.E. and Levin W., Purification and characterization of hepatic microsomal cytochrome P-450, *Pharmacol. Ther.*,**45**, 153-239, 1990.

43 Ortiz de Montellano, P.R. (1986), Oxygen activation and transfer In *Cytochrome P-450: Structure, mechanism and biochemistry* (Ortiz de Montellano, P.R., Ed.) pp 217-271, Plenum Press, New York.

44 Rietjens I.M.C.M., Cnubben N.H.P., van Haandel M., Tyrakowska B., Soffers A.E.M.F., and Vervoort J., Different metabolic pathways of 2,5-difluoronitrobenzene and 2,5-difluoroaminobenzene compared to molecular orbital substrate characteristics, *Chem. -Biol. Interactions*, **94**, 49-72, 1995.

45 Wray V., Fluorine nuclei in difluorobenzene derivatives. In: Annual reports on NMR spectroscopy **14**, Academic Press, 1983, (Webb, G.A. ed.), 273-281.

46 Ullrich V., Wolf J., Amadori E. and Staudinger H., *Hoppe-Seyler's Z. Physiol. Chem.*, **349**, 85-94, 1968.

47 Guengerich F.P., Oxidation of halogenated compounds by cytochrome P450 peroxidases and model metalloporphyrins. *J. Biol. Chem.* **264**, 17198-17205, 1989.

48 Burka L.T., Thorsen A. and Guengerich F.P., Enzymatic monooxygenation of halogen

atoms: cytochrome P450 catalyzed oxidation of iodobenzene by iodosobenzene, *J. Am. Chem. Soc.* **102**, 7615-7616, 1980.

49 Van Ommen B. and Van Bladeren P.J., Possible reactive intermediates in the oxidative biotransformation of hexachlorobenzene, *Drug Metab. and Drug Interact.*, **7**, 214-243, 1989.

50 Nastainczyk W., Ahr H.J. and Ullrich V., The reductive metabolism of halogenated alkanes by liver microsomal cytochrome P450. *Biochem. Pharmacol.* **31**, 391-396, 1982.

51 Rietjens I.M.C.M., Tyrakowska B., Veeger C. and Vervoort J., Reaction pathways for biodehalogenation of fluorinated anilines, *Eur. J. Biochem.*, **194**, 945-954, 1990.

CHAPTER 7

Relationships between the regioselectivity of the hydroxylation of C4-substituted 2-fluoroaniline derivates and their toxic endpoints.

N.H.P. Cnubben, C.L. van den Berg and I.M.C.M. Rietjens.

Accepted for publication in Toxicology and Applied Pharmacology.

SUMMARY.

The *in vitro* and *in vivo* metabolic profiles of a series of C4-substituted 2-fluoroanilines were determined and compared to their capacity to induce methemoglobinemia and nephrotoxicity in male Wistar rats. Qualitative and quantitative relationships between the biotransformation and the toxic end-point of the halogenated anilines could be defined. The rate of *in vitro* N-hydroxylation of the aniline-derivatives correlates with the capacity of the compounds to induce methemoglobinemia (r= 0.96). In the experiments on the nephrotoxicity, attention was focussed on the relative importance of the C4- and C6-hydroxylated metabolites of the C4-substituted 2-fluoroanilines. *In vivo*, the formation of 4-aminophenol metabolites was demonstrated to vary in the opposite order as the formation of the 6-aminophenol metabolites. ^{1}H-NMR urinalysis and characterization of a set of conventional biochemical urinary parameters revealed the occurrence of nephrotoxicity upon exposure to the aniline-derivatives and were most consistent with damage at the proximal tubular site. Comparison of the extent of nephrotoxicity to the extent of formation of respectively the 4-aminophenol and/or 6-aminophenol metabolites, indicates a predominant role for the C4-hydroxylation route, not the C6-hydroxylation route, in the induction of nephrotoxic effects. Thus, a qualitative relationship is observed for the extent of C4-hydroxylation of the aniline-derivatives and the extent of their *in vivo* nephrotoxicity. In addition, comparison of the extent of 4-aminophenol formation and nephrotoxicity of both 2-fluoroaniline and 2,4-

difluoroaniline pointed at a possible role for a bioactivation pathway through oxidative dehalogenation, resulting in direct formation of a 4-benzoquinoneimine as the primary metabolite in the case of 2,4-difluoroaniline. Altogether, it is concluded that reduced possibilities for C4-hydroxylation in the series of aniline-derivatives, results in increased possibilities for C6- and N-hydroxylation and, consequently, a shift in the type of toxic end-point observed, *i.e.* from nephrotoxicity to methemoglobinemia.

INTRODUCTION.

Halogenated aniline-derivatives are frequently used as industrial intermediates for the production of dyes, pharmaceuticals and agrochemicals. Exposure to these type of aromatic amines occurs primarily in the industrial setting, but also as a result of biotransformation or chemical degradation of their derivatives. The most frequently reported consequences of acute exposure to aniline-derivatives are methemoglobinemia [Eadsforth *et al.*, 1984; Harrison and Jollow, 1987; Kiese, 1974; McLean *et al.*, 1969] and nephrotoxicity [Lo *et al.*, 1990; Lo *et al.*, 1991; Rankin *et al.*, 1986 a & b; Yoshida *et al.*, 1989]. The cytochrome P450-catalyzed bioconversion of the aniline-derivatives to chemically reactive species, like nitrosobenzenes, N-hydroxyanilines, benzoquinoneimines and/or ring-hydroxylated metabolites, is generally accepted to be a prerequisite for the expression of the toxic effects exerted by these compounds [Eyer, 1983; Rankin *et al.*, 1994; Rietjens *et al.*, 1990; Sabbioni, 1992].

The N-hydroxyaniline metabolites are able to induce methemoglobin ($HbFe^{3+}$) formation [Eyer, 1988; Kiese, 1974; Lenk and Riedl, 1989; Maples *et al.*, 1989]. In addition, in *in vitro* studies 2- and 4-aminophenols were reported to be able to induce ferrihemoglobin upon their oxidation to quinoneimines within the erythrocytes [Blaauboer *et al.*, 1976; Eckert and Eyer, 1983]. *In vivo*, however, 2- and 4-aminophenols may hardly contribute to the aniline-induced methemoglobinemia. This can best be ascribed to their lower intrinsic ferrihemoglobin inducing capacity compared to N-oxidation products, in combination with their efficient conjugation in UDP-glucuronyltransferase and sulphotransferase-catalyzed reactions [Harrison and Jollow, 1987].

Nephrotoxicity of halogenated anilines, occuring predominantly at the proximal tubule and to a lesser extent at the distal tubule, is proposed to be linked to the formation of aminophenol-metabolites [Lo *et al.*, 1991; Rankin *et al.*, 1986a & b; Valentovic *et al.*, 1992]. The involvement of especially the 4-aminophenol metabolites in the nephrotoxicity of anilines has been reported, but the present

evidence is not conclusive. Rankin *et al.* [1994] demonstrated that the metabolite 2,6-dichloro-4-aminophenol may contribute to 3,5-dichloroaniline induced nephrotoxicity, but concluded that other metabolites may also be involved. Oxidation of 4-aminophenol to the reactive 4-benzoquinoneimine, subsequent conjugation with glutathione and further processing of the glutathione conjugate by the proximal tubular brush border enzyme γ-glutamyltransferase are thought to be involved in the selective toxicity of aminophenols [Calder *et al.*, 1975; Calder *et al.*, 1979; Fowler *et al.*, 1991; Fowler *et al.*, 1993; Fowler *et al.*, 1994, Gartland *et al.*, 1989b; Gartland *et al.*, 1990a; Josephy *et al.*, 1983; Klos *et al.*, 1993; Lock *et al.*, 1993].

Thus, the various aniline-metabolites resulting from N-, C4- and C6-hydroxylation, vary in their reactivities and toxic characteristics. This implies that the regioselectivity of the cytochrome P450-dependent hydroxylation is of importance for the toxic implications of aniline-derivatives, although the two aspects *i.e.* biotransformation and toxicity, have not yet been thoroughly investigated in one and the same study. The objective of the present study was to investigate in one study, for a series of related aniline-derivatives, possible relationships between the regioselectivity of their hydroxylation and their capacity to induce methemoglobinemia and/or nephrotoxicity. C4-Substituted 2-fluoroanilines were chosen as the substrates in these studies. The fluorine substituent at C2 provides the possibility for metabolite detection by ^{19}F-NMR, whereas the varying substituent at C4 (H, F, Cl, Br, I) can be expected to influence the regioselectivity of the aromatic hydroxylation with respect to N-hydroxylation and/or C4 and C2/6 aromatic hydroxylation [Cnubben *et al.*, 1995].

Qualitative and quantitative relationships between the biotransformation and the toxic endpoints of the halogenated anilines could be defined.

MATERIALS AND METHODS.

Chemicals.

2-Fluoro-, 2-fluoro-4-chloro- and 2-fluoro-4-bromoaniline were purchased from Janssen Chimica (Beerse, Belgium). 2-Fluoro-4-iodoaniline and 5-fluoro-2-nitrophenol were from Aldrich (Steinheim, Germany). 2,4-Difluoroaniline, 3-fluoro-4-nitrophenol, 3-fluoro-2-nitrophenol were obtained from Fluorochem (Derbyshire, UK). The purity of these compounds was > 97%. 3-Fluoro-4-aminophenol, 3-fluoro-2-aminophenol, 5-fluoro-2-aminophenol were synthesized by the chemical reduction of their nitro analogs in ethylacetate under 4 atm. H_2 using palladium on activated carbon (Janssen Chimica) as the catalyst essentially as described before [Rietjens and Vervoort, 1989 & 1991]. 3,5-Difluoro-2-aminophenol, 3-fluoro-5-chloro-2-amino-

phenol, 3-fluoro-5-bromo-2-aminophenol and 3-fluoro-5-iodo-2-aminophenol were synthesized according to Boyland and Sims [1954] using respectively 2,4-difluoroaniline, 2-fluoro-4-chloroaniline, 2-fluoro-4-bromoaniline and 2-fluoro-4-iodoaniline as the starting material. To a solution of 5 g of a halogenated aniline in 20 ml acetone, 250 ml water and 50 ml 2N potassium hydroxide, 15 g potassium persulphate (Janssen Chimica) were added as an aqueous solution during a time period of 8 hr under continuous stirring. The mixture was kept overnight and filtered. After washing with ether, the solution was acidified with 2N sulphuric acid and the precipitate was separated from the mixture by filtration. The filtrate was neutralized with 2N potassium hydroxide and the water-content was reduced by freeze-drying. The solution was extracted 3 times with 100 ml methanol, the solvent was removed by evaporation under reduced pressure. The sulphate esters were hydrolysed for 45 minutes at 100°C in 3N HCl. After cooling, the solution was neutralized and the 2-aminophenols were extracted from the mixture with diethylether. After evaporation of the solvent, the precipitate was dissolved in 3 ml dichloromethane and applied to a Silicagel 60 column (200 mm x 35 mm) (Merck, Darmstadt, FRG) using 5% (v/v) ethanol in dichloromethane as the eluens. The flow-rate was 5 ml/min and fractions of 5 ml were collected. The fractions were analyzed on halogenated 2-aminophenol content using a chemical assay [Cnubben *et al.*, 1994] and ^{19}F-NMR. The 2-aminophenol containing fractions were collected and after crystallization the purity of these aminophenols was checked on the basis of ^{19}F-NMR and also on the basis of their HPLC patterns. HPLC was carried out on a Kratos 400 HPLC system, with a LiChrosorb C8 column (100 mm x 3 mm) (Chrompack, Middelburg, The Netherlands). After eluting for 5 min with nanopure, a linear gradient from 0-80% (v/v) methanol in 22 min, followed by 80% (v/v) methanol for 6 min was applied. Detection was at 240 nm using a Waters^{TM} 996 photodiode array detector. The purity of the synthesized compounds was determined to be >98%. The identity of the 2-aminophenols was derived from their ^{1}H-NMR and ^{19}F-NMR spectral characteristics: 3,5-difluoro-2-aminophenol: ^{1}H-NMR (acetone-d$_6$, relative to acetone)(ppm): 9.17 (H6)(d)($^{3}J_{H6\text{-}F5}$ = 9.0 Hz), 9.10 (H4)(tr)($^{3}J_{H4\text{-}F3}$ = 9.0 Hz, $^{3}J_{H4\text{-}F5}$ = 9.0 Hz) and ^{19}F-NMR (0.1 M potassium phosphate, pH 7.6, relative to $CFCl_3$)(ppm): -134.5 (F3)(d, $^{3}J_{F3\text{-}H4}$ = 9.0 Hz), -127.1 (F5)(tr, $^{3}J_{F5\text{-}H6}$ = 9.0 Hz, $^{3}J_{F5\text{-}H4}$ = 9.0 Hz); 3-fluoro-5-chloro-2-aminophenol: ^{1}H-NMR (acetone-d$_6$, relative to acetone)(ppm): 6.69 (H6)(s), 6.67 (H4)(d)($^{3}J_{H4\text{-}F3}$ = 10.5 Hz) and ^{19}F-NMR (0.1 M potassium phosphate, pH 7.6, relative to $CFCl_3$)(ppm): -135.4 (F3)(d, $^{3}J_{F3\text{-}H4}$ = 10.5 Hz); 3-fluoro-5-bromo-2-aminophenol: ^{1}H-NMR (acetone-d$_6$, relative to acetone)(ppm): 6.76 (H6)(s), 6.74 (H4)(d)($^{3}J_{H4\text{-}F3}$ = 10.0 Hz) and ^{19}F-NMR (0.1 M potassium phosphate, pH 7.6, relative to $CFCl_3$)(ppm): -135.3 (F3)(d, $^{3}J_{F3\text{-}H4}$ = 10.0 Hz); 3-fluoro-5-iodo-2-aminophenol: ^{1}H-NMR (acetone-d$_6$, relative to acetone)(ppm): 6.92 (H6)(s), 6.88

(H4)(d)($^3J_{H4-F3}$ = 10.0 Hz) and ^{19}F-NMR (0.1 M potassium phosphate, pH 7.6, relative to $CFCl_3$)(ppm): -135.5 (F3)(d, $^3J_{F3-H4}$ = 10.0 Hz).

The N-acetylated derivatives of 2-fluoroaniline, 2,4-difluoroaniline, 2-fluoro-4-chloroaniline, 2-fluoro-4-bromoaniline, 2-fluoro-4-iodoaniline, 3-fluoro-4-aminophenol, 3-fluoro-2-aminophenol, 3,5-difluoro-2-aminophenol, 3-fluoro-5-chloro-2-aminophenol, 3-fluoro-5-bromo-2-aminophenol and 3-fluoro-5-iodo-2-aminophenol were synthesized as described by Vogel [1978]. N-hydroxy-2,4-difluoroaniline was synthesized by reduction of the nitroanalog 2,4-difluoronitrobenzene (Fluorochem) essentially as described by Vogel [1989] and Coleman [1943]. N-hydroxy derivatives of 2-fluoro-, 2-fluoro-4-chloro-, 2-fluoro-4-bromo- and 2-fluoro-4-iodoaniline were synthesized by the oxidation of the corresponding aniline to the nitrosobenzene analogue with potassium peroxymonosulphate in a water-acetic acid mixture using the procedure described by Kennedy and Stock for the synthesis of 1,4-dinitrosobenzene [Kennedy and Stock, 1960]. The characteristic green nitrosobenzenes were then converted to their N-hydroxyanilines by chemical reduction with 20 mM ascorbic acid. The ^{19}F-NMR chemical shifts of the synthesized compounds were as follows (0.1 M potassium phosphate, pH 7.6, relative to $CFCl_3$)(ppm): 2-fluoro-N-hydroxyaniline -135.3 ppm, 2,4-difluoro-N-hydroxyaniline -121.9 ppm (F4) and -130.6 (F2) ppm, 2-fluoro-4-chloro-N-hydroxyaniline -132.7 ppm, 2-fluoro-4-bromo-N-hydroxyaniline -132.6 ppm and 2-fluoro-4-iodo-N-hydroxyaniline -132.8 ppm.

Preparation of microsomes.

Microsomes were prepared from the perfused livers of male Wistar rats (ca. 300 g) [Rietjens and Vervoort, 1989]. Cytochrome P450 contents were determined as described by Omura and Sato [1964]. Protein was assayed by the method of Lowry *et al.* [1951] using bovine serum albumin (Sigma) as the standard.

Microsomal incubations.

Microsomal incubations were carried out at 37°C in 0.1 M potassium phosphate (pH 7.6) containing 2 µM microsomal cytochrome P450 and 0-10 mM aniline-derivative added as 1% (v/v) of a stock solution in dimethylsulphoxide. The reaction was started by the addition of 1 mM NADPH and terminated after 10 min. by freezing the sample into liquid nitrogen. Samples were stored at -20°C, thawed, centrifuged (5 min at 13000 rpm) and analysed by ^{19}F-NMR. To 1.6 ml of sample, 100 µl D_2O and 10 µl 8.4 mM 4-fluorobenzoic acid as the internal standard were added. These samples for ^{19}F-NMR analysis were made oxygen free by four cycles of evacuation and filling with argon. Incubations for ^{19}F-NMR analysis additionally contained 1 mM ascorbic acid to prevent autoxidation of the aminophenols especially

during the overnight ^{19}F-NMR measurement.

In vivo exposure of rats

Male Wistar rats (body weight 275-300 g) with a permanent cannulation of the jugular vein in combination with a head attachment apparatus allowing easy connection of cannulae for blood sampling were used [*Remie et al.*, 1990]. The rats were housed individually in metabolism cages. Food and water were allowed *ad libitum*. Groups of rats (2-4) were dosed by oral injection with olive oil at 2 ml kg^{-1} bodyweight (controls), or the desired aniline-derivatives in olive oil at indicated doses. Urine was collected for 24 hr before dosing and at 0-24 and 24-48 hr after dosing. The urine samples were stored at -20°C after centrifugation at 13000 rpm for 5 min to remove food particels and other debris. Blood samples (approximately 250 µl) were collected from the cannulated rats into heparinized tubes at 3 days before dosing (t=0) and at 1, 2, 4, 8, 24 and 48 hr after dosing and were immediately analysed for the percentage of methemoglobin present. Additionally, 1 ml blood samples were collected 3 days before dosing (t=0) and at 24 and 48 hr after dosing for determination of blood urea nitrogen (BUN) in order to assess the nephrotoxicity.

Enzyme hydrolysis of urinary aniline metabolites.

Enzyme-catalyzed hydrolysis of urine samples was carried out as described before (Cnubben *et al.*, 1992) using either β-glucuronidase from *Escherichia coli* K12 (Boehringer, Mannheim, Germany) or arylsulphatase/β-glucuronidase from *Helix pomatia* (Boehringer). Samples were made oxygen free by four cycles of evacuation and filling with argon. Urine samples were analyzed by ^{19}F NMR after 1:1 dilution in 0.2 M potassium phosphate (pH 7.6) containing 20% acetonitrile. Acetonitrile was added to the urine samples for a better resolution of some of the ^{19}F-NMR resonances [Vervoort *et al.*, 1990].

Determination of methemoglobinemia.

Methemoglobin content was determined by the method of Harrison and Jollow [1987]. All samples were analysed immediately after they had been collected in order to prevent decomposition of the unstable methemoglobin.

Determination of biochemical parameters in plasma and urine.

Urines were tested for glucose by the hexokinase method (Sigma kit, No. 16-UV). Creatinine concentrations in urine were measured by the so-called Jaffé reaction, based on the reaction between picric acid and creatinine to form a complex which absorbance is determined at 530 nm [Tietz, 1987]. Protein content in the urine was determined using the method of Lowry *et al.* [1951] using bovine serum

albumine as the standard. Plasma was tested for urea nitrogen using a diagnostic kit (BUN, Sigma kit No. 640A).

NMR measurements.

^{19}F-NMR measurements were performed on a Bruker AMX 300 spectrometer as described before [Vervoort *et al.*, 1990]. Between 1500 and 50000 scans were recorded, depending on the concentrations of the fluorine containing compounds and the signal to noise ratio required. Chemical shifts are reported relative to $CFCl_3$. Concentrations of the various metabolites could be calculated by comparison of the integrals of the ^{19}F-NMR resonances of the metabolites to the integral of the ^{19}F-NMR resonance of 4-fluorobenzoic acid, added as an internal standard. The splitting patterns of the ^{1}H-NMR and ^{19}F-NMR resonances of the synthesized 2-aminophenols dissolved in acetone-d_6 were measured on a Bruker AMX 500. ^{19}F-NMR measurements were performed using a ^{1}H probehead tuned to the ^{19}F frequency (470.5 MHz).

Urines were analyzed by ^{1}H-NMR measurements on a Bruker AMX 500 after lyophilization and solvation of the residue in D_2O. Fifty free induction decays were collected using 7 μsec pulses with a repetition time of 2.4 sec. Saturation of the resonance frequency of water was applied to prevent the appearance of an intense water signal in the spectrum. Chemical shifts are presented relative to sodium 3-trimethylsilyl-(2,2,3,3-$^{2}H_4$)-propionate (TSP at 0 ppm). TSP also served as an internal standard for quantitation of urinary marker metabolites indicative for site-specific renal damage [Gartland, 1989a; Anthony *et al.*, 1994]. Such marker metabolites were trimethylamine N-oxide (TMAO) at 3.27 ppm (singlet, $(CH_3)_3$), dimethylglycine (DMG) at 2.89 ppm (singlet, $(CH_3)_2$), dimethylamine (DMA) at 2.71 ppm (singlet, $(CH_3)_2$), citrate at 2.55 ppm (AB, $(CH_2)_2$), succinate at 2.45 ppm (singlet, $(CH_2)_2$), acetate at 1.94 ppm (singlet, CH_3), lysine at 1.71 ppm (multiplet, δ-CH_2), alanine at 1.48 ppm (doublet, CH_3), lactate at 1.33 ppm (doublet, CH_3), valine at 0.99, 1.04, 2.29, 3.62 ppm and isoleucine at 0.92, 1.01, 1.33, 1.70 and 3.68 ppm and [Anthony *et al.*, 1994, Bales *et al.*, 1984; Iles *et al.*, 1985]. Quantitation by NMR in samples with high protein contents has been reported to be hampered by the fact that TSP tends to bind to protein resulting in a broadening and reduction in the intensity of the TSP resonance as described by Gartland [1989a]. However, in our system the method was validated by measuring the creatinine concentration in 10 urine samples by another, independent method. Determinations of the amounts of creatinine in urine by the chemical assay based on the Jaffé reaction compared well ($r = 0.89$) with the creatinine concentrations as determined by ^{1}H-NMR spectroscopy using TSP as the standard.

Statistical analysis

Statistical analysis of the data was carried out using one-way analysis of variance (ANOVA), followed by Students *t*-tests. A p value of < 0.05 was considered to be statistically significant.

RESULTS.

In vivo metabolic profiles of the halogenated aniline-derivatives.

First, the effect of variation in the C4-substituent in the C4-substituted 2-fluoroanilines on the regioselectivity of their cytochrome P450-mediated conversion was investigated *in vivo*. The ^{19}F-NMR spectra of the 24 h urines of the rats exposed to the 2-fluoroaniline-derivatives having different substituents at the C4 position (H, F, Cl, Br or I respectively) are shown in Figure 1. The resonances of the metabolites, summarized in Table 1, were identified on the basis of synthesized reference compounds. Enzyme hydrolysis of the urine with β-glucuronidase and/or arylsulphatase identifies the resonances as the sulphated or glucuronidated metabolites in a similar way as described before [Cnubben *et al.*, 1992; Vervoort *et al.*, 1990]. The quantitative urinary metabolic profiles derived from these spectra are presented in Table 2. The results demonstrate that the contribution of 4-aminophenol derived metabolites to the overall metabolite pattern decreases when the C4-substituent varies and in the order 2-fluoroaniline, 2,4-difluoroaniline, 2-fluoro-4-chloroaniline, 2-fluoro-4-bromoaniline and 2-fluoro-4-iodoaniline being respectively 86.1, 21.5, 8.5, 6.6 and 5.6% of the total amount of metabolites in the urine. The contribution of 6-aminophenol derived metabolites to the metabolite pattern decreases in the opposite order. As a consequence, the total amount of aminophenol metabolites did not vary significantly for the various aniline derivatives, but the ratio 4-aminophenol to 6-aminophenol-derived metabolites decreases significantly when the C4 substituent varies from H >> F > Cl > Br ≥ I (Table 3). In the urine of 2-fluoroaniline exposed rats the ratio 4- to 6-aminophenol derived metabolites is 2 orders of magnitude higher than in the urine of rats exposed to the C4-halogenated derivatives.

Excretion of metabolites in urine resulting from N-hydroxylation was detected only to a limited extent for 2-fluoro-4-bromoaniline and 2-fluoro-4-iodoaniline. Finally, it is of importance to note that 4-hydroxylation of the C4-halogenated 2-fluoroanilines is accompanied by oxidative dehalogenation (Table 2) and, thus, without formation of NIH-shifted metabolites.

Table 1: Chemical shifts of ^{19}F-NMR resonances of identified urinary metabolites from 2-fluoroaniline (2FA), 2,4-difluoroaniline (2,4-diFA), 2-fluoro-4-chloroaniline (2F4ClA), 2-fluoro-4-bromoaniline (2F4BrA) and 2-fluoro-4-iodoaniline (2F4IA) in 0.1 M potassium phosphate (pH 7.6) containing 20% acetonitrile.

	chemical shift (ppm)				
Halogenated derivatives	**2FA**	**2,4-diFA**	**2F4ClA**	**2F4BrA**	**2F4IA**
Parent compound	-138.4	n.d.	n.d.	n.d.	n.d.
Fluoride anion	-123.0	-123.0	-123.0	-123.0	-123.0
N-Acetanilide	n.d.	n.d.	n.d.	n.d.	-126.1
6-Aminophenol	n.d.	-127.3 / -133.7	-135.4	-135.3	-135.5
6-Aminophenylglucuronide	n.d.	-127.4 / -133.6	-135.2	-135.0	-135.2
6-Aminophenylsulphate	-138.2	-127.7 /- 132.6	-133.6	-133.6	-133.9
6-Acetamidophenol	n.d.	-113.3 / -120.0	n.d.	n.d.	n.d.
6-Acetamidophenylglucuronide	n.d.	n.d.	-119.7	-119.6	-120.5
6-Acetamidophenylsulphate	n.d.	n.d.	-124.3	-124.2	-124.6
4-Aminophenol	n.d.	n.d.	n.d.	n.d.	n.d.
4-Aminophenylglucuronide	-135.0	-135.0	n.d.	n.d.	n.d.
4-Aminophenylsulphate	-135.2	-135.2	-135.2	-135.2	-135.2
4-Acetamidophenol	-125.4	n.d.	-125.4	n.d.	n.d.
4-Acetamidophenylglucuronide	-124.8	-124.8	-124.8	-124.8	-124.8
4-Acetamidophenylsulphate	-125.1	-125.1	-125.1	-125.1	-125.1
N-Hydroxyaniline	-135.3	-121.8 / -130.6	-132.9	-132.8	-133.3
N-O-glucuronylaniline	n.d.	n.d.	-131.3	-131.3	-131.7

n.d. means not detected.

In vitro N-hydroxylation of the halogenated aniline-derivatives.

As metabolites from N-hydroxylation are generally not efficiently converted into urine excretable metabolites, but either reactive or reduced to the corresponding aniline derivatives [Eyer, 1983], the exact contribution of N-hydroxylation to the metabolic patterns of the C4-substituted 2-fluoroanilines could not be derived from the *in vivo* metabolite patterns. Therefore, the extent and rate of N-hydroxylation of the various aniline derivatives was investigated and characterized *in vitro* using ^{19}F-NMR. The apparent V_{max} values for the cytochrome P450-mediated N-hydroxylation of the aniline-derivatives were determined using microsomes from the liver of male Wistar rats. The results from these experiments are presented in Table 4 and demonstrate that the reaction rate for N-hydroxylation decreases in the order 2,4-difluoroaniline > 2-fluoro-4-chloroaniline > 2-fluoro-4-bromoaniline > 2-fluoro-4-iodoaniline > 2-fluoroaniline.

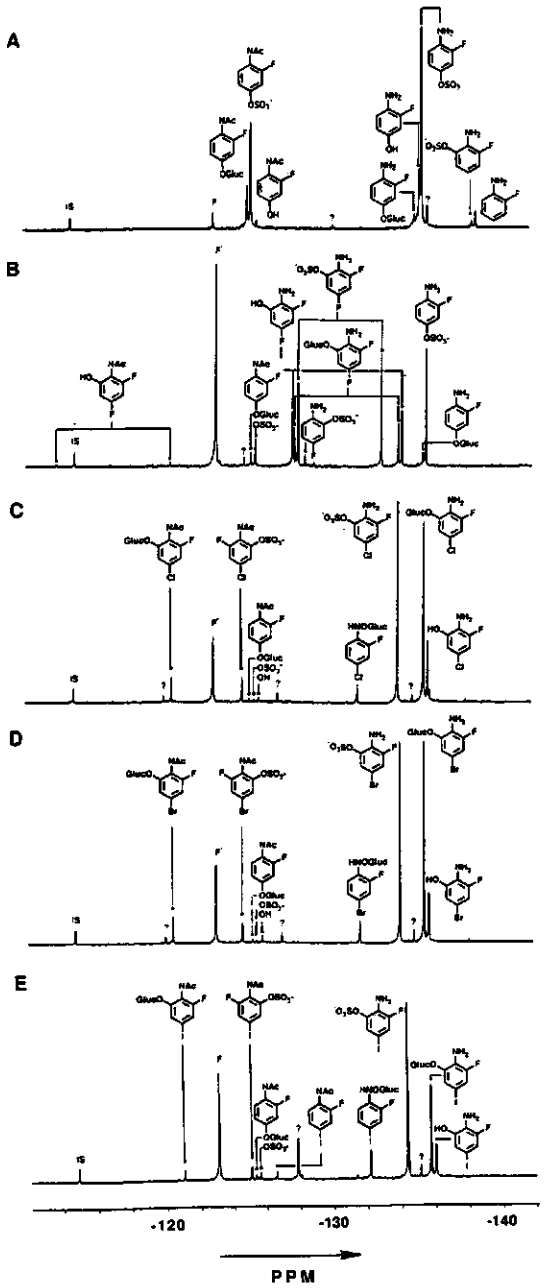

Figure 1: ^{19}F-NMR spectra of the urine of rats exposed to (a) 2-fluoroaniline, (b) 2,4-difluoroaniline, (c) 2-fluoro-4-chloroaniline, (d) 2-fluoro-4-bromoaniline and (e) 2-fluoro-4-iodoaniline. The resonance marked "IS" is from the internal standard 4-fluorobenzoic acid. Resonances marked with "?" represent unidentified metabolites.

Table 2: Quantitative metabolic patterns in 24 hr urine samples of rats exposed to 2-fluoroaniline (2FA), 2,4-difluoroaniline (2,4-diFA), 2-fluoro-4-chloroaniline (2F4ClA), 2-fluoro-4-bromoaniline (2F4BrA) or 2-fluoro-4-iodoaniline (2F4IA) as derived from ^{19}F NMR analysis (n=2-3 rats). Data are presented as mean ± standard error of the mean (for n=3).

	% of total F-containing metabolites					
Urine metabolite **Halogenated derivative**	**2FA**	**2,4-diFA**	**2F4ClA**	**2F4BrA**	**2F4IA**	
Parent compound	5.5 ± 2.6	n.d	n.d.	n.d.	n.d.	n.d.
Fluoride anion	1.7 ± 0.1	29.9 ± 2.2	10.3 ± 2.5	14.4 ± 0.3	13.2	17.2
N-Acetanilide	n.d	n.d.	n.d.	n.d.	2.9	2.4
6-Aminophenol	n.d.	10.4 ± 6.4	5.2 ± 0.9	4.4 ± 0.8	4.0	3.4
6-Aminophenylglucuronide	n.d	6.0 ± 1.2	36.4 ± 6.5	30.1 ± 2.4	23.0	25.5
6-Aminophenylsulphate	2.3 ± 0.8	26.7 ± 2.9	21.8 ± 4.9	27.6 ± 2.0	35.5	34.5
6-Acetamidophenol	n.d.	1.8 ± 0.1	n.d.	n.d.	n.d.	n.d.
6-Acetamidophenylglucuronide	n.d.	n.d.	4.5 ± 1.0	4.8 ± 1.4	2.4	1.0
6-Acetamidophenylsulphate	n.d.	n.d	4.3 ± 0.9	3.9 ± 0.7	2.3	2.3
4-Aminophenol	n.d.	n.d.	n.d.	n.d.	n.d.	n.d.
4-Aminophenylglucuronide	5.5 ± 0.9	1.2 ± 0.2	n.d.	n.d.	n.d.	n.d.
4-Aminophenylsulphate	48.4 ± 2.2	13.6 ± 2.4	3.6 ± 0.5	1.4 ± 0.3	2.1	1.0
4-Acetamidophenol	1.1 ± 0.3	n.d.	1.6 ± 1.6	n.d.	n.d.	n.d.
4-Acetamidophenylglucuronide	10.1 ± 0.8	1.5 ± 0.2	1.2 ± 0.2	1.2 ± 0.5	0.7	1.4
4-Acetamidophenylsulphate	21.0 ± 1.7	5.2 ± 0.6	2.1 ± 0.2	4.0 ± 1.6	2.9	2.8
N-O-Glucuronylaniline	n.d.	n.d.	2.5 ± 0.8	4.4 ± 1.6	4.6	6.9
Σ *Unidentified*	4.5 ± 0.7	2.0 ± 0.9	2.0 ± 0.9	4.0 ± 0.4	6.4	1.6
Recovery						
0.75 mmol•kg^{-1} (0-24 hr)	96.6 ± 4.5	67.1 ± 5.2	59.0 ± 15.0	68.0 ± 0.5	60.0	45.3
(24-48 hr)	1.2 ± 0.0	6.8 ± 1.7	6.4 ± 1.1	4.5 ± 1.3	8.1	15.2
1.00 mmol•kg^{-1} (0-24 hr)	83.3 ± 12.9	55.0 ± 12.0	55.0 ± 1.0	76.0 ± 3.5	58.5 ± 4.5	
(24-48 hr)	5.8 ± 2.3	7.0 ± 0.0	22.0 ± 2.0	4.0 ± 0.9	10.4 ± 2.9	

n.d. means not detected

Table 3: Formation of 6-aminophenol (6-AP) and 4-aminophenol (4-AP) derived metabolites in 24 h urine of rats exposed to the halogenated anilines (2-3 rats). Values are presented as mean ± standard error of the mean (for n=3).

Compound	**% of the dose administered**		**Σ**	**ratio**
	4-AP	**6-AP**	**4-AP+6-AP**	**4-AP : 6-AP**
2-Fluoroaniline	87.1 ± 2.9	2.3 ± 0.8	89.4	37.9
2,4-Difluoroaniline	21.5 ± 3.0	44.9 ± 4.4	66.4	0.48
2-Fluoro-4-chloroaniline	8.5 ± 0.3	72.2 ± 0.8	80.7	0.12
2-Fluoro-4-bromoaniline	6.6 ± 0.4	70.8 ± 1.9	77.4	0.09
2-Fluoro-4-iodoaniline (n=2)	5.5	67.2	72.9	0.08
	5.7	66.7	71.9	0.08

Table 4: Apparent V_{max} for the cytochrome P450-catalyzed N-hydroxylation of 2-fluoroaniline (2FA), 2,4-difluoroaniline (2,4-diFA), 2-fluoro-4-chloroaniline (2F4ClA), 2-fluoro-4-bromoaniline (2F4BrA) and 2-fluoro-4-iodoaniline (2F4IA) using liver microsomes of male Wistar rats as determined using ^{19}F-NMR. The apparent V_{max} is expressed in nmol N-hydroxyaniline • 10 min^{-1} • $nmol^{-1}$ cytochrome P450. Values are presented as mean ± standard error of the mean (for n=4).

Substrate	**Apparent V_{max}**
2-Fluoroaniline	< 0.25 [a]
2,4-Difluoroaniline	6.32 ± 0.79
2-Fluoro-4-chloroaniline	4.48 ± 0.79
2-Fluoro-4-bromoaniline	2.63 ± 0.16
2-Fluoro-4-iodoaniline	1.08 ± 0.08

[a] amount was below detection limit of the overnight ^{19}F-NMR measurement.

Methemoglobinemia.

Rats were orally exposed to a series of halogenated anilines and the changes of methemoglobin content were monitored in time as presented in Figure 2. From these results it follows that the induction of methemoglobinemia increases in the order 2-fluoroaniline < 2-fluoro-4-iodoaniline < 2-fluoro-4-bromoaniline < 2-fluoro-4-chloroaniline < 2,4-difluoroaniline. The N-hydroxylation rate, determined *in vitro* using ^{19}F-NMR, appeared to correlate well with the capacity (expressed as AUC) of the aniline-derivatives to induce methemoglobinemia *in vivo* (r=0.96), thus providing a quantitative biotransformation-toxicity relationship.

Upon dosing rats with 1 mmol 3-fluoro-4-aminophenol or 3,5-difluoro-2-aminophenol per kilogram bodyweight, no formation of methemoglobinemia was observed (unpublished data), indicating that metabolites resulting from aromatic hydroxylation do not significantly contribute to the formation of methemoglobinemia in rats.

Nephrotoxicity.

The nephrotoxic potential of the aniline-derivatives was assessed on the basis of ^{1}H-NMR analysis of urine in combination with a set of conventional biochemical parameters. The ^{1}H-NMR urinalysis was applied since this technique provides the possibility to screen toxic effects in a more sensitive way than the conventional biochemical determination of urine components [Gartland, 1989a&b]. Furthermore, ^{1}H-NMR analysis provides information on site-specific nephrotoxicity in a non-invasive way.

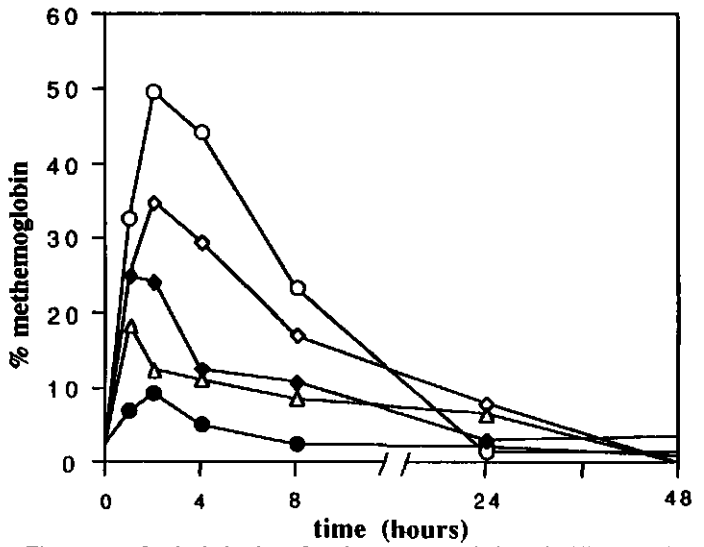

Figure 2: Time course for the induction of methemoglobinemia in male Wistar rats by a series of halogenated anilines; ●, 2-fluoroaniline, O, 2,4-difluoroaniline, ◇, 2-fluoro-4-chloroaniline, ◆, 2-fluoro-4-bromoaniline and , Δ, 2-fluoro-4-iodoaniline. Groups of two cannulated rats were orally exposed to 0.75 mmol aniline-derivative kg^{-1} bodyweight. The observed differences in the extent of methemoglobinemia formation between two rats within one group were less than 5%.

As an example, Figure 3 presents ^{1}H-NMR spectra of rat urine collected 24 hr before as well as 0-24 hr and 24-48 hr after dosing a rat with 1 mmol 2-fluoroaniline per kg bodyweight. Comparison of the spectrum of urine of a 2-fluoroaniline exposed rat to that of the control urine reveals marked changes in the metabolic profiles. In the ^{1}H-NMR spectrum of the urine of the exposed rat a number of resonances can be observed, that are absent in the spectrum of control urine. The quantitative metabolic profiles derived from the ^{1}H-NMR spectra are summarized in Table 5. The signals observed in the aromatic region (ring protons) as well as in the aliphatic region between 2.21 and 2.23 ppm (N-acetyl moieties) can be ascribed to 2-fluoroaniline metabolites. Furthermore, elevations in urinary excretion of the endogenous compounds succinate, acetate, lactate, lysine, alanine as well as changing levels of citrate were observed. Based on comparison to results of Gartland [1989a] it can be derived that the changes observed are most consistent with damage to the proximal tubular site. A similar pattern was observed for all aniline-derivatives tested. Analysis of the same urine samples by conventional biochemical methods revealed only moderate elevations of glucose and protein in urine for 2-fluoroaniline and to a lesser extent elevations of protein in urine for 2,4-difluoroaniline (Table 6). For 2-fluoro-4-chloroaniline a decrease in the BUN concentration was detetced, which might be caused by a reduced food intake rather than chemically-induced damage [Rankin *et al.*, 1986a; Traina and Sather, 1973].

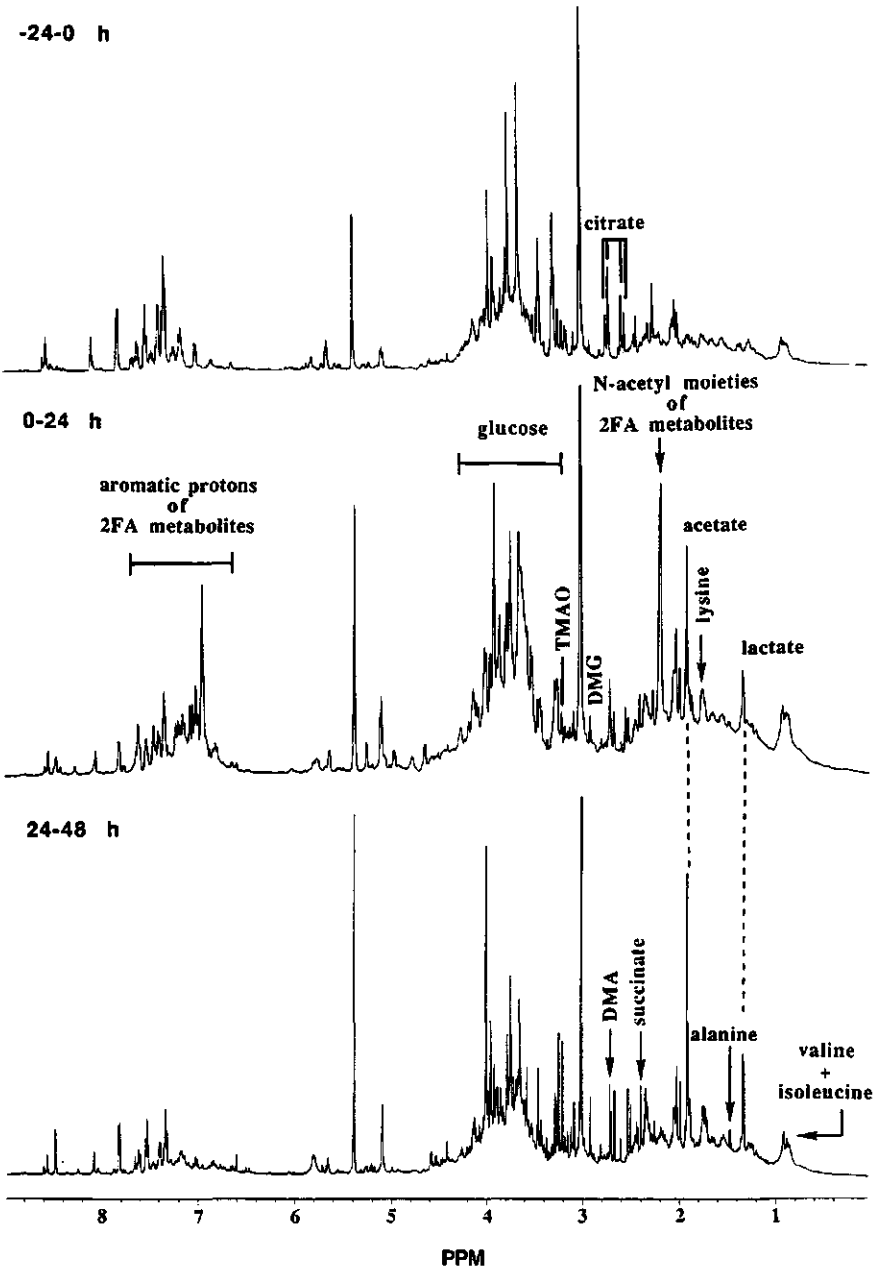

Figure 3: 500 MHz ^{1}H-NMR spectra of urine from a rat before (-24-0 hr) and after (0-24 hr and 24-48 hr) dosing with 1 mmol 2-fluoroaniline kg^{-1} bodyweight.

The urine volume (data not shown) was not significantly decreased upon haloaniline administration, possibly due to the mild nephrotoxic potential of the tested anilines. Although a mild nephrotoxic effect for the 2-fluoro-4-chloroaniline, 2-fluoro-4-bromoaniline and 2-fluoro-4-iodoaniline treated animals was observed, the changes in excretion of endogenous compounds succinate, acetate, lactate, alanine (Table 5) and the changes of some conventional biochemical parameters (Table 6), were demonstrated not to be significant. The rats exposed to 2-fluoroaniline and 2,4-difluoroaniline showed the greatest and significant nephrotoxicity. The excretion of glucose (0-24 hr), protein (0-24 hr & 24-48 hr), lactate (0-24 hr), succinate (24-48 hr) and alanine (24-48 hr) in the 2,4-difluoroaniline treated group was significant lower than observed for the 2-fluoroaniline treated group. Based on these results it was concluded that the order of decreasing nephrotoxicity was 2-fluoroaniline > 2,4-difluoroaniline > 2-fluoro-4-chloro-, 2-fluoro-4-bromo- and 2-fluoro-4-iodoaniline for which no statistically significant nephrotoxic effect was observed.

DISCUSSION.

In the present study the relationship between biotransformation and toxicity of a series of C4-substituted 2-fluoroanilines was investigated. Although it has been suggested that aniline-derivatives require bioactivation to either N-hydroxy- or aminophenol-derivatives to exert their toxic effects [Eyer, 1983; Rankin *et al.*, 1994; Rietjens *et al.*, 1990; Sabbioni, 1992], a combined study on a full metabolite profile and the actual toxic endpoint of a series of aniline derivatives has not been reported so far.

The results of the present study support, as expected, that the main metabolites involved in formation of methemoglobinemia are the N-hydroxyaniline metabolites. It was even demonstrated that the *in vitro* rate of N-hydroxylation of the series of C4-substituted 2-fluoroanilines correlates quantitatively (r=0.96) with the extent of methemoglobinemia observed upon *in vivo* exposure of rats.

Besides methemoglobinemia, the series of C4-substituted 2-fluoroanilines exerted nephrotoxicity as another toxic endpoint. Conventional biochemical parameters in combination with ^{1}H-NMR urinalysis as a sensitive method to detect kidney damage were used to investigate the nephrotoxicity in rats exposed to these aniline-derivatives. The results from the conventional parameters and ^{1}H-NMR urinalysis were most consistent with damage at the tubular site as judged from the increase in protein, succinate, acetate, lactate and alanine and fluctuation of citrate [Gartland *et al.*, 1989a, Kuesel *et al.*, 1991]. These findings are in agreement with studies on the nephrotoxicity of various aniline-derivatives reported previously by

Table 5: ^{1}H-NMR urinalysis on specific low molecular weight marker metabolites indicative for nephrotoxicity at 0-24 hr and 24-48 hr after exposure of rats to a series halogenated anilines. Groups of male Wistar rats (N=3-4) were orally dosed with vehicle (controle) or 1 mmol kg^{-1} bodyweight of 2-fluoroaniline (2FA), 2,4-difluoroaniline (2,4-diFA), 2-fluoro-4-chloroaniline (2F4ClA), 2-fluoro-4-bromoaniline (2F4BrA) and 2-fluoro-4-iodoaniline (2F4IA). See material and method section for exact experimental conditions. Values are presented as the mean ± standard error of the mean.

Compound	µmol • kg^{-1} bodyweight							
	TMAO	DMG	DMA	citrate	succ	acetate	lactate	alanine
0-24 hr								
control	25 ± 4	15 ± 4	48 ± 9	388 ± 50	40 ± 9	10 ± 4	9 ± 7	4 ± 1
2FA	64 ± 13	35 ± 12	56 ± 11	644 ± 34	129 ± 11*	92 ± 25	250 ± 26**	34 ± 13**
2,4-diFA	51 ± 16	28 ± 0	62 ± 29	584 ± 140	144 ± 36*	217 ± 80*	95 ± 32^{a}	20 ± 4
2F4ClA	45 ± 16	29 ± 18	37 ± 9	545 ± 148	123 ± 38	72 ± 45	106 ± 56^{a}	23 ± 10*
2F4BrA	22 ± 4	11 ± 2	40 ± 16	279 ± 23	68 ± 26	125 ± 17	68 ± 21^{a}	17 ± 2
2F4IA	46 ± 20	28 ± 11	38 ± 15	521 ± 219	87 ± 32	148 ± 90	66 ± 31^{a}	14 ± 2^{a}
24-48 hr								
control	25 ± 6	25 ± 2	50 ± 10	420 ± 57	39 ± 10	19 ± 10	19 ± 11	4 ± 1
2FA	74 ± 34	55 ± 17	55 ± 22	370 ± 127	168 ± 38*	380 ± 31**	298 ± 41**	36 ± 9**
2,4-diFA	92 ± 44*	48 ± 21	61 ± 22	456 ± 130	57 ± 17^{a}	261 ± 96*	202 ± 78*	13 ± 0^{a}
2F4ClA	39 ± 6	27 ± 4	35 ± 3	302 ± 19	64 ± 10^{a}	82 ± 16^{a}	95 ± 22^{b}	12 ± 0^{a}
2F4BrA	25 ± 8	17 ± 7	30 ± 5	143 ± 41	44 ± 13^{a}	198 ± 63	100 ± 33^{a}	11 ± 3^{a}
2F4IA	34 ± 7	22 ± 9	35 ± 3	175 ± 65	44 ± 16^{a}	108 ± 21^{a}	63 ± 20^{b}	13 ± 4^{a}

Abbreviations used are TMAO (trimethylamine-N-oxide), DMG (dimethylglycine), DMA (dimethylamine), succ (succinate).
Statistics: * $p < 0.05$ and ** $p < 0.01$ when compared to control; ^{a} $p < 0.05$ and ^{b} $p < 0.01$ when compared to 2FA.

Table 6: Effect of administration of a series of halogenated anilines at a dose of 1 mmol kg^{-1} bodyweight on excretion of urinary glucose and protein over 0-24 hours and 24-48 hours and urea nitrogen content in blood (BUN) at 24 and 48 hours post treatment. Values are presented as mean ± standard error of the mean (for n=3-4).

Compound	**glucose** (mmol kg^{-1} bodyweight)		**protein** (mg kg^{-1} bodyweight)		**BUN** (mg dl^{-1})	
	0-24 hr	**24-48hr**	**0-24 hr**	**24-48hr**	**at 24 hr**	**at 48 hr**
control	80 ± 8	81 ± 8	301 ± 22	283 ± 20	22.7 ± 1.0	22.7 ± 1.7
2FA#	121 ± 30*	72 ± 2	593 ± 41**	461 ± 63**	22.7 ± 1.2	20.5 ± 1.8
2,4-diFA	65 ± 16b	53 ± 9	425 ± 12*a	306 ± 25a	19.1 ± 1.6	22.9 ± 1.5
2F4ClA	71 ± 6b	69 ± 12	371 ± 39b	393 ± 38	17.1 ± 1.5*a	23.0 ± 2.0
2F4BrA	57 ± 5b	66 ± 10	325 ± 32b	356 ± 17	17.1 ± 2.0*a	20.1 ± 0.5
2F4IA	60 ± 9b	61 ± 14	398 ± 86b	315 ± 46a	20.5 ± 1.4	20.5 ± 1.3

Statistic analysis: * $p < 0.05$ and ** $p < 0.01$ when compared to control; a $p < 0.05$ and b $p < 0.01$ when compared to 2-fluoroaniline.

For explanation of abbreviations see legends of tables 1, 2, and 4.

others [Lo *et al.*, 1991; Rankin *et al.*; 1986; Valentovic *et al.*, 1992]. Nephrotoxicity of the C4-substituted 2-fluoroanilines decreased in the order 2-fluoroaniline > 2,4-difluoroaniline.

Although a mild nephrotoxic effect could be observed upon treatment with 2-fluoro-4-chloroaniline, 2-fluoro-4-bromoaniline and 2-fluoro-4-iodoaniline, the nephrotoxicity was observed not to be significantly different from the untreated animals. The extent of nephrotoxicity exerted by the anilines did not follow their methemoglobin-producing activity, indicating that the nephrotoxicity is not a result from tissue hypoxia. An alternative factor has been proposed to be involved in the nephrotoxicity exerted by aniline-derivatives, namely the formation of aminophenol metabolites [Lo *et al.*, 1991; Rankin *et al.*, 1986a & b; Valentovic *et al.*, 1992].

In the present study, the use of ^{19}F-NMR provided possibilities for identification of the complete urinary metabolite profiles of the C4-substituted 2-fluoroanilines. From the results obtained it appears that the type of C4-substituent only influences the regioselectivity of the hydroxylation and not the actual extent of aromatic hydroxylation. In other words, a lower extent of C4-hydroxylation is accounted for by a higher extent of C6-hydroxylation, whereas the formation of 4-

plus 6-aminophenol derived metabolites is similar for the different aniline-derivatives tested. The presence of a C4-substituent hampers cytochrome P450-catalyzed oxidation at this position and increases possibilities for C6-hydroxylation and also for N-hydroxylation. This observation is in accordance with results previously obtained for series of C4-fluorinated aniline-derivatives [Cnubben *et al.*; 1995]. Comparison of the extent of nephrotoxicity to the extent of formation of respectively the 4-aminophenol and/or 6-aminophenol metabolites, indicates a predominant role for the C4-hydroxylation route, not the C6-hydroxylation route, in the induction of nephrotoxic effects. These findings are in agreement with the observation that derivatives of 6-aminophenol are generally less nephrotoxic than 4-aminophenol derived isomers [Calder *et al.*, 1975].

It is especially of interest to notice that the 4-aminophenol pathway leading to nephrotoxicity may proceed through oxidation of the 4-aminophenol to the 4-benzoquinoneimine. Glutathione conjugation of this reactive electrophilic quinoneimine and transport of the conjugate to the kidney, ultimately leads to degradation of the conjugate to a toxic intermediate as is also seen with other nephrotoxic quinone glutathione conjugates [Monks *et al.*, 1985; Monks *et al.*, 1991; Monks and Lau, 1992]. Previous results for C4-halogenated anilines even demonstrated that the reactive quinoneimine metabolite can be formed as the primary metabolite upon the cytochrome P450-catalyzed oxidative dehalogenation of a C4-halogenated aniline such as the C4-halogenated 2-fluoroanilines of the present study. The pathway is schematically presented in Figure 4 [Cnubben *et al.*, 1995; Rietjens *et al.*, 1990; Rietjens *et al.* 1991]. Previous *in vitro* results reported the preferential removal of a fluorine over a chlorine, bromine or iodine substituent in such a cytochrome P450-catalyzed oxidative dehalogenation [Cnubben *et al.*, 1995], and this is clearly in line with the *in vivo* results of the present study indicating a larger extent of C4 oxidation, and nephrotoxicity, for the C4-fluorinated 2-fluoroaniline than for the C4-chlorinated, -brominated or -iodinated derivative.

Additional results of the present study demonstrate that 2,4-difluoroaniline, but also 2-fluoroaniline induces marked nephrotoxicity, whereas the amount of 4-aminophenol metabolites formed from 2,4-difluoroaniline is several-fold lower than the amount of 4-aminophenol derived metabolites observed in the metabolite pattern of 2-fluoroaniline [Table 3]. Presumably, this discrepancy can be understood on the basis of a direct formation of the fluorinated 1,4-benzoquinoneimine from 2,4-difluoroaniline by the alternative and effective pathway depicted in Figure 4.
Biotransformation of 2,4-difluoroaniline results in an amount of fluoride anions that is always significantly higher than the amount that could be accounted for by the formation of 4-aminophenol-derived metabolites. Previously, this phenomenon was also observed for other 4-fluorinated aniline derivatives [Rietjens and Vervoort,

1991]. It was concluded that the excretion of fluoride anions by 4-fluorinated aniline exposed rats results from a loss of fluoride anions accompanied by formation of the reactive benzoquinoneimine as the primary reaction product. This intermediate has to be chemically reduced to the aminophenol-metabolite [Riejens and Vervoort, 1991]. In contrast, upon biotransformation of 2-fluoroaniline formation of the fluorinated 1,4-benzoquinoneimine has to result from secondary oxidation of the initially formed fluorinated 4-aminophenol (Figure 4).

An alternative explanation for the observed differences in nephrotoxic potential of the C4-substituted 2-fluoroanilines might be, that the change in lipophilicity caused by the different halogens alters the disposition of the various aniline-derivatives. However, recently it has been demonstrated that the nephrotoxic potential of 2-haloaniline derivatives in rats was not influenced by the nature of the halogen [Valentovic *et al.*, 1992]. In addition, in a study of Rankin [1986] the *in vivo* and *in vitro* nephrotoxicity of monochloroanilines was investigated and it appeared that, despite an equal lipophilicity of the compounds, 2-chloroaniline was more toxic than 3-chloroaniline and 4-chloroaniline. Although an effect of the halogen type on

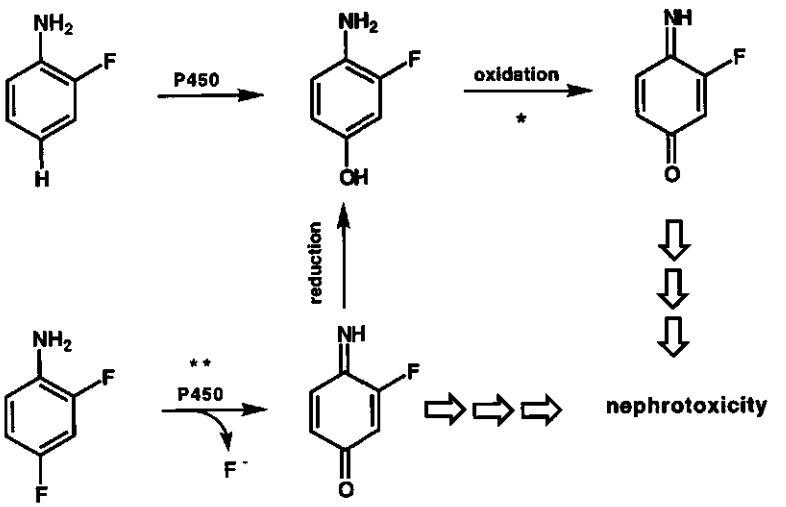

Figure 4: Outline of the importance of cytochrome P450-catalyzed oxidative dehalogenation as an additional route for the bioactivation of C4-substituted 2-fluoroanilines to nephrotoxic intermediates. Formation of the reactive benzoquinoneimine proceeds by oxidation of the aminophenol (*) or by a cytochrome P450-mediated oxidative dehalogenation of a C4-substituted 2-fluoroaniline (**). The resulting benzoquinoneimine can react non-enzymatically with glutathione to thioadducts that are translocated to the kidney. Eventually, metabolites which are formed upon further processing and oxidation of the aminophenol thioadducts bind to cellular macromolecules in the kidney to cause toxicity [Eckert *et al.*, 1990; Eyanagi *et al.*, 1991; Gartland *et al.*, 1990a; Klos *et al.*, 1992].

the disposition cannot be excluded in our study, results of these other studies indicate that not the lipophilicity, but other factors, such as biotransformation must contribute to the nephrotoxic potential of these compounds. The results of the present study provide support for the importance of the cytochrome P450-catalyzed C4-hydroxylation and oxidative dehalogenation of C4-substituted 2-fluoroanilines as a bioactivation pathway to nephrotoxic metabolites. Clearly, this provides an additional perspective to the present views on bioactivation pathways for aniline derivatives.

Morphological studies indicating the exact location of the renal lesion upon aniline-exposure may further elucidate whether the lesion is at the corticomedullary junction as this would further strengthen that 4-aminophenol metabolites contribute to the nephrotoxicity mechanism. Such morphological studies were beyond the scope of the present study but serve as an interesting topic for future research.

Altogether, it is concluded that reduced possibilities for C4-hydroxylation in the series of aniline-derivatives, results in increased possibilities for C6- and N-hydroxylation and, consequently in a shift in the type of toxic end-point observed, *i.e.* from nephrotoxicity to methemoglobinemia.

Acknowledgements.

This study was supported by the Netherlands Organization for the Advancement of Scientific Research (N.W.O.). The authors thank Ms. M.A.W. Peters for cannulation of the animals, Dr. J. Vervoort for help with ^{1}H-NMR measurements and Mr. P.W.J. Heinen and Mr. J. Bogaards for statistical analysis of the data.

REFERENCES.

Anthony M.L., Sweatman B.C., Beddell C.R., Lindon J.C. and Nicholson J.K. (1994). Pattern recognition classification of the site of nephrotoxicity based on metabolic data derived from proton nuclear magnetic resonance spectra of urine, *Molec. Pharmacol.* **46**, 199-211.

Bales J.R., Higham D.P., Howe I., Nicholson J.K. and Sadler P.J. (1984). Use of high-resolution proton nuclear magnetic resonance spectroscopy for multi-component analysis of urine, *Clin. Chem.* **30**, 426-432.

Blaauboer B.J., Van Holsteijn C.W.M. and Wit J.G. (1976). Ferrihemoglobin formation by monohydroxy aniline derivatives in erythrocytes of some avian species in comparison with mammals. *Naunyn-Schmiedeberg's Arch. Pharmacol.* **292**, 255-258.

Boyland E. and Sims P. (1954). The oxidation of some aromatic amines with persulphate, *J. Chem. Soc.*, 980-985.

Calder I.C., Williams P.J., Woods R.A., Funder C.C., Green C.R., Ham K.N. and Tange J.D. (1975). Nephrotoxicity and molecular structure, *Xenobiotica* **5**, 303-307.

Calder I.C., Yong A.C., Woods R.A., Crowe C.A., Ham K.N. and Tange J.D. (1979). The nephrotoxicity of p-aminophenol. II The effect of metabolic inhibitors and inducers, *Chem.-Biol. Interact.* **27**, 245-254.

Cnubben N.H.P., Blaauboer B., Juyn S., Vervoort J. and Rietjens I.M.C.M. (1994). A spectrophotometric assay for the detection of 2-aminophenols in biological samples, *Analytical Biochemistry* **220**, 165-171.

Cnubben N.H.P., Vervoort J., Boersma M.G. and Rietjens M.C.M. (1995). The effect of varying halogen substituent patterns on the cytochrome P450 catalysed dehalogenation of 4-halogenated anilines to 4-aminophenol metabolites, *Biochemical Pharmacology* **49**, 1235-1248.

Cnubben N.H.P., Vervoort J., Veeger C. and Rietjens M.C.M. (1992). Study on the regioselectivity and mechanism of the aromatic hydroxylation of monofluoroanilines, *Chem.-Biol. Interact.* **85**, 151-172.

Coleman G.H., McCloskey Ch.M. and Stuart F.A. (1943). Nitrosobenzene, *Organic Syntheses* **25**, 81-83.

Eadsforth C.V., Logan C.J., Morrison B.J. and Warburton P.A. (1984). 2,4-difluoroaniline and 4-fluoroaniline exposure: monitoring by methaemoglobin and urine analyses, *Int. Arch. Occup. Environ. Health* **54**, 223-232.

Eckert K.G. and Eyer P. (1983). Differences in the reactions of isomeric *ortho-* and *para-*aminophenols with hemoglobin, *Biochemical Pharmacology* **32**, 1019-1027.

Eyanagi R., Hisanari Y. and Shigematsu H. (1991). Studies of paracetamol/phenacetin toxicity: isolation and characterization of p-aminophenol-glutathione conjugate, *Xenobiotica* **21**, 793-803.

Eyer P. (1988). Detoxication of N-oxygenated arylamines in erythrocytes. An overview, *Xenobiotica* **18**, 1327-1333.

Eyer P. (1983). The red cell as a sensitive target for activated toxic arylamines. *Arch. Toxicol.*, Suppl. **6**, 3-12.

Fowler L.M., Foster J.R. and Lock E.A. (1993). Effect of ascorbic acid, acivicin and probenecid on the nephrotoxicity of 4-aminophenol in the Fischer 344 rat, *Arch. Toxicol.* **67**, 613-621.

Fowler L.M., Foster J.R. and Lock E.A. (1994). Nephrotoxicity of 4-amino-3-S-glutathionylphenol and its modulation by metabolism or transport inhibitors, *Arch. Toxicol.* **68**, 15-23.

Fowler L.M., Moore R.B., Foster J.R. and Lock E.A. (1991). Nephrotoxicity of 4-aminophenol glutathione conjugate, *Human & Experimental Toxicology* **10**, 451-459.

Gartland K.P.R., Bonner F.W. and Nicholson J.K. (1989a). Investigations into the biochemical effect of region-specific nephrotoxins, *Molec. Pharmacol.* **35**, 242-250.

Gartland K.P.R., Bonner F.W., Timbrell J.A. and Nicholson J.K. (1989b). Biochemical characterisation of *para*-aminophenol-induced nephrotoxic lesions in the F344 rat, *Arch.*

Toxicol. **63**, 97-106.

Gartland K.P.R., Eason C.T., Bonner F.W. and Nicholson J.K. (1990a). Effects of biliary cannulation and buthionine sulphoximine pretreatment on the nephrotoxicity of *para*-aminophenol in the Fischer 344 rat, *Arch. Toxicol.* **64**, 14-25.

Gartland K.P.R., Beddell C.R., Lindon J.C. and Nicholson J.K. (1990b) A pattern recognition approach to the comparison of PMR and clinical chemical data for classification of nephrotoxicity, *J. Pharmaceutical & Biomedical Analysis* **8**, 963-968.

Harrison J.H. and Jollow D.J. (1987) Contribution of aniline metabolites to aniline-induced methemoglobinemia, *Molec. Pharmacol.* **32**, 423-431.

Iles R.A., Hind A.J. and Chalmers R.A. (1985). Use of proton nuclear magnetic resonance spectroscopy in detection and study of organic acidurias, *Clin. Chem.* **31**, 1795-1801.

Josephy P.D., Eling T.E. and Mason R.P. (1983). Oxidation of p-aminophenol catalysed by horseradish peroxidase and prostaglandin synthase, *Molec. Pharmacol.* **23**, 461-466.

Kennedy R.J. and Stock A.M. (1960). The oxidation of organic substances by potassium peroxymonosulphate, *J. Org. Chem.* **25**, 1901-1906.

Kiese M. (1974). *Methemoglobinemia: A comprehensive treatise*. Chapter 7, CRC Press, Cleveland, Ohio.

Klos C, Koob M., Kramer C. and Dekant W. (1992). *p*-Aminophenol nephrotoxicity: Biosynthesis of toxic glutathione conjugates, *Toxicol. Appl. Pharmacol.* **115**, 98-106.

Kuesel A.C., Kroft T. and Smith I.C.P. (1991). Nuclear magnetic resonance spectroscopy, *Clin. Chem.* **63**, 237-246

Lenk W. and Riedl M. (1989). N-hydroxy-N-arylacetamides. V. Differences in the mechanism of haemoglobin oxidation in vitro by N-hydroxy-4-chlroacetaniline and N-hydroxy-4-chloroaniline. *Xenobiotica* **19,** 453-475.

Lo H.H., Brown P.I., Rankin G.O. (1990). Acute nephrotoxicity induced by isomeric dichloroanilines in Fischer 344 rats, *Toxicology* **63**, 215-231.

Lo H.H., Brown P.I. and Rankin G.O. (1991). Trichloroaniline effects on renal function in vivo and in vitro, *Toxicology Letters* **57**, 319-328.

Lock E.A., Cross T.J. and Schnellmann R.G. (1993). Studies on the mechanism of 4-aminophenol-induced toxicity to renal proximal tubules, *Human & Experimental Toxicology* **12**, 383-388.

Lowry O.H., Rosebrough N.J. Farr A.L. and Randall A.J. (1951). Protein measurements with Folin phenol reagent. *J. Biol. Chem.* **193**, 265-275.

Maples K.R., Eyer P. and Mason R.P. (1989). Aniline-, phenylhydroxylamine-, nitrosobenzene-, and nitrobenzene-induced hemoglobin thiyl free radical formation in vivo and in vitro, *Molec. Pharmacol.***37**, 311-318.

McLean S., Starmer G.A. and Thomas J. (1969). Methaemoglobin formation by aromatic amines, *J. Pharm. Pharmac.* **2**, 441-450.

Monks T.J., Jones T.W., Hill B.A. and Lau S.S. (1991). Nephrotoxicity of 2-bromo-(cysteinyl)hydroquinone and 2-bromo-(N-acetyl-L-cysteinyl) hydroquinone thioethers,

Toxicol. Appl. Pharmacol. **111**, 279-298.

Monks T.J. and Lau S.S. (1992). Toxicology of quinone-thioethers, *Crit. Rev. Toxicol.* **22**, 243-270.

Monks T.J., Lau S.S., Highet R.J. and Gillette J.R. (1985). Glutathione conjugates of 2-bromohydroquinone are nephrotoxic, *Drug Metab. Dispos.* **13**, 553-559.

Omura T. and Sato R. (1964). The carbon monoxide-binding pigment of liver microsomes. I. Evidence for its hemoprotein nature. *J. Biol. Chem.* **239**, 2370-2378.

Rankin G.O., Valentovic M.A., Nicoll D.W., Ball J.G., Anestis D.K., Wang R.-T., Brown P.I. (1994), In vivo and in vitro 4-amino-2,6-dichlorophenol nephrotoxicity and hepatotoxicity in the Fischer 344 rat. *Toxicology* **90**, 115-128.

Rankin G.O., Yang D.J., Cressey-Veneziano K., Casto S., Wang R.T. and Brown P.I. (1986a). In vivo and in vitro nephrotoxicity of aniline and its monochlorophenylderivatives in the Fischer 344 rat, *Toxicology* **38**, 269-283.

Rankin G.O., Yang D.J., Teets V.J., Lo H.H. and Brown P.I. (1986b). 3,5-Dichloroaniline-induced nephrotoxicity in the Sprague-Dawley rat, *Toxicology Letters* **30**, 173-179.

Remie R., Van Dongen J.J. and Rensema J.W. (1990). *Manual of microsurgery on the laboratory rat, Part I.* (J.J. Van Dongen, R. Remie, J.W. Rensema and G.H.J. Van Wunnik, Eds.) pp. 159-169, Elsevier, Amsterdam.

Rietjens I.M.C.M., Tyrakowska B., Veeger C. and Vervoort J. (1990). Reaction pathways for biodehalogenation of fluorinated anilines, *Eur. J. Biochem.* **194**, 945-954.

Rietjens I.M.C.M. and Vervoort J. (1991). Bioactivation of 4-fluorinated anilines to benzoquinoneimines as primary reaction products, *Chem.-Biol. Interactions* **77**, 263-281.

Rietjens I.M.C.M. and Vervoort J. (1989). Microsomal metabolism of fluoroanilines, *Xenobiotica.* **19**, 1297-1305.

Sabbioni G. (1992). Hemoglobin binding of monocyclic aromatic amines: molecular dosimetry and quantitative structure activity relationships for the N-oxidation, *Chem.-Biol. Interactions* **81**, 91-117.

Tietz N.W. (1987). Fundamentals of clinical chemistry, 3rd ed. W.B. Saunders Co. Philadelphia.

Traina V.M. and Sather B.T. (1973). Effect of starvation on renal function. *Lancet* **2**, 620.

Valentovic M.A., Ball J.G., Anestis D.K., Beers K.W., Madan E., Hubbard J.L. and Rankin G. (1992). Acute renal and hepatic toxicity of 2-haloanilines in Fischer 344 rats, *Toxicology* **75**, 121-131.

Vervoort J., De Jager P.A., Steenbergen J. and Rietjens I.M.C.M. (1990). Development of a ^{19}F-n.m.r. method for studies on the in vivo and in vitro metabolism of 2-fluoroaniline, *Xenobiotica* **20**, 657-670.

Vogel A.J. (1978). *Vogel's textbook of practical organic chemistry.* (B.S. Furniss, A.J. Hannaford, P.W.G. Smith and A.R. Fatchell, Eds.) p. 684, Longman Scientific & Technical, London.

Vogel A.J. (1989). *Vogel's textbook of practical organic chemistry.* (B.S. Furniss, A.J. Hannaford, P.W.G. Smith and A.R. Fatchell, Eds.) John Wiley & Sons, New York.

Yoshida M., Yoshikawa H., Goto H. and Hara I., Evaluation of the nephrotoxicity of aromatic nitro-

amino compounds by urinary enzyme activities, The Journal of Toxicological Sciences (1989) 14, 257-268.

CHAPTER 8

Different metabolic pathways of 2,5-difluoronitrobenzene and 2,5-difluoroaminobenzene compared to molecular orbital substrate characteristics.

Ivonne M.C.M. Rietjens, Nicole H.P. Cnubben, Marjon van Haandel, Bozena Tyrakowska, Ans E.M.F. Soffers and Jacques Vervoort.

Chemico-Biological Interactions **94**, 49-72, 1995.

SUMMARY

The *in vivo* metabolite patterns of 2,5-difluoroaminobenzene and of its nitrobenzene analogue, 2,5-difluoronitrobenzene, were determined using ^{19}F-NMR analysis of urine samples. Results obtained demonstrate significant differences between the biotransformation patterns of these two analogues. For the aminobenzene, cytochrome P450-catalyzed aromatic hydroxylation presents the main metabolic pathway. 2,5-Difluoronitrobenzene was predominantly metabolized through glutathione conjugation leading to excretion of 5-fluoro-2-(N-acetylcysteinyl)-nitrobenzene and fluoride anions, and, to a minor extent, through cytochrome P450-catalyzed hydroxylation and nitroreduction. Pretreatment of the rats with various inducers of cytochrome P450 enzymes, known to influence glutathione S-transferase enzyme patterns as well, followed by exposure to the 2,5-difluoroamino- or 2,5-difluoronitrobenzene, generally resulted in metabolite patterns that varied only to a small ($\leq$ 12%) extent. Based on this results it was concluded that the biotransformation enzyme pattern is not the predominant factor in determining the metabolic route of these two model compounds. Additional *in vitro*

microsomal and cytosolic incubations with 2,5-difluoroaminobenzene and 2,5-difluoronitrobenzene qualitatively confirmed the *in vivo* results. NADPH/oxygen-supported microsomal cytochrome P450-catalyzed hydroxylation was observed only for 2,5-difluoroaminobenzene, whereas cytosolic GSH conjugation occurred only in incubations with 2,5-difluoronitrobenzene as the substrate. Outcomes from molecular orbital calculations provided a working hypothesis that can explain the difference in metabolic pathways of the nitro- and amino benzene derivative on the basis of their chemical characteristics. This hypothesis states that the chances for a nitro- or aminobenzene derivative to enter either a cytochrome P450 or a glutathione conjugation pathway are determined by the relative energy levels of the frontier orbitals of the compounds. The aminobenzene derivative has relatively high energy molecular orbitals leading to an efficient reaction of its highest occupied molecular orbital (HOMO) with the singly occupied molecular orbital of the cytochrome P450 $(FeO)^{3+}$ intermediate, but a low reactivity of its lowest unoccupied molecular orbital (LUMO) with the HOMO of glutathione. The nitrobenzene, on the other hand, has molecular orbitals of relatively low energy, explaining the efficient interaction, and, thus, reaction between its LUMO and the HOMO electrons of glutathione, but resulting in low reactivity with the SOMO electron of the cytochrome P450 $(FeO)^{3+}$ reaction intermediate.

INTRODUCTION.

Aromatic xenobiotics like substituted benzenes, are generally converted to more polar metabolites before they can be excreted from the mammalian body. Reactions available for this conversion are so-called phase I or modification reactions and phase II or conjugation reactions. The present paper focusses on the marked difference in biotransformation pathways known to occur upon exposure to nitrobenzenes on one hand and to their chemically reduced analogues aminobenzenes (anilines). Previous papers reported that the biotransformation of aminobenzene derivatives proceeds predominantly through cytochrome P450-catalyzed aromatic hydroxylation, accompanied by N-acetylation, glucuronidation and/or sulphation (1-6). In contrast, however, the metabolic pathways of nitrobenzenes have been reported to proceed only to a minor extent through cytochrome P450-catalyzed aromatic ring hydroxylation. For nitrobenzenes, nitroreduction leading to aminobenzene derivatives and their glutathione conjugation leading to mercapturic acids have been reported to be important metabolic pathways (7-13).

The objective of the present study was to obtain more insight in these differences in metabolic pathways for nitro- and aminobenzene derivatives.

Model compounds used were 2,5-difluoronitrobenzene and 2,5-difluoroaminobenzene. The *in vivo* and *in vitro* metabolite patterns of these analogues were investigated to quantify the differences between the metabolic pathways of the two benzene derivatives. Molecular orbital calculations were performed to find a rational for possible differences observed.

MATERIALS AND METHODS.

Chemicals

2,5-Difluoroaminobenzene and 2,5-difluoronitrobenzene were purchased from Fluorochem (Derbyshire, UK). 5-Fluoro-2-(N-acetylcysteinyl)-nitrobenzene, 5-fluoro-2-cysteinyl-nitrobenzene and 5-fluoro-2-glutathionyl-nitrobenzene were synthesized from 2,5-difluoronitrobenzene as follows: to 0.3 g (1.9 mmol) 2,5-difluoronitrobenzene dissolved in 2.5 ml methanol, 2.5 ml of a solution containing 0.1 g (1.9 mmol) sodium methanolate and 0.5 mmol N-acetylcysteine, cysteine or reduced glutathione dissolved in methanol, were added over a period of 30 minutes. The mixture was stirred at room temperature overnight. Upon cooling to 4°C and centrifugation (10 minutes 13000 rpm in an Eppendorf centrifuge), the supernatant was mixed with one volume of demineralized water and one volume of 0.2 M potassium phosphate pH 7.6. Following a second centrifugation step, resulting in a 2,5-difluoronitrobenzene containing pellet, the supernatant was washed three times with diethylether to remove the final 2,5-difluoronitrobenzene. The water phase was evaporated under vacuum and the residue, containing the 5-fluoro-2-(N-acetylcysteinyl)-nitrobenzene, the 5-fluoro-2-cysteinyl-nitrobenzene or the 5-fluoro-2-glutathionyl-nitrobenzene, was dissolved in demineralized water, and analyzed by ^{19}F-NMR in 0.1 M potassium phosphate pH 7.6, or by ^{1}H-NMR, upon lyophilisation and dissolving in $^{2}H_2O$. Spectral characteristics of the compounds were as follows; 5-fluoro-2-(N-acetylcysteinyl)-nitrobenzene: ^{19}F-NMR (0.1 M potassium phosphate pH 7.6, relative to $CFCl_3$)(ppm): -119.1; ^{1}H-NMR ($^{2}H_2O$, relative to sodium 3-trimethylsilyl-(2,2,3,3-$^{2}H_4$)-propionate)(ppm): 8.01 (H6)(dd, $^{3}J_{H\text{-}F}$ = 8.6 Hz, $^{4}J_{H\text{-}H}$ = 2.9 Hz), 7.78 (H3) (dd, $^{4}J_{H\text{-}F}$ = 5.2 Hz, $^{3}J_{H\text{-}H}$ = 9.2 Hz), 7.57 (H4)(m, $^{3}J_{H\text{-}F}$ = 7.7 Hz, $^{3}J_{H\text{-}H}$ = 9.2 Hz, $^{4}J_{H\text{-}H}$ = 2.9 Hz), 4.44 (CH)(dd, $^{3}J_{H\text{-}H}$ = 9.0 Hz, $^{3}J_{H\text{-}H}$ = 4.1 Hz), 3.69 (1H of CH_2)(dd, $^{2}J_{H\text{-}H}$ = 14.1 Hz, $^{3}J_{H\text{-}H}$ = 4.1 Hz), 3.32 (1H of CH_2)(dd, $^{2}J_{H\text{-}H}$= 14.1 Hz, $^{3}J_{H\text{-}H}$= 9.0 Hz), 1.95 (CH_3)(s); 5-Fluoro-2-cysteinyl-nitrobenzene: ^{19}F-NMR (0.1 M potassium phosphate pH 7.6, relative to $CFCl_3$)(ppm): -118.5; ^{1}H-NMR ($^{2}H_2O$, relative to sodium 3-trimethylsilyl-(2,2,3,3-$^{2}H_4$)-propionate)(ppm): 8.07 (H6)(dd, $^{3}J_{H\text{-}F}$= 8.7 Hz, $^{4}J_{H\text{-}H}$ = 2.9 Hz), 7.74 (H3) (dd, $^{4}J_{H\text{-}F}$ = 5.1 Hz, $^{3}J_{H\text{-}H}$ = 9.1 Hz), 7.57 (H4)(m, $^{3}J_{H\text{-}F}$ = 7.7 Hz, $^{3}J_{H\text{-}H}$ = 9.1 Hz, $^{4}J_{H\text{-}H}$ = 2.9 Hz), 3.61

(CH)(dd, $^3J_{H-H}$ = 7.5 Hz, $^3J_{H-H}$ = 4.9 Hz), 3.49 (1H of CH_2)(dd, $^2J_{H-H}$ = 13.3 Hz, $^3J_{H-H}$ = 4.9 Hz), 3.28 (1H of CH_2)(dd, $^2J_{H-H}$ = 13.3 Hz, $^3J_{H-H}$ = 7.5 Hz); 5-fluoro-2-glutathionyl-nitrobenzene: ^{19}F-NMR (0.1 M potassium phosphate pH 7.6, relative to $CFCl_3$)(ppm): -118.5; ^{1}H-NMR (^2H_2O, relative to sodium 3-trimethylsilyl-(2,2,3,3-$^2H_4$)-propionate)(ppm): 8.02 (H6)(dd, $^3J_{H-F}$ = 8.6 Hz, $^4J_{H-H}$ = 2.8 Hz), 7.80 (H3) (dd, $^4J_{H-F}$ = 5.0 Hz, $^3J_{H-H}$ = 9.1 Hz), 7.58 (H4)(m, $^3J_{H-F}$ = 7.6 Hz, $^3J_{H-H}$ = 9.1 Hz, $^4J_{H-H}$ = 2.8 Hz), 4.65 (CH)(dd, $^3J_{H-H}$ = 9.3 Hz, $^3J_{H-H}$ = 4.6 Hz), 3.72 (1H of CH_2)(dd, $^2J_{H-H}$ = 14.5 Hz, $^3J_{H-H}$ = 4.6 Hz), 3.37 (1H of CH_2)(dd, $^2J_{H-H}$ = 14.5 Hz, $^3J_{H-H}$ = 9.3 Hz), 3.72 (1 H of CH_2)(br.s), 3.74 (1H of CH_2)(br.s), 3.61 (CH)(tr, $^3J_{H-H}$ = 6.4 Hz), 2.04 (m), 2.44 (CH_2)(tr, $^3J_{H-H}$= 7.8 Hz).

2,5-Difluoro-N-hydroxyaminobenzene was synthesized by the procedure described by Coleman *et al.* (14) for the synthesis of phenylhydroxylamine from nitrobenzene. In short, a mixture of 0.9 g of NH_4Cl and 2.33 g (14.6 mmol) of 2,5-difluoronitrobenzene in 30 ml of water was stirred vigorously and 2.23 g (30.9 mmol) of zinc powder (Merck, Darmstadt, FRG) was added in small portions over a period of 5 minutes. Following the addition of the zinc, the temperature of the reaction mixture increased spontaneously to 50-55°C after approximately 5 minutes. The mixture was maintained at 50-55°C for 15 minutes, adding ice as necessary. The solution was then filtered and the zinc oxide residue washed with 30 ml of hot water. The filtrate was cooled immediately to 0°C, to avoid decomposition of the hydroxylamine. A sample of the reaction mixture was analyzed by ^{19}F-NMR in 0.1 M potassium phosphate pH 7.6 to identify the ^{19}F-NMR resonances of the 2,5-difluoro-N-hydroxyaminobenzene. ^{19}F-NMR (0.1 M potassium phosphate pH 7.6, relative to $CFCl_3$)(ppm): -122.0 (F5), -142.0 (F2).

2,5-Difluoronitrosobenzene was synthesized by oxidation of 2,5-difluoroaminobenzene with potassium peroxymonosulphate in a water-acetic acid mixture, as described by Kennedy and Stock (15) for the synthesis of 1,4-dinitrosobenzene from 1,4-diaminobenzene. 2,5-Difluoronitrosobenzene was purified by preparative column chromatography on Silicagel 60 (0.015-0.040 mm)(Merck, Darmstadt, FRG) with 5 % (v/v) ether in petroleum benzine as the eluent. The green 2,5-difluoronitrosobenzene containing fractions were collected and concentrated by evaporation and a sample of this fraction was analyzed by ^{19}F-NMR in 0.1 M potassium phosphate pH 7.6 to identify the ^{19}F-NMR resonances of the compound. ^{19}F-NMR (0.1 M potassium phosphate pH 7.6, relative to $CFCl_3$)(ppm): -122.4 (F5), -138.0 (F2).

In vivo exposure of rats

Male Wistar rats (400 g) were exposed to 20 mg of the desired fluorinated benzene, administered in olive oil by oral injection. After dosing, 24 h urine samples

were collected. The 24 h urinary recovery was over 65 % of the dose administered for the 2,5-difluoronitrobenzene and over 95 % for the 2,5-difluoroaminobenzene. Pretreatment of the rats with inducers of cytochrome P450 enzymes before administration of the 2,5-difluoroaminobenzene or the 2,5-difluoronitrobenzene was carried out as previously described (16). Inducers used were phenobarbital, β-naftoflavone (used instead of the carcinogenic 3-methylcholanthrene, administered in a similar way), isosafrole (1,2-(methylenedioxy)-4-propenylbenzene) and acetone. Some of these inducers of cytochrome P450 enzymes influence the enzyme pattern of the glutathione S-transferases as well (17).

Analysis of urine samples

Urine samples were analyzed by ^{19}F-NMR after 1:1 dilution in 0.2 M potassium phosphate pH 7.6. Enzyme hydrolysis of urine samples was carried out as previously described (5) using either β-glucuronidase from *Escherichia coli* K12 (Boehringer, Mannheim, Germany) or arylsulphatase/β-glucuronidase from *Helix pomatia* (Boehringer, Mannheim, Germany). Samples were routinely made oxygen free by four cycles of evacuation and filling with argon.

For determination of ^{1}H-NMR and ^{19}F-NMR splitting patterns of the metabolite with its ^{19}F-NMR resonances at -121.7 and -145.1 ppm, 4 ml of an arylsulphatase/β-glucuronidase treated urine sample was diluted with 2 ml of 0.2 M potassium phosphate pH 7.6 and extracted three times with 2 ml of ethyl acetate. The collected ethyl acetate fractions were evaporated to dryness and dissolved in 0.5 ml $CDCl_3$, followed by evaporation to dryness and dissolving in 0.5 ml $CDCl_3$. This sample contained the metabolite to be identified and was analyzed by ^{1}H-NMR and ^{19}F-NMR as described below.

^{19}F-NMR measurements.

^{19}F-NMR measurements were performed on a Bruker AMX 300 spectrometer as described previously (5;16-18). Between 1500 and 50000 scans were recorded, depending on the concentrations of the fluorine containing compounds and the signal to noise ratio required. The detection limit of these measurements was 1 μM for an overnight run (50000 scans). The sample volume was 1.71 ml containing 100 μl $^{2}H_2O$ for locking the magnetic field and 10 μl of a 8.4 mM 4-fluorobenzoic acid solution, added as an internal standard. The ethyl acetate extract from the tert.butylhydroperoxide supported microsomal incubation was analyzed using a coaxial insert in the 10 mm NMR tube. The sample consisted of 1.6 ml of the ethyl acetate extract. The coaxial insert contained $^{2}H_2O$ for locking the magnetic field and a known amount of the internal standard (4-fluorobenzoic acid) for quantification of the measurement. Concentrations of the various metabolites could be calculated by

comparison of the integrals of the ^{19}F-NMR resonances of the metabolites to the integral of the ^{19}F-NMR resonance of 4-fluorobenzoic acid.

The splitting pattern of the ^{19}F-NMR resonances of the metabolite identified as 2,5-difluoro-4-hydroxynitrobenzene was measured on a Bruker AMX 500 MHz using a ^{1}H probehead tuned to the ^{19}F frequency (470.5 MHz). The sample volume was 0.5 ml and the solvent $CDCl_3$ was used for locking the magnetic field. Because of a smaller and thus more homogeneous sample as well as the higher magnetic field, resolution in these ^{19}F-NMR measurements on the Bruker AMX 500 MHz were improved over that obtained at the AMX 300 spectrometer, resulting in well resolved splitting patterns and *J*-values that could be compared to those of the ^{1}H-NMR signals of this metabolite.

^{1}H-NMR measurements.

^{1}H NMR measurements were performed on a Bruker AMX 500 spectrometer. Upon freeze drying, the synthesized compounds were dissolved in $^{2}H_2O$ to give a final sample volume of 0.5 ml. Spectra were recorded using 60° pulses (6 μs), a 10 kHz spectral width, a repetition time of 1.9 s, quadrature phase detection and quadrature phase cycling (CYCLOPS). About 150 scans were recorded. ^{1}H chemical shift values are presented relative to sodium 3-trimethylsilyl-(2,2,3,3-$^{2}H_4$)-propionate. The splitting pattern of the ^{1}H-NMR resonances of the metabolite identified as 2,5-difluoro-4-hydroxynitrobenzene was also measured on a Bruker AMX 500 MHz. The sample was dissolved in $CDCl_3$ and this solvent was used for locking the magnetic field.

Preparation of microsomes and cytosol.

Microsomes were prepared from the perfused livers of male Wistar rats (400 g) either untreated or treated with isosafrole as described before (16). Cytosol was obtained as the supernatant from the first 105000 g ultracentrifugation step performed during preparation of microsomes from control rats. Cytochrome P450 content of the microsomes was measured as described by Omura and Sato (20). Protein content was determined by the method of Lowry *et al.* (21) using bovine serum albumin as the standard.

Microsomal incubations.

Cytochrome P450 dependent conversion was studied *in vitro* in microsomal incubations containing (final concentrations) 0.1 M potassium phosphate pH 7.6, 2 μM microsomal cytochrome P450, 5 mM of the 2,5-difluoroamino- or 2,5-difluoronitrobenzene added as 1% (v/v) of a 0.5 M stock solution in dimethyl sulphoxide and 1.0 mM NADPH. The reaction was started by the addition of the

NADPH and carried out at 37°C for 10 min. The total reaction volume was 2 ml and the reaction was carried out in a closed reaction vessel to prevent evaporation of the substrate. The reaction was terminated by freezing the sample into liquid nitrogen. Upon thawing and centrifugation (10 min, 13000 rpm in an Eppendorf centrifuge), 1.6 ml of the supernatant was analyzed by ^{19}F-NMR as described above.
When tert.butylhydroperoxide was used as the artificial electron donor the sample volume was 20 ml and tert.butylhydroperoxide (2.5 mM final concentration, added as 5% (v/v) of a 50 mM tert.butylhydroperoxide suspension in water) was added instead of NADPH to start the reaction. After 10 minutes at 37°C the reaction was terminated by addition of 1 ml of 12 N HCl and the reaction mixture was extracted with 5 ml ethyl acetate. The ethyl acetate layer was collected and 1.6 ml of this sample was analyzed by ^{19}F-NMR.

Cytosolic incubations.

Glutathione S-transferase catalyzed conversion was studied in cytosolic incubations containing (final concentrations) 0.1 M sodium phosphate pH 6.5, 1 mM glutathione (reduced form)(Sigma St. Louis, MO, USA), 3.5 mg cytosolic protein/ml and 5 mM 2,5-difluoroaminobenzene or 2,5-difluoronitrobenzene, added as 1% of a 0.5 M stock solution in dimethyl sulphoxide. The reaction was started by the addition of the benzene derivative and carried out at 37°C for 10 min in a closed reaction vessel to prevent evaporation of the substrate. Reactions were terminated by freezing the samples into liquid nitrogen. For ^{19}F-NMR measurements, carried out as described above, the samples were thawed and centrifuged (10 min, 13000 rpm) in an Eppendorf centrifuge.

Chemical determination of 2,5-difluoro-4-hydroxyaminobenzene and 2,5-difluoro-4-hydroxynitrobenzene.

Chemical detection of 2,5-difluoro-4-hydroxyaminobenzene was carried out as described previously (16), using the method of Brodie and Axelrod (22), in which the 4-hydroxyaminobenzene reacts with phenol in a base environment to give the indophenol which can be quantified on the basis of its absorption at 630 nm. Extraction of the 2,5-difluoro-4-hydroxyaminobenzene from the acid hydrolyzed, neutralized urine of the 2,5-difluoroaminobenzene exposed rat into ethyl acetate, followed by purification of the compound on silicagel 60 (70-230 Mesh)(Merck, Darmstadt, Germany) using a mixture of ethyl acetate-ethanol-acetic acid (15:3:2 by vol.) as eluent, resulted in a stock solution of which the exact concentration was determined by ^{19}F-NMR. Analysis of diluted samples of this stock solution in the chemical assay for detection of 4-hydroxylated aminobenzenes (16;22) resulted in a molar extinction coefficient for the indophenol derived from 2,5-difluoro-4-

hydroxyaminobenzene of 20 $mM^{-1}cm^{-1}$.

In the urine of a 2,5-difluoronitrobenzene exposed rat the presence of 2,5-difluoro-4-hydroxynitrobenzene was detected essentially as described by Piotrowski (9). In short, 0.5 ml of urine was diluted with 0.5 ml of 0.1 M sodium acetate pH 5.2 and treated with arylsulphatase/β-glucuronidase as described previously (5). Half (0.5 ml) of this sample was extracted 2 times with 0.5 ml ethyl acetate. The collected ethyl acetate extracts were combined and diluted 1:10 in 4 N HCl. This diluted sample was divided in two parts. To 1.5 ml of one of these samples 0.25 g of zinc powder (Merck, Darmstadt, FRG) was added to reduce the 2,5-difluoro-4-hydroxynitrobenzene to 2,5-difluoro-4-hydroxaminobenzene. The 1.5 ml of the other sample served as a control sample which was analyzed without the zinc reduction step, leading to quantification of the excreted 2,5-difluoro-4-hydroxyaminobenzene. The ultimate difference between the two samples quantifies the actual amount of 2,5-difluoro-4-hydroxynitrobenzene in the urine sample. After 5 minutes of vigorous shaking the samples were centrifuged (5 min, 2500 rpm) and to 1.2 ml of each supernatant 0.8 ml of demineralised water was added. To 1.0 ml of this sample 63 µl of phenol reagent (5% w/v, phenol in water) and 650 µl of conc. NH_3 (25%) were added. After 60 minutes at room temperature the absorbance at 630 nm was determined, against a blank consisting of the urine of a non-exposed rat treated in a similar way. On the basis of the $A_{630\ nm}$ values thus obtained, concentrations of the hydroxylated metabolites in the urine were calculated using the extinction coefficient determined for the indophenol derived from 2,5-difluoro-4-hydroxyaminobenzene to be 20 $mM^{-1}cm^{-1}$.

Molecular orbital calculations.

Molecular orbital calculations were carried out on a Silicon Graphics Iris 4D/85 using Quanta/Charmm (Molecular Simulations, UK). The semi-empirical molecular orbital method was used, applying the AM1 Hamiltonian from the AMPAC program. All calculations were carried out with PRECISE criteria. For all calculations the self-consistent field was achieved. Geometries were optimized for all bond lengths, bond angles and torsion angles using the Fletcher-Powell criteria.

Frontier electron densities were calculated from HOMO (highest occupied molecular orbital) and HOMO-1 characteristics and from LUMO (lowest unoccupied molecular orbital) and LUMO+1 characteristics using the equation given by Fukui *et al.* (23). In this study, the outcomes of the semi-empirical calculations on molecules in vacuum are related to the electronic characteristics of the substrates in the active site of the cytochromes P450. Due to solvation effects and a different dielectric constant, the intrinsic properties of the compounds might be influenced upon binding to this active site. However, it is assumed that this phenomenon will not influence the

relative differences of parameters between a series of closely related compounds or between centers in a given molecule to a significant extent. The outcomes of the in vacuo computer calculations can thus be used as an approach to study relative differences within a series of related compounds or relative differences between sites in one molecule.

RESULTS.

In vivo metabolite pattern of 2,5-difluoroaminobenzene

Figure 1a shows the ^{19}F-NMR spectrum of the arylsulphatase/β-glucuronidase treated 24 h urine of a rat exposed to 2,5-difluoroaminobenzene. Resonances of the metabolites were identified as follows; extraction of the metabolite with ^{19}F-NMR resonances at -141.2 and -145.9 ppm into ethyl acetate, followed by its purification on silicagel 60 using a mixture of ethyl acetate-ethanol-acetic acid (15:3:2 by vol) as eluent, resulted in a compound that reacted in a chemical assay for detection of 4-hydroxyaminobenzenes, identifying the compound as a C4-hydroxylated aminobenzene metabolite. Furthermore, incorporation of the hydroxyl moiety at C4 in 2,5-difluoroaminobenzene results in a chemical shift change of the ^{19}F-NMR resonance of F2 (-144.5 ppm) and F5 (-123.3 ppm) in 2,5-difluoroaminobenzene to, -141.2 (F2) and -145.9 ppm (F5), respectively in 2,5-difluoro-4-hydroxy-aminobenzene. This implies a shift of +3.3 ppm and -22.6 ppm as a result of the hydroxyl incorporation with respect to F2 and F5 respectively. Based on analogy to the effect of hydroxyl incorporations into a series of other benzene derivatives (Table 1) (6,19), this observation corroborates that the hydroxyl group is incorporated at C4, i.e. *meta* with respect to F2 and *ortho* with respect to F5.

Identification of the 2,5-difluoro-4-hydroxy-N-acetylaminobenzene metabolite followed from the observation that upon acid hydrolysis of the urine, but not on its treatment with arylsulphatase/β-glucuronidase, the resonances at -131.8 and -145.3 ppm disappeared accompanied by a proportional increase of the resonances of 2,5-difluoro-4-hydroxyaminobenzene. The resonances of 2,5-difluoroaminobenzene could be identified on the basis of addition of the reference compound. Table 2 presents quantitative data of the metabolite pattern of 2,5-difluoroaminobenzene as derived from the ^{19}F-NMR spectra of the urine of two rats. From the results obtained it follows that of all urinary metabolites at least 96% results from a cytochrome P450-catalyzed conversion of the aminobenzene.

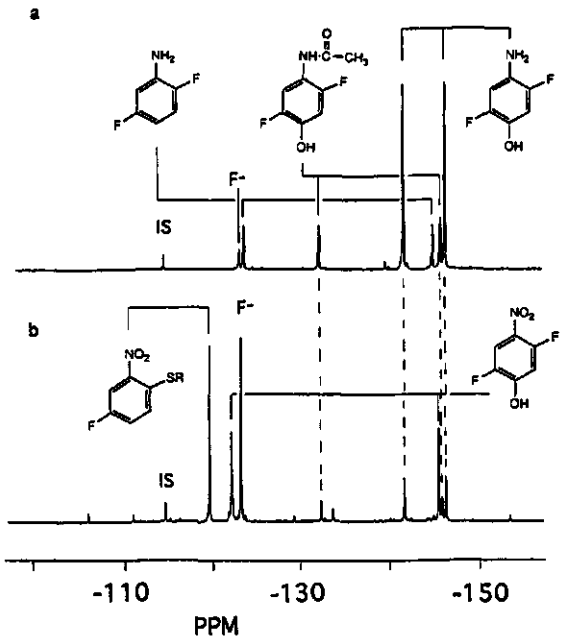

Figure 1: ^{19}F-NMR spectra of the arylsulphatase/β-glucuronidase treated 24 h urine of a Wistar rat exposed to (a) 2,5-difluoroaminobenzene and (b) 2,5-difluoronitrobenzene. Resonances were identified as described in the text. The resonance marked IS is from the internal standard 4-fluorobenzoic acid. The fluoride anions observed in (a) originate from the food, as a similar amount of fluoride anions was observed in the urine of a non exposed control rat. The SR adduct presents 5-fluoro-2-(N-acetylcysteinyl)-nitrobenzene.

In vivo metabolite pattern of 2,5-difluoronitrobenzene.

The ^{19}F-NMR spectrum of the arylsulphatase/β-glucuronidase treated 24 h urine of a rat exposed to 2,5-difluoronitrobenzene is presented in Figure 1b. Metabolites identical to those observed in Figure 1a, and, thus, representing aminobenzene derived metabolites are observed.

The main metabolite observed in the urine of the 2,5-difluoronitrobenzene exposed rat, however, could be identified as 5-fluoro-2-(N-acetylcysteinyl)-nitrobenzene because addition of the synthesized reference compound resulted in an increase of this resonance. The glutathione and cysteine adduct of the above-mentioned compound have resonances at slightly, but markedly, different positions, again showing that the resonance at -119.1 ppm belongs to 5-fluoro-2-(N-acetylcysteinyl)-nitrobenzene. In addition to this mercapturic acid metabolite, an almost equal amount of fluoride anion is observed in the urine (Figure 1b) resulting from the defluorination which accompanies the glutathione addition at C2.

Finally, another metabolite is observed with ^{19}F-NMR resonances at -121.7 and -145.1 ppm. These resonances could be ascribed to 2,5-difluoro-4-hydroxynitrobenzene on the basis of the following results. First, the resonances occur in the ^{19}F-NMR spectrum of the urine upon treatment with arylsulphatase, suggesting that they should be ascribed to a phenolic metabolite, excreted as the sulphate conjugate. Furthermore, zinc reduction of the acid hydrolysed urine resulted in disappearance of the resonances of this metabolite, accompanied by a proportional increase of the resonances of 2,5-difluoro-4-hydroxyaminobenzene. Besides, chemical analysis of the urine sample clearly identified the presence of a 4-hydroxy-

Table 1: Changes in ^{19}F-NMR chemical shift values in aromatic model compounds upon introduction of a hydroxyl moiety at positions, *ortho, meta or para* with respect to the fluorine substituent.

Conversion from in	**Converted to**	**OH incorporation with respect to the fluorine**	**Change chemical shift (ppm)**
3-fluorophenol	3-fluorocatechol	*ortho* to F3	-23.9
3,4-difluorophenol	3,4-difluorocatechol	*ortho* to F3	-23.1
3,5-difluorophenol	3,5-difluorocatechol	*ortho* to F3	-23.4
3,6-difluorophenol	3,6-difluorocatechol	*ortho* to F3	-23.0
3,4,5-trifluorophenol	3,4,5-trifluorocatechol	*ortho* to F3	-22.4
3-fluoroaminobenzene	3-fluoro-4-hydroxyaminobenzene	*ortho* to F3	-22.5
3-fluoroaminobenzene	3-fluoro-2-hydroxyaminobenzene	*ortho* to F3	-23.7
2-fluorophenol	3-fluorocatechol	*meta* to F2	+ 1.5
4-fluorophenol	4-fluorocatechol	*meta* to F4	+ 2.4
2,3-difluorophenol	3,4-difluorocatechol	*meta* to F2	+ 2.9
3,4-difluorophenol	3,4-difluorocatechol	*meta* to F4	+ 2.1
2,4-difluorophenol	3,5-difluorocatechol	*meta* to F2	-0.6
2,4-difluorophenol	3,5-difluorocatechol	*meta* to F4	+ 0.3
2,5-difluorophenol	3,6-difluorocatechol	*meta* to F2	+ 1.9
3,4-difluorophenol	4,5-difluorocatechol	*meta* to F4	+ 1.9
2-fluoroaminobenzene	2-fluoro-4-hydroxyaminobenzene	*meta* to F2	+ 3.5
2-fluoroaminobenzene	2-fluoro-6-hydroxyaminobenzene	*meta* to F2	+ 1.5
4-fluoroaminobenzene	4-fluoro-2-hydroxyaminobenzene	*meta* to F4	+ 2.5
3-fluorophenol	4-fluorocatechol	*para* to F3	-10.2
2,3-difluorophenol	3,4-difluorocatechol	*para* to F3	- 9.3
3,5-difluorophenol	3,5-difluorocatechol	*para* to F3	-11.2
3,4-difluorophenol	4,5-difluorocatechol	*para* to F3	-11.4
3,4,5-trifluorophenol	3,4,5-trifluorocatechol	*para* to F3	-14.0
3-fluoroaminobenzene	3-fluoro-6-hydroxyaminobenzene	*para* to F3	- 9.9

Chemical shift values of the various compounds were determined in 0.1 M potassium phosphate pH 7.6, or in urine 1:1 diluted in 0.2 M potassium phosphate pH 7.6 at 7^{o}C, and were derived from previous results (6,18).

Table 2. Metabolite patterns in arylsulphatase/β-glucuronidase treated 24 h urine samples as derived from ^{19}F-NMR analysis (n=3 rats).

Compound **Urine metabolite**	**Chemical shift in ppm**	**% of total F-containing metabolites**
2,5-Difluoroaminobenzene		
Parent compound	-123.3 (F5); -144.5 (F2)	15.3 ± 2.5
2,5-Difluoro-4-hydroxyaminobenzene	-141.2 (F2); -145.9 (F5)	63.3 ± 0.5
2,5-Difluoro-4-hydroxy-N-acetylaminobenzene	-131.8 (F2); -145.3 (F5)	15.0 ± 1.7
Σ Unidentified		5.7 ± 3.1
2,5-Difluoronitrobenzene		
2,5-Difluoro-4-hydroxyaminobenzene	-141.2 (F2); -145.9 (F5)	15.0 ± 1.7
2,5-Difluoro-4-hydroxy-N-acetylaminobenzene	-131.8 (F2); -145.3 (F5)	6.3 ± 1.6
5-Fluoro-2-(N-acetylcysteinyl)-nitrobenzene	-119.2 (F5)	19.1 ± 1.5
Fluoride anions	-123.0	20.9 ± 2.1
2,5-Difluoro-4-hydroxynitrobenzene	-121.7 (F2); -145.1 (F5)	25.4 ± 6.3
Σ Unidentified		13.3 ± 3.9

Total 24 h urinary recovery amounted to > 95% and > 65% of the dose administered for 2,5-difluoroaminobenzene and 2,5-difluoronitrobenzene, respectively.

lated nitrobenzene metabolite in the arylsulphatase/β-glucuronidase treated urine of the 2,5-difluoronitrobenzene exposed rat, at a concentration corresponding to that of the metabolite with the ^{19}F-NMR resonances at -121.7 and -145.1 ppm.

Further unequivocal identification of the metabolite with its resonances at -121.7 and -145.1 ppm comes from the results presented in Figure 2. This figure presents the splitting patterns of the two ^{19}F-NMR signals and the two ^{1}H-NMR signals of this metabolite. The $J_{F\text{-}F}$ -coupling value observed for this metabolite is 13.8 Hz. Literature data published for $J_{F\text{-}F}$ values in fluorinated benzene derivatives (24) indicate that $^{3}J_{F\text{-}F}$ values (fluorine substituents *ortho* with respect to each other) vary between 19.0 and 20.9 Hz, $^{4}J_{F\text{-}F}$ values (fluorine substituents *meta*) between 1.6 and 6.6 Hz and $^{5}J_{F\text{-}F}$ values (fluorine substituents *para*) between 10.9 and 17.6 Hz. This implies that the $J_{F\text{-}F}$ value of 13.8 Hz demonstrates that in the metabolite the two fluorine substituents are still at a position *para* with respect to each other.

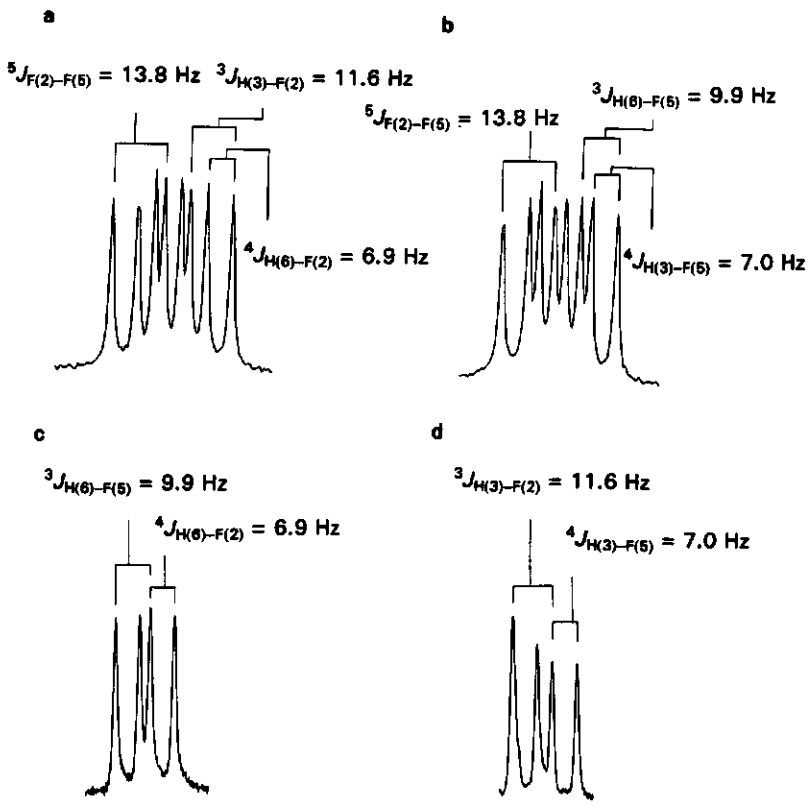

Figure 2: ^{19}F-NMR and ^{1}H-NMR splitting patterns of the fluorine and proton signals of 2,5-difluoro-4-hydroxynitrobenzene. (a)^{19}F-NMR resonance at -121.7 ppm (F2), (b) ^{19}F-NMR resonance at -145.1 ppm (F5), (c) ^{1}H-NMR resonance at 7.92 ppm (H6) and (d) ^{1}H NMR spectrum showing the resonance at 6.90 ppm (H3).

Thus, it can be concluded that the metabolite does not result from a hydroxylation accompanied by an NIH shift. The absence of a $^4J_{H\text{-}H}$ coupling in the ^{1}H-NMR signals of the metabolite indicates that the two proton substituents present in this metabolite are not *meta* with respect to each other. In addition, the two $J_{H\text{-}F}$ couplings of each of the fluorine substituents are significantly different, and, thus, result from a proton *ortho* and a proton *meta* with respect to the fluorine, i.e. represent a $^3J_{H\text{-}F}$ and a $^4J_{H\text{-}F}$ for each of the fluorine substituents. Finally, the splitting pattern of this metabolite is similar to the one reported for another C4 substituted 2,5-difluoronitrobenzene derivative, namely 2,5-difluoro-4-S-methyl nitrobenzene (25). Together these data indicate that, in this metabolite of 2,5-

difluoronitrobenzene the modification is at C4, and demonstrates that this phenolic metabolite with its resonances at -121.7 and -145.1 ppm must be 2,5-difluoro-4-hydroxynitrobenzene.

The metabolite pattern derived from the ^{19}F-NMR spectra of urine samples of two 2,5-difluoronitrobenzene exposed rats is summarized in Table 2. From these data it follows that glutathione conjugation, represented by the sum of the mercapturic acid and fluoride anion elimination (together being 40.0 ± 3.6 %), is the major pathway for 2,5-difluoronitrobenzene metabolism.

Metabolite patterns in rats pretreated with inducers of biotransformation enzymes.

To investigate the extent to which the metabolite patterns observed in rats exposed to 2,5-difluoroaniline and 2,5-difluoronitrobenzene would vary upon changes in the pattern of biotransformation enzymes, rats were pretreated with various inducers of the cytochrome P450 system. Some of these inducers are known to influence the glutathione S-transferase enzyme pattern also (17). Upon pretreatment, the rats were exposed to either 2,5-difluoroaminobenzene or 2,5-difluoronitrobenzene. The collected 24 h urines were treated with arylsulphatase/β-glucuronidase and analyzed by ^{19}F-NMR. The results obtained are presented in Table 3. The rats pretreated with phenobarbital, β-naftoflavone or acetone did not show marked changes in the metabolite profiles of 2,5-difluoroaminobenzene or 2,5-difluoronitrobenzene. Generally, the variations observed were only a few ($\leq$ 12 %) percent. The amount of metabolites that resulted from the glutathione conjugation pathway (5-fluoro-2-(N-acetylcysteinyl)-nitrobenzene plus fluoride anions) is $\geq$ 40 % of all the fluorinated metabolites. For 2,5-difluoronitrobenzene, the amount of metabolites resulting from glutathione conjugation is higher than the amount of 2,5-difluoro-4-hydroxybenzene resulting from the cytochrome P450-catalyzed hydroxylation of 2,5-difluoronitrobenzene, and also higher than the amount of 2,5-difluoro-4-hydroxyaminobenzene plus 2,5-difluoro-4-hydroxy-N-acetylamino-benzene resulting from nitroreduction followed by N-acetylation and/or cytochrome P450-catalyzed hydroxylation. Together the results presented in Table 3 demonstrate that the marked difference in the metabolic profile of the nitro- and the amino analogue, observed *in vivo* in non-pretreated rats (table 2) is still observed when rats are pretreated with inducers of the biotransformation enzymes. This implies that the marked difference in the contribution of the various pathways to the overall metabolic profile of these two model compounds cannot be ascribed to the pattern of the biotransformation enzymes, but is more likely due to differences in chemical characteristics of the amino and the nitro analogue. The results presented in Table 3 also demonstrate that, surprisingly, in the rats pretreated with isosafrole excretion of the hydroxylated metabolites of 2,5-difluoroaminobenzene is no longer observed. *In*

vitro microsomal incubations with 2,5-difluoroaminobenzene and isosafrole indicated that isosafrole is able to inhibit the cytochrome P450-catalyzed hydroxylation of 2,5-difluoroaminobenzene in a competitive way (data not shown). Thus, the pretreatment of the rats with isosafrole apparently loads the animals with a concentration of this compound that appears to be high enough to efficiently inhibit the cytochrome P450-catalyzed aromatic hydroxylation. Exposure of isosafrole pretreated rats to 2,5-difluoronitrobenzene not only resulted in a significant decrease of the formation of the hydroxylated aminobenzene derivatives, but also in a significant reduction in the formation of the metabolite identified as 2,5-difluoro-4-hydroxynitrobenzene. This result supports the supposition that this metabolite is also formed by the cytochrome P450 system. Formation of the mercapturic acid from 2,5-difluoronitrobenzene is however still observed in the isosafrole pretreated rats. Furthermore, in the ^{19}F-NMR metabolite pattern of the isosafrole pretreated rat exposed to 2,5-difluoronitrobenzene 15.3% of the total fluorine intensity, (45.8% of the fraction characterized as unidentified metabolites), could be ascribed to 2,5-difluoroaniline. This indicates that nitroreduction is also still observed.

Table 3: Metabolite patterns in arylsulphatase/β-glucuronidase treated 24 h urine samples as derived from ^{19}F-NMR analysis (n=3 rats for the control animals, same data as in Table 2, presented once more for comparison)(n=1 rat for the pretreatments).

Compound/Metabolite	**% of total F-containing urine metabolites**				
	CON	**PB**	**β-NF**	**ISF**	**ACE**
2,5-Difluoroaminobenzene					
Parent compound	17.7 ± 1.4	18.1	10.5	39.0	12.1
2,5-Difluoro-4-hydroxyaminobenzene	62.8 ± 0.2	53.1	58.1	2.3	64.0
2,5-Difluoro-4-hydroxy-N-acetylaminobenzene	16.8 ± 0.2	21.1	26.9	2.3	17.8
Unidentified	2.7 ± 1.8	7.7	4.5	56.4	6.2
2,5-Difluoronitrobenzene					
2,5-Difluoro-4-hydroxyaminobenzene	15.0 ± 1.7	14.4	6.9	NO	27.0
2,5-Difluoro-4-hydroxy-N-acetylaminobenzene	6.3 ± 1.6	7.0	6.4	NO	8.6
5-Fluoro-2-(N-acetylcysteinyl)-nitrobenzene	19.1 ± 1.5	22.9	22.5	36.3	20.8
Fluoride anions	20.9 ± 2.1	26.2	29.4	30.3	24.9
2,5-Difluoro-4-hydroxynitrobenzene	25.4 ± 6.3	15.1	25.9	NO	13.3
unidentified	13.3 ± 3.9	14.4	8.9	33.4[a]	5.4

CON, control; PB, phenobarbital pretreated; βNF, β-naftoflavone pretreated; ISF, isosafrole pretreated and ACE, acetone pretreated. Total 24 h urinary recovery always amounted to > 95% and > 65% of the dose administered for 2,5-difluoroaminobenzene and 2,5-difluoronitrobenzene respectively. NO, not observed.

[a]45.8 % of this fraction of unidentified metabolites, can be ascribed to 2,5-difluoroaminobenzene.

Microsomal incubation of 2,5-difluoroaminobenzene and 2,5-difluoronitrobenzene.

Microsomal incubations with 2,5-difluoroaminobenzene and 2,5-difluoronitrobenzene were performed to further confirm the difference in possibilities for cytochrome P450-catalyzed hydroxylation of these compounds. Figure 3a and b present the ^{19}F-NMR spectra of these microsomal incubations. Formation of a hydroxylated metabolite is observed for the amino analogue, but for the nitro analogue formation of the 4- hydroxylated metabolite is not observed to a detectable level within the 10 minutes of the microsomal incubation. Nevertheless, microsomal conversion of the nitro analogue results in formation of two metabolic products, identified as 2,5-difluoroaminobenzene and 2,5-difluoro-N-hydroxy-aminobenzene on the basis of (synthesized) reference compounds, i.e. as metabolites resulting from nitroreduction.

Apparently in the *in vitro* microsomal incubation, the cytochrome P450 cycle rather enters the reductive pathway when 2,5-difluoronitrobenzene is bound to the active site, than proceeding by oxygen binding, reduction by a second electron, formation of the reactive $(FeO)^{3+}$ species and substrate hydroxylation. When tert. butylhydroperoxide was used as the artificial oxygen donor for the cytochrome P450 cycle, thus circumventing the electron donating steps, formation of 2,5-difluoro-4-hydroxynitrobenzene could be observed. This can be seen in the ^{19}F-NMR spectrum of the ethyl acetate extract from a microsomal incubation without NADPH and with tert.butylhydroperoxide as the oxygen donor to support the reaction (Figure 4). The ^{19}F-NMR spectrum of the ethyl acetate extract of the blank incubation carried out in the absence of microsomes did not show formation of this metabolite (^{19}F-NMR spectrum not shown).

Glutathione dependent cytosolic conversion of 2,5-difluoroaminobenzene and 2,5-difluoronitrobenzene

To investigate the difference in reactivity of the amino and nitro model compound of the present study in a glutathione S-transferase catalyzed reaction, cytosolic incubations in the presence of glutathione were performed, the results of which are presented in Figure 5. In accordance with the *in vivo* metabolite pattern, the 2,5-difluoroaminobenzene does not show any product formation in a glutathione S-transferase catalyzed reaction (Figure 5a). The nitro analogue shows formation of a significant amount of the glutathione adduct accompanied by formation of a similar amount of fluoride anion resulting from the aromatic substitution reaction by which this glutathione addition proceeds. Besides, a small amount of a metabolite with resonances at -122.0 and -142.0 ppm, identified as 2,5-difluoro-N-hydroxyamino-benzene on the basis of the resonances of a synthesized reference compound, is observed (Figure 5b). Blanc incubations carried out in the absence of cytosol did not show this product formation (^{19}F-NMR spectrum not shown).

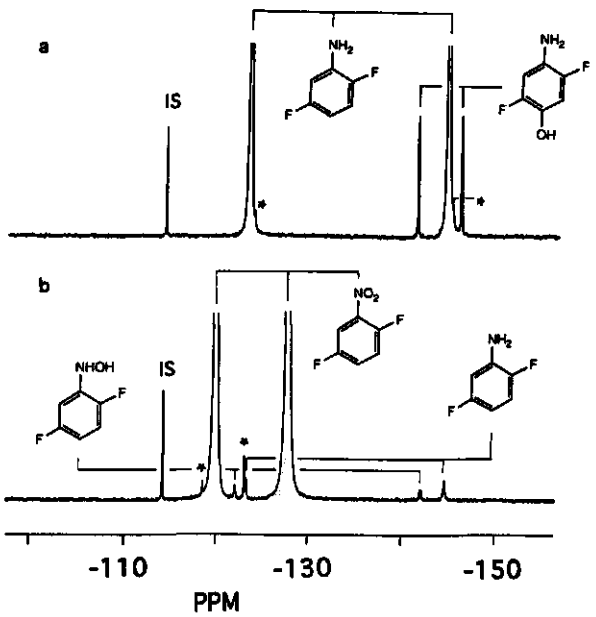

Figure 3: ^{19}F-NMR spectra of microsomal incubations with (a) 2,5-difluoroaminobenzene and (b) 2,5-difluoronitrobenzene. The resonances marked with an asterisk were also present in the ^{19}F-NMR spectra of control incubations carried out in the absence of NADPH. The resonance marked IS is from the internal standard 4-fluorobenzoic acid.

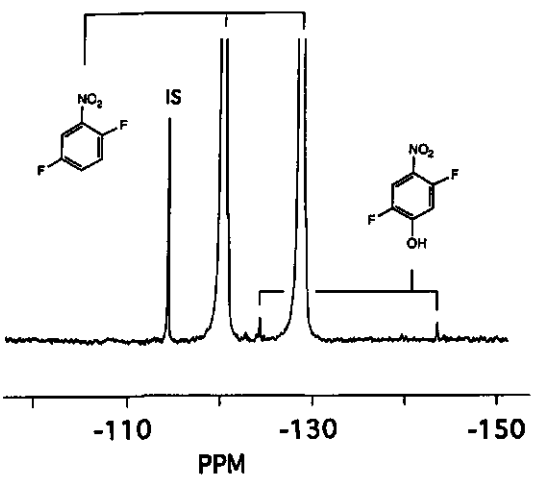

Figure 4: ^{19}F-NMR spectrum of the ethyl acetate extract of a microsomal incubation with 2,5-difluoronitrobenzene and tert.butylhydroxyperoxide as the artificial oxygen donor for the cytochrome P450 reaction. In ethyl acetate the resonances of the 2,5-difluoro-4-hydroxymetabolite are at -124.1 (F2) and -143.2 (F5), which could be derived from the ethyl acetate extract of the arylsulphatase/β-glucuronidase treated urine sample.

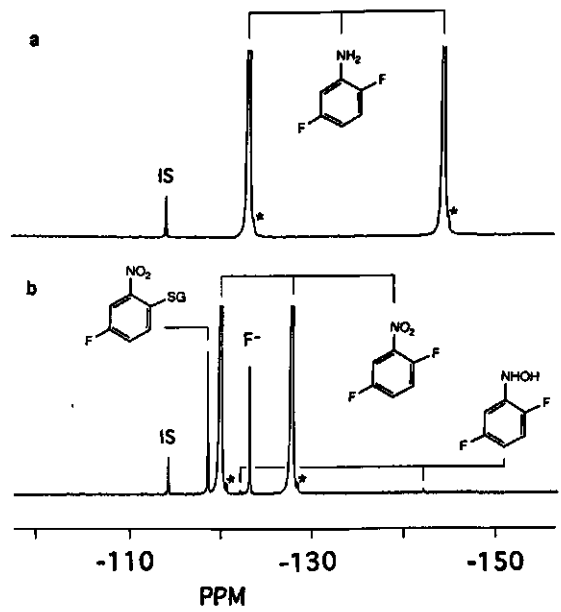

Figure 5: ^{19}F-NMR spectra of glutathione (GSH) containing cytosolic incubations with (a) 2,5-difluoroaminobenzene and (b) 2,5-difluoronitrobenzene. The resonances marked with an asterisk were also present in the ^{19}F-NMR spectra of control incubations carried out in the absence of cytosol. The resonance marked IS is from the internal standard 4-fluorobenzoic acid.

Molecular orbital characteristics

Molecular orbital characteristics of the 2,5-difluoroaminobenzene and 2,5-difluoronitrobenzene model compounds were calculated in order to investigate to which extent the observed differences in their biotransformation characteristics may originate from electronic differences between the compounds. Table 4 presents the results obtained for the energy levels of their so-called frontier orbitals , i.e. the orbitals which are of importance for their chemical reactivity, and, thus for their conversion in the active site of the biotransformation enzymes. The data obtained demonstrate that the nitro analogue has orbitals of relatively lower energy than those of the amino analogue. The difference between the energy of their frontier orbitals is

1.0 to 1.5 eV, those of the nitro analogue being more negative.

Additional results from the MO calculations are presented in Table 5, namely the density distribution of the frontier orbitals of importance for nucleophilic and electrophilic attack on the compounds. Previous results on the cytochrome P450-catalyzed aromatic hydroxylation of a series of monofluoroaminobenzenes and a series of fluorinated benzenes demonstrated that the preferential site for the cytochrome P450-catalyzed hydroxylation could be qualitatively (6) and even quantitatively (19) predicted on the basis of the frontier density for electrophilic attack of the substrate. The results presented in Table 5 for 2,5-difluoroaminobenzene show that for this aminobenzene derivative the preferential site for hydroxylation of a hydrogen substituted aromatic carbon centre, also corresponds with the position of the highest frontier orbital density for an electrophilic attack by the cytochrome P450 $(FeO)^{3+}$ intermediate, C4 being the preferential site for hydroxylation (Figure 1a). An attack at C2, substituted with a fluorine substituent and also containing relatively high frontier density for an electrophilic attack, does not result in product formation as no significant formation of hydroxylated products resulting from hydroxylation accompanied by an NIH shift or defluorination is observed (Figure 1a and 3a). Furthermore, hydroxylation at C3 resulting from an $(FeO)^{3+}$ attack at C2, followed by formation of the 2,3-arene oxide and opening of the epoxide moiety to give the 3-hydroxylated product is not observed to a significant extent either. Thus, the $(FeO)^{3+}$ attack at a fluorinated centre is more likely to be reversible than to lead to significant product formation.

For the nitrobenzene, the situation is different than for the 2,5-difluoroaminobenzene for which the preferential site for an electrophilic attack is the site of hydroxylation. The main frontier electron density for an electrophilic attack by the cytochrome P450 $(FeO)^{3+}$ is located on C5 and C2 of the 2,5-difluoro-nitrobenzene, whereas the hydroxylation observed occurs at C4. The frontier density for a nucleophilic attack, calculated from the LUMO and LUMO+1 is at this C4 centre (Table 5).

In addition to the frontier orbital density distributions of the 2,5-difluoronitrobenzene and 2,5-difluoroaminobenzene, Table 5 also presents the frontier orbital density distributions of three other nitrobenzene compounds, namely nitrobenzene itself, 2-fluoronitrobenzene and 3-fluoronitrobenzene. This is to enable comparisons between literature data on their aromatic hydroxylation (26-28) and the calculated chemical reactivity of their aromatic carbon centres (see discussion section). The results of the calculations demonstrate that, as for 2,5-difluoronitrobenzene, the preferential site for an electrophilic attack on a hydrogen substituted carbon centre is at the position(s) *meta* with respect to the nitro moiety.

Table 4: Energy levels of the frontier orbitals of 2,5-difluoroaminobenzene and 2,5-difluoronitrobenzene as calculated with the AM1 Hamiltonian.

Molecular orbital	E in eV in		Difference in eV
	2,5-Difluoro-aminobenzene	2,5-Difluoro-nitrobenzene	
LUMO+1	+ 0.06	- 0.97	- 1.03
LUMO	- 0.08	- 1.57	- 1.49
HOMO	- 8.83	-10.29	- 1.46
HOMO-1	- 9.75	-11.31	- 1.56

HOMO = highest occupied molecular orbital, LUMO = lowest unoccupied molecular orbital, HOMO-1 and LUMO+1 are the orbitals respectively just below the HOMO and just above the LUMO.

Table 5: Frontier density distributions of 2,5-difluoroaminobenzene, 2,5-difluoronitrobenzene, nitrobenzene, 2-fluoronitrobenzene and 3-fluoronitrobenzene as calculated with the AM1 Hamiltonian.

Compound	Distribution of	Density on						
		C1	C2	C3	C4	C5	C6	rest of molecule
2,5-diF-NH_2-benzene	HOMO	0.14	0.22	0.00	0.21	0.08	0.04	0.31
	HOMO/HOMO-1	0.26	0.43	0.03	0.39	0.16	0.11	0.62
	LUMO	0.04	0.29	0.13	0.03	0.33	0.12	0.06
	LUMO/LUMO+1	0.30	0.35	0.32	0.24	0.20	0.28	0.31
2,5-diF-NO_2-benzene	HOMO	0.07	0.22	0.09	0.05	0.26	0.12	0.19
	HOMO/HOMO-1	0.16	0.43	0.20	0.12	0.49	0.24	0.36
	LUMO	0.21	0.15	0.03	0.24	0.04	0.10	0.23
	LUMO/LUMO+1	0.36	0.33	0.11	0.41	0.14	0.25	0.40
NO_2-benzene	HOMO	0.00	0.25	0.25	0.00	0.25	0.25	0.00
	HOMO/HOMO-1	0.29	0.34	0.37	0.25	0.37	0.34	0.04
	LUMO	0.19	0.12	0.03	0.23	0.03	0.12	0.28
	LUMO/LUMO+1	0.34	0.27	0.10	0.42	0.10	0.27	0.50
2-F-NO_2-benzene	HOMO	0.07	0.24	0.15	0.02	0.29	0.11	0.12
	HOMO/HOMO-1	0.22	0.41	0.32	0.12	0.50	0.23	0.20
	LUMO	0.20	0.16	0.02	0.24	0.04	0.11	0.23
	LUMO/LUMO+1	0.35	0.33	0.10	0.41	0.11	0.26	0.44
3-F-NO_2-benzene	HOMO	0.04	0.15	0.27	0.08	0.07	0.27	0.12
	HOMO/HOMO-1	0.15	0.31	0.47	0.21	0.19	0.46	0.21
	LUMO	0.21	0.12	0.03	0.23	0.04	0.12	0.25
	LUMO/LUMO+1	0.36	0.27	0.12	0.41	0.12	0.27	0.45

HOMO/HOMO-1 and LUMO/LUMO+1 density distributions were calculated as described by Fukui et al. (23), and represent the contribution of two orbitals, resulting in a total density distribution of 2.0.

DISCUSSION.

The present paper presents *in vivo* and *in vitro* biotransformation characteristics of a model aminobenzene and its nitrobenzene analogue, namely 2,5-difluoroaminobenzene and 2,5-difluoronitrobenzene. The data presented demonstrate a marked difference in the relative contribution of cytochrome P450-catalyzed aromatic hydroxylation of the parent compound and, especially, of the glutathione S-transferase catalyzed glutathione conjugation, to the metabolism of the amino and nitro analogue. For the aminobenzene the cytochrome P450-catalyzed aromatic hydroxylation is the major pathway (62.8%), whereas for the nitrobenzene its conjugation with glutathione is the predominant route (40.0 %). The metabolic pattern of 2,5-difluoroaminobenzene is in accordance to what can be expected on the basis of metabolic characteristics of other aminobenzene derivatives. Cytochrome P450-catalyzed hydroxylation accompanied by N-acetylation and sulphate or glucuronide conjugation of the phenolic metabolites present the major routes for biotransformation (1-6). Furthermore, the preferential site for the cytochrome P450-catalyzed aromatic hydroxylation of 2,5-difluoroaminobenzene appeared to correlate with the one predicted on the basis of the highest frontier electron density for electrophilic attack. This result is in accordance with previous results on the cytochrome P450-catalyzed aromatic hydroxylation of monofluoroaminobenzenes (6) and fluorinated benzenes (19). It was demonstrated that the preferential site of cytochrome P450-catalyzed hydroxylation could be predicted qualitatively (6) and even quantitatively (19) on the basis of the calculated frontier orbital density distribution for electrophilic attack on the substrate, i.e. the preferential site for the attack on the substrate by the reactive cytochrome P450 $(FeO)^{3+}$ species initiating the hydroxylation.

For the 2,5-difluoronitrobenzene, however, its direct cytochrome P450-catalyzed aromatic hydroxylation appeared to be less efficient than for the amino analogue, other routes, like glutathione conjugation and nitroreduction being able to compete. Although *in vivo* the formation of some 2,5-difluoro-4-hydroxynitrobenzene was observed, NADPH/oxygen supported microsomal incubations with 2,5-difluoronitrobenzene did not show formation of a ring hydroxylated metabolite. The microsomal incubations with 2,5-difluoronitrobenzene, however, did show formation of two metabolites, identified as 2,5-difluoroaminobenzene, resulting from a six electron reduction of the nitro group, and as 2,5-difluoro-N-hydroxyaminobenzene, the 4 electron reduced intermediate in this reductive pathway (11;12). Formation of the 2 electron reduced 2,5-difluoronitrosobenzene reaction intermediate was not observed. Although this microsomal reduction of nitro compounds was reported before (12) quantification of

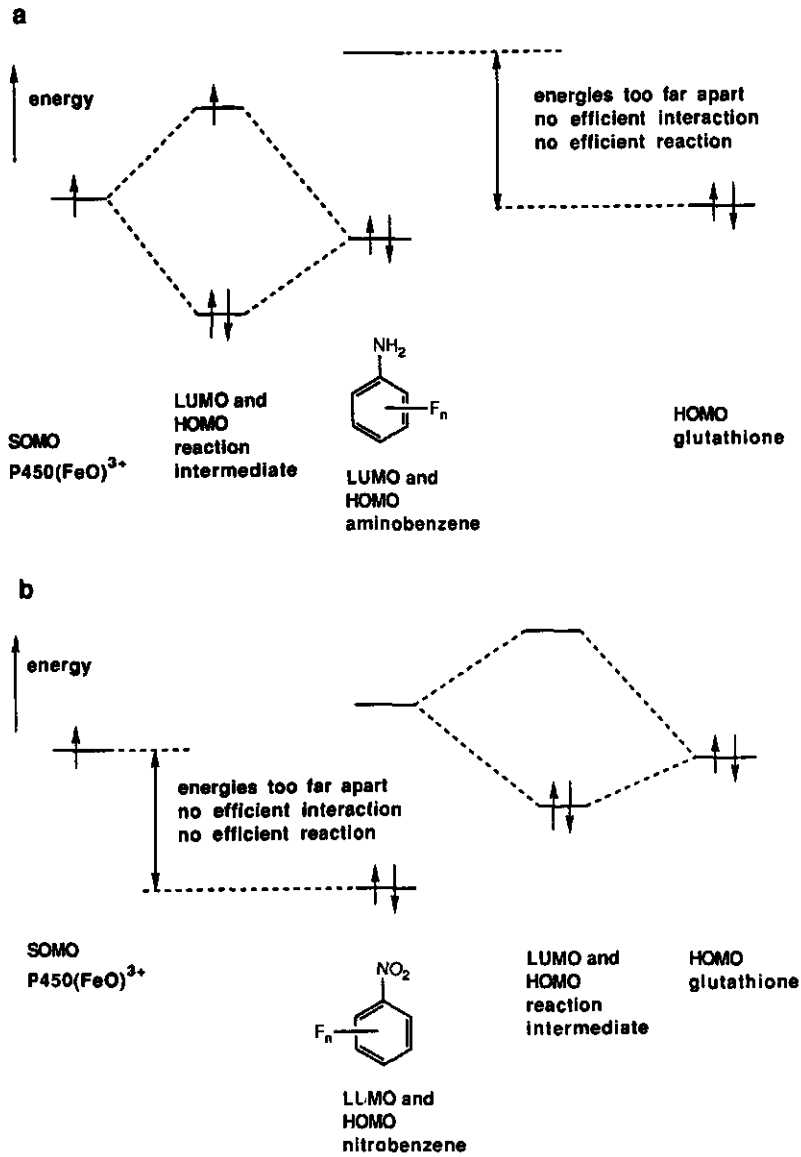

Figure 6: Molecular orbital scheme presenting the working hypothesis for possibilities for cytochrome P450 and/or glutathione S-transferase catalyzed biotransformation of (a) fluoroaminobenzenes and (b) fluoronitrobenzenes. Glutathione is reacting in its thiolate anionic form (32;33).

the hydroxylamino, and not the nitroso, as the main accumulating reaction intermediate has not been reported as unequivocally as in the present study.
However, in spite of these *in vitro* results it is of importance to stress that *in vivo* the contribution of the cecal microflora to this reductive pathway might be of more importance than the observed microsomal nitro reduction (11). In line with this, additional results of the present study supported the possibility that *in vivo* the cytochrome P450 cycle has better chances to complete the oxidative cycle resulting in hydroxylation, instead of resulting in nitroreduction. This can be derived as follows; the use of tert.butylhydroperoxide as the artificial oxygen donor in the microsomal conversion of 2,5-difluoronitrobenzene surpasses the electron donation steps and appeared to result in aromatic hydroxylation instead of nitroreduction of the 2,5-difluoronitrobenzene. This suggests that the difference between the formation of 2,5-difluoro-4-hydroxynitrobenzene observed *in vivo*, but not in a NADPH/oxygen supported *in vitro* microsomal incubation, is not only due to the fact that *in vivo* the metabolism continues for 24 h (24 h urine is analyzed), whereas *in vitro* a 10 minutes incubation is carried out. An additional factor adding to this difference in the extent of hydroxylation of 2,5-difluoronitrobenzene *in vitro* and *in vivo* might be that *in vivo* oxygen binding and donation of the second electron to the cytochrome P450 cycle is more efficient, leading to a full-turn P450 cycle, whereas in the microsomal system chances for nitroreduction upon the donation of the first electron are higher. *In vivo* the nitroreduction might then mainly result from the activity of the cecal microflora, whereas the cytochrome P450 conversion results in aromatic hydroxylation. Additional results of the present study showing inhibition of this *in vivo* hydroxylation of 2,5-difluoronitrobenzene, but not of the nitroreduction, by pretreatment of the animals with isosafrole (1,2-(methylenedioxy)-4-propenylbenzene), supports that the *in vivo* hydroxylation of 2,5-difluoronitrobenzene, but not its nitroreduction, is catalyzed by the cytochromes P450. The fact that isosafrole pretreatment did not inhibit the glutathione conjugation indicates that the effect on the formation of hydroxylated metabolites is not due to limitation of the uptake of the compound.

Furthermore, it is noteworthy that the cytochrome P450-catalyzed aromatic hydroxylation of the 2,5-difluoronitrobenzene occurs predominantly at C4 not at C3 or C5, in spite of the *meta* directing effect of the nitrogroup. The results of the molecular orbital calculations demonstrate that in 2,5-difluoronitrobenzene the highest frontier orbital density for an electrophilic attack, i.e. the highest HOMO/HOMO-1 density, is located at the fluorinated centres C2 and C5, C4 being much less reactive. When C4 hydroxylation is indeed initiated by an electrophilic attack of the cytochrome P450$(FeO)^{3+}$ on C5 of the substrate, this implies that the C4 hydroxylation must result from formation of an intermediate 4,5-epoxide.

However, in such a case formation of the 5,6-epoxide leading to C6 hydroxylation can be expected to occur in addition to formation of the 4,5-epoxide and C4 hydroxylation. This is, however, not observed. Another explanation might be that due to an orienting interaction between the active center of the cytochrome P450$(FeO)^{3+}$ and the 2,5-difluoronitrobenzene the substrate is oriented towards the oxygen of the $(FeO)^{3+}$ moiety in such a way that the C4 becomes the preferential site for a reaction in spite of its lower reactivity for an electrophilic attack. The observation that in the metabolite patterns of the rats pretreated with cytochrome P450 inducers and exposed to 2,5-difluoronitrobenzene the hydroxylation is always at C4 suggests that the orienting effect might be the result of an interaction that occurs in a similar way in the active site of different cytochromes P450. Thus, the interaction might be the result of an orienting interaction between the porphyrin $(FeO)^{3+}$ and the nitrobenzene. Definite prove for such a possible orienting interaction has to await further investigations on other nitrobenzene derivatives. The preferential hydroxylation of the 2,5-difluoronitrobenzene at the position *para*, not *meta*, with respect to the nitro moiety is similar to what was reported up to now for nitrobenzene derivatives. Bray *et al.* (26) using color formation of TLC spots as means for identification of urine metabolites of rabbits, reported C5 but also C4 hydroxylation of 2-chloronitrobenzene, as well as C4-hydroxylation of 3-chloronitrobenzene. In further studies on 2- and 3-fluoro-, chloro-, bromo- or iodo-nitrobenzenes they reported that the predominant nitrophenols from all the halogenated nitrobenzenes were paranitrophenols (27). More recently, Rickert *et al.* (28) reported hydroxylation of nitrobenzene at both the positions *para* and *meta* with respect to the nitro moiety, hydroxylation of the C4 position being generally 1.65 ± 0.16 times higher than that of the C3 position. Comparison of these biotransformation data to the relative reactivity of the various carbon centres in nitrobenzene and in 2- and 3-fluoronitrobenzene indicates that, as for 2,5-difluoronitrobenzene, the hydroxylation is not observed at the carbon centre that is most reactive towards an electrophilic attack. However, as for the 2,5-difluoronitrobenzene, the preferential site for a nucleophilic attack is at the C4. This implies that, in addition to the explanations given above, a third factor might in theory be responsible for the regioselectivity of the aromatic hydroxylation. A radical attack by the cytochrome P450$(FeO)^{3+}$ SOMO (singly occupied molecular orbital) can in theory proceed not only electrophilic, the SOMO interacting with the HOMO of a substrate, but also nucleophilic, the SOMO interacting with the LUMO of a substrate (29). Based on this consideration and the results of the present study it could be proposed that the cytochrome P450-catalyzed hydroxylaton of the 2,5-difluoronitrobenzene proceeds by a nucleophilic, instead of by an electrophilic, attack of the cytochrome P450$(FeO)^{3+}$ SOMO on the substrate. The fact that the preferential site for hydroxylation of 2,5-difluoronitrobenzene

appears to be at C4, combined with the fact that the LUMO/LUMO+1 density is highest and predicts this C4 site as the preferential site for a nucleophilic attack, supports this explanation. However, the fact that the cytochrome P450$(FeO)^{3+}$ species is known to be highly electrophilic seems to argue against this explanation and leaves the specific stereoselective orientation of the nitrobenzene and/or the involvement of epoxide intermediates as the best working hypotheses for further research.

Finally, Figure 6 schematically presents a molecular orbital based model for the explanation of the observed difference in metabolic pathways for the amino- and the nitrobenzene derivative, as reported in the present study. From molecular orbital calculations it followed that the molecular orbitals of the nitro analogue are generally 1 to 1.5 eV lower in energy than those of the amino analogue. As a result, the LUMO of the 2,5-difluoronitrobenzene might be closer in energy to the HOMO of the thiolate anion of glutathione than the LUMO of the 2,5-difluoroaminobenzene. Taking into account the fact that the frontier orbital theory (29) describes that the reactivity of two reactants is higher when the energy difference between the reacting orbitals is lower this might result in a more efficient glutathione conjugation of 2,5-difluoronitrobenzene than of the 2,5-difluoroaminobenzene. In a similar way the relatively lower energy orbitals of the nitro analogue might explain the lower reactivity of the HOMO of 2,5-difluoronitrobenzene than of the HOMO of 2,5-difluoroaminobenzene with the SOMO of the cytochrome P450$(FeO)^{3+}$ intermediate. Previous MO-QSAR studies on the aromatic hydroxylation by flavin dependent monooxygenases have demonstrated an energy difference in the HOMO of the substrate of 1.0 eV to correspond to a change in the reaction rate of a factor 10 to 50 (30;31), whereas a recently obtained MO-QSAR for the cytochrome P450-catalyzed 4-hydroxylation of a series of aminobenzene derivatives (32) demonstrates that halogenated anilines with a E(HOMO) value below -9.2 eV appeared to be converted at relatively low rates by the cytochromes P450. These results imply that the relatively low energy of the frontier orbitals of the nitrobenzene might indeed explain its relatively lower reactivity in a cytochrome P450-catalyzed hydroxylation as well as its relatively higher reactivity in a glutathione S-transferase catalyzed reaction. Thus, together the results of the present study indicate that, on the basis of the molecular orbital characteristics of a substrate it must be possible to predict some of the characteristics of its biotransformation pathways. Further development of this approach is currently under investigation.

REFERENCES.

1 J.W. Gorrod and D. Manson, The metabolism of aromatic amines. *Xenobiotica* **16** (1986) 933-955.

2 J.W. Daly, G. Gurrof, S. Udenfriend and B. Witkop, Hydroxylation of alkyl and halogen substituted anilines and acetanilides by microsomal hydroxylases. *Biochem. Pharmacol.* **17** (1968) 31-36.

3 C.V. Eadsforth, C.J. Logan, B.J. Morrison and P.A. Warburton, 2,4-Difluoroaniline and 4-fluoroaniline exposure: monitoring by methaemoglobin and urine analysis. *Int. Arch. Occ. Env. Health* **54** (1984) 223-232.

4 C.V. Eadsforth, P.C. Coveney, D.H. Hutson, C.J. Logan and A.J. Samuel, The metabolism of o-fluoroaniline by rats, rabbits and marmosets. *Xenobiotica*, **16** (1986) 555-566.

5 J. Vervoort, P.A. de Jager, J. Steenbergen and I.M.C.M. Rietjens, Development of a ^{19}F NMR method for studies on the in vivo and in vitro metabolism of 2-fluoroaniline. *Xenobiotica*, **20** (1990) 657-670.

6 N.H.P. Cnubben, J. Vervoort, C. Veeger and I.M.C.M. Rietjens, Study on the regioselectivity and mechanism of the aromatic hydroxylation of monofluoroanilines. *Chem.-Biol. Interactions*, **85** (1992) 151-172.

7 D.E. Rickert, Metabolism of nitroaromatic compounds, *Drug Metabolism Reviews*, **18** (1987) 23-53.

8 T. Yoshida, K. Andoh and T. Tabuchi. Identification of urinary metabolites in rats treated with p-chloronitrobenzene. *Arch. Toxicol.* **65** (1991) 52-58.

9 T. Yoshida, T. Tabuchi and K. Andoh, Identification of human subjects acutely poisoned by p-chloronitrobenzene. *Xenobiotica* **22** (1992) 1459-1470.

10 J. Piotrowski, Further investigations on the evaluation of exposure to nitrobenzene, *Brit. J. Industr. Med.*, **24** (1967) 60-65.

11 A. A. Levin and J.G. Dent, Comparison of the metabolism of nitrobenzene by hepatic microsomes and cecal microflora from Fischer-344 rats in vitro and the relative importance of each in vivo. *Drug Metabolism and Dipos.* **10** (1982) 450-454.

12 N. Harada and T. Omura, Participation of cytochrome P450 in the reduction of nitro compounds by rat liver microsomes. *J. Biochem.* **87** (1980) 1539-1554.

13 D. Rickert and S.D. Held, Metabolism of chloronitrobenzenes by isolated rat hepatocytes. *Drug Metabolism and Dispos.* **18** (1990) 5-9.

14 G.H. Coleman, Ch. M. McCloskey and F.A. Stuart: Nitrosobenzene. *Organic Syntheses* **25** (1943) 81-83.

15 R.J. Kennedy and A.M. Stock, The oxidation of organic substances by potassium peroxymonosulphate. *J. Org. Chem.* **25** (1960) 1901-1906.

16 I.M.C.M. Rietjens and J. Vervoort, Microsomal metabolism of fluoroanilines. *Xenobiotica*, **19** (1989) 1297-1305.

17 R.M.E. Vos, M.C.Snoek, W.J.H. van Berkel, F. Müller and P.J. van Balderen, Differential induction of rat hepatic glutathione S-transferase isoenzymes by hexachlorobenzene and benzyl isothiocyanate: comparison with induction by phenobarbital and 3-methylcholanthrene. *Biochem. Pharmacol.* **37** (1988) 1077-1082.

18 I.M.C.M. Rietjens and J. Vervoort, A new hypothesis for the mechanism for cytochrome P-450 dependent aerobic conversion of hexahalogenated benzenes to pentahalogenated phenols. *Chem. Res. Toxicol.* **5** (1992) 10-19.

19 I.M.C.M. Rietjens, A.E.M.F. Soffers, C. Veeger and J. Vervoort, Regioselectivity of cytochrome P450 catalyzed hydroxylation of fluorobenzenes predicted by calculated frontier orbital substrate characteristics. *Biochemistry,* **32** (1993) 4801-4812.

20 T. Omura and R. Sato, The carbon monoxide pigment of liver microsomes, I. Evidence for its haemoprotein nature. *J. Biol. Chem.*, **239** (1964) 2370-2378.

21 .H. Lowry, N.J. Rosebrough, A.L. Farr and A.J. Randall, Protein measurements with Folin phenol reagent. *J. Biol. Chem.*, **193** (1951) 265-275.

22 B.B. Brodie and J. Axelrod, The estimation of acetanilide and its metabolic products, aniline, N-acetyl p-aminophenol and p-aminophenol (free and conjugated) in biological fluids and tissues. *J. Pharmacol. Exp. Ther.*, **94** (1948) 22-28.

23 K. Fukui, T. Yonezawa, C. Nagata and H. Shingu, Molecular orbital theory of orientation in aromatic, heteroaromatic and other conjugated molecules. *J. Chem. Phys.*, **22** (1954) 1433-1442.

24 M.A. Cooper, H.E. Weber and S.L Manatt, The fluorine-19 nuclear magnetic resonance spectra of some fluoroaromatic compounds. Studies using nise decoupling of protons. *J. Am. Chem. Soc.* **93** (1971) 2369-2380.

25 V. Wray, Fluorine nuclei in difluorobenzene derivatives. In : Annual reports on NMR spectroscopy, vol 14, Academic Press. 1983, (Webb, G.A. ed.) p 273-281.

26 H.G. Bray, S.P. James and W.V. thorpe, The metabolism of monochloronitrobenzenes in the rabbit. *Biochem. J.* **64** (1956) 38-44.

27 H.G. Bray, S.P. James and W.V. Thorpe, Metabolism of o-, m- and p-fluoro, -bromo and -iodo-nitrobenzenes in the rabbit. *Biochem. J.* **68** (1958) 561-568.

28 D.E. Rickert, J.A. Bond, R.M. Long and J.P. Chism, Metabolism of nitrobenzene by rats and mice, *Toxicol. Applied Pharmacol.*, **67** (1983) 206-214.

29 I. Fleming (Ed). Frontier orbitals and organic chemical reactions, John Wiley & Sons, New York, 1976, pp 1-249.

30 J. Vervoort, I.M.C.M. Rietjens, W.J.H. van Berkel and C. Veeger, Frontier orbital study on the 4-hydroxybenzoate-3-hydroxylase-dependent activity with benzoate derivatives. *Eur. J. Biochem.* **206** (1992) 479-484.

31 I.M.C.M. Rietjens, M.G. Boersma, A.E.M.F. Soffers, N.H.P. Cnubben, J. Koerts, S. Peelen, W.J.H. van Berkel, C. Veeger and J. Vervoort, Use of molecular orbital calculations in studies on mechanisms of enzyme catalysis. In: Flavins and Flavoproteins 1993. Kunio Yagi

(ed), Walter de Gruyter & Co, Berlin, (1993)(in press).

32 N.H.P. Cnubben, S. Peelen, J.W. Borst, J. Vervoort, and I.M.C.M. Rietjens, Molecular orbital based quantitative structure activity relationship for the cytochrome P450-catalyzed 4-hydroxylation of halogenated anilines, *Chem. Res. Tox.*, (1994) in press.

33 W.J. Chen, G.F. Graminski and R.N. Armstrong, Dissection of the catalytic mechanism of isozyme 4-4 of glutathione S-transferase with alternative substrates, *Biochemistry* **27** (1988) 647-654.

34 G.F. Graminski, G.F., Y. Kubo and R.N. Armstrong, Spectroscopic and kinetic evidence for the thiolate anion of glutathione at the active site of glutathione S-transferase. *Biochemistry* **28** (1989) 3562-3568.

CHAPTER 9

Influence of the halogen-substituent pattern of fluoronitrobenzenes on their biotransformation and capacity to induce methemoglobinemia.

Nicole H.P. Cnubben, Ans E. M. F. Soffers, Maria A.W. Peters, Jacques Vervoort and Ivonne M.C.M. Rietjens.

Accepted for publication in Toxicology and Applied Pharmacology.

SUMMARY.

In the present study both the biotransformation patterns and the capacity to induce methemoglobinemia of a series of fluoronitrobenzenes were investigated. This was done to investigate to what extent variation in the number and position of the halogen substituents influence the metabolic fate of the fluoronitrobenzenes, thereby influencing their capacity to induce methemoglobinemia. The results obtained were compared to the effect of the fluorine substituent patterns on the calculated electronic characteristics, and, thus, on the chemical reactivity of the fluoronitrobenzenes.

Analysis of the *in vivo* metabolic profiles demonstrates a dependence of the extent of nitroreduction, of glutathione conjugation and of aromatic hydroxylation with the pattern of halogen substitution. With increasing number of fluorine substituents at electrophilic carbon centres, 24 h urine recovery values decreased and fluoride anion elimination increased, due to increased reactivity of the fluoronitrobenzenes with cellular nucleophiles. *In vitro* studies even demonstrated a clear correlation between calculated parameters for the electrophilicity of the fluoronitrobenzenes and the natural logarithm of their rate of reaction with glutathione or with bovine serum albumin, taken as a model for cellular nucleophiles ($r=0.97$ and $r=0.98$ respectively). Increased possibilities for the conjugation of the

fluoronitrobenzenes to cellular nucleophiles was accompanied by decreased contributions of nitroreduction and aromatic hydroxylation to the overall *in vivo* metabolite patterns, as well as by a decreased capacity of the fluoronitrobenzenes to induce the methemoglobinemia. In vitro studies on the rates of nitroreduction of the various fluoronitrobenzenes by cecal microflora and rat liver microsomes, revealed that the changes in the capacity of the fluoronitrobenzenes to induce methemoglobinemia were not due to differences in their intrinsic reactivity in the pathway of nitroreduction, leading to the methemoglobinemia inducing metabolites.

Thus, the results of the present study clearly demonstrate that the number and position of fluorine substituents in the fluoronitrobenzenes influence the capacity of the fluoronitrobenzenes to induce methemoglobinemia, not because their intrinsic chemical reactivity for entering the nitroreduction pathway is influenced. The different methemoglobinemic capacity must rather result from differences in the inherent direct methemoglobinemic capacity and/or reactivity of the various toxic metabolites, and/or from the fact that the halogen substituent pattern influences the electrophilic reactivity, thereby changing the possibilities for reactions of the nitrobenzenes with glutathione and, especially, other cellular nucleophiles. When the number of fluorine substituents increases, the electrophilicity of the fluoronitrobenzenes can become so high that glutathione conjugation is no longer able to compete efficiently with covalent binding of the fluoronitrobenzenes to cellular macromolecules. As a consequence, it can be suggested that with an increasing number of fluorine substituents at electrophilic carbon centres in a nitrobenzene derivative, a toxic endpoint of the nitrobenzene other than formation of methemoglobinemia can be foreseen.

INTRODUCTION.

Halogenated nitrobenzenes are frequently used as industrial intermediate reagents in the production of dyes, rubbers, pharmaceuticals or are used as agrochemicals, like for instance the soil pesticide pentachloronitrobenzene [Rickert, 1987]. Nitrobenzene derivatives are mutagenic in several bacterial strains [Shimizu *et al.*, 1983; Debnath *et al.*, 1992], cause DNA damage in vivo [Cesarone *et al.*, 1983], are hepatotoxic [Beauchamp *et al.*, 1982] and nephrotoxic [Yoshida *et al.*, 1989]. However, the most frequently reported consequence of exposure to nitrobenzenes is methemoglobinemia and it is generally accepted that the intermediate oxidation states formed in the process of nitroreduction by the intestinal microflora (nitrosobenzene, N-hydroxyarylamine or the radical intermediates, all formed in the six-electron reduction pathway leading to aniline formation) are responsible for

inducing methemoglobinemia [for review, see Kiese, 1974]. Thus, some of the toxic effects require reactive intermediates formed upon the biotransformation of nitrobenzenes. From several studies it became evident that both the toxicity as well as metabolism of nitrobenzenes can be dependent on their substituent pattern [O'Brien *et al.*, 1990; Shimizu *et al.*, 1983; Debnath *et al.*, 1991; Sabbioni, 1992; Sabbioni, 1994]. The wide variation in capacity of nitrobenzene-derivatives to cause toxic effects has been partially related to their different susceptibility to nitroreduction to give their corresponding nitro radical anions, nitrosobenzenes or N-hydroxyarylamines [Debnath *et al.*, 1991; Lopez de Compadre *et al.*, 1990; O'Brien *et al.*, 1990; Sabbioni, 1992; Sabbioni, 1994; Tatsumi *et al.*, 1978]. On the other hand, it has been suggested that differences in occurence of methemoglobinemia or in the formation of hemoglobin adducts with a change in the substituent pattern, are related to the effectiveness of biotransformation pathways competing with nitroreduction [Debnath *et al.*, 1991; Kiese, 1974; Sabbioni, 1994; Rickert and Held, 1990]. A combined study on biotransformation and methemoglobin formation of a series of nitrobenzenes may provide insight in the relative importance of these two suggestions, but has not been published yet. Therefore, the objective of the present study was to investigate both the induction of methemoglobinemia as well as in vivo metabolic profiles of a series of nitrobenzene derivatives. This was done using a series of fluoronitrobenzenes. The fluorine label makes it possible to use ^{19}F NMR as a tool to characterize the complete urine metabolic patterns of the nitrobenzene derivatives. Besides, the Van der Waals radius of a fluorine substituent is slightly larger compared to that of a hydrogen substituent, limiting possible steric influences of the substituents. Finally, the fluorine substituents can be expected to influence the chemical reactivity characteristics of the substrates that are of importance in electrophilic reactions like aromatic hydroxylation [Cnubben *et al.*, 1992; Cnubben *et al.*, 1994; Rietjens *et al.*, 1993], in nucleophilic reactions like glutathione conjugation [Rietjens *et al.*, 1995 a+b], and in reductions, like nitroreduction [Lopez de Compadre *et al.*, 1990]. To elucidate the actual influence of the various fluorine substituents patterns on these electronic characteristics of the nitrobenzene model compounds, molecular orbital calculations were performed and the results obtained were compared to the biotransformation characteristics of the nitrobenzenes observed both *in vivo* as well as *in vitro.*

MATERIALS AND METHODS.

Chemicals.

2-Fluoronitrobenzene, 3-fluoronitrobenzene, 4-fluoronitrobenzene and 3,5-difluoronitrobenzene were obtained from Aldrich (Steinheim, FRG). 2,5-

Difluoronitrobenzene, 2,4-difluoronitrobenzene, 2,3,4-trifluoronitrobenzene, 2,4,6-trifluoronitrobenzene and 2,3,4,6-tetrafluoronitrobenzene were purchased from Fluorochem (Derbyshire, UK). 2-Fluoroaniline, 3-fluoroaniline and 4-fluoroaniline were from Janssen Chimica (Beerse, Belgium). 2,4-Difluoroaniline, 2,5-difluoroaniline, 3,5-difluoroaniline, 2,3,4-trifluoroaniline, 2,4,6-trifluoroaniline and 2,3,4,6-tetrafluoroaniline were from Fluorochem. 3-Fluoro-4-nitrophenol and 2-fluoro-4-nitrophenol were from Fluorochem.

The ^{19}F-NMR resonances of the 2-fluoro-3-nitrophenol, 2-fluoro-5-nitrophenol, 5-fluoro-3-nitrophenol and 4,6-difluoro-2-aminophenol were identified on the basis of a characteristic shift of the ^{19}F-NMR resonance known to exist upon the introduction of a hydroxyl moiety at positions ortho, meta or para with respect to the fluorine [Rietjens *et al.*, 1995a]. The ^{19}F-NMR resonances of 2,5-difluoro-4-nitrophenol and 2,6-difluoro-4-nitrophenol were identified by reducing the nitro moiety to the amino moiety with zinc powder yielding respectively 2,5-difluoro-4-nitrophenol and 2,6-difluoro-4-aminophenol [Rietjens *et al.*, 1995a; Piotrowski, 1967].

3-Fluoro-4-aminophenol, 3-fluoro-2-aminophenol, 4-fluoro-2-aminophenol, 2-fluoro-4-aminophenol, 5-fluoro-2-aminophenol, 2,5-difluoro-4-aminophenol, 3,5-difluoro-4-aminophenol and 2,6-difluoro-4-aminophenol were synthetised essentially as described before [Cnubben *et al.*, 1992; Cnubben *et al.*, 1994]. 3-Fluoro-4-acetamidophenol, 2-fluoro-4-acetamidophenol, 5-fluoro-2-acetamidophenol, 3-fluoroacetanilide, 2,6-difluoro-4-acetamidophenol, 3,5-difluoro-4-acetamidophenol and 2,5-difluoro-4-acetamidophenol were synthetised by acylation of the corresponding amino-compounds following the procedure described by Vogel [1978].

All (fluorinated) glutathionyl-nitrobenzene and mercapturic acid derivatives were synthetised from suitable fluoronitrobenzenes essentially as described before [Rietjens *et al.*, 1995 a+b]. ^{19}F-NMR and ^{1}H-NMR spectral characteristics of 4-fluoro-2-glutathionyl-nitrobenzene, 2-fluoro-4-glutathionyl-nitrobenzene, 5-fluoro-2-glutathionyl-nitrobenzene, 5-fluoro-2-(N-acetylcysteinyl)-nitrobenzene, 2,6-difluoro-4-glutathionyl-nitrobenzene, 2,4-difluoro-6-glutathionyl-nitrobenzene, 3,4,6-trifluoro-2-glutathionyl-nitrobenzene and 2,3,6-trifluoro-4-glutathionyl-nitrobenzene were previously described [Rietjens *et al.*, 1995 a+b]. Spectral characteristics of all other synthetised compounds, used for identification of the various adducts, are presented in Table 1. Chemical shift values are in D_2O and presented relative to $CFCl_3$ for ^{19}F-NMR and relative to TSP (sodium 3-trimethylsilyl-(2,2,3,3-$^{2}H_4$)-propionate) (Isotec, INC) for ^{1}H-NMR.

Fluoronitrosobenzenes were synthetised according to Kennedy and Stock [1960]. During 3 min 25 mL 15% (w/v) potassiumperoxomonosulphate (minimal 4.5 % active oxygen, Janssen Chimica) were added to a solution of 10 mmol of the

Table 1: ^{1}H-NMR and ^{19}F-NMR spectral characteristics of the aromatic substituents of the various glutathionyl-fluoronitrobenzene and mercapturic acid derivatives. Chemical shift values are in D_2O and presented relative to $CFCl_3$ for ^{19}F-NMR and relative to TSP (sodium 3-trimethylsilyl-(2,2,3,3-$^{2}H_4$)-propionate) for ^{1}H-NMR.

Compound		Spectral characteristics
2,3-difluoro-4-glutathionyl-nitrobenzene		
^{1}H-NMR	8.01	(H5)(dd;$^{3}J_{H5-H6}$ = 8.0 Hz, $^{4}J_{H5-F3}$ = 5.7 Hz)
	7.45	(H6)(dd;$^{3}J_{H6-H5}$ = 8.0 Hz)($^{4}J_{H6-F2}$ = 7.1 Hz)
^{19}F-NMR	-146.2	(F2)(dd; $^{3}J_{F2-F3}$ = 21.6 Hz, $^{4}J_{F2-H6}$ = 7.1 Hz)
	-135.5	(F3)(dd; $^{3}J_{F3-F2}$ = 21.6 Hz, $^{4}J_{F3-H5}$ = 5.7 Hz)
3,4-difluoro-2-glutathionyl-nitrobenzene		
^{1}H-NMR	7.51	(H5)(m; $^{3}J_{H5-H6}$ = 9.2 Hz, $^{3}J_{H5-F4}$ = 8.9 Hz, $^{4}J_{H5-F3}$ = 7.1 Hz)
	7.90	(H6)(dd; $^{3}J_{H6-H5}$ = 9.2 Hz, $^{4}J_{H6-F4}$ = 4.4 Hz)
^{19}F-NMR	-129.2	(F3)(dd; $^{3}J_{F3-F4}$ = 21.6 Hz, $^{4}J_{F3-H5}$ = 7.1 Hz)
	-131.0	(F4)(m; $^{3}J_{F4-F3}$ = 21.6 Hz, $^{3}J_{F4-H5}$ = 8.9 Hz, $^{4}J_{F4-H6}$ = 4.4 Hz)
2-(N-acetylcysteinyl)-nitrobenzene		
^{1}H-NMR	7.49	(H6)(d, $^{3}J_{H6-H5}$ = 8.0 Hz),
	7.12	(H5)(tr, $^{3}J_{H5-H4}$ = 8.0 Hz, $^{3}J_{H5-H6}$ = 8.0 Hz)
	7.00	(H4)(tr, $^{3}J_{H4-H5}$ = 8.0 Hz, $^{3}J_{H4-H3}$ = 8.0 Hz)
	6.76	(H3)(d, $^{3}J_{H3-H4}$ = 8.0 Hz)
4-(N-acetylcysteinyl)-nitrobenzene		
^{1}H-NMR	7.49	(H2/6)(d, $^{3}J_{H2/6-H3/5}$ = 9.0 Hz)
	6.87	(H3/5)(d, $^{3}J_{H3/5-H2/6}$ = 9.0 Hz)
2-fluoro-4-(N-acetylcysteinyl)-nitrobenzene		
^{1}H-NMR	7.24	(H3)(dd; $^{3}J_{H3-F2}$ = 12.3 Hz, $^{4}J_{H3-H5}$ = 2.1 Hz)
	7.18	(H5)(dd; $^{3}J_{H5-H6}$ = 8.8 Hz, $^{4}J_{H5-H3}$ = 2.1 Hz)
	7.96	(H6)(tr of dd; $^{3}J_{H6-H5}$ = 8.8 Hz, $^{4}J_{H6-F2}$ = 8.2 Hz)
^{19}F-NMR	-121.5	(F2)(dd; $^{3}J_{F2-H3}$ = 12.3 Hz, $^{4}J_{F2-H6}$ = 8.2 Hz)
4-fluoro-2-(N-acetylcysteinyl)-nitrobenzene		
^{1}H-NMR	7.30	(H3)(dd; $^{3}J_{H3-F4}$ = 10.0 Hz, $^{4}J_{H3-H5}$ = 2.6 Hz)
	7.05	(H5)(m; $^{3}J_{H5-F4}$ = 7.1 Hz, $^{3}J_{H5-H6}$ = 9.4 Hz, $^{4}J_{H5-H3}$ = 2.6 Hz)
	8.20	(H6)(dd; $^{3}J_{H6-H5}$ = 9.4 Hz, $^{4}J_{H6-F4}$ = 6.0 Hz)
^{19}F-NMR	-106.3	(F4)(m; $^{3}J_{F4-H3}$ = 10.0 Hz, $^{3}J_{F4-H5}$ = 7.1 Hz, $^{4}J_{F4-H6}$ = 6.0 Hz)
2,6-difluoro-4-(N-acetylcysteinyl)-nitrobenzene		
^{1}H-NMR	7.18	(H3/5)(d; $^{3}J_{H3/5-F2/6}$ = 9.7 Hz)
^{19}F-NMR	-122.1	(F2/6)(d; $^{3}J_{F2/6-H3/5}$ = 9.7 Hz)

4,6-difluoro-2-(N-acetylcysteinyl)-nitrobenzene

^{1}H-NMR	7.11	(H5)(m; $^{3}J_{H5-F6}$ = 10.7 Hz, $^{3}J_{H5-F4}$ = 8.6 Hz, $^{4}J_{H5-H3}$ = 2.5 Hz)
	7.32	(H3)(m; $^{3}J_{H3-F4}$ = 9.1 Hz, $^{4}J_{H3-H5}$ = 2.5 Hz, $^{5}J_{H3-F6}$ = 1.5 Hz)
^{19}F-NMR	-119.5	(F6)(m; $^{3}J_{F6-H5}$= 10.7 Hz, $^{4}J_{F6-F4}$ = 11.8 Hz, $^{5}J_{F6-H3}$ = 1.5 Hz)
	-105.2	(F4)(m; $^{3}J_{F4-H3}$ = 9.1 Hz, $^{3}J_{F4-H5}$ = 8.6 Hz, $^{4}J_{F4-F6}$ = 11.8 Hz)

2,3-difluoro-4-(N-acetylcysteinyl)-nitrobenzene

^{1}H-NMR	7.93	(H5)(dd; $^{3}J_{H5-H6}$= 7.5 Hz, $^{4}J_{H5-F3}$ = 6.1 Hz)
	7.63	(H6)(dd; $^{3}J_{H6-H5}$ = 7.5 Hz, $^{4}J_{H6-F2}$ = 6.1 Hz)
^{19}F-NMR	-146.7	(F2)(dd; $^{3}J_{F2-F3}$ = 21.6 Hz, $^{4}J_{F2-H6}$ = 6.1 Hz)
	-136.3	(F3)(dd; $^{3}J_{F3-F2}$ = 21.6 Hz, $^{4}J_{F3-H5}$ = 6.1 Hz)

3,4-difluoro-2-(N-acetylcysteinyl)-nitrobenzene

^{1}H-NMR	7.46	(H5)(m; $^{3}J_{H5-H6}$ = 9.2 Hz, $^{3}J_{H5-F4}$ = 8.9 Hz, $^{4}J_{H5-F3}$ = 7.5 Hz)
	7.85	(H6)(m; $^{3}J_{H6-H5}$ = 9.2 Hz, $^{4}J_{H6-F4}$ = 4.4 Hz)
^{19}F-NMR	-129.4	(F3)(dd; $^{3}J_{F3-F4}$ = 21.5 Hz, $^{4}J_{F3-H5}$ = 7.5 Hz)
	-131.3	(F4)(m; $^{3}J_{F4-F3}$ = 21.5 Hz, $^{3}J_{F4-H5}$ =8.9 Hz, $^{4}J_{F4-H6}$ = 4.4 Hz)

3,4,6-trifluoro-2-(N-acetylcysteinyl)-nitrobenzene

^{1}H-NMR	7.55	(H5)(m; $^{3}J_{H5-F6}$ = 10.2 Hz, $^{3}J_{H5-F4}$ = 9.5 Hz, $^{4}J_{H5-F3}$ = 6.3 Hz)
^{19}F-NMR	-134.9	(F3)(m;$^{3}J_{F3-F4}$ = 22.3 Hz, $^{4}J_{F3-H5}$ = 6.3 Hz, $^{5}J_{F3-F6}$ = 12.4 Hz)
	-129.6	(F4)(m; $^{3}J_{F4-F3}$ = 22.3 Hz, $^{3}J_{F4-H5}$ = 9.5 Hz, $^{4}J_{F4-F6}$ = 6.3 Hz)
	-127.0	(F6)(m;$^{3}J_{F6-H5}$ = 10.2 Hz, $^{4}J_{F6-F4}$ = 6.3 Hz, $^{5}J_{F6-F3}$ = 12.4 Hz)

2,3,6-trifluoro-4-(N-acetylcysteinyl)-nitrobenzene

^{1}H-NMR	7.40	(H5)(dd; $^{3}J_{H5-F6}$ = 11.0 Hz, $^{4}J_{H5-F3}$ = 5.3 Hz)
^{19}F-NMR	-145.1	(F2)(dd; $^{3}J_{F2-F3}$ = 21.6 Hz, $^{4}J_{F2-F6}$ = 3.7 Hz)
	-140.9	(F3)(m; $^{3}J_{F3-F2}$= 21.6 Hz, $^{4}J_{F3-H5}$ = 5.3 Hz, $^{5}J_{F3-F6}$ = 12.0 Hz)
	-126.9	(F6)(m; $^{3}J_{F6-H5}$= 11.0 Hz, $^{4}J_{F6-F2}$ = 3.7 Hz, $^{5}J_{F6-F3}$ = 12.0 Hz)

desired fluoroaniline in 20 mL glacial acetic acid, cooled in an ice bath. After 2 minutes mixing, the reaction mixture was immediately extracted two times with 25 mL hexane. The characteristic green colored nitrosobenzene containing hexane-phase was immediately analysed by ^{19}F-NMR in 0.1 M potassium phosphate pH 7.6 to identify the ^{19}F-NMR resonances of the compounds. Synthesis of the fluoro-N-hydroxyanilines was performed by the chemical reduction of the synthetised fluoronitrosobenzenes with 20 mM ascorbic acid. Chemical shift values are in 0.1 M potassium phosphate and presented relative to $CFCl_3$. The ^{19}F-NMR spectral characteristics of the compounds are as follows: 2-fluoronitrosobenzene (F2) -133.7 ppm; 3-fluoronitrosobenzene (F3) -116.2 ppm; 4-fluoronitrosobenzene (F4) -102.6 ppm; 2,4-difluoronitrosobenzene (F4) -96.9 ppm, (F2) -128.0 ppm; 2,5-difluoronitrosobenzene (F5) -122.4 ppm, (F2) -138.0 ppm; 3,5-difluoronitrosobenzene (F3/F5) -115.1 ppm; 2,4,6-trifluoronitrosobenzene (F2/F6) -132.5 ppm, (F4) -126.5 ppm; 2,3,4-trifluoronitrosobenzene (F3) -152.5 ppm, (F1) -158.8, (F2) -165.7 ppm; 2,3,4,6-tetrafluoronitrosobenzene (F6) -139.4 ppm, (F4) -152.8 ppm, (F2) -156.7 ppm and (F3) -170.6 ppm. 2-Fluoro-N-hydroxyaniline (F2)

-135.3 ppm; 3-fluoro-N-hydroxyaniline (F3) -116.8 ppm; 4-fluoro-N-hydroxyaniline (F4) -125.7 ppm; 2,4-difluoro-N-hydroxyaniline -121.9 ppm (F4), -130.6 ppm (F2); 2,5-difluoro-N-hydroxyaniline -122.0 ppm (F5), -142.0 ppm (F2); 3,5-difluoro-N-hydroxyaniline (F3/5) -114.0 ppm; 2,4,6-trifluoro-N-hydroxyaniline -114.3 ppm (F4), -124.8 ppm (F2/6); 2,3,4-trifluoro-N-hydroxyaniline -147.2 ppm (F3), -155.6 ppm (F1), -165.2 ppm (F2); 2,3,4,6-tetrafluoro-N-hydroxyaniline -131.6 ppm (F6), -140.1 ppm (F4), -148.1 ppm (F2) and -168.5 ppm (F3).

NMR measurements.

^{19}F-NMR measurements were performed on a Bruker AMX 300 NMR spectrometer essentially as described before by Vervoort *et al.* [1990]. The splitting patterns of the ^{1}H-NMR and ^{19}F-NMR resonances of the synthetised compounds were measured on a Bruker AMX 500 spectrometer. ^{19}F-NMR measurements were performed using a ^{1}H-probehead tuned to the ^{19}F-frequency (470.5 MHz). Upon freeze drying the synthetised compounds were dissolved in D_2O to give a final sample volume of 0.5 ml. Spectra were recorded using 60° pulses (6μs), a 10 kHz spectral width a repetition time of 1.9 s, quadrature phase detection and quadrature phase cycling (CYCLOPS). Chemical shift values are presented relative to $CFCl_3$ for ^{19}F-NMR and relative to TSP (sodium 3-trimethylsilyl-(2,2,3,3-$^{2}H_4$)-propionate)(Isotec, INC) for ^{1}H-NMR.

In vivo exposure of rats to fluoronitrobenzenes.

Male Wistar rats (body weight 300-325 g) with a permanent cannulation of the jugular vein in combination with a head attachment apparatus allowing easy connection of cannulae for blood sampling were used. The animals were placed in metabolism cages and allowed free access to food and tapwater. Groups of rats (N=3) were orally dosed with olive oil (controls) or 0.5 mmol of the desired fluoronitrobenzene per kg body weight in olive oil administered by oral gavage. The urine was collected for a period of 24 h prior to dosing and at times of 24 and 48 hr after dosing. The collected urine samples were stored at -20°C prior to analysis. Blood samples (approximately 250 μl) of the cannulated rats were collected by cannules into heparinized tubes 3 days before dosing (t=0) and at 1, 2, 4, 8, 24 and 48 h after dosing for the determination of methemoglobin content.

Determination of methemoglobinemia.

Methemoglobin content was determined by the method of Harrison and Jollow [1987]. All samples were immediately analysed after collection in order to prevent decomposition of the unstable methemoglobin.

Enzyme hydrolysis of urine samples.

The urine samples of the fluoronitrobenzene exposed rats were subjected to analysis by ^{19}F-NMR before and after β-glucuronidase and/or arylsulphatase treatment essentially as described before [Cnubben *et al.*, 1992].

HPLC analysis of the non-fluorinated N-acetylcysteinyl-nitrobenzene metabolites in urine.

The presence of N-acetylcysteinyl-nitrobenzene metabolites in the urine of the 2- and 4-fluoronitrobenzene exposed rats were quantified and detected using a Kratos 400 HPLC system, with a LiChrosorb C8 column 10 RP (250 x 9.0 mm) (Chrompack, Middelburg, The Netherlands) equiped with a Waters^{TM} 996 photodiode array detector. This was done because the loss of the fluorine atom prevents detection of this metabolite by ^{19}F-NMR. After eluting for 1 min with 0.1% trifluoroacetic acid a linear gradient from 0-100% (v/v) methanol in 60 min was applied. The synthetised 2- or 4-(N-acetylcysteinyl)-nitrobenzene were used as the reference compounds for the identification of these metabolites excreted in the urine of resp. 2- and 4-fluoronitrobenzene exposed rats. The urinary metabolites eluting from the column at the same retention time as the respective reference compounds were collected, freeze-dried and resolved in D_2O. Their identity was confirmed by means of ^{1}H-NMR analysis as being respectively 2-(N-acetylcysteinyl)-nitrobenzene as the urinary metabolite of a 2-fluoronitrobenzene exposed rat and 4-(N-acetylcysteinyl)-nitrobenzene as the metabolite of a 4-fluoronitrobenzene exposed rat.

Quantitation of urinary fluoronitrobenzene derived metabolites.

Quantitation of fluoro-containing nitrobenzene derived metabolites, using ^{19}F-NMR, was performed by comparison of the integrals of the ^{19}F-NMR resonances of the metabolites to the integral of the ^{19}F-NMR resonance of 4-fluorobenzoic acid used as the internal standard.

Quantitation of the urinary non-fluorinated N-acetylcysteinyl-nitrobenzene metabolites was carried out on a Kratos 400 HPLC system equiped with a LiChrosorb C8 column (100 x 3.0 mm) (Chrompack, Middelburg, The Netherlands), eluted isocratically with 37% methanol/0.1% trifluoroacetic acid. Detection was performed at 370 nm and quantitation was done by integration of the peak areas and comparison to a calibration curve obtained with the synthetised 2- or 4-(N-acetylcysteinyl)-nitrobenzene. The concentration of the stock solution of the synthetised N-acetylcysteinyl-nitrobenzene was determined using ^{1}H-NMR by comparison of the integrals of the ^{1}H-NMR resonances to the integral of the ^{1}H-

NMR resonance of sodium 3-trimethylsilyl-(2,2,3,3-$^2H_4$)-propionate (Isotec, INC) used as the internal standard.

Incubations of fluoronitrobenzenes with GSH and BSA.

The chemical reaction of fluoronitrobenzene derivatives with reduced glutathione (GSH) or bovine serum albumine (BSA) was studied in incubations containing 0.1 M potassium phosphate pH 7.6, 3 mM fluoronitrobenzene derivative and 2 mM GSH (Sigma, St. Louis, MO, USA) or 10 mg BSA/ml (= 0.15 mM)(Boehringer Mannheim, FRG). The reaction was started by the addition of the fluoronitrobenzene and carried out at 37°C. At different time intervals, 1 ml samples were taken from the incubation mixture and frozen into liquid nitrogen. Fluoride anion elimination and/or fluoro-glutathionyl-nitrobenzene formation was monitored using ^{19}F-NMR. The rate of the chemical reaction between the fluoronitrobenzenes and GSH or BSA was calculated from the linear increase in time of fluoride anion and/or adduct content in the incubation mixture. Incubations without GSH or BSA served as the control. For 2-fluoronitrobenzene the chemical reaction with GSH was monitored by the decrease of GSH, since the ^{19}F-NMR resonance of the fluoride anion overlaps with the ^{19}F-NMR resonance of the substrate. In short, 200 µl samples were taken from the incubation mixture, mixed with 30 µl 33% trichloroacetic acid to stop the reaction and assayed for GSH content using Ellman's reagent (5,5' dithiobis-(2-nitrobenzoic acid))(Boehringer Mannheim, FRG). The rate of the chemical reaction between GSH and the 2-fluoronitrobenzene was calculated from the linear decrease in time of the GSH content. Incubations without 2-fluoronitrobenzene served as the control in order to correct for the oxidation of the GSH in time.

Incubations with a suspension of rat intestinal microflora.

A suspension of the intestinal microflora was prepared according to Levin and Dent [1982]. Anaerobic incubations were carried out at 37°C in 0.1 M potassium phosphate pH 7.6, containing 2% glucose. The reaction was started by the addition of fluoronitrobenzene dissolved in dimethylsulphoxide (up to 8 mM final concentration) and carried out at 37°C in a sealed reaction vessel upon four cycles of evacuating and filling with argon. At different time intervals, 2 ml samples were taken from the incubation mixture and immediately frozen into liquid nitrogen. Formation of reduced metabolites, e.g. corresponding N-hydroxyaniline and/or aniline-derivatives, was monitored using ^{19}F-NMR. Accumulation of the nitroso-derivative did not occur to a detectable level. Using increasing substrate concentrations, the V_{max} for reduction of fluoronitrobenzenes by the intestinal microflora was determined. To compare apparent V_{max} values for nitroreduction for all compounds, sommation of the amount of the fluorinated N-hydroxyaniline and aniline was performed as such or

in an electron-weighted manner, by taking into account that for reduction of nitrobenzene to nitrosobenzene, N-hydroxyaniline or aniline respectively two, four or six electrons are required.

Molecular orbital computer calculations.

Molecular orbital computer calculations were performed essentially as described before using a semi-empirical molecular orbital method, applying the AM1 Hamiltonian from the AMPAC program (Quantum Chemistry Program Exchange, no. 506, Indiana University, Bloomington, IN, USA) [Cnubben *et al.*, 1992]. The frontier orbital densities for electrophilic and nucleophilic atttack were calculated from respectively HOMO/HOMO-1 and LUMO/LUMO+1 characteristics of the fluoronitrobenzene-derivatives as indicated by Fukui *et al.* [1954].

RESULTS.

Fluoronitrobenzene induced methemoglobinemia in male Wistar.

Male Wistar rats were orally dosed with different fluoronitrobenzenes and blood was sampled for determination of methemoglobin content at several time intervals for 48 hours. Table 2 shows the relative amounts of methemoglobin observed at various times after exposure to the fluoronitrobenzenes. These results demonstrate that fluorobenzenes without a fluorine at the C2, C4 or C6 position, like 3-fluoronitrobenzene and 3,5-difluoronitrobenzene, possess the highest capacity for inducing methemoglobinemia. For the various fluoronitrobenzenes containing a fluorine at the C2, C4 and/or C6 position, a decrease in the potency to induce methemoglobinemia was generally observed with an increase in the number of fluorine substituents.

Rate of nitro-reduction of the nitrobenzenes by cecal microflora and liver preparations.

Reduction of unsubstituted nitrobenzene is generally accepted to proceed predominantly by the microflora of the intestine [Reddy *et al.*, 1976]. For a series of monochloronitrobenzenes, it was demonstrated that hepatocytes of rat liver are also able to take part in the reduction [Rickert and Held, 1990]. In vitro, the reduction of the fluoronitrobenzenes was studied using a suspension of rat cecal microflora and rat liver preparations. This was done in order to elucidate whether the observed differences in methemoglobin formation with changes in the fluorine substituent pattern originate from a possible influence of the substituent pattern on chances for reduction of the nitro moieties to methemoglobin-inducing intermediates.

Table 2: Formation of methemoglobinemia by fluoronitrobenzene-derivatives in male Wistar rats (N=2-3). Rats were orally dosed with 0.5 mmol fluoronitrobenzene per kilogram bodyweight.

nitrobenzene	**% methemoglobinemia at time (h)***					
	1	**2**	**4**	**8**	**24**	**48**
2-fluoro-	28 ± 4	29 ± 1	22 ± 3	25 ± 3	13 ± 5	6 ± 3
3-fluoro-	37 ± 9	43 ± 9	34 ± 6	36 ± 3	19 ± 2	14 ± 5
4-fluoro-	< 2	5 ± 3	10 ± 2	7 ± 5	8 ± 5	< 2
2,5-difluoro-	16 ± 2	20 ± 5	10 ± 2	15 ± 3	3 ± 1	3 ± 1
3,5-difluoro-	51 ± 5	56 ± 6	45 ± 5	41 ± 4	45 ± 6	9 ± 4
2,4-difluoro-	6 ± 3	4 ± 4	3 ± 3	< 2	5 ± 3	< 2
2,4,6-trifluoro-	< 2	4 ± 2	2 ± 1	< 2	< 2	< 2
2,3,4-trifluoro-	2 ± 2	5 ± 2	< 2	< 2	< 2	< 2
2,3,4,6-tetrafluoro-	2 ± 2	2 ± 2	< 2	< 2	< 2	< 2

* Before dosing (t=0) methemoglobin content was determined to be < 2% in all cases.

Table 3 presents the V_{max} and K_m values for the reduction of the fluoronitrobenzenes to their corresponding N-hydroxyaniline and aniline-analogs as determined using ^{19}F-NMR analysis of the incubations of a rat cecal microflora suspension with the different fluoronitrobenzenes. The incubation times were chosen in such a way that the reaction was linear over the whole time period. Thus, incubation times for the mono-, di-, tri- and tetrafluoronitrobenzenes were respectively resp. 240, 120, 60 and 30 minutes. Generally, a shift from N-hydroxyaniline to aniline was observed upon increasing incubation time. Such a shift in the pattern of metabolites resulting from nitro-reduction in time was reported before for the nitroreduction of nitrobenzene [Levin and Dent, 1982]. Sommation of the amount of the fluorinated N-hydroxyaniline and aniline, either as such or in an electron-weighted manner (see methods), makes it possible to compare apparent V_{max} values for nitroreduction for all compounds (Table 3). From the data thus obtained, it can be concluded that the rates of reduction do not vary to a large extent i.e. at most two-fold. Furthermore, the K_m value for reduction of the fluoronitrobenzenes generally decreases upon increasing number of fluorine substituents (Table 3). Because V_{max} hardly varies and K_m decreases with increasing number of fluorine substituents, these observations indicate that other factors than the relative reducibility of the fluoronitrobenzene must be contributing to the observed differences in induction of methemoglobinemia by these derivatives.

Table 3: Nitroreduction of fluoronitrobenzenes to their N-hydroxyaniline (N-OH) and aniline (NH_2) derivatives by extract of rat cecal microflora under anaerobic conditions (N=2).

nitrobenzene	NH_2	N-OH	Σ	Σ	NH_2	N-OH
	V_{max}^{app} in nmol • ml cecal microflora suspension^{-1} • hour $^{-1}$		sommation reduced metabolites	electron weighted sommation	K_m^{app} in mM	
2-fluoro-	180.1 ± 15.8	89.7 ± 50.5	269.8 ± 66.3	1439 ± 297	0.6 ± 0.1	1.7 ± 0.6
3-fluoro-	228.5 ± 8.0	131.0 ± 3.6	359.5 ± 11.6	1895 ± 62	1.1 ± 0.1	1.3 ± 0.2
4-fluoro-	212.1 ± 14.5	6.3 ± 3.6	218.4 ± 18.1	1298 ± 101	0.8 ± 0.1	1.7 ± 0.0
2,5-difluoro-	210.3 ± 0.4	364.0 ± 43.6	574.3 ± 44.0	2718 ± 177	0.6 ± 0.1	3.9 ± 2.5
3,5-difluoro-	222.2 ± 34.7	243.8 ± 16.6	466.0 ± 51.3	2308 ± 275	0.4 ± 0.1	3.1 ± 0.3
2,4-difluoro-	171.0 ± 11.0	197.6 ± 117.0	368.6 ± 128.0	1816 ± 534	0.3 ± 0.1	1.6 ± 0.0
2,4,6-trifluoro-	87.0 ± 7.5	421.5 ± 78.3	508.5 ± 85.8	2208 ± 358	0.2 ± 0.0	1.4 ± 0.7
2,3,4-trifluoro-	118.1 ± 2.7	179.0 ± 62.5	297.1± 65.2	1425 ± 266	0.1 ± 0.0	0.6 ± 0.2
2,3,4,6-tetrafluoro-	123.3 ± 26.7	408.7 ± 116.4	532.0 ± 143.1	2375 ± 626	0.1 ± 0.0	0.6 ± 0.1

Table 4: Metabolite pattern of the fluoronitrobenzene-derivatives in arylsulphatase/β-glucuronidase treated 24 h urine samples of male Wistar rats as derived from ^{19}F-NMR analysis (N=2-3 rats).

NO_2-benzene	metabolite	chemical shifts in ppm	% of total fluoro-containing metabolites
2-F-	3-F-4-nitrophenol	-117.9	21.6 ± 1.0
	fluoride anion	-123.0	46.5 ± 1.7
	3-F-4-acetamidophenol	-125.7	7.2 ± 1.4
	3-F-4-aminophenol	-134.9	11.5 ± 0.4
	3-F-2-aminophenol	-136.9	0.5 ± 0.2
	2-F-aniline	-138.3	0.7 ± 0.1
	2-F-3-nitrophenol	-148.9	6.0 ± 0.6
	Σ unidentified metabolites		6.0 ± 0.7
3-F-	5-F-3-nitrophenol	-114.0	3.0 ± 1.0
	3-F-aniline	-117.5	4.7 ± 0.4
	fluoride anion	-123.0	5.7 ± 0.1
	4-F-2-aminophenol	-127.5	3.6 ± 0.7
	2-F-4-acetamidophenol	-139.7	17.2 ± 4.0
	2-F-4-nitrophenol	-140.5	63.2 ± 5.4
	Σ unidentified metabolites		2.8 ± 0.9
4-F-	5-F-2-acetamidophenol	-117.6	17.3 ± 1.4
	fluoride anion	-123.0	49.7 ± 1.3
	5-F-2-aminophenol	-127.5	4.2 ± 1.4
	2-F-5-nitrophenol	-130.1	25.1 ± 2.4
	Σ unidentified metabolites		3.7 ± 1.5
2,4-diF-	4-F-2-(N-acetylcysteinyl)nitrobenzene	-106.7	18.5 ± 2.6
	2-F-4-(N-acetylcysteinyl)nitrobenzene	-121.5	1.1 ± 0.2
	fluoride anion	-123.0	62.9 ± 2.8
	3-F-4-acetamidophenol	-125.7	0.8 ± 0.3
	3-F-4-aminophenol	-134.9	1.0 ± 0.0
	Σ unidentified metabolites		15.7 ± 1.0
3,5-diF-	3,5-diF-nitrobenzene	-110.7	1.2 ± 0.2
	3,5-diF-aniline	-115.2	8.7 ± 0.4
	fluoride anion	-123.0	5.6 ± 0.8
	4,6-diF-2-aminophenol	-125.3/-137.8	8.9 ± 1.6
	2,6-diF-4-acetamidophenol	-137.5	7.4 ± 2.7
	2,6-diF-4-aminophenol	-137.8	27.8 ± 2.0
	2,6-diF-4-nitrophenol	-139.1	20.3 ± 0.8
	Σ unidentified metabolites		20.1 ± 2.7
2,5-diF-	5-F-2-(N-acetylcysteinyl)nitrobenzene	-119.1	19.1 ± 4.5
	2,5-diF-4-nitrophenol	-121.7/-145.0	36.7 ± 9.6
	fluoride anion	-123.0	26.0 ± 5.5
	2,5-diF-4-acetamidophenol	-131.8/-145.3	5.0 ± 0.4
	2,5-diF-4-aminophenol	-141.2/-145.9	7.1 ± 1.8
	Σ unidentified metabolites		6.1 ± 2.5

2,3,4-triF-	fluoride anion	-123.0	60.0 ± 0.4
	3,4-diF-2-(N-acetylcysteinyl)-nitrobenzene	-129.2/-131.2	12.9 ± 2.2
	3,4,5-triF-2-acetamidophenol	-153.6/ -158.7/-176.9	8.6 ± 4.3
	2,3-diF-4-aminophenol	-160.5/-165.3	1.9 ± 0.9
	Σ unidentified metabolites		16.6 ± 3.3
2,4,6-triF-	4,6-diF-2-(N-acetylcysteinyl)-nitrobenzene	-105.5/-119.5	2.2 ± 0.1
	2,6-diF-4-(N-acetylcysteinyl)-nitrobenzene	-122.1	0.1 ± 0.1
	fluoride anion	-123.0	72.6 ± 4.6
	3,5-diF-4-acetamidophenol	-123.6	7.9 ± 1.9
	3,5-diF-4-aminophenol	-133.7	4.5 ± 1.3
	Σ unidentified metabolites		12.7 ± 2.4
2,3,4,6-tetraF	fluoride anion	-123.0	67.6 ± 1.2
	3,4,6-triF-2-(N-acetylcysteinyl)-nitrobenzene	-126.8/-129.5 / -134.7	6.1 ± 3.3
	Σ unidentified metabolites		26.3 ± 2.2

Since preparations of rat liver also have been demonstrated to contribute to the reduction of halogenated nitrobenzenes [Rickert and Held, 1990], microsomes of rat liver were incubated with 2-fluoro-, 3-fluoro-, 4-fluoro- and 2,5-difluoronitrobenzene. The rates were determined to be respectively 8.3, 11.1, 11.1, and 9.5 nmol fluorinated N-hydroxyaniline and aniline per mg protein per 10 minutes. Thus, also for the aerobic incubations with liver preparations no differences were observed for the relative rate of reduction of the fluoronitrobenzenes that could explain the differences in induction of methemoglobinemia. This again indicates that other factors than the relative reducibility of the fluoronitrobenzene by rat liver microsomes must be contributing to the observed differences in induction of methemoglobinemia by these derivatives.

The in vivo metabolic pathways of the fluoronitrobenzenes.

In order to investigate whether differences in metabolic pathways can account for the observed differences in induction of methemoglobinemia by the various fluoronitrobenzenes, the in vivo biotransformation of the fluoronitrobenzenes was elucidated. The ^{19}F-NMR resonances of the metabolites in the urines of the various fluoronitrobenzene exposed rats were identified by comparison to (synthetised) reference compounds. Enzyme hydrolysis of the urine with β-glucuronidase and/or arylsulphatase identifies the resonances of the sulphated or glucuronidated metabolites in a similar way as described before [Cnubben *et al.*, 1992; Rietjens *et al.*, 1995]. Table 4 summarizes the ^{19}F-NMR resonances of the urinary metabolites and the quantitative data of the in vivo biotransformation patterns of the fluoronitrobenzenes as derived from the ^{19}F-NMR spectra. These data demonstrate

Table 5: Relative contribution of nitro reduction (NH_2), glutathione conjugation (GSH), fluoride anion formation and aromatic hydroxylation (NO_2-OH) to the *in vivo* biotransformation of a series of fluoronitrobenzenes in male Wistar rats (n=2-3).

nitrobenzene	**% of metabolites as total ^{19}F intensity in urine**					
	nitro reduction	**glutathione conjugation**	**fluoride anion**	**aromatic hydroxylation**	**unknown**	**recovery in 48 hrs**
2-fluoro-	19.9	#	46.5	27.6	6.0	68.0
3-fluoro-	25.5	0	5.7	66.2	2.6	63.2
4-fluoro-	21.5	#	49.7	25.1	3.7	60.9
2,5-difluoro-	12.1	19.1	26.0	36.7	6.1	69.6
3,5-difluoro-	54.0	0	5.6	20.3	20.1	91.6
2,4-difluoro-	1.8	19.6	62.9	0	15.7	50.9
2,4,6-trifluoro-	12.4	2.3	72.6	0	12.7	42.5
2,3,4-trifluoro-	10.5	12.9	60.0	0	16.6	43.4
2,3,4,6-tetrafluoro-	0	6.1	67.6	0	26.3	22.6

The N-acetylcysteinyl conjugates of 2- and 4-fluoronitrobenzene are ^{19}F-NMR invisible, since the fluorine is eliminated from the nitrobenzene upon glutathione conjugation. Quantification of these conjugates was, therefore, performed by HPLC and amount to respectively 54.6% and 60.7%.

-as expected- a main contribution of three different biotransformation pathways for the fluoronitrobenzenes, i.e. aromatic hydroxylation, nitroreduction to the amino derivatives and glutathione conjugation. In addition, fluoride anion elimination is observed. The relative contribution of these different metabolic routes to the urinary metabolite pattern as derived from analysis of urine samples by ^{19}F-NMR and HPLC (see hereafter), is presented in Table 5 and appears to vary with the substituent pattern of the fluoronitrobenzene derivatives. Focussing on the position of the fluorine substituents, the results presented in Table 5 demonstrate that fluoronitrobenzenes with a fluoro-substituent at the C2 and/or C4 position are predominantly metabolised through glutathione conjugation leading to replacement of the halogen by glutathione and excretion of (fluorinated) 2- or 4-(N-acetylcysteinyl) nitrobenzenes. No formation of N-acetylcysteinyl metabolites resulting from a replacement of a fluorine at the C3 or C5 position of a nitrobenzene was observed. Comparison of the excreted amount of fluoride anion to the amount of metabolites resulting from glutathione-conjugation, demonstrates that the fluoride

anion formation is higher and only partially accounts for the formation of the glutathione-derived nitrobenzene metabolites. When the number of fluorine substituents is taken into account, the relative contribution of fluoride anions to the overall metabolic patterns increases with increasing number of fluoro-substituents at C2, C4 and/or C6 positions in the nitrobenzene-derivative. Furthermore, it is observed that increased possibilities for glutathione conjugation and/or fluoride anion formation, are accompanied by decreased relative contributions of the aromatic hydroxylation and/or nitroreduction pathway to the overall metabolite pattern of the fluoronitrobenzenes.

Determination of 2- and 4-(N-acetylcysteinyl)-nitrobenzene in urine by HPLC analysis.

The N-acetylcysteinyl adducts of 2-fluoro- and 4-fluoronitrobenzene no longer contain the fluorine substituent which eliminates the possibility for their quantification by ^{19}F-NMR. Therefore, urine samples of the 2-fluoro- and 4-fluoronitrobenzene exposed rats were analysed by HPLC in order to detect 2- and 4-(N-acetylcysteinyl)-nitrobenzene. From the elution profiles it appears that the 2- and 4-fluoronitrobenzene exposed rats indeed excrete respectively 2- or 4-(N-acetylcysteinyl)-nitrobenzene (HPLC-patterns not shown). These metabolites were quantified using HPLC in combination with ^{1}H-NMR (see material and methods for details). The amounts of 2- and 4-(N-acetylcysteinyl)-nitrobenzene detected in the urine are respectively 54.6% and 60.7% of the total amount of metabolites in the urine of 2- and 4-fluoronitrobenzene dosed animals. These amounts are slightly higher than those of fluoride anions excreted, which are determined to be 46.5% and 49.7% of the total amount of metabolites in the urine of 2- and 4-fluoronitrobenzene dosed rats. The small discrepancy between the excreted amounts of fluoride anions and the N-acetylcysteinyl conjugates might be due to the fact that fluoride anions are not fully excreted from the body.

Chemical reactivity of fluoronitrobenzenes with reduced glutathione and with bovine serum albumine.

As outlined above, the results of the metabolic patterns presented in Table 4 and 5 demonstrate that the amount of fluoride anions, resulting from the elimination upon glutathione adduct formation, almost equals the amount of N-acetylcysteinyl nitrobenzenes in the urine of 2-fluoronitrobenzene, 4-fluoronitrobenzene and 2,5-difluoronitrobenzene exposed rats. However, for 2,4-difluoronitrobenzene, 2,3,4-trifluorobenzene, 2,4,6-trifluoronitrobenzene and 2,3,4,6-tetrafluoronitrobenzene the fluoride anion resonance becomes the major metabolite signal in the ^{19}F-NMR urine spectra, while the amounts of excreted fluorinated N-acetylcysteinyl conjugates is

Table 6: The regioselectivity for the in vivo and in vitro (spontaneous and enzymatic) GSH conjugation of the fluorinated nitrobenzenes and the reaction rates for the conjugation of these nitrobenzenes with GSH and BSA as determined by ^{19}F-NMR. The reaction rate was monitored by elimination of fluoride anions from these nitrobenzene-derivatives (3 mM) upon their reaction with reduced glutathione (2 mM) and bovine serum albumine (10 mg/ml). The structural characteristics of the fluorinated glutathionyl-fluoronitrobenzenes for identification are presented in Table 1.

nitrobenzene		**regioselectivity**			**reaction rates in μM.min^{-1} for conjugation with**	
	reaction centre	**in vivo**	**in vitro chemical***	**in vitro enzymatic***	**GSH**	**BSA**
2-fluoro-	C1:C2	0:100	0:100	0:100	2.6 ± 0.6**	n.d.***
3-fluoro-	C1:C3	0:0	0:0	n.d.	0.0 ± 0.0	0.0 ± 0.0
4-fluoro	C1:C4	0:100	0:100	0:100	1.6 ± 0.4	0.2 ± 0.0
2,4-difluoro-	C1:C2:C4	0:94:6	0:91:9	0:63:37	14.1 ± 2.0	2.7 ± 0.3
2,5-difluoro-	C1:C2:C5	0:100:0	0:100:0	n.d.	2.7 ± 0.3	0.5 ± 0.1
3,5-difluoro-	C1:C3:C5	0:0:0	0:0:0	n.d.	0.0 ± 0.0	0.0 ± 0.0
2,4,6-trifluoro-	C1:C2/6:C4	0:96:4	0:97:3	0:78:22	219.3 ± 32.5	18.1 ± 2.7
2,3,4-trifluoro-	C1:C2:C3:C4	0:100:0:0	0:100:0:0	n.d.	204.5 ± 20.1	18.3 ± 3.1
2,3,4,6-tetrafluoro-	C1:C2:C3:C4:C6	0:100:0:0:0	0:96:0:4:0	0:70:0:30:0	2240 ± 255	553 ± 59

* data obtained from literature [Rietjens *et al.*, 1995]

** rate of reaction was determined by the decrease of GSH. GSH was assayed using Ellman's reagens as described in the material and method section.

*** n.d. means not determined, since the ^{19}F-NMR resonance of 2-fluoronitrobenzene overlaps the ^{19}F-NMR resonance of fluoride anion.

considerably lower. Furthermore, the total 48 hours recovery of the fluoronitrobenzenes strongly decreases with increasing number of fluoro-substituents (Table 5). Together, these observations point at formation of fluoronitrobenzene adducts, resulting in fluoride anion formation and metabolites which are withheld in the body.

To investigate the above-mentioned hypothesis, the reactivity of the various fluoronitrobenzenes in a spontaneous (non-enzymatic) nucleophilic substitution reaction with GSH and also with a model protein (bovine serum albumin) was studied. A nucleophilic substitution of a fluorine substituent in a fluoronitrobenzene by a cellular macromolecule will lead to formation of a covalent macromolecular-nitrobenzene adduct accompanied by the elimination of a fluoride anion. Table 6 presents the reaction rates for the chemical reaction between the various fluoronitrobenzene derivatives with GSH or with BSA. The results demonstrate that C2, C4 and/or C6 fluorinated carbon centres of the fluoronitrobenzenes are sensitive towards a spontaneous attack by nucleophiles like GSH and BSA. In case of GSH the molecular weight of the resulting adduct is low enough to detect this product by ^{19}F-NMR and, thus, the regioselectivity of the GSH conjugation with fluoronitrobenzenes could be determined. A strong preference for glutathione conjugation at a fluorinated C2 position over a fluorinated C4 position is observed. The regioselectivity for the spontaneous conjugation of GSH with the various fluoronitrobenzenes resembles the regioselectivity for the in vivo formation of the fluorinated N-acetylcysteinyl nitrobenzenes (Table 2). The results in Table 6 additionally demonstrate that the reactivity of the fluoronitrobenzenes with nucleophilic entities as GSH and BSA increases remarkably with increasing number of fluoro-substituents.

Molecular orbital calculations.

The electronic substrate characteristics of the nitrobenzene derivatives were calculated in order to investigate whether the observed differences in biotransformation pathways, methemoglobin formation as well as the almost similar rate of their in vitro nitroreduction could be explained by electronic characteristics of the fluoronitrobenzenes.

Table 7 presents the AM1 calculated values for the energy level of the frontier orbital of importance for a nucleophilic attack on the fluoronitrobenzenes, i.e. the energy of the lowest unoccupied molecular orbital (E(LUMO)). A decrease in E(LUMO) with increasing number of electron withdrawing substituents at the aromatic ring is observed and can be expected to lead to a more efficient interaction with a nucleophile.

Table 7: Frontier density distributions and energy levels of fluoronitrobenzenes for nucleophilic (GSH/BSA) reactions as calculated with the AM1 Hamiltonian. The LUMO/LUMO+1 density distributions were calculated as described by Fukui *et al.* [1954] and represent the contribution of two orbitals, resulting in a total density distribution of 2.0.

Compound	E_{LUMO} in eV	C1	C2	C3	C4	C5	C6	rest of molecule
		distribution of LUMO/LUMO+1						
2-F	-1.30	0.35	0.33	0.10	0.42	0.11	0.26	0.43
3-F	-1.34	0.36	0.27	0.12	0.41	0.12	0.27	0.45
4-F	-1.35	0.34	0.26	0.11	0.47	0.11	0.26	0.45
2,5-diF	-1.57	0.36	0.33	0.11	0.41	0.14	0.25	0.40
3,5-diF	-1.60	0.38	0.26	0.14	0.40	0.14	0.26	0.42
2,4-diF	-1.58	0.34	0.32	0.10	0.47	0.12	0.25	0.40
2,4,6-triF	-1.81	0.33	0.30	0.12	0.47	0.12	0.30	0.36
2,3,4-triF	-1.85	0.35	0.31	0.13	0.46	0.13	0.24	0.38
2,3,4,6-tetraF	-2.07	0.34	0.30	0.14	0.46	0.13	0.29	0.34

In Figure 1 the logarithm of the reaction rate for the spontaneous reaction of fluoronitrobenzenes with the nucleophiles GSH and BSA is plotted against the calculated E(LUMO). Clear correlations (resp. r=0.97 and r=0.98) are obtained. Fluoronitrobenzenes with C3 and/or C5 fluorinated centres were not taken into account, because the low density of the LUMO at these carbon centres (Table 7) prevents efficient reaction and explains why C3 and/or C5 fluorinated sites in the nitrobenzenes do not become conjugated. The logarithm of the rate of reduction by the intestinal microflora (Table 3) does not correlate with the E(LUMO) (r=0.57 or r=0.43, for respectively the plain sommation and the electron weighted sommation of fluorinated N-hydroxyaniline and aniline).

The regioselectivity for the cytochrome P450 catalyzed hydroxylation of various aromatic compounds has been demonstrated to be directed and even predicted by the calculated reactivity of the carbon centres for an electrophilic attack by the high-valent-iron-oxo intermediate of cytochromes P450. Aromatic hydroxylation of fluoronitrobenzene derivatives was recently demonstrated to be mediated by

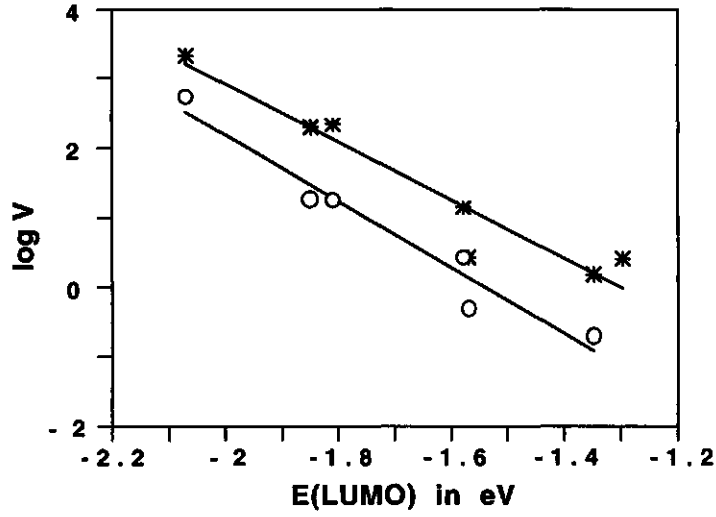

Figure 1: Molecular orbital based quantitative structure activity relationship for the spontaneous conjugation of a series of fluoronitrobenzenes with the nucleophilic entities glutathione (*) and bovine serum albumine (O). Correlation coefficients were respectively r = 0.97 and r = 0.98. The chemical reactions are dependent on the concentrations of both substrates and were carried out at fixed concentrations of fluoronitrobenzenes (3 mM) and glutathione (2 mM) or BSA (0.15 mM). For both reactions V is in μM of fluoride anion formed per minute.

cytochromes P450 [Rietjens *et al.*, 1995]. Table 8 presents the regioselectivity for the cytochrome P450 mediated aromatic hydroxylation of the fluoronitrobenzenes of the present study compared to calculated reactivity parameters for electrophilic or nucleophilic attack on those fluoronitrobenzenes. Only nitrobenzenes for which nitrophenol derived metabolites were actually detected in the urine of the exposed rats are taken into account. The results show that aromatic hydroxylation predominantly occurs at the non-fluorinated C4 position, whereas hydroxylation at the C3 position occurs to a much smaller extent and C2/C6-hydroxylation is not observed at all. The regioselectivity for aromatic hydroxylation of the fluoronitrobenzenes does not correspond with the position of the frontier orbital density for electrophilic attack on the nitrobenzenes e.g. HOMO/HOMO-1, which is predominantly located on the C2 and C3 carbon centres, whereas the hydroxylation occurs mainly at C4. Surprisingly, the frontier orbital density for a nucleophilic attack on the nitrobenzenes, calculated from their LUMO/LUMO+1, is

predominantly located at the hydroxylated C4 carbon centres of the fluoronitrobenzene and to a much smaller extent at C3 (Table 7). The C2 and C6 positions with reasonable reactivity for either an electrophilic or nucleophilic attack, become never hydroxylated, apparently due to factors other than their intrinsic reactivity.

Table 8: Regioselectivities for the in vivo aromatic hydroxylation of fluoronitrobenzene derivatives as determined by ^{19}F-NMR urinalysis compared to calculated frontier orbital characteristics.

nitro-benzene derivative	aromatic hydroxylation at carbon centres C2 : C3 : C4 : C5 : C6	LUMO/LUMO+1 frontier orbital densities at carbon centres C2 : C3 : C4 : C5 : C6	HOMO/HOMO-1 frontier orbital densities at carbon centres C2 : C3 : C4 : C5 : C6
2-F-	0.00 : 0.22 : 0.78 : 0.00 : 0.00	0.33 : 0.10 : 0.42 : 0.11 : 0.26	0.41 : 0.32 : 0.12 : 0.51 : 0.23
3-F-	0.00 : 0.00 : 0.95 : 0.05 : 0.00	0.27 : 0.12 : 0.41 : 0.12 : 0.27	0.31 : 0.47 : 0.21 : 0.19 : 0.46
4-F-	0.00 : 0.50 : 0.00 : 0.50 : 0.00	0.26 : 0.11 : 0.47 : 0.11 : 0.26	0.17 : 0.30 : 0.39 : 0.30 : 0.17
2,5-diF-	0.00 : 0.00 : 1.00 : 0.00 : 0.00	0.33 : 0.11 : 0.41 : 0.14 : 0.25	0.43 : 0.20 : 0.12 : 0.49 : 0.24
3,5-diF-	0.00 : 0.00 : 1.00 : 0.00 : 0.00	0.26 : 0.14 : 0.40 : 0.14 : 0.26	0.44 : 0.31 : 0.13 : 0.31 : 0.44

DISCUSSION.

In this study, possible relationships between various biotransformation pathways and the methemoglobin inducing capacity of a series of fluoronitrobenzene were investigated. Induction of methemoglobinemia by fluoronitrobenzenes was observed to decrease with increasing number of fluorine substituents, especially when these fluoro-substituents are positioned at the carbon centres C2, C4 and/or C6, calculated to be most reactive for a nucleophilic attack.

The primary reduction of nitrobenzene-derivatives to nitrosobenzenes and N-hydroxyarylamines is the crucial step for the methemoglobin inducing activity of this class of compounds [for review, see Kiese, 1974; Suzuki *et al.*, 1989] as schematically presented in Figure 2. This reductive metabolism of unsubstituted nitrobenzene to the reactive methemoglobin inducing species is predominantly accomplished by the bacterial nitroreductases present in the intestinal environment [Levin and Dent, 1982]. Besides, for a series of monochloronitrobenzenes, it was demonstrated that hepatocytes of rat liver are able to reduce these halogenated nitrobenzenes to their corresponding aniline-derivatives under aerobic conditions [Rickert and Held, 1990]. In vitro experiments with a suspension of rat cecal

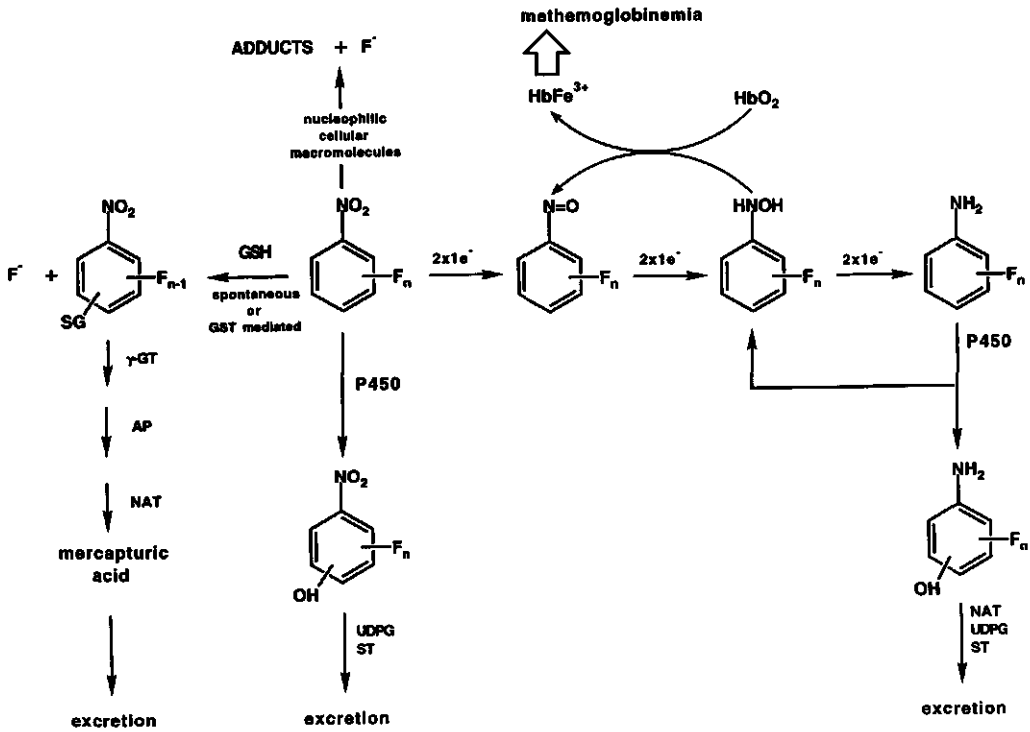

Figure 2: Schematic representation of the metabolic fate of fluorinated nitrobenzenes. GST: glutathione S-transferase, γGT: γ-glutamyl transpeptidase, AP: aminopeptidase M and cysteinylglycine dipeptidase, UDPG: UDP-glucuronyltransferase, ST: sulphotransferase, NAT: N-acetyltransferase.

microflora or with a preparation of rat liver demonstrate that the rate of reduction of the various fluoronitrobenzenes varies only slightly, and not in a way that can account for the differences in extent of methemoglobin formation. Apparently, the induction of methemoglobinemia by the various fluoronitrobenzenes is not predominantly determined by their intrinsic capacity to enter the nitro reduction pathway. The different methemoglobinemic capacity must rather result from differences in the inherent direct methemoglobinemic capacity and/or reactivity of the various toxic metabolites, and/or from the fact that the halogen substituent pattern influences the electrophilic reactivity, thereby changing the possibilities for reactions with glutathione and, especially, other cellular nucleophiles.

In vivo metabolite patterns of the fluoronitrobenzenes, derived from the urinary ^{19}F-NMR metabolite profiles of the fluoronitrobenzene exposed rats provided support for the latter explanation. The metabolite patterns indicate that the differences in the extent of methemoglobin induction with changing fluorine substituent patterns in the nitrobenzenes is more likely to be related to the presence of competing reaction pathways. Excretion of mercapturic acids, increased fluoride anion elimination and reduced recoveries with increasing number of fluorine substituents were observed, pointing at reactions of the fluoronitrobenzenes with GSH and/or other cellular nucleophiles (as could be jugded from the yellow colour of the intestinal tract (unpublished)). A reaction with GSH and/or cellular macromolecules is a factor that prevents the fluoronitrobenzenes to become reduced by and/or, as a consequence, reduces their chances to induce methemoglobinemia. Additional in vitro studies demonstrated QSAR's for these conjugation pathways relating the natural logarithm of the rates of conjugation of fluoronitrobenzenes with GSH as well as BSA to a calculated parameter representative for the electrophilicity of the nitrobenzenes *i.e.* the energy of their lowest unoccupied molecular orbital (E(LUMO)). The correlation coefficients obtained were respectively r=0.97 and r=0.98. Conjugation with GSH at a halogenated C3 or C5 centre is not observed, which can be ascribed to a low reactivity for a nucleophilic attack at these positions reflected by the relatively low calculated LUMO/LUMO+1 frontier orbital densities. Thus, depending on the position and number of fluorine substituents the reactivity of the fluoronitrobenzenes for nucleophilic attack by either glutathione or cellular macromolecules is influenced, and this results in more or less efficient alternatives for the nitro reduction pathway that gives rise to methemoglobin inducing metabolites.

The exception to this general consideration might be the results obtained for 2- and 4-fluoronitrobenzene. The amounts of reduced metabolites and mercapturic acids in urine (Table 5), as well as the rate of conjugation with GSH and BSA (Table 6), were almost similar for 2- and 4-fluoronitrobenzene, 2-fluoronitrobenzene appeared to be a more potent inducer of methemoglobinemia compared to 4-fluoronitrobenzene (Table 2). An explanation for this observation might be that the nitroso- and N-hydroxy-metabolites of 4-fluoronitrobenzene are relatively more efficiently reduced to their aniline-analogs compared to 2-fluoronitrobenzene as demonstrated in Table 3. Thus, besides the presence of competing reaction pathways with GSH and/or cellular macromolecules, the extent and rate of complete nitroreduction also seems to be involved in the in vivo regeneration of methemoglobinemia inducing metabolites of fluoronitrobenzenes. Furthermore, additional factors that might contribute to these observed differences might originate from possible differences in the inherent direct methemoglobinemic capacity of the

N-hydroxy and nitroso metabolites and/or differences in the stability of the N-hydroxylamine/nitroso redox pair in the erythrocyt. Conclusive evidence on the involvement of these factors, however, are not provided yet and these interesting considerations may serve as a basis for future research.

Finally, the metabolic profiles obtained for the various fluoronitrobenzenes in the present study demonstrated that the extent of cytochrome P450 mediated aromatic hydroxylation of the fluoronitrobenzenes did not vary significantly with the substituent patterns. A recent study on the biotransformation of 2,5-difluoronitrobenzene clearly demonstrated that cytochrome P450 is the enzyme-system responsible for the aromatic hydroxylation of this derivative [Rietjens *et al.*, 1995]. This cytochrome P450 mediated aromatic hydroxylation is generally regarded as a detoxification route, due to the efficient conjugation of nitro- and aminophenols with sulphate or glucuronyl moieties and their subsequent elimination from the body (Figure 2). For the aniline metabolites of the present study their (non)preferential site of hydroxylation can qualitatively be explained on the basis of the calculated reactivity of the carbon centres for an electrophilic attack by the activated cytochrome P450 high-valent-iron-oxo intermediate (data not shown), similar to what was previously reported for other aromatic compounds [Cnubben *et al.*, 1992; Rietjens *et al.*, 1993]. For the nitrobenzenes, however, the preferential site for hydroxylation is more related to the frontier orbital density distribution for a nucleophilic attack. It may be hypothesized that the aromatic hydroxylation of substrates with a relatively high electrophilicity proceeds not by an electrophilic attack of the high-valent-iron-oxo species of the cytochromes P450, but by a nucleophilic attack of another intermediate in the catalytic cytochrome P450 cycle, for instance the nucleophilic cytochrome Fe^{3+}-O-O^{-} intermediate. The Fe^{3+}-O-O^{-} intermediate might react with the substrate instead of decomposing to the usual $(FeO)^{3+}$ intermediate, in a way as is proposed for the cleavage of C-C bonds during oestrogen biosynthesis [Akhtar and Wright, 1991; Ortiz de Montellano 1985]. The high electrophilic reactivity of the nitrobenzenes may support the preferential occurence of such a nucleophilic attack by the Fe^{3+}-O-O^{-} intermediate over a pathway proceeding by an attack of the electrophilic $(FeO)^{3+}$ intermediate.

REFERENCES.

Akhtar M., and Wright J.N. (1991). A unified mechanistic view of oxidative reactions catalyzed by P-450 and related Fe-containing enzymes. *Nat. Prod. Rep.* **8**, 527-551.

Beauchamp R.O., Irons R.D., Rickert D.E., Couch D.B., and Hamm T.E. (1982). A critical review of the literature on nitrobenzene toxicity. *CRC Critical Reviews in Toxicology* **11**, 33-84.

Cesarone C.F., Bolognesi C., and Santi L. (1983). DNA damage induced in vivo in various tissues by nitrochlorobenzene derivatives. *Mutation Research* **116**, 239-246.

Cnubben N.H.P., Peelen S., Borst J.W., Vervoort J., and Rietjens I.M.C.M. (1994). Molecular orbital based quantitative structure activity relationship for the cytochrome P450-catalyzed 4-hydroxylation of halogenated anilines. *Chem. Res. Toxicol.* **7**, 590-598.

Cnubben N.H.P., Vervoort J., Veeger C., and Rietjens I.M.C.M. (1992). Study on the regioselectivity and mechanims of the aromatic hydroxylation of monofluoroanilines. *Chem.-Biol. Interactions* **85**, 151-172.

Debnath A.K., Lopez de Compadre R.L., Debnath G., Shusterman A.J., and Hansch C. (1991). Structure activity relationship of mutagenic aromatic and heteroaromatic nitrocompounds. Correlation with molecular orbital energies and hydrophobicity. *J. Med. Chem.* **34**, 785-797.

Debnath A.K., Lopez de Compadre R.L., Shusterman A.J., and Hansch C. (1992). Quantitative structure activity relationship investigation of the role of hydrophobicity in regulating mutagenicity in the Ames test: 2. Mutagenicity of aromatic and heteroaromatic nitrocompounds in Salmonella Typhimurium TA 100. *Environmental and Molecular Mutagenesis* **19**, 53-70.

Fukui K., Yonezawa T., Nagata C., and Shingu H. (1954). Molecular orbital theory of orientation in aromatic, heteroaromatic and other conjugated molecules. *J. Chem. Phys.* **22**, 1433-1442.

Harada N., and Omura T. (1980). Participation of cytochrome P-450 in the reduction of nitro compounds by rat liver microsomes. *J. Biochem.* **87**, 1539-1554.

Harrison J.H., and Jollow D.J. (1987). Contribution of aniline metabolites to aniline-induced methemoglobinemia. *Molec. Pharmac.* **32**, 423-31.

Kennedy R.J., and Stock A.M. (1960). The oxidation of organic substances by potassium peroxymonosulphate. *J. Org. Chem.* **25**, 1901-1906.

Kiese M. (1974). *Methemoglobinemia: A comprehensive treatise*. Chapter 7, CRC Press, Cleveland, Ohio.

Levin A.A., and Dent J.G. (1982). Comparison of the metabolism of nitrobenzene by hepatic microsomes and cecal microflora from Fischer-344 rats in vitro and the relative importance of each in vivo. *Drug Metab. Dispos.* **10**, 450-454.

Lopez de Compadre R.L., Debnath A.K., Shusterman A.J., and Hansch C. (1990). LUMO energies and hydrophobicity as determinants of mutagenicity by nitroaromatic compounds in *Salmonella typhimurium*. *Environmental and molecular mutagenesis* **15**, 44-55.

Maples K.R., Eyer P., and Mason R.P. (1989). Aniline-, phenylhydroxylamine-, nitrosobenzene-, and nitrobenzene-induced hemoglobin thiyl free radical formation in vivo and in vitro. *Molec. Pharmac.* **37**, 311-318.

O'Brien P.J., Wong W.C., Silva J., and Khan S. (1990). Toxicity of nitrobenzene compounds towards isolated hepatocytes: Dependence on reduction potential. *Xenobiotica* **20**, 945-955.

Ortiz de Montellano P. (1985). *Cytochrome P-450, structure, mechanism and biochemistry.* chapter 11, Plenum Press, New York.

Piotrowski J. (1967). Further investigations on the evaluation of exposure to nitrobenzene. *Br. J. Ind. Med.* **24**, 60-65.

Reddy B.G., Pohl L.R., and Krishna G. (1976). The requirement of the gut flora in nitrobenzene-induced methemoglobinemia in rats. *Biochem. Pharmac.* **25**, 1119-1122.

Rickert D.E. (1987). Metabolism of nitro aromatic compounds. *Drug Metab. Rev.* **18**, 23 -53.

Rickert D.E., and Held S. (1990). Metabolism of chloronitrobenzenes by isolated rat hepatocytes. *Drug Metab. Disp.* **18**, 5-9.

Rietjens I.M.C.M., Cnubben N.H.P., van Haandel M., Tyrakowska B., Soffers A.E.M.F., and Vervoort J. (1995a). Different metabolic pathways of 2,5-difluoronitrobenzene and 2,5-difluoroaminobenzene compared to molecular orbital substrate characteristics. *Chem.-Biol. Interactions* **94**, 49-72.

Rietjens I.M.C.M., Soffers A.E.M.F., Hooiveld G., Veeger C., and Vervoort J. (1995b). Quantitative structure activity relationships based on computer calculated parameters for the overall rate of glutathione S-transferase catalyzed conjugation of a series of fluoronitrobenzenes. *Chem. Res. Toxicol.* **8**, 481-488, 1995.

Rietjens I.M.C.M., Soffers A.E.M.F., Veeger C., and Vervoort J. (1993). Regioselectivity of cytochrome P450 catalyzed hydroxylation of fluorobenzenes predicted by calculated frontier orbital substrate characteristics. *Biochemistry* **32**, 4801-4812.

Sabbioni G. (1992). Hemoglobin binding of monocyclic aromatic amines: molecular dosimetry and quantitative structure activity relationships for the N-oxidation. *Chem.-Biol. Interact.* **81**, 91-117.

Sabbioni G. (1994). Hemoglobin binding of nitroarenes and quantitative structure-activity relationships. *Chem. Res. Toxicol.* **7**, 267-274.

Shimizu M., Yasui Y., and Matsumoto N. (1983). Structural specificity of aromatic compounds with special reference to mutagenic activity in *Salmonella typhimurium* -a series of chloro- or fluoro-nitrobenzene derivatives. *Mutation Research* **116**, 217-238.

Suzuki J., Meguro S., Moriat O., Hirayama S., and Suzuki S. (1989). Comparison of in vivo binding of aromatic nitro and amino compounds to rat hemoglobin. *Biochem. Pharmac.* **38**, 3511-3519.

Tatsumi K., Kitamura S., Yoshimura H., and Kawazoe Y. (1978). Susceptibility of aromatic nitro compounds to xanthine oxidase-catalyzed reduction. *Chem. Pharm. Bull.* **26**, 1713-1717.

Vervoort J., de Jager P.A., Steenbergen J., and Rietjens I.M.C.M. (1990). Development of a ^{19}F NMR method for studies on the in vivo and in vitro metabolism of 2-fluoroaniline. *Xenobiotica* **20**, 657-670.

Vogel A.J. (1978). *Vogel's textbook of practical organic chemistry.* (B.S. Furniss, A.J. Hannaford, P.W.G. Smith and A.R. Tatchell, Eds.) p. 684., Longman Scientific & Technical, London.

Yoshida M., Yoshikawa H., Goto H., and Hara I. (1989). Evaluation of the nephrotoxicity of aromatic nitro-amino compounds by urinary enzyme activities. *The Journal of Toxicological Sciences* **14**, 257-268.

CHAPTER 10

Comparative MO-QSAR studies in various species including man.

Bozena Tyrakowska, Nicole H.P. Cnubben, Ans E.M.F. Soffers, Th. Wobbes and Ivonne M.C.M. Rietjens·

In press Chemico-Biological Interactions.

SUMMARY.

In the present study it is demonstrated that MO-QSAR's (quantitative structure-activity relationships based on calculated molecular orbital substrate characteristics) of cytochrome P450-catalyzed biotransformation of benzene derivatives obtained in previous studies for Wistar rats, can be extrapolated to other species, including man.

First, it was demonstrated that the regioselectivity of the *in vivo* aromatic hydroxylation of two fluorobenzene derivatives can be quantitatively predicted, on the basis of the calculated density distribution of the reactive π-electrons in the aromatic ring of the fluorobenzene derivative, for all experimental animal species tested. Second, it was investigated whether the preferential site for *in vitro* aromatic hydroxylation of 3-fluoroaniline could be predicted on the basis of the same calculated parameter. This was done because extrapolation to human systems requires *in vitro* instead of *in vivo* experiments. The results obtained indicated that the variation in the regioselectivity of the aromatic hydroxylation of 3-fluoroaniline by liver microsomes from different species, including man, was only a few percent, and was mainly directed by calculated chemical reactivity characteristics of the 3-fluoroaniline substrate. Finally, possibilities for the extrapolation from rat to other species, of the MO-QSAR for the rate of *in vitro* C4 hydroxylation of a series of aniline derivatives converted in a iodosobenzene-supported microsomal cytochrome P450 system, were investigated. Experiments with liver microsomes from rats, mice,

rabbit and man resulted in clear MO-QSAR's with correlation coefficients for the relationship between the ln k_{cat} and the E(HOMO) of the aniline substrates that were ≥ 0.97 in all cases.

Thus, the results of the present study clearly demonstrate that MO-QSAR's previously described for Wistar rats can be extrapolated to mice, rabbit, guinea pig and even to man. Regioselectivities obtained and QSAR lines for the rate of conversion plotted against calculated E(HOMO) values of the aniline derivatives are similar for the various species investigated. Altogether, these results strongly support the conclusion that the conversion of the relatively small benzene derivatives in the relatively large and aspecific active sites of the mammalian cytochromes P450, even when derived from various species, are mainly dependent on chemical reactivity parameters of the substrates. Therefore, the results of the present study support the hypothesis that MO-based QSAR's obtained in rat for the cytochrome P450-catalyzed aromatic hydroxylation of benzene derivatives can provide a basis for prediction of biotransformation pathways in different species, including man.

INTRODUCTION.

Upon exposure of mammals to benzene derivatives these compounds are known to be metabolised in phase I and phase II type biotransformation reactions before they can be excreted from the body, or before they exert their toxic effects (1, 2). Phase I metabolism of substituted benzene derivatives is mediated by the cytochrome P450 enzyme system, which consists of a series of isoenzymes with broad, and partially overlapping substrate specificity. Metabolic patterns resulting from cytochrome P450-catalyzed biotransformation may vary with variation in the cytochrome P450 enzyme pattern. This enzyme pattern is dependent on both external and internal factors. Among the internal factors species differences are known to influence the cytochrome P450 enzyme pattern. Species differences have been reported for both Phase I and Phase II enzymes and can result in variation in both routes and rates of metabolite formation (3-6). Such species differences, and, as a result, variations in metabolic profiles, may hamper extrapolation of results obtained in biotransformation studies with one type of experimental animal to other animal species, or, ultimately, to man.

Variations in the cytochrome P450 enzyme pattern of the microsomal preparations, due to pretreatment of animals by specific inducers or due to species differences, are well-known to be able to affect the outcomes of the biotransformation. For example, the metabolic profile of chlorobenzenes was influenced by the type of cytochrome P450 enzymes present in the microsomal

preparations (7,8). For bromobenzene it has been reported that 3-methylcholanthrene induced cytochrome P450 patterns result in preferential hydroxylation at the position ortho with respect to the bromine substituent, leading to relatively harmless metabolites, whereas metabolism by a phenobarbital induced cytochrome P450 population results in preferential para hydroxylation of bromobenzene leading to formation of intermediates that induce liver damage (9,10). In contrast to these results, previous studies demonstrated that for the cytochrome P450-catalyzed conversion of relatively small substrates, like fluorinated benzenes or monofluoroanilines, QSAR's (quantitative structure activity relationships) for their conversion by cytochromes P450 could be obtained and the influence of variations in the cytochrome P450 enzyme pattern appeared to be relatively small (11-13). These QSAR's were based on calculated molecular orbital characteristics, and, thus, chemical reactivity characteristics of the substrates. It was demonstrated for instance that the actual regioselectivity of the cytochrome-P450 catalyzed conversion of a series of fluorinated benzenes could be predicted within 6% accuracy and a correlation coefficient of 0.96 on the basis of the calculated reactivity of the various carbon centres in the benzene derivatives for electrophilic attack (11). In a similar way the preferential site of hydroxylation for a series of monofluoroanilines could be predicted (12). Moreover, the actual rate of 4-hydroxylation of a series of halogenated aniline derivatives in a iodosobenzene-supported cytochrome P450-catalyzed conversion was demonstrated to correlate with the calculated energy of the reactive π-electrons in the aniline substrate, providing another MO-QSAR (QSAR based on calculated molecular orbital characteristics) for a cytochrome P450-mediated reaction (13).

Thus, for relatively small substrates, chemical reactivity characteristics of the substrates may dominate over the influence of the specific P450 enzymes in determining the regioselectivity of the biotransformation both *in vitro* and *in vivo* and also in setting the rate of the reaction in a iodosobenzene supported system *in vitro*. This observation would imply that MO-QSAR's obtained up to now for cytochrome P450 catalysed reactions using the cytochromes P450 from Wistar rats, may be valid for other species as well. The present study was undertaken to investigate whether the MO-QSAR's obtained up to now for rat cytochromes P450, are also valid for the prediction of the metabolism of substituted benzene derivatives by other species than rat, and, thus, may provide a basis for extrapolation to man. Therefore, in the present study, the validity of QSAR's previously described for reactions catalysed by cytochromes P450 from Wistar rats, was investigated for cytochromes P450 obtained from mice, guinea pig, rabbit and also from man.

MATERIALS AND METHODS.

Chemicals.

Aniline, 2-fluoroaniline, 3-fluoroaniline, 2-chloroaniline, 3-chloroaniline and 2,3-difluoroaniline were purchased from Janssen Chimica (Beerse, Belgium). 1,3-Difluorobenzene was obtained from Fluorochem (Derbyshire, UK). 1,2,4-Trifluorobenzene was purchased from Aldrich Chemie (Steinheim, FRG). The purity of all compounds was >98%. Iodosobenzene was synthesized by the base-catalyzed hydrolysis of diacetoxyiodobenzene (Fluka, Switzerland), essentially as described by Saltzman and Sharefkin (14), and added to the incubations from a 20 mM sonicated suspension in 10% DMSO in demineralised water.

In vivo exposure of different species to 1,3-difluoro- and 1,2,4-trifluorobenzene.

Male U inbred, R inbred and Spraque Dawley (SD) rats (400 g) were exposed to 200 µmol (500 µmol per kg body weight) of the 1,3-difluoro- or 1,2,4-trifluorobenzene, administrated in olive oil by oral injection. Male NMRi, C57/BL mice (40 g) were exposed to 20 µmol (500 µmol per kg body weight), male New Zealand White (NZW) rabbit (4000 g) was exposed to 2000 µmol (500 µmol per kg body weight) and male guinea pig (800g) was exposed to 400 µmol (500 µmol per kg body weight) of the 1,3-difluorobenzene or 1,2,4-trifluorobenzene, administrated in olive oil by oral injection. After dosing, 0-24 h and 24-48 h urine samples were collected and stored at -20°C until analysis.

Analysis of urine samples.

Urine samples were analysed by ^{19}F-NMR after 1:1 dilution in 0.2 M potassium phosphate (pH 7.6). Enzyme hydrolysis of urine samples was carried out as described previously (15) using either ß-glucuronidase from *Escherichia coli* K12 (Boehringer, Mannheim, Germany) or arylsulphatase/ß-glucuronidase from *Helix pomatia* (Boehringer, Mannheim, Germany). Samples were made oxygen free by four cycles of evacuation and filling with argon.

^{19}F NMR measurements.

^{19}F NMR measurements were performed on a Bruker AMX 300 spectrometer as described previously (15-17). Between 1500 and 20000 scans were recorded, depending on the concentrations of the fluorine-containing compounds and the signal to noise ratio required. The sample volume was 1.71 ml, containing 100 µl of D_2O for locking the magnetic field and 10 µl of 8.4 mM 4-fluorobenzoic acid solution added as an internal standard. Chemical shifts are reported relative to $CFCl_3$ (18). Concentrations of the various metabolites observed in ^{19}F-NMR spectra were

calculated by comparison of the integrals of their ^{19}F-NMR resonances to the integral of the ^{19}F-NMR of 4-fluorobenzoic acid, as an internal standard.

Preparation of microsomes.

Microsomes were prepared from the perfused livers of male rats (400 g), male mice (40 g) and male NZW rabbit (4000 g), which were treated with isosafrole (Sigma, St Louis, MO), 150 mg/kg body weight, using a stock solution 100 mg/ml in olive oil, administrated i.p., daily for 3 days. Following homogenisation of the livers in Tris-sucrose buffer (50 mM Tris/HCl, 0.25 M sucrose, pH 7.4) and centrifugation at 10 000 * g (20 min), the supernatants were centrifuged for 75 min at 105 000 * g. The microsomal pellet was washed once with Tris-sucrose buffer and finally suspended in 0.1 M potassium phosphate pH 7.25 containing 20% glycerol and 1 mM EDTA. The final preparation was immediately frozen in liquid nitrogen and stored at -80° C, until use.

Cytochrome P450 contents were determined as described by Omura and Sato (19). Protein was assayed by the method of Lowry (20) using bovine serum albumin (Sigma, St Louis, MO) as the standard.

Microsomes from human livers (labelled A, B, C and D) were prepared in a similar way from specimens obtained from patients who underwent resection of one or two liver segments for metachronous liver metastases of colorectal carcinoma. In all patients preoperative liver function tests were normal. Some characteristics of the patients are given in Table1. Immediately after resection a representative specimen of normal liver tissue was excised from the resected segment and cooled. All patients had epidural anaesthesia and after introduction (fentanylcitrate, thiopental, vecuroniumbromide) nitrous oxide and isoflurane as anaesthetic agent were applicated continously during the operation. All patients gave permittance preoperatively for the use of some liver tissue for scientific purposes.

Microsomal incubations.

Microsomal incubations were carried out at 37° C in 0.1 M potassium phosphate (pH 7.6) containing 1 μM microsomal cytochrome P450 and 0-20 mM (halogenated) aniline added as 1% (v/v) of a stock solution in DMSO. The reaction was started by the addition of NADPH or iodosobenzene (both at 1mM final concentration) and terminated after 10 min (NADPH) or 1 min (iodosobenzene) by freezing the reaction mixture in liquid nitrogen for ^{19}F-NMR measurements or by adding 1.0 ml of the reaction mixture to 0.3 ml 20% trichloroacetic acid (TCA) for the chemical detection of 4-aminophenol. The cytochrome P450-mediated microsomal conversion of the aniline derivatives to their 4-aminophenols was observed to be linear in time for at least 10 min in a NADPH/O_2-supported reaction

and for at least 75 s in a iodosobenzene-supported reaction. In order to correct for the chemical reaction between iodosobenzene and the aniline substrates resulting in 4-hydroxylation of the substituted anilines, control incubations were carried out for each substrate concentration in the absence of microsomal cytochrome P450. This correction was 5-40%, depending on the substrate concentration and aniline derivative used.

Conditions for the ^{19}F-NMR samples for determination of the regioselectivity of 3-fluoroaniline hydroxylation in a NADPH/O_2 driven reaction were essentially similar using a final volume of 2 ml, 2 µM microsomal cytochrome P450, a 3-fluoroaniline concentration of 10 mM and adding 2 mM ascorbic acid and 0.2 mg/ml of superoxide dismutase (SOD) to prevent autoxidation of the aminophenol metabolites especially during the overnight ^{19}F-NMR measurement.

Chemical detection of 4-aminophenol.

Halogenated 4-aminophenols were determined essentially by the method of Brodie and Axelrod (21). In short, to 1ml of TCA-precipitated supernatant 100 µl of phenol reagent (5% phenol in 2.5 M NaOH) and 200 µl of 2.5 M Na_2CO_3 were added. After 60 min at room temperature the absorbance at 630 nm was measured. Halogenated 4-aminophenols were quantified using the values of molar extinction coefficients at 630 nm for their corresponding halogenated 4-aminophenol-derived indophenols reported by Cnubben *et al.* (13).

Kinetic analysis

The apparent Michaelis constant K_m (mM) for the aniline substrates and the apparent maximum reaction rate k_{cat} (nmol of halogenated 4-aminophenol per nmol of cytochrome P450 per minute) at infinite aniline concentration, for the 4-hydroxylation of the aniline derivatives by the microsomal cytochrome P450 were determined by fitting the data to the standard Michaelis-Menten equation $V = V_{max}[S]/(K_m+[S])$ using the program of KaleidaGraph, version 2.0.2. (Abelbeck Software). In spite of its multistep reaction cycle, it appeared possible to analyze the kinetics of the cytochrome P450-catalyzed 4-hydroxylation of the various anilines by Michaelis-Menten kinetics, the correlation coefficient "r" of the fits being greater than 0.97 in all cases.

Molecular orbital parameters

Molecular orbital parameters needed for the various comparisons of experimental data to calculated molecular orbital reactivity parameters were taken from the literature (11-13) and were calculated using the AM1 Hamiltonian (22). The parameters used were either the reactivity of the π-electrons characterised by their

calculated energy of the highest occupied molecular orbital (E_{HOMO}), or the calculated density distribution of the reactive π-electrons in the aromatic ring. This density distribution was calculated from the density distribution of the HOMO and the HOMO-1 (i.e. first occupied orbital at the highest energy level below the HOMO) as described by Fukui et al. (23).

RESULTS.

QSAR's for the in vivo aromatic ring hydroxylation of fluorinated benzenes .

To investigate whether the MO-QSAR for the prediction of the regioselectivity of the in vivo aromatic ring hydroxylation of fluorinated benzenes can be extrapolated from Wistar rats to other species, the regioselectivity of the aromatic hydroxylation of 1,3-difluorobenzene and 1,2,4-trifluorobenzene was determined in U and R inbred rats and SD rats, in two mice strains, in a rabbit strain and in the guinea pig. As an example, Figure 1 shows the ^{19}F-NMR spectra of the arylsulphatase/ß-glucuronidase-treated urine samples of NMRi mice exposed to 1,3-difluorobenzene (Figure 1a) or 1,2,4-trifluorobenzene (Figure 1b). The ^{19}F-NMR spectra of urine from Wistar rats exposed to these fluorobenzenes were previously reported (11). Results obtained from ^{19}F-NMR analysis of urine samples of the various animals exposed to 1,3-difluorobenzene or 1,2,4-trifluorobenzene are summarised in Table 2 and 3 respectively. For both 1,3-difluorobenzene and 1,2,4-trifluorobenzene all urinary metabolite patterns contain large amounts (> 48% of total

Table 1: Some characteristics of the patients of which liver specimens were obtained.

patient	**sex**	**age**	**histology liver**	**alkohol**	**smoking**	**medication**
A	male	63	steatosis±	2U/day	no	no
B	male	67	normal	4U/day	no	no
C	female	66	steatosis± fibrosis+	no	no	no
D	female	60	steatosis+	no	no	no

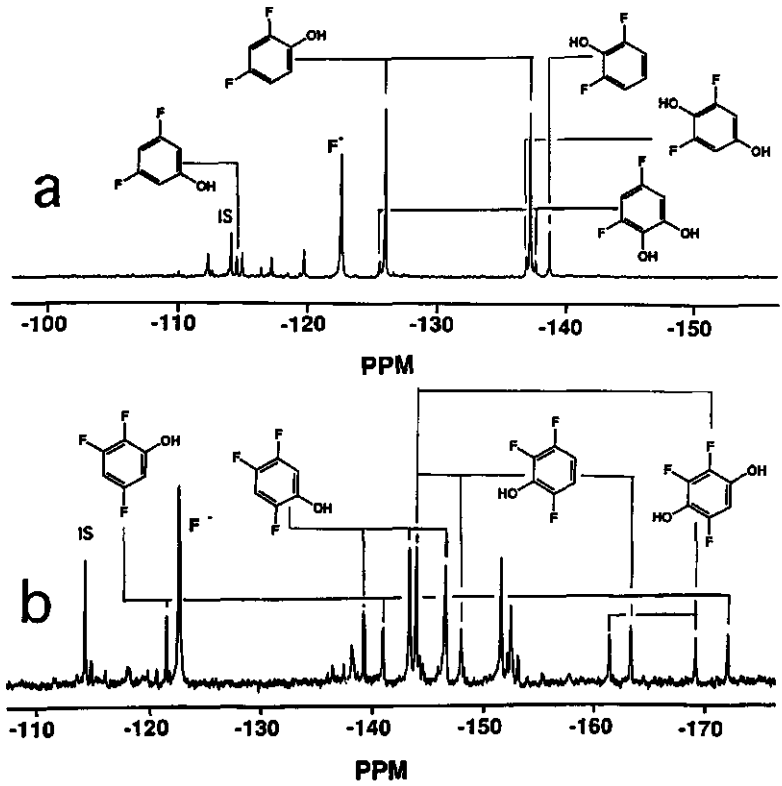

Figure 1: ^{19}F-NMR spectra of the arylsulphatase/ß-glucuronidase -treated 24 h urine of NMRi mice exposed to a) 1,3-difluorobenzene and b) 1,2,4-trifluorobenzene. The resonances of the hydroxylated metabolites were identified as previously described (11). The resonance marked IS is from the internal standard 4-fluorobenzoic acid.

fluorine containing metabolites) of phenolic metabolites. Formation of some ortho hydroxylated phenol (catechol) from 1,3-difluorobenzene is observed in all species, the relative amount being slightly higher in rabbit than in the other species (Table 2). This observation is accompanied by a slightly lower amount of monophenols in the urine of 1,3-difluorobenzene exposed rabbits compared to the urine from the other species exposed to 1,3-difluorobenzene. Catechol formation from 1,2,4-trifluorobenzene is not observed (Table 3). Formation of para hydroxylated phenols (hydroquinones) is observed only in mice for both fluorobenzenes. Some resonances in the ^{19}F-NMR spectrum of 1,3-difluoro- and 1,2,4-trifluorobenzene remain unidentified. Since these unidentified peaks do not represent primary halogenated phenolic metabolites, they were not investigated in detail in this study.

Table 2: Phenolic metabolite pattern in urine of different species exposed to 1,3-difluorobenzene as determined by ^{19}F-NMR analysis of the arylsulphatase/β-glucuronidase treated 24 h urine of exposed animals.

	phenolic metabolites (% of total fluorine containing aromatic metabolites)				**regioselectivity at carbon centers**
species	phenols	2-OH-phenol	4-OH-phenol	total	C2 : C4/6 : C5
Wistar rat [a]	46.5	2.1	n.o.[b]	48.6	0.12 : 0.82 : 0.06
SD rat	60.8	6.0	n.o.[b]	66.8	0.09 : 0.85 : 0.06
U inbred rat	55.2	4.4	n.o.[b]	59.6	0.11 : 0.84 : 0.05
R inbred rat	53.7	4.9	n.o.[b]	58.6	0.11 : 0.84 : 0.05
C57/BL mouse	61.3	3.7	2.7	67.7	0.11 : 0.84 : 0.05
NMRi mouse	66.3	5.5	3.3	75.1	0.10 : 0.85 : 0.05
NZW rabbit	42.1	11.7	n.o.[b]	53.8	0.12 : 0.79 : 0.09
Guinea pig	65.4	7.8	n.o.[b]	73.2	0.13 : 0.81 : 0.06

[a] Data were taken from the literature (11).

[b] n.o. means not observed in the ^{19}F-NMR spectrum based on the known position of the resonance of 2,6-difluoro-4-hydroxyphenol at -137.1 ppm (11).

Most interesting for the objective of the present study, however, are the regioselectivities of the aromatic hydroxylation also presented in Table 2 and 3. The results obtained show that conversion of 1,3-difluorobenzene and 1,2,4-trifluorobenzene by various species results in similar regioselectivity for the aromatic hydroxylation. The regioselectivities observed in all species closely match the regioselectivity predicted on the basis of the calculated reactivity of the various carbon centers for an electrophilic attack, i.e. C2 : C4/6 : C5 = 0.16 : 0.74 : 0.10 for 1,3-difluorobenzene and C3 : C5 : C6 = 0.19 : 0.60 : 0.21 for 1,2,4-trifluorobenzene (11).

Table 3: Phenolic metabolite pattern in urine of different species exposed to 1,2,4-trifluorobenzene as determined by ^{19}F-NMR analysis of the arylsulphatase/β-glucuronidase treated 24 h urine of exposed animals.

	phenolic metabolites (% of total fluorine containing aromatic metabolites)			**regioselectivity at carbon centers**
species	phenols	4-OH-phenol	total	C3 : C5 : C6
Wistar rat [a]	48.6	n.o.[b]	48.6	0.25 : 0.51 : 0.24
U inbred rat	51.9	n.o.[b]	51.9	0.31 : 0.49 : 0.20
R inbred rat	53.7	n.o.[b]	53.7	0.34 : 0.46 : 0.20
C57/BL mouse	59.6	6.3	65.9	0.31 : 0.50 : 0.19
NMRi mouse	55.3	7.8	63.1	0.30 : 0.50 : 0.20
NZW rabbit	69.6	n.o.[b]	69.6	0.29 : 0.44 : 0.27
Guinea pig	67.8	n.o.[b]	67.8	0.31 : 0.42 : 0.27

[a] Data were taken from the literature (11).

[b] n.o. means not observed in the ^{19}F-NMR spectrum based on the known position of the resonances of 2,3,5-trifluoro-4-hydroxyphenol at -144.4, -162.2 and -169.7 ppm (11).

Regioselectivity for the in vitro aromatic hydroxylation of 3-fluoroaniline

In addition to extrapolation to other experimental animals than the Wistar rat, it is of interest to investigate whether the regioselectivity obtained for the aromatic hydroxylations catalyzed by cytochromes P450 from Wistar rats can be extrapolated to man. As, for obvious ethical reasons, the *in vivo* regioselectivity of the aromatic hydroxylation can not be investigated in man, *in vitro* experiments with 3-fluoroaniline were performed. 3-Fluoroaniline was used for these *in vitro* studies instead of the fluorobenzenes because the rate of its conversion is higher and therefore results in metabolite patterns that can be quantified by ^{19}F-NMR analysis. Figure 2 presents the ^{19}F-NMR spectrum of an incubation of 3-fluoroaniline with human liver microsomes.

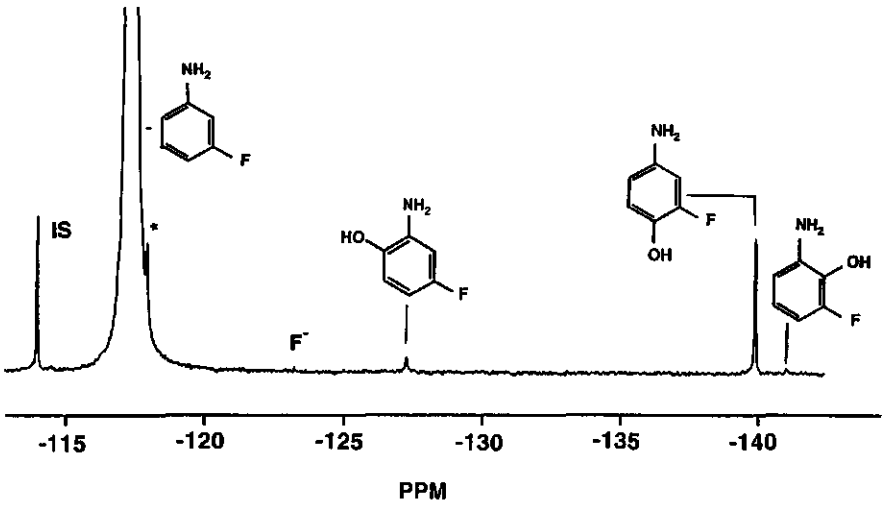

Figure 2.: ^{19}F-NMR spectrum of an incubation of 3-fluoroaniline with microsomes from human liver. Metabolites were identified as previously described (12,16). The resonance marked IS is from the internal standard 4-fluorobenzoic acid. The resonance marked with an asterisk is also present in blank incubation without NADPH.

Table 4 presents the regioselectivity derived from this and additional ^{19}F-NMR spectra obtained for incubations with various microsomal preparations. The results presented clearly demonstrate that the regioselectivity of the 3-fluoroaniline hydroxylation observed with microsomes from different species, and also with different human liver microsomal preparations, vary by only a few percent. Qualitatively, the regioselectivity observed follows the calculated density distribution for an electrophilic attack on the reactive π-electrons of 3-fluoroaniline. This frontier electron densitry distribution for an electrophilic attack is 0.20 : 0.47 : 0.05 : 0.36 for C2 : C4 : C5 : C6 (12). These MO results qualitatively explain that C5 is not hydroxylated, that C6-hydroxylation is favoured over C2-hydroxylation and that C4 is the preferential site for hydroxylation of 3-fluoroaniline. Apparently, the type of cytochromes P450 present in the microsomal preparation, and, thus, the species from which the P450 preparation is derived, is not a main factor influencing the regioselectivity of the hydroxylation of 3-fluoroaniline.

Table 4: The regioselectivity for the *in vitro* aromatic ring hydroxylation of 3-fluoroaniline in microsomal incubations from different species as determined by ^{19}F-NMR.

species		regioselectivity observed at the carbon centers C2 : C4 : C5 : C6
Wistar rat [a]		0.05 : 0.84 : 0.00 : 0.11
NMRi mouse		0.05 : 0.80 : 0.00 : 0.15 0.06 : 0.77 : 0.00 : 0.17
NZW rabbit		0.06 : 0.84 : 0.00 : 0.10 0.06 : 0.85 : 0.00 : 0.09
human	batch A	0.04 : 0.76 : 0.00 : 0.20
	batch B	0.06 : 0.79 : 0.00 : 0.15
	batch C	0.08 : 0.78 : 0.00 : 0.14
	batch D	0.05 : 0.86 : 0.00 : 0.09

[a] data were taken from the literature (12).

QSAR's for the rate of in vitro conversion of halogenated aniline derivatives in a iodosobenzene-supported cytochrome P450-catalysed C4-hydroxylation.

In a final set of experiments it was investigated whether the MO-QSAR describing a correlation between the rates of conversion of a series of aniline derivatives in a iodosobenzene-supported cytochrome P450-mediated C4-hydroxylation and the energy of the reactive π-electrons of these aniline derivatives (13), can be extrapolated to other species than the Wistar rat. To allow comparison of the data of the present study to those previously reported, isosafrole pretreatment of the animals was performed before preparing the microsomes for the present *in vitro* studies. Previous studies demonstrated aniline hydroxylation in a NADPH/O_2 driven microsomal reaction to be highest with microsomes from isosafrole pretreated rats (13,16). Table 5 presents the k_{cat} values obtained for the C4-hydroxylation of a series of (halogenated) anilines by liver microsomes from isosafrole-pretreated rats, rabbit and mice. It also presents k_{cat} values obtained for a iodosobenzene driven microsomal system derived from human liver. It appears from the data presented in Table 5, that k_{cat} values for C4-hydroxylation of aniline derivatives obtained using microsomes from various species vary at most two-fold. Furthermore, the results presented in Table 5 show considerable differences in k_{cat} values for the C4-hydroxylation of the different aniline derivatives.

Table 5: Apparent k_{cat} (maximum velocity in nmoles converted per nmol of cyt P450 per min) for the iodosobenzene-supported microsomal cytochrome P450-catalyzed C4-hydroxylation of aniline derivatives with liver microsomes from different species. Values presented are the mean ± standard error of the mean (n=2-4).

substrate	**k_{cat} (min^{-1})**			
	Wistar rats	NZW rabbit	NMRi mice	human (batch A and B)
aniline	115.8 ± 21.6	111.4 ± 32.2	124.7 ± 22.2	223.3 ± 77.5
2-chloroaniline	104.8 ± 10.5	95.9 ± 24.4	75.6 ± 15.4	164.1 ± 53.6
2-fluoroaniline	74.1 ± 10.0	55.1 ± 5.1	58.9 ± 20.2	132.9 ± 55.7
3-chloroaniline	36.5 ± 5.2	28.7 ± 1.3	26.8 ± 3.2	69.2 ± 13.7
3-fluoroaniline	41.1 ± 3.8	30.8 ± 3.8	29.6 ± 2.6	60.4 ± 5.1
2,3-difluoroaniline	15.5 ± 1.0	15.1 ± 0.0	15.7 ± 0.0	18.8 ± 0.0

In Figure 3 the natural logarithm of the k_{cat} values for the iodosobenzene-supported C4-hydroxylation of the (halogenated) anilines is plotted against the E(HOMO) values calculated for the aniline derivatives. These E(HOMO) values of the aniline derivatives are of importance for their reactivity in the electrophilic attack by the high-valent-iron-oxo cytochrome P450 intermediate. The results presented in Figure 3 clearly demonstrate that MO-QSAR's are obtained not only for rat, but also for mice, rabbit and even human microsomal systems. The correlation coefficients for the QSAR's describing the relation between the ln k_{cat} values and the E(HOMO) values are r=0.97 for rats, r=0.98 for mice, r=0.97 for rabbit and r= 0.99 for human microsomes.

Besides, Figure 3 clearly shows that the QSAR's obtained for the various species are similar. These similar QSAR lines obtained for different species indicate that the relative change in the rate of conversion with a change in the reactivity of the aniline substrate is about the same for all species.

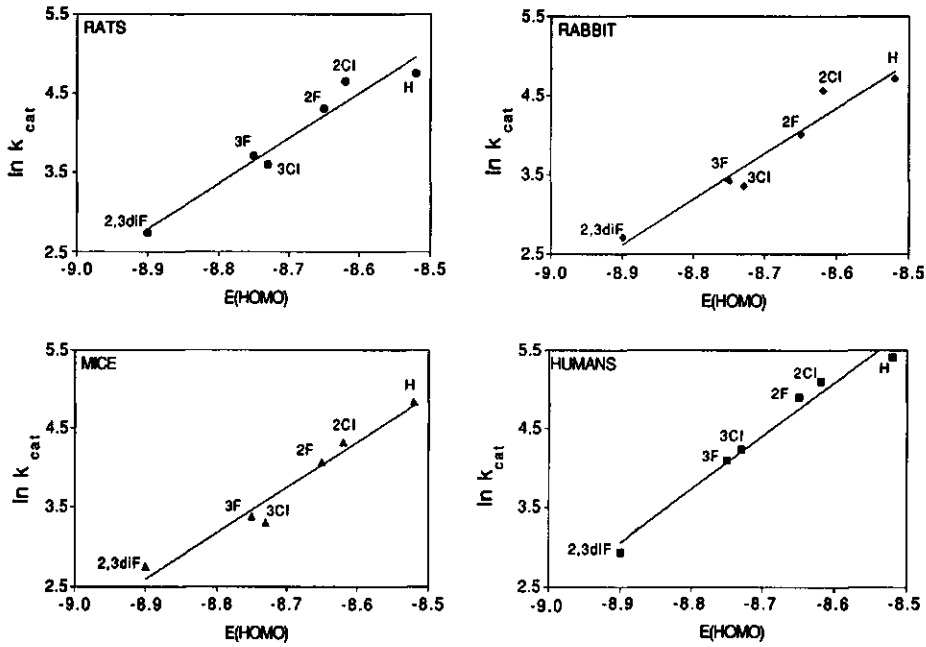

Figure 3: Relationship between the ln k_{cat} for 4-hydroxylation of a series of halogenated anilines in a iodosobenzene-supported microsomal P450 conversion and the E(HOMO) of these substrates for rats (r=0.97), mice (r=0.98), rabbit (r=0.97) and human (r=0.99) liver microsomes. k_{cat} is expressed in min^{-1}, E(HOMO) is expressed in eV. Theoretically, k_{cat} should be multiplied by h/kT to make the parameter dimensionless before calculating the natural logarithm. However, because this would result in a change of the y-axis values by a constant factor, this theoretically appropriate correction was omitted and the natural logarithm of k_{cat} was plotted. Frontier orbital characteristics of the aniline derivatives calculated using the AM1 Hamiltonian. The E_{HOMO} in eV was calculated to be -8.52, -8.62, -8.65, -8.73, -8.75 and -8.90 for aniline, 2-chloroaniline, 2-fluoroaniline, 3-chloroaniline, 3-fluoroaniline and 2,3-difluoroaniline, respectively.

DISCUSSION.

In the present study it was investigated whether MO-QSAR's (quantitative structure activity relations based on molecular orbital parameters) described previously for aromatic hydroxylation reactions of halogenated benzene derivatives catalysed by cytochromes P450 from Wistar rats can be extrapolated to cytochrome P450 reactions of other species. Because these MO-QSAR's describe relationships between experimental parameters and a calculated reactivity parameter of the P450 substrate, it might be foreseen that such MO-QSAR's obtained for one species may be valid for other species including man. Previous results with differently induced Wistar rat microsomal preparations as well as with different induced rats metabolising substrates *in vivo*, already demonstrated that a change in the cytochrome P450 enzyme pattern did not influence the regioselectivity of the aromatic hydroxylation of relatively small substrates like fluorinated benzene derivatives or monofluoroanilines (11,12). These results imply that chemical characteristics of the substrate instead of the types of cytochromes P450 involved, are of major importance in determining the outcomes of the catalysis. The present study was undertaken to provide further support for this hypothesis, and especially to investigate whether this MO-QSAR approach would indeed form a basis for extrapolation of biotransformation results from one species to another including man. First, the regioselectivity of the *in vivo* hydroxylation of two model fluorinated benzenes with three discernable sites for aromatic hydroxylation (1,3-difluorobenzene and 1,2,4-trifluorobenzene), was tested in three additional rat strains, in two mice strains, in a rabbit strain and in guinea pig. Second, the regioselectivity of the in vitro 3-fluoroaniline hydroxylation by mice, rabbit and human microsomes was determined and compared to the results obtained with rat microsomes. Finally, it was investigated whether the MO-QSAR for the rate of conversion of a series of aniline derivatives in a iodosobenzene-supported cytochrome P450-catalysed C4-hydroxylation can be extrapolated to studies with mice, rabbit and human microsomes.

The results obtained demonstrate that for all three biotransformation QSAR's the results obtained with mice, guinea pig, rabbit and even human systems were similar to those obtained for the rat system. The regioselectivity of the in vivo aromatic hydroxylation of 1,3-difluorobenzene and 1,2,4-trifluorobenzene could be predicted on the basis of the calculated electron densitry distribution for an electrophilic attack by the activated high-valent-iron-oxo species of the cytochromes P450. Thus, in *in vivo* studies with mice, guinea pig, other rats strains and rabbit, this MO-QSAR for the prediction of the regioselectivity of the fluorobenzene hydroxylation was valid, indicating that the chemical reactivity of the various sites in

the fluorinated benzenes, rather than a stereoselective influence of the active site of the cytochromes P450, determines the regioselectivity of the aromatic hydroxylation. This observation implies that the regioselectivity of the hydroxylation of these fluorinated benzenes in man can be expected to be similar. The similar regioselectivity observed in the present study for the *in vitro* hydroxylation of 3-fluoroaniline by microsomes from experimental animals or man, supports this view. Furthermore, the qualitative correlation between the regioselectivity predicted for 3-fluoroaniline on the basis of the calculated reactivity of the various carbon centres for an electrophilic attack and the regioselectivity actually observed, also supports this conclusion.

Finally, it was demonstrated that the relationship between the natural logarithm for the k_{cat} for iodosobenzene-supported microsomal C4 hydroxylation of a series of aniline derivatives and the energy of the reactive π-electrons of these derivatives can be obtained not only for liver microsomes from Wistar rats as previously described (13) but also for liver microsomes from mice, from rabbit and even from human liver. This MO-QSAR indicates that in the iodosobenzene-supported cytochrome P450-catalysed aniline C4-hydroxylation the actual electrophilic attack of the high-valent-iron-oxo P450 intermediate on the reactive π-electrons of the aniline substrate is the rate limiting step in catalysis. The two-fold variation in the various k_{cat} values observed when comparing results from human liver microsomes with those obtained for rats, rabbit or mice microsomes, is the only significant species-dependent difference observed in the present study. Nevertheless, the QSAR lines describing the relationship between the ln k_{cat} for the conversion of the various aniline derivatives and their E(HOMO) are similar for all species investigated. This implies that the relative influence of a change in the chemical reactivity of an aniline derivative on its rate of conversion is about the same for all species.

Altogether, the results of the present study strongly support the conclusion that the conversion of the relatively small benzene derivatives in the relatively large and aspecific active sites of the mammalian cytochromes P450, are mainly dependent on chemical reactivity parameters of the substrates. Therefore, the results of the present study support the hypothesis that MO-based QSAR's obtained in rat can provide a basis for prediction of biotransformation pathways in different species, including man.

Acknowledgements.
The authors gratefully acknowledge Prof. dr. C. Veeger for continuous support and helpfull discussion. Thanks are extended to Mr. J. Haas and Mrs. M.A.W. Peters for assistance with animal handling.

REFERENCES.

1. R.N. Armstrong, Enzyme-catalyzed detoxication reactions: mechanisms and stereochemistry. CRC Crit. Rev. Biochem., 22 (1987) 39-88.
2. I.G. Sipes and A.J. Gandolfi, Biotransformation of toxicants, in: Casarett and Doull's Toxicology. The Basic Science of Poisons. M.O. Amdur, J. Doull and C.D. Klaassen (Eds.), 4th edn. Pergamon, Oxford, (1991) pp. 64-98.
3. R.T. Williams, Species variations in the pathways of drug metabolism. Environ. Health Perspect., 22 (1978) 133-138.
4. R. Kato, Characteristics and differences in the hepatic mixed function oxidases of different species. Pharmac. Ther., 6 (1979) 41-98.
5. J. Caldwell, Problems and opportunities in toxicity testing arising from species differences in xenobiotic metabolism.Toxicol. Letters, 64/65 (1992) 651-659.
6. E. Dybing and H.S. Huitfeldt, Species differences in carcinogen metabolism and interspecies extrapolation. IARC Sci. Publ., 116 (1992) 501-522.
7. H.G. Selander, D. Jerina and J.W. Daly, Metabolism of chlorobenzene with hepatic microsomes and solubilised cytochrome P-450 systems. Arch. Biochem. Biophys., 168 (1975) 309-321.
8. J.J.P. Bogaards, B. van Ommen, C.R. Wolf and P.J. van Bladeren, Human cytochrome P450 enzyme selectivities in the oxidation of chlorinated benzenes. Toxicol. Appl. Pharmacol. 132 (1995) 44-52.
9. S.S. Lau, G.D. Abrams and V.G. Zannoni, Metabolic activation and detoxification of bromobenzene leading to cytotoxicity. J. Pharmacol. Exp. Ther., 214 (1980) 703-708.
10. T.J. Monks and S.S. Lau, Reactive intermediates and their toxicological significance. Review paper. Toxicology, 52 (1988) 1-53.
11. I.M.C.M.Rietjens , A.E.M.F. Soffers , C. Veeger and J. Vervoort, Regioselectivity of cytochrome P-450 catalyzed hydroxylation of fluorobenzenes predicted by calculated frontier orbital substrate characteristics. Biochemistry, 32 (1993) 4801-4812.
12. N.H.P.Cnubben , J.Vervoort , C.Veeger and I.M.C.M. Rietjens, Study on theregioselectivity and mechanism of the aromatic hydroxylation of monofluoroanilines. Chem.-Biol. Interact., 85 (1992) 151-172.
13. N.H.P. Cnubben , S. Peelen, J.W. Borst, J. Vervoort and I.M.C.M. Rietjens, Molecular orbital-based quantitative structure activity relationship for the cytochrome P450-catalysed 4-hydroxylation of halogenated anilines. Chem. Res. Toxicol., 7 (1994) 590-598.
14. H. Saltzman and J.G. Sharefkin, Iodosobenzene. in:Organic Syntheses, Collect. Vol. V, John Wiley & Sons, New York, (1973) 658-659.
15. I.M.C.M. Rietjens and J. Vervoort, A new hypothesis for the mechanism for cytochrome P-450 dependent aerobic conversion of hexahalogenated benzenes to pentahalogenated phenols. Chem. Res. Toxicol., 5 (1992) 10-19.

16. I.M.C.M. Rietjens and J. Vervoort, Microsomal metabolism of fluoroanilines. Xenobiotica, 19 (1989) 1297-1305.

17. J. Vervoort, P.A. De Jager, J. Steenbergen and I.M.C.M. Rietjens, Development of a ^{19}F NMR method for studies on the in vivo and in vitro metabolism of 2-fluoroaniline. Xenobiotica, 20 (1990) 657-670.

18. V. Wray, Fluorine nuclei in fluorobenzene derivatives, in: G.A. Webb (Ed), Annual Reports on NMR Spestroscopy, Vol. 14, Academic Press, London, (1983) p. 252.

19. T. Omura and R. Sato, The carbon monoxide pigment of liver microsomes, I. Evidence for its haemoprotein nature. J. Biol. Chem., 239 (1964) 2370-2378.

20. O.H. Lowry, N.J. Rosenbrough, A.L. Farr and A.J. Randall, Protein measurements with Folin phenol reagent. J. Biol. Chem. 193 (1951) 2370-2378.

21. B.B. Brodie and J. Axelrod, The estimation of acetanilide and its metabolic products, aniline, N-acetyl *p*-aminophenol and *p*-aminophenol (free and conjugated) in biological fluids and tissues. J. Pharmacol. Exp. Ther., 94 (1948) 22-28.

22. M.J.S. Dewar, E.G. Zoebisch, E.F. Healy and J.J.P. Stewart, AM1: a new general purpose quantum mechanical molecular model. J. Am. Chem. Soc., 107 (1985) 3902-3909.

23. K. Fukui, T. Yonezawa, C. Nagata and H. Shingu, Molecular orbital theory of orientation in aromatic, heteroaromatic and other conjugated molecules. J. Chem. Phys., 22 (1954) 1433-1442.

CHAPTER 11

Summary and conclusions.

Organisms are frequently exposed to low molecular weight xenobiotic compounds. An advanced enzymatic machinery modifies these compounds into more hydrophilic metabolites which are subsequently excreted from the body. This process of biotransformation aims to detoxify bodyforeign compounds. Ironically, reactive intermediates may also be formed during the biotransformation process and can interact with macromolecules or receptors, with possible toxicological consequences (bioactivation). Toxicological testing of all new and existing compounds is a money- and time-consuming problem and therefore alternatives are urgently needed. The main objective of the studies decribed in this thesis, which is outlined in **chapter 1**, was to describe QSARs (quantitative structure-activity relationships) for the biotransformation and toxicity of halogenated amino- and nitrobenzene derivatives. Special attention was focussed on the most important phase 1 biotransformation enzyme involved, the cytochrome P450 system. In addition, in the course of the investigations some attention was paid to the glutathione/glutathione S-transferase dependent phase 2 biotransformation pathway.

Chapter 2 gives an overview of the biotransformation enzymes primarily involved in the metabolism of halogenated amino- and nitrobenzene derivatives with respect to their function, regulation, occurrence, molecular/biochemical mechanisms and role in bioactivation and detoxication of xenobiotics. Biotransformation of amino- and nitrobenzene derivatives plays a crucial role in the generation of reactive intermediates assumed to contribute to the toxicity of this class of compounds. Since biotransformation of nitro- and aminobenzene derivatives is known to include pathways leading to both detoxication and bioactivation, insight into factors that direct the rates and regioselectivities of biotransformation processes or interactions with nucleophiles, like macromolecules or the tripeptide glutathione, will help to gain insight in factors that direct processes of, and chances on, bioactivation or detoxication of these compounds. Regioselective enzymatic conversion of relatively small aromatic substrates in the relatively large and aspecific active sites of cytochromes P450 is assumed to depend predominantly on chemical characteristics

of the substrates, whereas for relatively large substrates stereoselective positioning through steric constraints of the protein core in the active site becomes more important (see also **chapter 2**). Therefore, the relative differences in reactivity of various sites in a small aromatic compound can be expected to affect the possibilities for enzymatic conversion of the molecule. These considerations prompted us to investigate whether computer calculated molecular orbital characteristics of halogenated benzene derivatives, in combination with insight into the molecular mechanisms of their enzymatic conversion, could provide a basis for the prediction of their metabolic fate.

Chapter 3 presents a study on the regioselectivity and underlying mechanisms for the cytochrome P450-catalyzed aromatic hydroxylation of monofluoroanilines. This study provides insight into the molecular mechanism of the cytochrome P450-catalyzed aromatic hydroxylation of molecules containing a heteroatom as well as factors that influence the regioselectivity of hydroxylation. Three mechanisms for aromatic hydroxylation can be proposed; hydrogen abstraction (I), or electron abstraction followed by proton release (II) both leading to formation of a NH • radical. Upon rearrangement of the radical and OH-rebound from the $(FeOH)^{3+}$ species, the aminophenol product is formed. Aromatic hydroxylation might also proceed by a direct interaction of the high-valent iron-oxo cytochrome $(FeO)^{3+}$ intermediate with the π-electrons of the aromatic ring resulting in a so-called σ-adduct (III), which rearranges to the aminophenol, either directly or through formation of epoxides and/or ketones as intermediates. First, it was demonstrated that the regioselectivity of the aromatic hydroxylation was influenced by the position of fluoro-substituents at the aniline-ring and that the observed regioselectivity for hydroxylation of these small aromatics was not influenced by the relatively aspecific and large hydrophobic active sites of the cytochromes P450. As expected, a fluorine-substituent induces an effect on the electronic characteristics of the aniline-molecule and this effect was quantified using molecular orbital calculations. Considering the possible molecular mechanisms for aromatic hydroxylation, it appeared that the observed *in vitro* and *in vivo* regioselectivity correlated best with the frontier orbitals of importance for a direct interaction of the $(FeO)^{3+}$ species with the π-electrons of the aromatic molecule *e g.* the density distribution of the HOMO/HOMO-1. The spin density distribution of the NH • radicals -a parameter of importance for the hydrogen abstraction as well as electron abstraction plus proton release mechanisms- could not explain the observed regioselectivities, indicating that the regarding mechanisms are less likely. In a later study it was demonstrated that for a series of fluorobenzenes the regioselectivity for aromatic hydroxylation could even be predicted on the basis of the frontier orbital density distribution for electrophilic attack within 6% accuracy

(r=0.96) [Rietjens *et al.*, 1993]. For the fluoroanilines the C4 position is hydroxylated to higher extent, whereas the C2/C6 positions are hydroxylated to an extent lower than their chemical reactivity predicts. This deviation might result from steric hindrance of the amino moiety for electrophilic attack, a stereoselective positioning of the substrate through an interaction of the amino moiety with amino acid residues in the active site as has been described for P450 debrisoquine 4-hydroxylase, or a dipole-dipole or electronic interaction between the substrate and the activated cytochrome P450 $(FeO)^{3+}$ species. It is stressed here that the juxtaposition of these small substrates in the active site with respect to the Fe^{3+} resting state as determined on the basis of ^{1}H-NMR T1 relaxation or cristallography studies, might not represent the actual orientation with respect to the reactive $(FeO)^{3+}$ intermediate actually performing the hydroxylation step [Koerts *et al.*, 1995].

In **chapter 4** the aromatic hydroxylation of anilines was further investigated with special emphasis on possible relationships between kinetic parameters and both the physicochemical and electronic substrate characteristics. This was done in order to provide a basis for molecular orbital based quantitative structure activity relationships (MO-QSARs) for kinetic characteristics of the cytochrome P450-mediated aromatic hydroxylation of a homologous series of aniline-derivatives. It was demonstrated that the k_{cat} for C4-hydroxylation in a series of substituted anilines strongly correlates with the HOMO energy of the anilines for the iodosobenzene supported P450 reaction in isosafrole induced microsomes. This observation is in accordance with a mechanism that proceeds by an initial electrophilic interaction of the $(FeO)^{3+}$ intermediate with the frontier π electron of the aniline-substrate. In a NADPH/oxygen-supported P450 system, however, it was demonstrated that the interaction of the $(FeO)^{3+}$ species on the aniline-substrate is no longer rate-limiting, and therefore cannot be described by this QSAR. However, when the electrophilic reactivity of the substrates becomes too low, as is the case for 2,3,5,6-tetrafluoroaniline (E_{HOMO} of -9.24 eV) the initial attack of the cytochrome $(FeO)^{3+}$ on the substrate might become the rate-limiting step in the overall catalysis. The relatively low conversion rate observed for aromatic hydroxylation of fluorobenzenes for example [Rietjens *et al.*, 1993], might be explained by the relatively low electrophilic reactivity of these compounds. If the resulting metabolite is less toxic than its parent compound, a decreased conversion might have implications for the toxicity and the other way around.

To fully describe the cytochrome P450-mediated biotransformation of these aniline-derivatives, a sensitive and efficient analytical technique was developed for the detection and quantification of 2-aminophenols (**chapter 5**). The principle of the

method was based on a dimerization reaction of 2-aminophenols to an intensively colored 2-hydroxy-isophenoxazin-3-one in an acidic environment using ferric ions as the catalyst. It was demonstrated that this method was also applicable for the detection and quantification of halogenated 2-aminophenol derivatives.

Besides aromatic hydroxylation reactions, also oxidative dehalogenation reactions mediated by cytochromes P450 were investigated. Halogen substituents are often introduced into molecules to block positions at the aromatic ring of drugs or agrochemicals for bioactivation or biodegradation. Fluorine substituents are frequently used for this purpose, due to the strong C-F bond, and a Van der Waals radius that almost equals that of a hydrogen. In order to study the molecular mechanism of oxidative aromatic dehalogenation as well as the consequences of halogen substitution for regioselective hydroxylation and the formation of reactive intermediates, the study described in **chapter 6** was undertaken. Using halogenated anilines as the model compound, the effect of a varying halogen substituent patterns on the cytochrome P450-catalyzed dehalogenation of 4-halogenated anilines to 4-aminophenols was investigated. In the case of C4-fluorinated aniline derivatives, the cytochrome P450-mediated metabolic pathway has been unequivocally demonstrated to result in direct formation of a reactive 1,4-benzoquinoneimine and fluoride anions the primary reaction products [Rietjens *et al.*, 1993]. These reactive benzoquinoneimine metabolites may interact with cellular macromolecules and hence can lead to destruction of molecules essential to living cells.

The study described in **chapter 6** clearly demonstrated that upon the cytochrome P450-mediated oxidative dehalogenation to the primary reactive 1,4-benzoquinoneimine a fluorine substituent at C4 position of the aromatic aniline-ring was more easily eliminated than a chloro-, bromo- or iodo-substituent. A similar decrease in dehalogenation was observed in a NADPH/O_2 supported microsomal P450 system, as well as in a tBuOOH supported microsomal P450 system, or a system with purified reconstituted P4502B1, or in a system with the heme-based mini-enzyme microperoxidase 8. This indicates that the decrease in dehalogenation was not a result of a change in rate-limiting steps in the P450 catalysis or a change in the contribution of P450 enzymes with a change in the halogen substituent. Structure-activity relationship principles were applied to investigate the reaction mechanism of dehalogenation. The results obtained strongly indicate that the possibilities for the cytochrome P450-mediated dehalogenation of 4-halogenated anilines to 4-aminophenol metabolites are dependent on i) the characteristics of the halogen that has to be eliminated, the most electronegative and smallest halogen (fluorine) being the one most easily eliminated and ii) the electron-withdrawing capacities of the other

substituents in the aromatic ring, electron-withdrawing substituents decreasing the relative rate of the reaction. The conclusion that not only a fluoro-, but also a chloro-, bromo- and iodo- substituent, is eliminated as a halogen anion serves as the best explanation for the observations in this study. In addition, it was demonstrated that blocking the C4-position for aromatic hydroxylation by cytochromes P450 resulted in a metabolic switch from dehalogenation and 4-aminophenol formation, to formation of 2-aminophenol- and N-hydroxyaniline-derivatives. Although halogen substitution at the C4-position of an aniline indeed leads to a decreased metabolism at that site, the formation of the reactive 1,4-benzoquinoneimine instead of 4-aminophenol as the primary metabolite, as well as the switch to N-hydroxylation, giving rise to reactive hydroxylamino- and nitroso-derivatives may have considerable toxicological implications.

The biological activity of numerous aniline derivatives has been shown to be closely related to the cytochrome P450 mediated oxidative attack at their nitrogen center, yielding products with increasing toxic properties, namely N-hydroxyaniline and nitrosobenzene derivatives. Reactive N-hydroxyanilines cause for example ferrihemoglobin formation (methemoglobinemia) with concomittant co-oxidation to nitrosobenzenes. The resulting nitrosobenzenes in turn are able to interact with cysteine residues of hemoglobin or with the tripeptide glutathione [Eyer, 1988]. On the other hand, the cytochrome P450 mediated aromatic hydroxylation of anilines may represent a detoxification pathway due to the efficient conjugation of the resulting phenolic metabolites and subsequent excretion from the body. However, the cytochrome P450 mediated formation of aminophenol metabolites has been proposed to play a role in the nephrotoxicity of halogenated anilines, occuring predominantly at the proximal tubule and to a lesser extent at the distal tubule [Lo *et al.*, 1990 & 1991; Rankin *et al.*, 1986a & b; Valentovic *et al.*, 1992]. **Chapter 7** presents a clear example of a metabolism-toxicity relationship study. Since the cytochrome P450 mediated regioselective hydroxylation seems to direct the toxicity of aniline compounds, a study was performed on the relationships between the regioselectivity of the hydroxylation of C4-substituted 2-fluoroaniline derivatives and their toxic endpoints nephrotoxicity and/or methemoglobinemia. Depending on the derivative, nephrotoxicity at the tubular site and/or methemoglobinemia was shown to occur. The extent of nephrotoxicity induced by C4-substituted 2-fluoroanilines was shown to be related to the extent of C4-hydroxylation, and the extent of methemoglobinemia was shown to be related to the extent of N-hydroxylation. Consequently, a change in the regioselective hydroxylation from the cytochrome P450-mediated C4-hydroxylation to N-hydroxylation resulted in a change of toxic endpoint from nephrotoxicity to methemoglobinemia.

In **chapter 8** a study was directed at understanding the marked differences in biotransformation pathways of anilines and their chemically oxidized analogues nitrobenzenes. *In vivo* and *in vitro*, 2,5-difluoroaniline was demonstrated to become predominantly metabolized through a cytochrome P450-mediated pathway, whereas 2,5-difluoronitrobenzene is predominantly converted through glutathione conjugation, and the a minor extent through nitroreduction and cytochrome P450-mediated aromatic hydroxylation. On the basis of computer calculations a hypothesis was presented that might explain the differences in metabolic pathways on the basis of their molecular orbital substrate characteristics. It was suggested that the HOMO of the thiolate anion of glutathione will interact more efficiently with the LUMO of a nitro compound (E_{LUMO} = -1.57 eV) than with the LUMO of a less electrophilic amino compound (E_{LUMO} = -0.08 eV). Concerning the aromatic hydroxylation on the other hand, it was suggested that the SOMO of the cytochrome P450 $(FeO)^{3+}$ intermediate can interact more efficiently with the amino compound (E_{HOMO} = -8.83 eV) than with the nitro compound (E_{HOMO} = -10.29 eV). These considerations are in accordance with the observation in chapter 4, that the reaction rate of the cytochrome P450-mediated C4-hydroxylation decreases with decreasing electrophilic reactivity of an aniline substrate. Substrates with an E_{HOMO} value below -9.2 eV were converted at a relatively low rate by the cytochromes P450. The considerations are also in accordance with the recent observation that the rate of both the chemical and glutathione S-transferase catalyzed glutathione conjugation of fluoronitrobenzenes increases with decreasing E_{LUMO} values [Rietjens *et al.*, 1995].

Halogenated nitrobenzenes are known to become metabolized by nitroreduction, glutathione conjugation and aromatic hydroxylation. For some of the toxic effects of nitrobenzenes, the formation of reactive metabolites is a prerequisite. Reduction of nitrobenzenes to the aminobenzene analogues, via the formation of methemoglobinemia-inducing intermediates (nitrosobenzene, N-hydroxyaniline or radical intermediates), is a clear example of bioactivation of nitrobenzenes. The different susceptibility for nitroreduction, and also the presence of competing biotransformation pathways, like glutathione conjugation and aromatic hydroxylation, have been proposed to set the chances for methemoglobinemia exerted by nitrobenzene-derivatives. Applying QSAR approaches, a study was performed in order to investigate whether a metabolism-toxicity relationship exists for a series of fluoronitrobenzenes providing insight in the relative importance of these two suggestions. **Chapter 9** describes a combined study concerning the influence of the substituent pattern of fluoronitrobenzenes on their biotransformation and their capacity to induce methemoglobinemia. It was demonstrated that increased possibilities for the conjugation of fluoronitrobenzenes to cellular nucleophiles was

accompanied by decreased contributions of aromatic hydroxylation and nitroreduction. A QSAR could be described for the rate of conjugation with the tripeptide glutathione or with bovine serum albumine (a model for cellular nucleophiles) and calculated parameters for electrophilicity of the fluoronitrobenzenes, showing that with increasing number of fluoro-substituents the conjugation pathway will become more important. In addition, the intrinsic reactivity of the fluoronitrobenzenes for nitroreduction by cecal microflora and rat liver preparations was not related to the *in vivo* methemoglobin-forming capacity. This observation, in combination with the QSAR for conjugation, led to the conclusion that the different methemoglobinemic capacity must rather result from differences in the inherent direct methemoglobinemic reactivity of the various toxic metabolites, and/or from the difference in reactivity of the fluoronitrobenzenes with glutathione or other cellular nucleophiles. As a result of an increased electrophilic reactivity of fluoronitrobenzenes, another toxic endpoint than methemoglobinemia can be expected.

In the final study described in **chapter 10**, comparative MO-QSAR studies clearly demonstrated that outcomes on both the regioselectivity and the rate of the cytochrome P450-catalyzed aromatic hydroxylation could be described on the basis of frontier orbital characteristics of the substrates. The MO-QSARs obtained for rats, were also valid for other species, including man. These results strongly support the conclusion that the conversion of the relatively small halogenated benzene derivatives in the relatively large and aspecific active sites of the mammalian cytochromes P450 -even when derived from various species- are mainly dependent on chemical reactivity parameters of the substrates. This importance of the substrate characteristics also dominates over the influence of the specific P450 enzymes in determining the regioselectivity of biotransformation both *in vitro* and *in vivo*.

In conclusion, the studies described in this thesis cleary demonstrate that molecular orbital calculations in combination with the frontier orbital theory are a usefull additional tool to study the mechanism of cytochrome P450 enzyme catalysis. In addition to the theoretical considerations on the molecular reaction mechanisms and enzyme catalysis, empirical data on the metabolism are essential to construct valid rules or even quantitative structure activity relationships for the biotransformation and toxicity of series of related compounds. Insight into the possibilities for biotransformation have been demonstrated to provide insight into the formation of toxicity determining reactive intermediates. Defining QSARs for biotransformation have been shown to offer an approach to explain the type and extent of the toxic effects exerted by the series of halogenated amino- and

nitrobenzene derivatives.

Refined models, which do not only focus on the chemical reactivity parameters of the substrates, but also take into account possible stereoselective positioning or interactions with specific amino acid residues in the active site, will contribute to a better prediction of metabolic profiles of existing and new drugs, agrochemicals and other industrially relevant compounds.

Finally, it is challenging to apply the approaches described in this thesis to other enzymes with more specific active sites than the relatively large aspecific active sites of the biotransformation enzyme cytochrome P450.

REFERENCES.

Eyer P., Detoxication of N-oxygenated arylamines in erythrocytes. An overview, *Xenobiotica* **18**, 1327-1333, 1988.

Koerts J., Rietjens I.M.C.M., Boersma M.G. and Vervoort J., ^{1}H NMR T_1 relaxation rate study on substrate orientation of fluoromethylanilines in the actives sites of microsomal and purified cytochrome P450 1A1 and 2B1, *FEBS Letters* **368**, 279-284, 1995.

Lo H.H., Brown P.I., Rankin G.O., Acute nephrotoxicity induced by isomeric dichloroanilines in Fischer 344 rats, *Toxicology* **63**, 215-231, 1990.

Lo H.H., Brown P.I. and Rankin G.O., Trichloroaniline effects on renal function in vivo and in vitro, *Toxicology Letters* **57**, 319-328, 1991.

Rankin G.O., Yang D.J., Cressey-Veneziano K., Casto S., Wang R.T. and Brown P.I., In vivo and in vitro nephrotoxicity of aniline and its monochlorophenylderivatives in the Fischer 344 rat, *Toxicology* **38**, 269-283, 1986a.

Rankin G.O., Yang D.J., Teets V.J., Lo H.H. and Brown P.I., 3,5-Dichloroaniline-induced nephrotoxicity in the Sprague-Dawley rat, *Toxicology Letters* **30**, 173-179, 1986b.

Rietjens I.M.C.M., Soffers A.E.M.F., Hooiveld G., Veeger C. and Vervoort J., Quantitative structure activity relationships based on computer calculated parameters for the overall rate of glutathione S-transferase catalyzed conjugation of a series of fluoronitrobenzenes. *Chem. Res. Toxicol.* **8**, 481-488, 1995.

Rietjens I.M.C.M., Soffers A.E.M.F., Veeger C. and Vervoort J., Regioselectivity of cytchrome P450 catalyzed hydroxylation of fluorobenzenes predicted by calculated frontier orbital substrate characteristics, *Biochemistry* **32**, 4801-4812, 1993.

Rietjens I.M.C.M. and Vervoort J., Bioctivation of 4-fluorinated anilines to benzoquinoneimines as primary reaction products, *Chem.-Biol. Interact.* **22**, 263-281, 1991.

Valentovic M.A., Ball J.G., Anestis D.K., Beers K.W., Madan E., Hubbard J.L. and Rankin G., Aute renal and hepatic toxicity of 2-haloanilines in Fischer 344 rats, *Toxicology* **75**, 121-131, 1992.

Samenvatting voor niet-vakgenoten.

In de huidige moderne samenleving worden organismen veelvuldig blootgesteld aan lichaamsvreemde verbindingen zoals medicijnen, agrochemicaliën, oplosmiddelen, milieuverontreinigende stoffen en hun afbraakprodukten met mogelijk nadelige gevolgen. Het lot van deze stoffen is in het algemeen afhankelijk van hun fysisch-chemische eigenschappen. Zeer goed vetoplosbare stoffen hebben de neiging om te accumuleren in vettige weefsels (bijvoorbeeld de PCBs), terwijl goed wateroplosbare stoffen juist efficient uit het lichaam worden verwijderd via onder andere de urine (denk maar aan de gekleurde urine na het eten van rode bietjes). Reactieve stoffen kunnen in een cel schadelijke effecten teweegbrengen door een interactie aan te gaan met essentiële macromoleculen, zoals eiwitten, enzymen of DNA. Gelukkig zijn organismen uitgerust met een speciaal enzymatisch afweersysteem tegen deze verbindingen en dit enzymsysteem is met name gelocaliseerd in de lever, maar ook bijvoorbeeld in de nieren en longen. Dit complex systeem heeft tot doel lichaamsvreemde stoffen (xenobiotica) te modificeren tot meer wateroplosbare verbindingen (metabolieten), die vervolgens efficient via de gal of urine het lichaam verlaten. Dit proces van enzymatische modificatie van xenobiotica wordt ook wel biotransformatie genoemd. Biotransformatie dient lichaamsvreemde verbindingen onschadelijk te maken. Ironisch genoeg kunnen tijdens de biotransformatie ook ongewenste reactieve produkten ontstaan met mogelijk toxische (schadelijke) consequenties (bioactivering).

Het toxicologisch testen van alle nieuwe en bestaande verbindingen is een zeer kostbare en tijdrovende aangelegenheid, en daarom zijn alternatieven hiervoor zeer gewenst. Het voornaamste doel van het onderzoek dat beschreven is in dit proefschrift was om regels ofwel "QSARs" (quantitatieve structuur-activiteit relaties) te formuleren voor de biotransformatie en toxiciteit van gehalogeneerde amino- en nitrobenzeen derivaten (**hoofdstuk 1**). Deze verbindingen worden frequent gebruikt in de agrochemische en pharmaceutische industrie ten behoeve van de produktie van pesticiden, herbiciden, kleurstoffen, medicijnen en andere industriëel relevante verbindingen. Het cytochroom P450 systeem en glutathion S-transferase zijn

belangrijke biotransformatie enzymen, die betrokken zijn bij de detoxificatie (ontgifting) en bioactivering van deze stoffen. In deze studies is voornamelijk aandacht besteed aan cytochroom P450, en in mindere mate aan de glutathion/glutathion S-transferase afhankelijke biotransformatie route.

Hoofdstuk 2 geeft een overzicht van de enzymen die betrokken zijn bij de biotransformatie van gehalogeneerde amino- en nitrobenzeen derivaten, met betrekking tot hun functie, regulatie, voorkomen, moleculaire/biochemische werkingsmechanismen, alswel de rol in bioactivering en detoxificatie van xenobiotica. Biotransformatie van amino- en nitrobenzeen derivaten is essentieel voor de vorming van reactieve intermediairen die mogelijk verantwoordelijk zijn voor de toxische effecten van deze groep verbindingen. Inzicht in factoren die de biotransformatie van deze verbindingen bepalen, leiden tot een beter begrip van de processen en van de mogelijkheden tot bioactivering en detoxificatie. De regioselectieve enzymatische omzetting van relatief kleine aromatische substraten in het relatief grote aspecifieke katalytisch centrum van cytochroom P450 wordt verondersteld voornamelijk afhankelijk te zijn van de chemische substraat karakteristieken. Voor grotere substraten daarentegen, zal ook de stereoselectieve positionering tengevolge van sterische interacties in het katalytisch centrum de regioselectieve omzetting bepalen (zie hoofdstuk 2). De mogelijkheden voor de enzymatische omzetting van een klein aromatisch molecuul worden daarom waarschijnlijk bepaald door de verschillen in reactiviteit van de diverse plaatsen in het molecuul. Naar aanleiding van deze overwegingen werd onderzocht of computer berekende karakteristieken van de amino- en nitrobenzenen, in combinatie met inzicht in het moleculaire werkingmechanisme van de enzymatische omzetting, behulpzaam kunnen zijn bij het voorspellen van het metabole lot van deze stoffen.

Hoofdstuk 3 presenteert een studie naar de regioselectiviteit en mechanismen die ten grondslag liggen aan de cytochroom P450 gekatalyseerde aromatische hydroxylering van fluor aminobenzenen (= fluor anilines). Deze studie verschaft zowel inzicht in het mogelijke moleculaire werkingsmechanisme van de cytochroom P450 gekatalyseerde aromatische hydroxylering, als in de factoren die de regioselectieve hydroxylering beinvloeden. Op basis van computer-berekende substraat karateristieken en inzicht in de moleculaire werkingsmechanismen van cytochroom P450 kon zowel de regioselectiviteit (**hoofdstuk 3**) als de snelheid (**hoofdstuk 4**) van de aromatische hydroxylering van aminobenzenen verklaard worden. Bovendien kon een QSAR voor de snelheid van de aromatische hydroxylering worden geformuleerd op basis van de computer berekende substraat karakteristieken.

Teneinde de cytochroom P450 afhankelijke biotransformatie van aniline-derivaten volledig op te helderen, moest een gevoelige en efficiente methode worden ontwikkeld voor de detectie en quantificering van 2-aminophenol metabolieten, aangezien deze nog niet voorhanden was (**hoofdstuk 5**).

Naast de aromatische hydroxylerings reacties werd ook de oxidatieve dehalogenering door cytochroom P450 bestudeerd. Halogenen worden vaak gebruikt om specifieke plaatsen in medicijnen of agrochemicalien te bezetten, waardoor bioactivatie of biodegradatie door enzymen wordt verhinderd. Bij voorkeur worden daarvoor fluor atomen gebruikt, omdat ze bijna net zo klein zijn als waterstof atomen en vanwege de sterke C-F binding. In **hoofdstuk 6** werd aan de hand van SAR principes het mechanisme van de oxidatieve aromatische dehalogenering bestudeerd. Tevens werd de invloed van het halogeen substitutie op de regioselectieve hydroxylering en de vorming van reactieve deeltjes onderzocht. Er werd aangetoond dat tijdens de biotransformatie de fluoratomen een aminobenzeen gemakkelijker verlaten dan een chloor-, broom- of joodatoom. Alhoewel het metabolisme op de gehalogeneerde positie werd geremd, resulteerde deze blokkade tevens in de (verhoogde) vorming van andere metabolieten (het reactieve 1,4-benzoquinoneimine en N-hydroxyaniline), met mogelijke toxicologische consequenties.

De toxische effecten van aminobenzenen worden voor een gedeelte bepaald door de vorming van N-hydroxyaniline metabolieten, die methemoglobinemie veroorzaken. De aromatische hydroxyleringsmetabolieten (aminophenolen) daarentegen worden gekoppeld aan goed wateroplosbare groepen en verlaten dientengevolge efficient het lichaam via de urine. Daarnaast wordt de vorming van 4-aminophenolen verondersteld een rol te spelen bij het onstaan van aniline-geinduceerde niertoxiciteit. Daar de cytochroom P450 gekatalyseerde regioselectieve hydroxylering de toxiciteit van anilines lijkt te beinvloeden, werd in **hoofdstuk 7** een studie uitgevoerd naar de relatie tussen de regioselectieve hydroxylering en het optreden van toxische effecten als methemoglobinemie en niertoxiciteit. De mate van niertoxiciteit in een serie anilines bleek gerelateerd te zijn aan de mate van aromatische hydroxylering op de C4-positie. De mate van methemoglobinemie was gerelateerd aan de mate van N-hydroxylering. Een verandering in regioselectieve hydroxylering van 4-hydroxylering naar N-hydroxylering leidt dus tot een verandering in toxisch effect van niertoxiciteit naar methemoglobinemie. Hieruit blijkt dat in hoofdstuk 7 een duidelijk voorbeeld wordt gepresenteerd van een verband tussen het metabolisme enerzijds, en de mate en type van toxiciteit anderzijds.

Aminobenzenen worden voornamelijk door cytochroom P450 omgezet en niet door glutathion S-transferase. De chemisch geoxideerde nitrobenzeen analogen worden voornamelijk door glutathion S-transferase omgezet en in mindere mate door cytochroom P450. In **hoofdstuk 8** wordt een hypothese voorgesteld die verklaart waarom nitrobenzenen voornamelijk door de glutathion afhankelijke biotransformatie route worden omgezet, terwijl anilines juist via de P450 route worden gemodificeerd. De hypothese is gebaseerd op inzicht in de werkingsmechanismen van de enzymen en met de computer berekende substraat karakteristieken die van belang zijn voor de twee verschillende biotransformatie routes. Het actieve deeltje van glutathion S-transferase (thiolaat anion van glutathion) kan een betere interactie aangaan met het nitrobenzeen substraat dan met de aniline, terwijl het actieve deeltje van cytochroom P450 een betere interactie kan aangaan met het aniline substraat dan met de nitrobenzeen.

Gehalogeneerde nitrobenzenen worden via drie biotransformatie routes gemetaboliseerd, te weten nitro-reductie, glutathion conjugatie en aromatische hydroxylering. Voor enkele van de toxische effecten van nitrobenzenen is de vorming van reactieve metabolieten een vereiste. Zo ontstaan bijvoorbeeld tijdens de nitro-reductie methemoglobinemie vormende deeltjes. De mate van methemoglobinemie vorming wordt verondersteld afhankelijk te zijn van de mogelijkheden tot nitroreductie. Factoren die deze nitroreductie kunnen beinvloeden zijn de intrinsieke gevoeligheid van nitrobenzenen voor nitroreductie, en/of de aanwezigheid van concurrerende biotransformatie routes als glutathion conjugatie en aromatische hydroxylering. Met behulp van QSAR benaderingen werd in **hoofdstuk 9** een studie uitgevoerd naar een mogelijk verband tussen het metabolisme en de vorming van methemoglobinemie door een serie fluornitrobenzenen. Hierdoor ontstond inzicht in het relatieve belang van deze twee veronderstellingen. Er werd aangetoond dat verhoogde conjugatie mogelijkheden met glutathion of andere macromoleculen tot een afname in de bijdrage van aromatische hydroxylering en nitroreductie leiden. Deze conjugatie snelheid van fluornitrobenzenen kon zelfs voorspeld worden aan de hand van computer berekeningen. De mate van methemoglobinemie vorming bleek verder niet bepaald te worden door de intrinsieke gevoeligheid van fluornitrobenzenen voor nitroreductie door darm-microflora en leverpreparaten. Geconcludeerd werd dat de conjugatie met glutathion en macromoleculen fungeert als een voor nitroreductie concurrerende biotransformatie route en daardoor dus de mogelijkheden voor methemoglobinemie beinvloedt.

In **hoofdstuk 10** wordt een studie beschreven die aantoont dat de gedefinieerde QSARs voor de snelheid en regioselectiviteit van de P450

gekatalyseerde hydroxylering niet alleen gelden voor ratten, maar ook voor diverse andere species, waaronder de mens. Deze bevindingen ondersteunen de conclusie dat de omzetting van relatief kleine gehalogeneerde benzeen derivaten in de relatief grote en aspecifieke actieve centra van de cytochroom P450 enzymen, voornamelijk worden bepaald door de chemische reactiviteit parameters van de substraten. Het belang van deze substraat karakteristieken domineert zelfs over de invloed van de specifieke P450 enzymen op de regioselectiviteit *in vitro* als *in vivo*.

Samenvattend kan geconcludeerd worden, dat het onderzoek in dit proefschrift duidelijk aantoont dat moleculaire orbitaal berekeningen in combinatie met de frontier orbitaal theorie een bruikbare additionele benadering is om het mechanisme en de uitkomsten van de cytochroom P450 katalyse te bestuderen. Naast theoretische overwegingen betreffende het moleculaire reactie mechanisme en de enzym katalyse, zijn empirische gegevens essentieel om geldige regels of zelfs QSARs te formuleren voor biotransformatie en toxiciteit. In dit proefschrift wordt duidelijk geillustreerd dat inzicht in biotransformatie routes bijdraagt tot inzicht in de vorming van reactieve metabolieten. Het opstellen van QSARs voor biotransformatie bleek een zeer bruikbare benadering om zowel het type als de mate van de toxische effecten, die worden teweeggebracht door deze amino- en nitrobenzenen, te verklaren.

Meer geavanceerde modellen, die niet alleen rekening houden met de chemische reactiviteit van de substraten, maar ook met hun stereoselectieve positionering en interacties met specifieke aminozuurresiduen in het actieve centrum van cytochromen P450, zullen uiteindelijk leiden tot een betere voorspelling van metaboliet profielen van bestaande en nieuw te ontwikkelen medicijnen, agrochemicalien en andere industrieel relevante verbindingen.

Naar aanleiding van bovenstaande resultaten is het een uitdaging, de in dit proefschrift beschreven benaderingen toe te passen op andere enzymen met meer specifieke actieve centra dan de relatief grote aspecifieke actieve centra van het biotransformatie-enzym cytochroom P450.

Curriculum Vitae

Nicole Cnubben werd geboren op 13 februari 1967 te Meerssen. Zij behaalde het VWO diploma (Gymnasium β) in mei 1985 aan de Scholengemeenschap Stella Maris te Meerssen. Aansluitend startte zij de studie Moleculaire Wetenschappen aan de Landbouwuniversiteit te Wageningen. Tijdens de doctoraalstudie doorliep zij de hoofdvakken Biochemie en Toxicologie. In 1989 verrichtte zij op de vakgroep Biochemie onder leiding van professor C. Veeger, Dr. I.M.C.M. Rietjens en Dr. W.H.J. van Berkel onderzoek naar "De rol van FMO en cytochroom P450 in de biotransformatie van 4-fluoro-N-methylaniline". In 1990 bestudeerde zij op de vakgroep Toxicologie de invloed van 4OH-3,3',4',5-TCB op de plasmakinetiek, eliminatie en distributie van ^{125}I-TTR en ^{125}I-T4 onder begeleiding van professor J. H. Koeman en Dr. A. Brouwer. In november 1990 behaalde zij het doctoraal examen. Vervolgens trad zij als onderzoekster in opleiding in dienst van de Nederlandse organisatie voor Wetenschappelijk Onderzoek (NWO), werkgemeenschap farmaca en vergiften, gedetacheerd aan de vakgroep Biochemie van de Landbouwuniversiteit te Wageningen. De resultaten van dit onderzoek onder leiding van professor C. Veeger en Dr. I.M.C.M. Rietjens zijn vastgelegd in dit proefschrift. Tijdens deze periode volgde ze de Postdoctorale Opleiding Toxicologie ten behoeve van de registratie toxicoloog conform de SMBWO normen. In februari 1995 was zij werkzaam als toegevoegd onderzoeker bij de vakgroep Biochemie van de Landbouwuniversiteit en sinds juni 1995 is zij werkzaam bij TNO Voeding, divisie Toxicologie, te Zeist.

List of publications

Cnubben, N.H.P., Vervoort, J., Veeger, C., Rietjens, I.M.C.M. Study on the regioselectivity and the mechanism for the cytochrome P450 dependent aromatic hydroxylation of monofluoroanilines. *Chem.-Biol. Interactions* **85**, 151-172, 1992.

Cnubben, N.H.P., Peelen, S., Borst, J.W., Vervoort, J., Veeger, C., Rietjens, I.M.C.M. Molecular orbital based quantitative structure-activity relationship for the cytochrome P450-catalyzed 4-hydroxylation of halogenated anilines. *Chem. Res. Toxicol.* **7**, 590-598, 1994.

Cnubben, N.H.P., Blaauboer, B., Juyn, S., Vervoort, J., Rietjens, I.M.C.M. A spectrophotometric assay for the detection of 2-aminophenols in biological samples. *Anal. Biochem.* **220**, 165-171, 1994.

Cnubben, N.H.P., Vervoort, J., Boersma, M.G., Rietjens, I.M.C.M. The effect of varying halogen substituents on the cytochrome P450-catalyzed dehalogenation of 4-halogenated anilines to aminophenol metabolites. *Biochem. Pharmacol.* **49**, 1235-1248, 1995.

Cnubben, N.H.P., van den Berg, C.L., Rietjens, I.M.C.M. Relationships between the regioselectivity of the hydroxylation of C4-substituted 2-fluoroaniline derivatives and their toxic endpoints. Submitted for publication in *Toxicol. Appl. Pharmacol.*

Rietjens, I.M.C.M., Cnubben, N.H.P., van Haandel, M., Tyrakowska, B., Soffers, A.E.M.F., Vervoort, J. Different metabolic pathways of 2,5-difluoronitrobenzene and 2,5-difluoroaminobenzene compared to molecular orbital substrate characteristics *Chem.-Biol. Interact.* **94** , 49-75., 1995.

Cnubben, N.H.P., Soffers, A.E.M.F., Peters, M., Vervoort, J., Rietjens, I.M.C.M. Influence of the halogen-substituent pattern of fluoronitrobenzenes on their biotransformation and capacity to induce methemoglobinemia. Accepted for publication in *Toxicol. Appl. Pharmacol.*, 1996.

Tyrakowska, B., Cnubben, N.H.P., Soffers, A.E.M.F., Wobbes, Th., Rietjens, I.M.C.M. Comparative MO-QSAR studies in various species including man. Accepted for publication in *Chem. Biol.-Interactions*, 1996.

Boersma, M.G., Cnubben, N.H.P., van Berkel, W.J.H., Blom, M., Vervoort, J., Rietjens, I.M.C.M. Role of cytochrome P450 and flavin containing monooxyenase in the biotransformation of 4-fluoro-N-methylaniline. *Drug Metabolism and Disposition* **21**, 218-230, 1993.

Rietjens, I.M.C.M., Cnubben, N.H.P., de Jager, P.A., Boersma, M.G., Vervoort, J. Application of NMR in biotransformation studies. In: Developments and ethical considerations in toxicology, Michael I. Weitzner (Ed.), Royal Society of Chemistry, Redwood Press Ltd., Melksham, Wiltshire, 94-109, 1993.

Rietjens, I.M.C.M., Boersma, M.G., Soffers, A.E.M.F, Cnubben, N.H.P., Koerts, J., Peelen, S., van Berkel, W.H.J., Veeger, C., Vervoort, J. Use of molecular orbital calculations in studies on mechanisms of enzyme catalysis. In: Flavins and Flavoproteins 1993, K. Yagi (Ed), Walter de Gruyter & Co., Berlin, 3-12, 1994.

Vervoort, J., Boersma, M.G., Cnubben, N.H.P., van Berkel, W.H.J., Koerts, J., Rietjens, I.M.C.M. Mammalian flavin-containing monooxygenases catalyzed conversion of 4-halo-N-methylanilines. In: Flavins and Flavoproteins 1993, K. Yagi (Ed), Walter de Gruyter & Co. Berlin, 255-258, 1994.

Koerts, J., Soffers, A.E.M.F., Cnubben, N.H.P., de Kraker, J.W., Rietjens, I.M.C.M. The metabolism and bioavailability of teflubenzuron, in preparation.

Dankwoord

Met veel plezier denk ik terug aan de periode waarin dit onderzoek is uitgevoerd en daarbij niet te vergeten aan alle mensen die hebben bijgedragen aan de totstandkoming van dit proefschrift.

Allereerst wil ik Ivonne, mijn co-promotor, hartelijk bedanken voor haar enorm goede en enthousiaste ondersteuning. Discussies over experimenten en resultaten waren altijd zeer verhelderend én gezellig. Voor problemen die niet altijd puur van wetenschappelijke aard waren kon ik ook altijd bij je terecht. Kortom, ik heb het heel erg prettig gevonden om "jouw OIO" te zijn en ik weet zeker dat ik mij geen betere co-promotor had kunnen wensen.

Voorts ben ik mijn promotor, professor Cees Veeger, zeer erkentelijk voor zijn interesse in mijn onderzoek en voor zijn opbouwende kritieken. Het afgelopen jaar heb ik mij zeer gesterkt gevoeld door uw medeleven, steun en begrip.

Vervolgens wil ik Jacques bedanken voor zijn hulp bij de NMR metingen. Ondanks het feit dat je het altijd zo druk hebt, maakte je vaak tijd vrij voor een babbel. Wanneer ik mij weer eens vreselijk zat op te winden over bepaalde zaken, was jouw (soms te) nuchtere kijk op zaken een verfrissing voor mij.

De medewerkers van het CKP (Jo, Gerrit, etc.) en in het bijzonder Maria Peters, heel erg bedankt. Maria, jij was mijn grote steun en toeverlaat bij de dierexperimenten. Jouw professionele aanpak bij de ingewikkelde en arbeidsintensieve operaties, plus je bereidwilligheid om tijdens de experimenten gedurende 12 uren te assisteren, hebben het mogelijk gemaakt de studies in hoofdstuk 7 en 9 uit te voeren. Maria, ik en ook de studenten vonden het altijd heel erg leuk om met je samen te werken.

Fijne kamergenoten zijn essentieel voor een prettige werksfeer. En ik moet zeggen dat ik een héle prettige werksfeer heb gehad op onze kamer; Walter, Jan-Willem, Marelle, Janneke, Marion, Petra, Lars en Tatiana, de heerlijke kletspartijen waren een welkome afwisseling tijdens het nadenken, rommelen en schrijven van publicaties.

Ook Ans, Marelle en Sjef wil ik heel erg bedanken voor al hun professionele hulp, collegialiteit en gezelligheid.

Dear Bozena, I enjoyed our collaboration very much. I will never forget the thousands of tubes and "epjes". To me, it was always pleasant to perform these fruitful experiments together and to discuss the results (and other things.....).

Verder wil ik de studenten met wie ik nauw heb samengewerkt, Jan-Willem Borst, Jeannine, Saskia, Jack, Jan-Willem de Kraker, Elles, Mark, Caroline, Coralie en Guido heel erg bedanken voor hun inzet en plezierige samenwerking.

Alle collega's van de vakgroep Biochemie, ontzetttend bedankt voor jullie hulp en gezelligheid.
Verder wil ik mijn moeder, Theo, Marion, Lenardo, de familie van Peter en alle vrienden en kennissen heel erg bedanken voor hun interesse, goede raad (Nicole, rustig aan, er is meer tussen hemel en aarde dan werken) en steun.
Lieve Peter, jouw steun, engelen-geduld, enthousiasme en interesse (Nicole, hoe zit dat nu met die HOMO's en LUMO's en anilines en P450s en glutathion S-transferases?) hebben ook bijgedragen tot dit proefschrift. Je staat zelfs een keer vermeld in de acknowledgements van een publicatie. Misschien had ik dat bij al die andere ook wel moeten doen? Geamuseerd keek je toe en wijselijk hield je je mond, als ik het ene moment zat te grienen op de bank (wèèh, en nu wil ik huisvrouw worden en 10 kindertjes krijgen), en het andere moment tot middernacht vlijtig en vrolijk op het lab met reageerbuizen zat te worstelen. Peter, bedankt voor alles.

Nicole